# A Role for the Parkinson's Disease Kinase LRRK2 in Endo-Lysosomal and Cytoskeletal Function

Laura Pellegrini

Thesis submitted for the degree
of Doctor of Philosophy
University College London

*2017*

Supervisors:

Dr. Mark Cookson
*Laboratory of Neurogenetics*
*National Insitute of Aging*
*National Institutes of Health*

Prof. Kirsten Harvey
*Department of Pharmacology*
*School of Pharmacy*
*University College London*

## Declaration

I, Laura Pellegrini, confirm that the work presented in this thesis is my own, describing research completed between February 2014 and June 2017 under the supervision of Professor Kirsten Harvey and Dr. Mark Cookson. Where information has been derived from other sources of collaboration, I confirm that this has been indicated in the thesis. All text was written by me and those parts which have appeared in publications have been indicated by citation.

_____

Laura Pellegrini

_____

Date

# Abstract

Parkinson's disease (PD) is a progressive neurodegenerative disorder affecting millions of people globally. Like other age-related conditions, inheritance of genetic variations contributes to PD pathogenesis. Mutations in leucine-rich repeat kinase 2 (LRRK2) are linked with familial forms of late-onset PD. Importantly, the LRRK2 locus has been identified by genome-wide association studies to contribute to risk of sporadic disease. These observations suggest that the study of LRRK2 cell biological function and dysfunction might shed light on the pathogenesis of PD. LRRK2 is a large multidomain cytosolic protein reported to play a role in a variety of cellular functions such as cytoskeletal dynamics, vesicular trafficking and autophagy. Mouse models deficient of LRRK2 or harbouring the pathogenic human G2019S mutation do not show typical PD brain pathology. However, reported phenotypic kidney pathology in LRRK2 knockout mice provides a rationale to investigate LRRK2 knockout and G2019S knockin kidneys to further elucidate the biological role of LRRK2. Using an unbiased quantitative proteomic approach, significant alterations in protein levels associated with cytoskeletal, lysosomal, vesicular trafficking and control of protein translation were observed in Lrrk2 knockout but not G2019S knockin tissue. Lysosomal protein accumulation and changes in expression of a subset of cytoskeletal proteins were validated using orthogonal techniques in independent cohorts of mice across several age time points. Very few protein changes were observed in brain or varied in opposite directions in knockout versus knockin mice. A role for LRRK2 in the endo-lysosomal pathway was further confirmed in primary kidney cells from LRRK2 knockout mice. Overall, these results imply LRRK2 co-ordinated responses in protein trafficking and cytoskeletal dynamics, and argue against a simple dominant negative role for the G2019S mutation.

## Impact Statement

The work presented in this thesis has contributed to improve our knowledge on the biological role of leucine-rich repeat kinase 2 (LRRK2), which currently represents one of the most attractive therapeutic targets for Parkinson's disease. The results here discussed have been validated with different techniques and are in line with the literature.

First, the relevance of this study relies in the discovery, by unbiased proteomic screening, of multiple candidate proteins which are affected by alterations of the protein of interest, LRRK2. The large amount of data generated by the proteomic approach chosen, will benefit multiple promising follow-up projects and potentially each of the identified candidates could be further investigated.

Second, the experimental work here presented include the generation of an *in vitro* model in which to investigate the biological role of LRRK2 and which can be used for functional studies. The cell model of lysosomal dysfunction represents a helpful tool to monitor the accumulation of these organelles observed in several neurodegenerative pathologies and lysosomal storage disorders.

Overall, this work has shed light on a potential network of proteins affected by LRRK2 and has built evidence for future translational studies.

# Aknowledgements

There are many people who helped to this thesis and I would need a separate thesis to thank them all. For space reasons, I would limit myself to whom I am particularly grateful.

First, I would like to particularly thank my family. Mum, for your motivational speeches, for the life lessons that helped me throughout this experience, for being an invaluable role model. Dad, for your inconditional support, and for being an example of dedication and honesty. Francesco for always being a kind, understanding and caring brother. I am extremely lucky and I should never be grateful enough.

I would like to thank my supervisors Prof. Kirsten Harvey and Dr. Mark R Cookson for their constant scientific support, constructive critisism and enormous patience throughout this PhD. Thank you for giving me the possibily to work in such a stimulating research environment and for the encouragement in these last years.

From the NIH, I would like to thank my friends and colleagues Sasha and Alice for their inspiring energy, remarkable resilience, scientific and moral support; Dave Hauser for teaching me fundamental scientific techniques with extreme patience and enthusiasm; Thank you Adam, Kumaran, Dorien, Rebekah, Xyleena, Jillian, Louis for the creative scientific discussions and standing all my questions, but most of all, for creating such a great lab. You guys were my family in the US. I really hope that wherever we are in the world we will stay in touch.

Special thanks to Simone Grannò, Jonathon Nixon-Abell and Christopher Obara for their friendship and amazing help from the very beginning of this experience.

Obviously, huge thanks to all friends and workmates from UCL: Andrea, Ola, Archie, Emma, Giulia, Sam, Ed, Michael, Joana. You are all brilliant, beautiful

people and you made this experience a lot easier and fun!
Enormous thanks to David Gershlick for his inconditional moral and scientific support. For every crisis moment, for stopping me from going to "panic-town" and for all the scientific discussions which helped me immensely throughout this PhD. You are my favorite and I feel so lucky to have such a smart, kind and loving person in my life.
Finally, I would like to thank all my friends from from my lovely hometown Belluno and from the greatest Goodenough college in London, who have supported me over the years: Elena, Jessica, Federica, Paolo, Valerio, Simone, Chiara, Elisa, Alessandra, Pina, João, Matko, Ines and Omar. You all mean a great deal to me.

Thank you all so much!

# Contents

# List of Figures

# List of Tables

# Abbreviations

| Abbreviation | Name |
|---|---|
| **AD** | Alzheimer's disease |
| **ANK** | Ankyrin-like domain |
| **ARHGEF7** | Rho guanine exchange factor 7 |
| **ARM** | Armadillo region |
| **ATP** | Adenosine triphosphate |
| **BSA** | Bovine serum albumin |
| **CMA** | Chaperone-mediated autophagy |
| **COP** | Coatmer protein coated |
| **COR** | C-terminal of Ras of complex |
| **Coro1c** | Coronin1C |
| **CatD** | Cathepsin D |
| **DA** | Dopamine |
| **DMEM** | Dulbecco 's modified eagle 's medium |
| **DNA** | Deoxyribonucleic acid |
| **EGF** | Epidermal growth factor |
| **ER** | Endoplasmic reticulum |
| **ERES** | ER exit sites |
| **ERM** | Ezrin radixin moesin |
| **ESc** | Embryonic stem cell |
| **FBS** | Fetal bovine serum |
| **GAK** | Cyclin-D associated protein K |
| **GDP** | Guanosine diphosphate |
| **GI** | Gastrointestinal tract |
| **GO** | Gene ontology |
| **GTP** | Guanosine triphosphate |
| **GWAS** | Genome wide association studies |
| **HBSS** | Hank's buffered saline solution |
| **HEK293** | Human embryonic kidney 293 |
| **HPLC** | High-performance liquid chromatography |
| **HRP** | Horseradish peroxidase |
| **iTRAQ** | Isobaric Tag for Relative and Absolute Quantitation |
| **L-DOPA** | Levodopa |
| **LB** | Lewy body |
| **LC3** | Microtubule-associated protein 1 light chain 3 |
| **LC** | Liquid chromatography |
| **LRRK2** | Leucine rich repeat kinase 2 |
| **M6PR** | Mannose 6-phosphate receptor |
| **MAP** | Microtubule-associated protein |

| Abbreviation | Name |
|---|---|
| **MS** | Mass Spectrometry |
| **mTOR** | Mechanistic target of rapamycin |
| **Naa15** | N-alpha-acetyltransferase 15, NatA auxiliary subunit |
| **PBS** | Phosphate buffered saline |
| **PD** | Parkinson's disease |
| **PFA** | Paraformaldehyde |
| **PINK1** | PTEN-induced putative kinase 1 |
| **PM** | Plasma membrane |
| **PTM** | Post-translational modification |
| **PVDF** | Polyvinylidene fluoride |
| **qRT-PCR** | Quantitative real-time polymerase chain reaction |
| **RNA** | Ribonucleic acid |
| **Roc** | Ras of complex |
| **SDS-PAGE** | Sodium dodecyl sulphate polyacrylamide gel electrophoresis |
| **SNCA** | ∝-synuyclein |
| **SNpc** | Substantia nigra pars compacta |
| **TBS** | Tris-buffered saline |
| **TGN** | Trans-Golgi network |
| **TUBB** | Beta-tubulin |
| **UPS** | Ubiquitin proteasome system |
| **Vps35** | Vacuolar protein sorting-associated protein 35 |

# 1 Introduction

## 1.1 Parkinson's disease

### 1.1.1 History and overview of the *shaking palsy*

In 1817, the English physician James Parkinson published a document entitled "An Essay on the Shaking Palsy" in which he described for the first time a spectrum of symptoms that characterise the eponymous disease. The biochemical underpinning of Parkinson's disease (PD), however, only began to be unearthed around 1960, whereby altered dopamine synthesis, crucial for the control of movement circuits, was identified in PD patients (Reeve et al. 2014).

PD is classified as a late-onset degenerative movement disorder affecting 1% of people over the age of 60, rising to 4-5% in individuals 85 years or older (Berwick and Harvey 2014; Polito et al. 2016; Reeve et al. 2014). The typical age of onset is between 60 and 70, although 4% of patients develop early-onset disease before the age of 50 (Gandhi and Wood 2005; Reeve et al. 2014; Trinh and Farrer 2013).

PD has traditionally been considered a sporadic disorder due to its complex and poorly understood aetiology. The current consensus suggests multiple risk factors contribute to the risk of disease, such as environmental exposure and genetic predisposition (Polito et al. 2016). Ageing, however, appears to be the biggest risk factor for PD (Reeve et al. 2014). Therefore, the health, social, and economic impact arising from PD is continuously increasing with the longevity of the population (Reeve et al. 2014).

In the last 15 years, an increasing number of loci associated with Mendelian forms of PD have been identified (Greggio 2012; Kumaran and Cookson 2015). Genome Wide Association Studies (GWAS), by looking at ∼1 million polymorphisms in matched case and control cohorts, provided strong evidence that sporadic PD has a genetic component (Kumaran and Cookson 2015; Simón-Sánchez et al. 2009). These findings aroused great interest and renewed hope in discovering common molecular mechanisms shared by familial and sporadic PD (Gandhi and Wood 2005).

### 1.1.2 Symptomatology: motor and non-motor symptoms

PD is now recognised as a progressive and clinically heterogeneous movement disorder, characterised by neurological and non-motor deficiencies (Caligiore et al. 2016; Jellinger 2012; Lees et al. 2009; Van Den Eeden et al. 2003). The neurodegenerative process varies between individuals but is typically chronic and slowly progressive, meaning symptoms continue and worsen over a period of years. Life expectancy of patients from onset of symptoms is typically around 15 years. However, PD is not considered a fatal disease as death usually arises as a result of several secondary complications, the most common being pneumonia and bronchitis (Ben-Shlomo and Marmot 1995).

From a clinical viewpoint it is possible to highlight three typical manifestations of PD: resting tremor, rigidity and bradykinesia (slowness of movement) (Jankovic 2008; Lees et al. 2009). These symptoms are usually associated with other motor dysfunctions such as balance impairments, gait disturbances and postural instability. Non-motor symptoms defined as secondary symptoms often precedes the motor symptoms and can include depression, sleep difficulties, constipation and gastrointestinal tract (GI) dysfunctions (Kim and Sung 2015; Mukherjee et al.

2016), autonomic nervous system deregulation and, in the late stages, dementia (Lees et al. 2009).

### 1.1.3 Molecular pathology of PD

The histopathological examination of post-mortem brain sections from PD patients reveals two typical features. First, the macroscopic absence of melanin pigmentation within the substantia nigra represents a pathological hallmark of PD, correlated with loss of dopaminergic neurons in this brain region (Lees et al. 2009; Reeve et al. 2014). Dopaminergic neurons specialise in the synthesis of dopamine (DA). DA is a catecholamine neurotransmitter critical for several physiological functions such as movement initiation and execution but also reward-motivation behaviours. Dopaminergic neurons release DA to the striatum that sends projections to other components of the basal ganglia (Barbeau 1961; Chinta and Andersen 2005). Typical motor symptoms of PD appear only after neurodegeneration of the majority of substantia nigra *pars compacta* (SNpc). Denervation in the SNpc causes a dramatic reduction in DA levels that can be compensated pharmacologically with therapeutic administration of L-DOPA: a precursor of DA (Ehringer and Hornykiewicz 1998; Montagu 1957). This drug, unlike DA (that is not able to cross the blood brain barrier), easily reaches dopaminergic neurons where it is converted by decarboxylation into DA. However, despite the symptomatic relief promoted by L-DOPA, its efficacy decreases over years and the treatment often leads to adverse effects in the later stages of the disease (typically dyskinesias) (Varanese et al. 2011).

Second, cytoplasmic inclusions called Lewy bodies (LB) are routinely found in surviving dopaminergic neurons (Braak et al. 2003; Cookson 2010; Halliday et al. 2012). LB and related structures such as Lewy neurites are protein and

lipid aggregates chiefly composed of α-synuclein, but also other proteins such as ubiquitin, tubulin and tau (Jellinger 2012; Schneider et al. 2006). α-synuclein is a short-lived protein econded by the SNCA gene, which preferentially resides in the pre-synaptic terminal in close proximity of synaptic vesicles where it appears to have a role in neurotransmitter release in combination with the SNARE complex (Murphy et al. 2000; Polymeropoulos et al. 1997; Stefanis 2012). In addition to PD, α-synuclein seems to play a role in other diseases, such as Lewy body dementia, that are collectively called *synucleinopathies* (Spillantini et al. 1998). According to the Braak hypothesis, LB formation occurs in a stereotyped fashion starting from peripheral tissues through the midbrain and eventually to the neocortex (Braak et al. 2003). In particular, α-synuclein inclusions are detectable in the enteric nervous system and in the vagal nerve prior to accumulation in the central nervous system that is accompanied by inflammation and microglial activation (Braak et al. 2003; Shannon et al. 2012).

There may be relationships between α-synuclein and other proteins involved in different neurodegenerative diseases. For example, a toxic interaction between tau and α-synuclein has been shown to promote fibrillation of both proteins and to increase tau phosphorylation (Jensen et al. 1999; Moussaud et al. 2014). Neurofibrillary tangles, aggregates of hyperphosphorylated tau, in the substantia nigra have been associated with gait impairment in older patients with and without dementia (Schneider et al. 2006). Dementia often seems to correlate with the amount of tau-containing neurofibrillary tangles (Ghoshal et al. 2002).

Finally, microglial hyperactivation has also been reported in PD. Microglial cells are resident phagocytic cells that are normally quiescent but can provide an immune response when necessary. However, in a neurodegenerative condition,

these cells may become hyperactive leading to a chronic inflammatory state (Qian and Flood 2008).

## 1.2 LRRK2 and inherited PD

### 1.2.1 Overview

GWAS and genetic analysis of several kindreds have identified loci designated as PARK loci containing PD causative mutations and PD risk variants. Some of these mutations are robustly associated with PD, others refer to clinical parkinsonism rather then PD with LB pathology (Hardy et al. 2009). To date, eleven genes, listed below, have been associated with PD and other forms of parkinsonism (Table 1) (Beilina et al. 2014; Kumaran and Cookson 2015; Simón-Sánchez et al. 2009).

| Gene | Protein | Inheritance |
|---|---|---|
| SNCA (PARK1/PARK4) | α-synuclein | AD |
| Parkin (PARK2) | Parkin | AR |
| PINK1 (PARK6) | PTEN | AR |
| DJ-1 (PARK7) | DJ-1 | AR |
| LRRK2 (PARK8) | Leucine-rich repeat kinase 2 (LRRK2) | AD |
| ATP13A2 (PARK9) | Atp13a2 protein | AR |
| PLA2G6 (PARK14) | 85/88 kDa calcium-independent phospholipase A2 | AR |
| FBX07 (PARK15) | F-box protein 7 (FBX07) | AR |
| VPS35 (PARK17) | Vacuolar protein sorting-associated protein (VPS35) | AD |
| DNAJC6 (PARK19) | Putative tyrosine-protein phosphatase auxilin (DNAJC6) | AR |
| SYNJ1 (PARK20) | Synaptojanin-1 (SYNJ1) | AR |

Table 1: **Gene whose mutations are associated with PD and parkinsonism.**

### 1.2.2 LRRK2 mutations

Mutations in the LRRK2 gene represent a major cause of autosomal dominant, late-onset familial PD, observed in 6-10% of familial cases and in 0.5-2% of all Parkinson's cases (Van Den Eeden et al. 2003). Arguably, these mutations are the most relevant to sporadic disease since LRRK2 clinical features, although variable,

are indistinguishable from idiopathic PD (Gandhi et al. 2009). The interest in the study of LRRK2 is further reinforced by GWAS that have nominated the locus containing LRRK2 as conferring risk for sporadic PD (Satake et al. 2009; Simón-Sánchez et al. 2009).

In 2002, Funayama and collaborators identified the PARK8 locus through genome-wide linkage analysis of a dominantly inherited late-onset form of parkinsonism in a large Japanese family. Haplotype analysis pointed out that the disease locus in this family mapped to the 13.6cM interval of chromosome 12p11.23-q13.11 (Funayama et al. 2002). Concurrent studies in two families, the Western Nebraska Family D and German-Canadian Family A, who suffered from a similar form of autosomal-dominant and late-onset parkinsonism, confirmed linkage to the same chromosomal region (Zimprich et al. 2004).

Meanwhile, kindred studies provided further evidence that missense mutations in the PARK8 region segregate with PD (Paisan-Ruiz et al. 2004; Zimprich et al. 2004). LRRK2 identification and cloning revealed low but consistent expression levels throughout the brain. However, LRRK2 is not highly expressed in dopaminergic neurons (Han et al. 2008; MacLeod et al. 2006). LRRK2 has been detected also in other organs such as kidney, lung and heart and in different cell types such as immune cells (macrophages, dendritic cells, microglia, monocytes, T and B-cells), Purkinje cells and astrocytes (Baptista et al. 2013; Giasson et al. 2006; Herzig et al. 2011; Higashi et al. 2007).

To date, although many studies have identified several LRRK2 coding substitutions, only seven mutations, clustered in the catalytic core of the protein, convincingly segregate with PD (Table:2). For some mutations (the G2019S, for example), heterozygous and homozygous individuals have similar risk of developing PD

and similar pathological progression. Mutant gene dosage, therefore, seems not correlated with a phenotypic effect meaning that LRRK2 mutations display a true dominant effect (Ishihara et al. 2007). The study of these mutations, however, is complicated because of the low number of cases and the incomplete penetrance, since some carriers do not develop PD during their lifetime (Greggio et al. 2009).

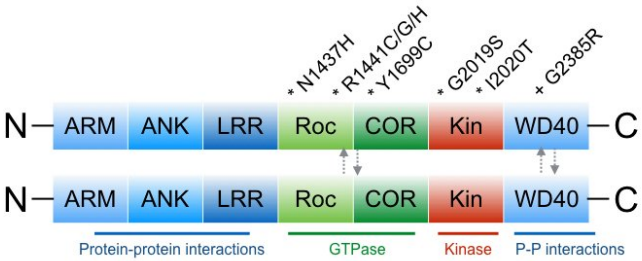


Figure 1.1: **LRRK2 domain structure.** Protein-protein interaction domains are coloured in blue, GTPase Roc-COR domain in green and kinase domain in red. Mutations segregating with PD are indicated with asterisks and the risk variant G2385R is indicated with a plus sign. LRRK2 dimerisation is possibly mediated by Roc-COR and/or WD40 domains. Figure adapted from Berwick and Harvey 2013.

| **LRRK2 mutation** | **Population identified** | **Reference** |
|---|---|---|
| I2020T | Funayama Japanese family | (Funayama et al. 2002) |
| Y1699C | German-Canadian family A | (Zimprich et al. 2004) |
| R1441C | Western Nebraska family D | (Zimprich et al. 2004) |
| R1441G | Basque families | (Paisan-Ruiz et al. 2004) |
| R1441H | European/Taiwanese families | (Mata et al. 2005) |
| G2019S | North American/European families | (Di Fonzo et al. 2005) |
| N1437H | Norwegian family F04 | (Aasly et al. 2010) |

Table 2: **LRRK2 mutations detected in families with PD or parkinsonisms.**

The most common LRRK2 mutation, the G2019S, increases the incidence of PD from 20% to 80% between the age of 50 and 70 (Bonifati 2006; Greggio et al. 2009; Healy et al. 2008). This mutation reaches a maximum of frequency in certain ethnicities such as Ashkenazi Jews (10-30% of PD patients) and some North African populations (35-40% of PD patients) (Healy et al. 2008). Mutation of the I2020 residue, adjacent to the G2019 residue, also segregates with PD (Gloeckner et al. 2006; Nichols et al. 2010). Three familial mutations have been identified at the residue R1441 (R1441C/G/H). Localised in the same domain, the N1437H mutation has been found in a large Norwegian Family (Aasly et al. 2010). Other substitutions such as G2385R or R1628P have much lower penetrance, and are therefore better described as risk factors variants for sporadic PD (Farrer et al. 2007; Rudenko et al. 2012)

### 1.2.3 LRRK2 structure

The LRRK2 gene is located on the position 12 in the long arm (q) of chromosome 12. LRRK2 contains 51 exons and its cDNA is 7.5kb long (Greggio and Cookson 2009; Greggio et al. 2009; Paisan-Ruiz et al. 2004; Zimprich et al. 2004). Its encoded protein has 2527 amino acids with a predicted molecular weight of 286kDa. LRRK2 is conserved across species, with *Drosophila melanogaster* and *Caenorhabditis elegans* expressing a single LRK.

LRRK2 is a large protein that belongs to the ROCO protein family. This family comprises proteins with a ROC (Ras of complex proteins) domain, invariably followed in tandem by a domain termed COR (C-terminal of ROC). ROC domains are highly conserved GTP binding domains often surrounded by additional protein domains, typically including a kinase domain (Marín et al. 2008). This arrangement is observed in LRRK2, which is composed of the following domains from the

N-terminal armadillo (ARM) region to the C-terminal domain: an ankyrin like (ANK) domain, a leucine-rich (LRR) domain, a Roc-COR GTPase domain, a kinase domain and a C-terminal WD40 domain (Fig.1.1).

The N-terminal region of LRRK2 is predicted to contain armadillo repeats, a repetitive amino acid sequence of about 40 residues, often present in tandem copies, important for the transduction of signals. The ANK domain, a 33-residue motif folded to form a solenoid structure is likely to be involved in protein-protein interactions. Following, the LRR is a conserved protein-protein interaction domain composed of 13 LRR regions each containing 20-30 repeating amino acid motifs rich in the hydrophobic amino acid leucine. Proteins containing LRRs participate in multiple cellular and sub-cellular processes including membrane vesicle trafficking, apoptosis and cell polarisation (Kobe and Deisenhofer 1995). The Roc-COR bi-domain forms the catalytic core together with the kinase domain. This domain shares similarity with Rab GTPases, implicated in vesicular trafficking and transport. It presents a dimeric fold structure connected with loops. Each loop contains $Mg^{2+}$ and guanine nucleotide binding regions allowing GTP hydrolysis (Gilsbach and Kortholt 2014). The kinase domain consists of a canonical, N-terminal loop connected with the C-terminal loop by the activation loop, a hinge-region binding $Mg^{2+}$-ATP and the substrate. This domain resembles receptor interacting protein kinases (RIPKs), sensors of cellular stress and activators of Mitogen-activated protein kinases (MAPK) (Zhang et al. 2010). Finally, the WD40 domain is involved in protein-protein and protein-lipid interactions. LRRK2 contains seven WD40 repeats together forming a propeller-like structure. In addition to its two catalytic activities, the presence of several protein-protein interaction domains suggests a scaffolding role (Fig.1.1).

LRRK2 dimerisation has been demonstrated by co-immunoprecipitation experiments (Greggio et al. 2008). Self-interaction seems to involve the Roc-COR and/or WD40 domains (Greggio et al. 2008), suggesting LRRK2 autoregulation. Several studies reported that kinase activity is increased in the dimeric form compared to the monomeric (Greggio et al. 2008; Sen et al. 2009). Concerning the catalytic activity, it has been shown that the kinase and the GTPase activity are interdependent, although the underlying mechanism is still unresolved (Greggio et al. 2009). The kinase activity might regulate LRRK2 overall function, by phosphorylating the GTPase domain (Gloeckner et al. 2006; Ito et al. 2007). LRRK2 kinase activity is of particular interest since kinases are generally attractive targets for small molecule therapies and kinase inhibitors have been promising in clinical studies (AlDakheel et al. 2014). Pharmacological inhibition of LRRK2 has been shown to be protective in a human neuroblastoma cell line (Liu et al. 2011) and in both *in vitro* and in PD animal models (Daher et al. 2015; Lee et al. 2010; Yao et al. 2013).

### 1.2.4 The mammalian paralogues LRRK2 and LRRK1

In mammals LRRK2 has a homologue, LRRK1, not linked to PD (Langston et al. 2016; Reyniers et al. 2014; Taylor et al. 2007). LRRK2 and LRRK1 are both large multidomain proteins sharing similar structure, with a kinase and a GTPase domain that equally binds GTP (Civiero et al. 2012). LRRK1, with 1981 amino acids, has a shorter N-terminal domain and contains different repeats in the C-terminal region (Civiero et al. 2012; Korr et al. 2006).

At a cellular level, LRRK1 and LRRK2 are both cytoplasmic proteins, widely expressed across different brain regions although LRRK2 mRNA levels in brain are more elevated compared to LRRK1 (Biskup et al. 2007). Radioactive *in situ*

hybridisation studies show ubiquitous and continuously increasing expression of both genes from embryonic stages to birth (Giesert et al. 2013). In postnatal brain, LRRK2 expression seems high in the striatum, particularly in dopaminergic neuronal populations, whereas LRRK1 mRNA seems less strongly expressed in this region (Giesert et al. 2013). LRRK2 and LRRK1 can interact when coexpressed in HEK293 cells forming heterodimers which can modulate LRRK2 enzymatic activity or binding properties (Dachsel et al. 2010). Thus, due to their similar structure and localisation it is reasonable to ask whether LRRK2 and LRRK1 have analogue functions or interaction partners (Reyniers et al. 2014).

It has been hypothesised that LRRK1 plays a role in LRRK2 signalling pathways and therefore might modify PD risk. Although LRRK1 variants have been identified (Dachsel et al. 2010), the link between LRRK1 and PD pathogenesis has yet to be confirmed. Introduction of equivalent LRRK2 pathogenic mutations in LRRK1 do not display the same cytotoxic effects (Greggio et al. 2007). At basal levels LRRK1 seems to display a weaker kinase activity compared to its paralogue LRRK2 (Korr et al. 2006), which also shows stronger autophosphorylation activity (Greggio et al. 2009). Binding with some specific interactors is mediated by different phosphosites. LRRK1 and LRRK2 display distinct sites of phosphorylation at basal level and specific subsets of interaction partners (Reyniers et al. 2014). In particular LRRK2 binds 14-3-3 protein via two phospho-residues not observed in LRRK1 (Reyniers et al. 2014). LRRK1 specifically interacts with the adaptor protein Grb2, mediating the formation of a complex with a tyrosine kinase involved in leukaemia (Titz et al. 2010). In addition, LRRK1, and not LRRK2, seems to bind and regulate the endosomal trafficking of the epidermal growth factor receptor (EGFR) (Hanafusa et al. 2011; Reyniers et al. 2014). Severe osteopetrosis, a dysfunction of bone resorption, was observed in LRRK1 knockout mice but not in

LRRK2 knockout models suggesting a role for LRRK1 in bone mass homoeostasis (Xing et al. 2013). The authors suggest that the specificity of LRRK1 repeats in the N-terminal domain, different from LRRK2 unique repeats, might mediate the binding with different interactors including regulators of bone resorption (Xing et al. 2013).

Unfortunately, the tools to study LRRK1 are still limited. Antibodies and pharmacological inhibitors are not as reliable as the ones optimised for LRRK2. However, given the close homology of these two proteins, future characterisations of overlapping pathways would give important insights into LRRK2 physiological function.

## 1.3 LRRK2 role in vesicular trafficking

### 1.3.1 Overview

In the cell secretory pathway, vesicles bud and selectively concentrate their protein cargo from a *donor* compartment, a process mediated by protein coats (Bonifacino and Glick 2004; Braulke and Bonifacino 2009; Jahn and Scheller 2006; Orci et al. 1986; Pearse 1976). Once formed, vesicles are shuttled to their target *acceptor* compartment into which the cargo is released (Fig. 1.2). This process requires fusion between membranes of the two compartments, a process mediated by SNARE protein complexes (Balderhaar et al. 2013; Bernard and Klionsky 2015; Bonifacino and Glick 2004; Seaman et al. 1997).

Given its complex structural organisation, it is not surprising that LRRK2 displays multiple functions and has been related to different steps of the secretory pathway. LRRK2 is a cytoplasmic protein that can be found associated with membranous structures such as lipid rafts, synaptic vesicles, the Golgi apparatus and the endoplasmic reticulum (Beilina et al. 2014; Biskup et al. 2006; Chia et al. 2014; Gloeckner et al. 2006). Its membrane association suggests a role in vesicular trafficking or membrane turnover. LRRK2 kinase activity, moreover, appears to be increased at the membrane, when recruited after extracellular stimuli (Berwick and Harvey 2012).

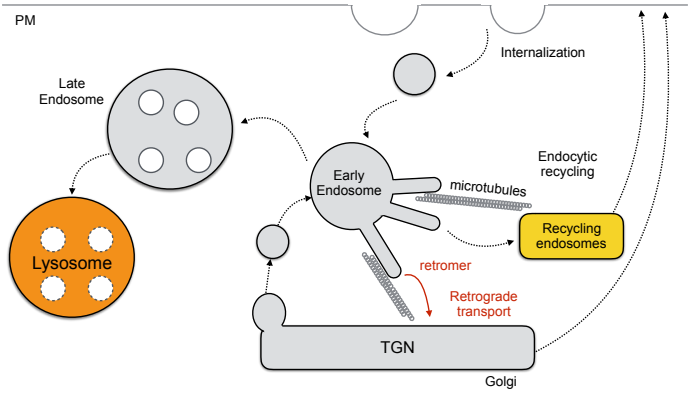


Figure 1.2: **Schematic representation of the endo-lysosomal pathway.** Early endosomes receive their cargos from the trans-Golgi network (TGN) or from the plasma membrane. Maturation of early endosomes involves pH acidification which causes release of the lysosomal hydrolase precursors. Retrograde transport allows recycling of cargo to the TGN or to the plasma membrane (PM), via the retromer complex tubules budding along microtubules. Figure adapted from Gershlick et al. 2016.

### 1.3.2 LRRK2 role in protein synthesis

Protein synthesis is a finely regulated process that involves myriads of factors and signalling complexes in order to maintain the correct levels of expression of a certain protein (Jackson et al. 2010). There are three major steps in protein synthesis: initiation, elongation and termination (Gebauer and Hentze 2004; Jackson et al. 2010). In eukaryotic cells, the initiation step is assisted by the eIF-4 initiation factors and the ribosomal subunits, which sequentially associate to form

a functional ribosome scanning the mRNA (Gebauer and Hentze 2004; Jackson et al. 2010). During the elongation phase, amino acids are added to the newly synthesized protein and peptide bonds are formed. In the termination step, the stop codon of the mRNA and the release factors cause ribosomes to destabilise and determines the end of the translation (Dever and Green 2012).

Abnormal regulation of protein synthesis has been linked to several pathologies including neurodegenerative diseases (Dasuri et al. 2013; Halliday et al. 2015; Liu-Yesucevitz et al. 2011). In the context of PD, overexpression of α-synuclein is one established example, as triplication of SNCA gene and corresponding protein levels cause PD (Singleton et al. 2003). LRRK2 has been recently found to interact with ribosomal proteins and translation initiation factors (Dorval and Hébert 2012; Imai et al. 2008; Martin et al. 2014), suggesting a role for LRRK2 in protein synthesis, although the functional mechanism leading to neurodegeneration still remains elusive (Dorval and Hébert 2012).

Previous studies show a link between LRRK2 and transcription (Häbig et al. 2008; Schulz et al. 2011). Using microarrays, significant changes in 187 mRNA transcripts in LRRK2-knockdown cells were reported (Häbig et al. 2008). Another microarray analysis of fibroblasts carrying the LRRK2 G2019S mutation with normal controls, did not report significant differences in basal gene expression (Devine et al. 2011). Additional studies, using LRRK2 haploinsufficient and control ES cell-derived neurons, report significant changes in 23 mRNA transcripts (Schulz et al. 2011). Among these transcripts, 4E-BP1 and the membrane-cytoskeletal proteins ezrin, radixin,and moesin (ERM) were confirmed as downregulated in LRRK2 haploinsufficient neurons (Schulz et al. 2011).

LRRK2 has been implicated in protein translation, specifically to the 4E-BP1 signalling pathway (Dorval and Hébert 2012; Imai et al. 2008). 4E-BP1 is an important regulator of protein synthesis (Gingras et al. 1998; Musa et al. 2016). In mammalian cells, 4E-BP1 activation is downstream of mTORC1, a key lysosomal sensing complex (Ramírez-Valle et al. 2008). When active, 4E-BP1 binds eIF4E, reducing overall protein translation. By contrast, phosphorylated 4E-BP1 is no longer able to bind eIF4E resulting in a general increase in protein translation (Musa et al. 2016). LRRK2 seems involved in the TOR/4E-BP1 pathway, promoting protein translation by binding and phosphorylating 4E-BP1 (Imai et al. 2008). A LRRK2 hyperactive kinase mutant further increases 4E-BP1 phosphorylation directly altering protein translation (Imai et al. 2008). However, evidence that LRRK2 phosphorylation directly alters protein synthesis is still lacking and two recent studies contradict these results showing that 4E-BP1 might not be a valid LRRK2 substrate (Kumar et al. 2010; Trancikova et al. 2012). In addition, LRRK2 transient knockdown has been reported to decrease 4E-BP1 protein levels (Pons et al. 2012), which is in turn associated with augmented cell proliferation. In post-mitotic neurons, upregulation of cell cycle may lead to defects in cell division leading to apoptosis, supporting the notion that abnormal protein translation can lead to neurodegeneration.

LRRK2 has also been reported to phosphorylate the ribosomal protein s15 in *Drosophila* and neurons derived from PD patients (Martin et al. 2014). The authors claim that abnormal phosphorylation of s15 by the mutant G2019S LRRK2 results in increased mRNA translation. Supporting this observation, phosphodeficient ribosomal protein s15 can rescue neuritic defects in G2019S neurons from PD patients (Martin et al. 2014).

Together these findings suggest that LRRK2 might be involved in regulation of the initial steps of protein translation by specifically interacting with key components of the protein synthesis machinery. However, the molecular mechanism is still controversial and future research is needed to understand whether and how deregulated protein translation leads to LRRK2-related neurodegeneration.

### 1.3.3 From ER to Golgi

Before entering the secretory pathway, proteins are transported from ER specialised regions called ER exit sites (ERES) to the Golgi within transport vesicles (Zanetti et al. 2012). These vesicles are coated with the Coatmer Protein II Coated (COPII) (Barlowe et al. 2017). Only correctly folded proteins are concentrated inside the lumen of the budding vesicle as they leave the ER, a process dependent on a small GTP binding protein SarI (Lee et al. 2005b). SarI associates to the membrane of the newly formed vesicle and helps the assembly of a complex that induces membrane curvature (Zanetti et al. 2012). Once the protein-vesicle complex is stabilised, SarI provides the energy to dissociate the vesicle via GTP hydrolysis (Zanetti et al. 2012).

Interestingly, a putative link between LRRK2 and anterograde ER-Golgi transport has been suggested (Cho et al. 2014). One essential element for ER to Golgi transport is Sec16A, a membrane protein involved in the formation of the ERES (Cho et al. 2014). LRRK2 interacts and colocalises with Sec16A and loss of LRRK2 seems to cause Sec16A dispersion and to consequently alter ER export (Cho et al. 2014). In particular, in LRRK2 knockout fibroblasts, COPII positive vesicles are larger compared to controls, suggesting a role for LRRK2 in stabilising COPII vesicle structure. However, no difference in levels of Sec16A between LRRK2 knockout and controls mouse brain extracts was observed (Cho et al. 2014).

Collectively, these data indicate that LRRK2 might play a role in anterograde trafficking and that loss of LRRK2 might impair cargo transport by altering the formation of ERES.

In addition, ERES are linked to dynamic microtubules via microtubule plus end binding proteins (Cho et al. 2014). Since LRRK2 has been shown to preferentially bind dynamic populations of microtubules (Law et al. 2014), it is reasonable to hypothesize that LRRK2 may act as a microtubule plus end binding protein, linking ER exit sites and Sec16A to microtubules. Experiments using microtubule-targeting agents suggest that LRRK2 stabilises the dynamic ends of microtubules helping the ER exit sites to cluster (Cho et al. 2014).

### 1.3.4 Arrival at the Golgi

From the ER, COPII-coated transport vesicles are delivered to the Golgi, a branching station of the secretory pathway (Fokin et al. 2014; Maday and Holzbaur 2014). From the Golgi, proteins can follow three distinct paths: to the ER via COPI vesicles, to the endo-lysosomal route, or to the plasma membrane (Bonifacino and Glick 2004). At the Golgi, newly synthesized lysosomal hydrolases are first modified by addition of mannose-6-phosphate residues and then subsequently conjugated to lysosomal sorting receptors (Braulke and Bonifacino 2009). The first characterised sorting receptor is the mammalian mannose-6-phosphate receptor (M6PR) (Braulke and Bonifacino 2009; Campbell et al. 1983; Le Borgne and Hoflack 1997; Young et al. 1991) (Fig. 1.3). The M6PR recognises and covalently binds M6P residues on lysosomal proteins in the late Golgi compartments mediating their segregation in the endosomal pathway (Braulke and Bonifacino 2009) (Fig. 1.3).

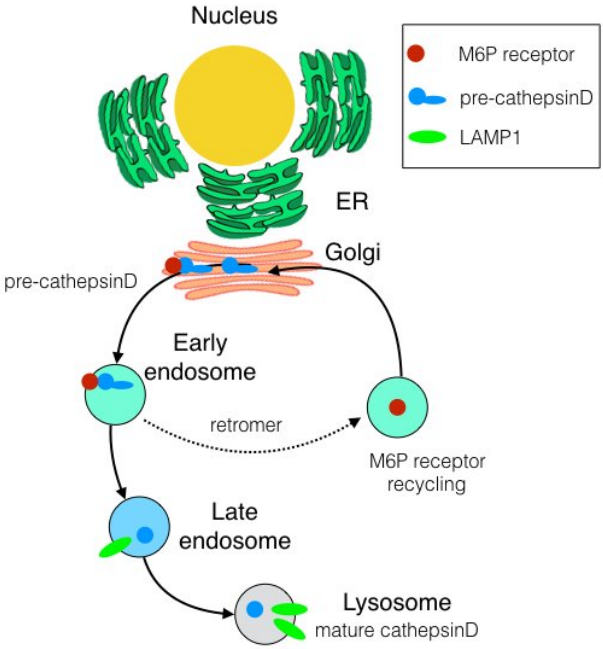


Figure 1.3: **Mannose-6-phosphate receptor recycling.** Schematic representation of mannose-6-phosphate (M6P) receptor cycle. M6P-receptors bind precursors of lysosomal hydrolases such as cathepsin D in the Golgi and deliver them to the endosomal compartment. Acidification of the endosomal lumen cause enzyme-receptor dissociation allowing maturation of cathepsin D and recycling of M6P receptors back to the Golgi.

One common example of a M6PR cargo is cathepsin D (Young et al. 1991), a protein encoded by the gene CTSD located on the p15.5 region of chromosome 11 (Minarowska et al. 2008; Redecker et al. 1991) (Fig. 1.3). Cathepsin D is a

ubquitously expressed lysosomal aspartyl protease composed of heavy and light chains linked by disulphide bonds and encoded by the same precursor (Metcalf and Fusek 1993). Lysosomal proteases such as cathepsin D are synthesized in the ER as inactive precursors, then recognised and transported via the trans-Golgi network (TGN) and sorting endosomes to the lysosomes where they undergo maturation by pH-dependent proteolytic cleavage (Sevlever et al. 2008) (Fig. 1.3).

### 1.3.5 Evidence for LRRK2 at the Golgi

Evidence for LRRK2 at the Golgi comes from *in vitro* and *in vivo* studies which support a functional and physical interaction between LRRK2 and RAB7L1 (or Rab29) (Beilina et al. 2014; MacLeod et al. 2013). RAB7L1 encodes for a small GTPase, involved in the transport of selective cargo between the lysosomes and the Golgi apparatus (Wang et al. 2014) Results from an unbiased screen point out RAB7L1 and the clathrin-uncoating protein cyclin G (GAK) as direct LRRK2 interactors (Beilina et al. 2014). Rab7L1 together with GAK and the co-chaperone BAG5, recruits LRRK2 to the TGN. In particular, RAB7L1, GAK and BAG5 form a complex that promotes the clearance and remodelling of Golgi-derived endosomes via the lysosomal autophagy pathway. Altered turnover of these vesicles may affect the autophagy machinery over time (Manzoni et al. 2013; Tong et al. 2010). In addition, overexpression of RAB7L1 rescued LRRK2-induced neurite shortening in rat primary cortical neurons, a process that involves autophagy (MacLeod et al. 2013). LRRK2 mutants seem to further promote this phenomena, suggesting that LRRK2 enzymatic activities might be involved and that some pathogenic mutations are likely to cause a toxic gain-of-function (Beilina et al. 2014; MacLeod et al. 2013; Roosen and Cookson 2016).

Together this evidence suggests that LRRK2 and RAB7L1 are cooperating in order to regulate vesicular trafficking and this could be related to the known role of LRRK2 in autophagy. It is important to point out that GAK and Rab7L1 are nominated as risk factors for sporadic PD by GWAS (Nalls et al. 2014; Simón-Sánchez et al. 2009). Identification and validation of these LRRK2 interactors from unbiased screens point towards a common mechanism that might be shared between sporadic and inherited PD.

### 1.3.6 Clathrin-mediated vesicle sorting

At the TGN, lysosomal precursors conjugated to M6PR are concentrated in the lumen of a newly budding endosome (Braulke and Bonifacino 2009; Hu et al. 2015; Young et al. 1991). The sorting signals in the receptor cytosolic tails determine the packaging and the recruitment of a number of adaptors and coat proteins that mediate vesicle budding and scission from the TGN (Braulke and Bonifacino 2009). A variety of adaptor proteins mediate the binding of clathrin which coat vesicles budding either from the TGN, for lysosomal sorting, or from the plasma membrane for endocytosis (Boehm and Bonifacino 2001; Lee et al. 2005a; Robinson and Bonifacino 2001). There are three mammalian monomeric GGA protein adaptors (GGA1, GGA2, GGA3) and five heterotetrameric adaptor protein (AP) complexes (AP1-5) which determine endosome's fate in the secretory system (Boehm and Bonifacino 2001; Braulke and Bonifacino 2009; Robinson and Bonifacino 2001).

Receptor cytosolic sorting signals are recognised by GGA protein adaptors, localised at the TGN (Braulke and Bonifacino 2009). In addition M6PR tails contain a binding motif for the AP1 complex (Lewin and Mellman 1998). Once the cargo-receptor-adaptin complex is assembled on the membrane of the budding vesicle, clathrin subsequently binds the adaptor with low affinity and high avidity,

or as alternatively described, *matricity* (Schmid et al. 2006). The clathrin-coat is composed of a combination of clathrin heavy and light chains assembled into a *triskelion* structure that aggregates and deforms membranes (Zimmerberg and Kozlov 2006). GTP-hydrolysis, catalysed by dynamin, is then required to detach the vesicle (Mettlen et al. 2009). Finally, clathrin-coated vesicles (CCVs) are uncoated by a process involving co-chaperones such as auxilin or GAK, which associate to clathrin and mediate Hsc70 binding (Lee et al. 2005a).

### 1.3.7 LRRK2 and endosome biogenesis

Mutations in genes associated with the endocytic pathway have been linked to PD (Kumaran and Cookson 2015). In particular, mutations in the genes encoding the clathrin adaptor protein auxilin 1 and GAK have been identified in cases of both familial and sporadic PD (Beilina et al. 2014; Edvardson et al. 2012; Nalls et al. 2011). In a recent study, LRRK2 has been reported to localise and physically interact with clathrin light chains (Schreij et al. 2015). According to this study, LRRK2-clathrin interaction regulates the activity of Rac1, a small GTPase involved in cytoskeletal reorganisation. Additional protein array studies identified the clathrin uncoating chaperone cofactor GAK as a direct LRRK2 interactor (Beilina et al. 2014), as previously discussed. Although LRRK2 interaction with clathrin still needs to be independently validated, these results together suggest that LRRK2 might act as a scaffold regulating endosomal biogenesis and sorting.

### 1.3.8 From early endosome maturation to lysosomes

The endosomal pathway is a highly dynamic tubulo-vesicular network where early, late and recycling endosomes are part of a *continuum* of vesicles moving along microtubules (Hu et al. 2015). In particular early endosomes follow a process

of maturation by increasing vacuolar-ATPase mediated pH acidification of their lumen (Braulke and Bonifacino 2009). Acidification of the endosomal lumen causes release of the lysosomal hydrolase precursors which are delivered to late endosomes and to lysosomes where they exert their functions such as protein digestion (Hu et al. 2015). Crucial players in trafficking of endosomes are the members of the Rab family small GTPases with conformational change between GTP-bound active state to GDP-bound inactive state acting as molecular switch that regulates their membrane association (Hu et al. 2015; Villarroel-Campos et al. 2014). Within the maturation progress, together with the increase in acidification, endosomes undergo a series of changes including the increase in number of intraluminal vesicles and modifications in their subset of Rab proteins (Hu et al. 2015). One example is the Rab5 to Rab7 conversion from early to late endosomes (Deinhardt et al. 2006; Rojas et al. 2008). Defects in endosomal trafficking and distribution play an important role in neurological disorders such as AD and PD (Hu et al. 2015).

### 1.3.9 LRRK2 functional interaction with retromer

The retromer complex is a pentameric complex localised on tubules that extend from the endosomal membrane (Attar and Cullen 2010; Lucas et al. 2016). This complex has the important function of recycling sorting receptors, once dissociated from their cargos during endosomal lumen maturation, from endosomes to the Golgi. The retromer structure can be divided into two complexes: the cargo recognition heterotrimer, composed of the subunits Vps26, Vps29 and Vps35, and the sorting nexin dimer which displays membrane association properties (Attar and Cullen 2010; Farias et al. 2014; Lucas et al. 2016). One example of a receptor recycled via retromer is the M6PR that, once dissociated from its enzyme cargo,

is retrieved back to the TGN, allowing constant replenishment of the receptor pool (Farias et al. 2014).

Disruption of retromer function has been linked to a number of neurodegenerative conditions such as AD and PD (Fjorback et al. 2012; McGough et al. 2014; Muhammad et al. 2008; Vilariño-Güell et al. 2011; Zimprich et al. 2011). The gene encoding for the Vacuolar Sorting Protein 35 (Vps35) has been linked to the LRRK2/Rab7L1 pathway (MacLeod et al. 2013). Specifically, Golgi defects caused by LRRK2 mutants are rescued by *VPS35* overexpression (MacLeod et al. 2013). In addition, knockdown of *VPS35* or expression of its mutant D620N result to a reduction in neurite length, a phenotype that matches the G2019S LRRK2 mutant effect (MacLeod et al. 2013). Another study showed that Vps35 rescues locomotor defects in *Drosophila* overexpressing the LRRK2 I2020T mutation, providing the evidence that LRRK2 and Vps35 are in the same pathway (Linhart et al. 2014).

### 1.3.10 LRRK2 functional interaction with Rab GTPases

Studies of LRRK2 interactors have been helpful in determining LRRK2 functions in cells. LRRK2 has been found to interact with Rab5b (Shin et al. 2008), a small GTPase that has a role in the transport from the plasma membrane to the early endosome and in synaptic vesicle recycling (Woodman 2000). LRRK2 may therefore be involved in synaptic function modulation. Consistent with this hypothesis, LRRK2 mutations (G2019S and R1441C) have been implicated in the hindrance of neurotransmitter release (Shin et al. 2008; Tong et al. 2012). In addition, LRRK2 studies in rat and human brain tissue (Biskup et al. 2006) suggest a potential role in biogenesis and/or modulation of intracellular vesicles in mammals.

A role for LRRK2 in vesicular pathways is further supported by a recent phosphoproteomic study revealing that LRRK2 phosphorylates a subset of Rab GTPases, key regulators in membrane trafficking (Rivero-Ríos et al. 2015; Steger et al. 2016). This study used a two-screen approach with either fibroblasts from LRRK2-G2019S kinase hyperactive mice or fibroblast from kinase inhibitor resistant LRRK2-A2016T mice, both treated with different LRRK2 kinase inhibitors. The authors found that LRRK2 directly phosphorylates Rab10 *in vivo* and *in vitro* (Roosen and Cookson 2016; Steger et al. 2016). Experiments conduced in HEK293FT cells further identified Rab8 and Rab12 as direct LRRK2 physiological substrates (Steger et al. 2016). Other small GTPases, Rab32 and Rab38, have been shown to directly interact with LRRK2. The authors propose a role for Rab32 in late endosomal trafficking of LRRK2, specifically, shuttling LRRK2 to lysosomes (Waschbüsch et al. 2014).

LRRK2 has been reported to regulate membrane trafficking via functional interaction with Rab7 (Gómez-Suaga et al. 2014). Rab7 is a small GTPase involved in multiple steps of the endo-lysosomal pathway such as endosome maturation, transport and lysosome positioning (Fujiwara et al. 2016; Gómez-Suaga et al. 2014; Vanlandingham and Ceresa 2009). Interestingly, expression of mutant LRRK2 decreases Rab7 activity and causes a delay in trafficking from early to late endosomes, as observed by the delay in Rab5 to Rab7 switch and the abnormal elongation of endosomal tubules (Gómez-Suaga et al. 2014). Together this evidence provides a possible mechanism for LRRK2 in late steps of the membrane trafficking pathway dependent on Rab7 activity.

### 1.3.11 LRRK2 and mitochondria

Due to their unique morphology, neuronal cells are highly dependent on mitochondrial respiration in order to perform their functions. Mitochondria are involved in a variety of intracellular functions such as producing ATP necessary for cell survival, regulating calcium homeostasis and oxidative stress. Numerous evidence point out an association between mitochondrial dysfunction and PD (Arduíno et al. 2012; Kazlauskaite and Muqit 2015; Matenia et al. 2012; Ryan et al. 2015; Wang et al. 2012b; Winklhofer and Haass 2010). Studies from the 1980s lead to the discovery that inhibition of the mitochondrial complex I caused by MPP+, a metabolite of a neurotoxic compound called MPTP, resulted in nigrostriatal degeneration with parkinsonism (Langston et al. 1983).

Further confirming the importance of mitochondria in PD is the evidence that several PD genes are associated with mitochondrial integrity and oxidative stress response (Winklhofer and Haass 2010). For example, mutations in *PINK1*, *PARK2*, and *DJ1* cause parkinsonisms and have been reported to cause different types of mitochondrial defects (Kazlauskaite and Muqit 2015; Valente et al. 2004; Wang et al. 2012b). Loss of the mitochondrial kinase PINK1 has been assiociated with decrease of mitochondrial membrane potential, impairments in calcium homeostasis and increase in ROS production (Valente et al. 2004). *PARK2* encodes for the E3 ubiquitin-ligase parkin that targets substrates to the proteasome and promotes autophagy of damaged mitochondria or mitophagy, helping to clear mitochondria with mutations in their mtDNA (Kazlauskaite and Muqit 2015). Studies from mutant flies lead to the discovery of a functional pathway where PINK1 is upstream of parkin in the control of mitochondrial function (Cookson 2012; Kazlauskaite and Muqit 2015). In particular, mutations in PINK1 impair parkin

recruitment to mitochondrial membrane resulting in misfunctional mitochondria quality control and accumulation of damaged mitochondria. Affecting parallel pathways, mutations in *DJ1*, a protein with anti-oxidant role, have been correlated with mitochondrial fragmentation and increased oxidative stress (Cookson 2012; Wang et al. 2012b).

Evidence of LRRK2 association with mitochondria has been of particular interest (Yue et al. 2015). LRRK2 abnormal kinase activity seems to be involved in mitochondrial fragmentation and transport of damaged organelles along microtubules via dynamin-like protein 1 (DLP1) (Wang et al. 2012a). Studies in *C.elegans*, moreover, point out a protective role for wild-type LRRK2, but not for its mutants, against rotenone and paraquat-induced mitochondrial toxicity (Saha et al. 2009).

Overall, impaired mitochondria quality control mechanisms have been functionally linked to PD and other neurodegenerative disorders. These defects can be caused by toxic compounds or by mutations in PD genes resulting in accumulation of swollen or damaged mitochondria which fail to undergo mitophagy.

### 1.3.12 LRRK2 as a signalling scaffold in multiple pathways

Several studies on LRRK2 interactors shed light on its possible role as a scaffolding protein in signalling pathways. Two examples are the MAPK and Wnt signalling pathways. In the MAPK pathway, LRRK2 was shown to interact with Jun N terminal kinase (JNK)/p38 signalling components and activate extracellular regulated kinase (ERK) 1 and 2 (Berwick and Harvey 2011). LRRK2 might form a scaffold along the microtubule tracks, recruiting other GTPases involved in

vesicular trafficking or helping the formation of signalling complexes that regulate cytoskeletal dynamics (Law et al. 2014).

Several studies point out a role for LRRK2 in regulation of neurite outgrowth (MacLeod et al. 2006). LRRK2 silencing in rat developing neurons resulted in longer neurites whereas mutations in LRRK2 caused neurite shortening and reduced complexity (MacLeod et al. 2006). This effect might involve LRRK2 interaction with microtubules (Law et al. 2014) or with components of the Wnt signalling pathway directly involved in cytoskeletal modulation (Berwick and Harvey 2011).

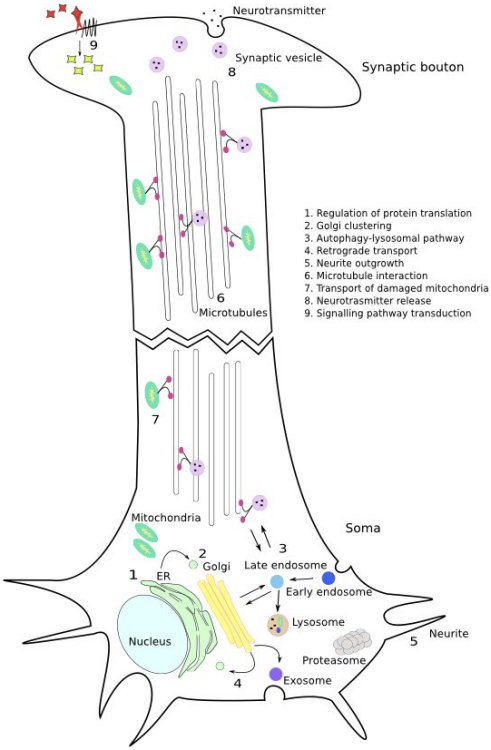


Figure 1.4: **Schematic representation of a neuronal cell divided in synaptic bouton and soma.** Delineation of LRRK2 subcellular functions linked to neurodegeneration. (1) Regulation of protein translation; (2) Golgi clustering; (3) LRRK2 mediated endocytosis and autophagy dysfunctions; (4) retrograde transport; (5) neurite outgrowth and (6) microtubule interaction; (7) transport of damaged mitochondria; (8) neurotransmitter release and (9) regulation of signalling cascades (figure adapted from: (Kumaran and Cookson 2015))

## 1.4 LRRK2 role in protein degradation pathways

### 1.4.1 Overview

A common pathological hallmark shared by age-related neurodegenerative disorders such as PD is the abnormal accumulation of undigested proteins in specific neuronal populations (Nixon 2006). The cause of this accumulation remains controversial. Protein aggregation can be due to increased protein synthesis or stability, but can also derive from dysfunctional protein clearance. Within a cell, protein quality control is constantly regulated by two major protein degradation pathways: the ubiquitin-proteasome system (UPS) and the autophagy pathway. Dysfunctions of either of these pathways have been associated with formation of aggregates of misfolded proteins. Interestingly, experimental evidence linking LRRK2 with protein degradation pathways is accumulating. In this section, the role of LRRK2 in autophagy and in proteasomal degradation will be discussed.

### 1.4.2 The autophagy machinery

Autophagy is a highly regulated physiological process that cells employ in order to monitor the quality of the cytoplasm (Roosen and Cookson 2016; Rubinsztein et al. 2012). A basal level of autophagy is maintained to remove organelles such as damaged mitochondria and protein aggregates. Autophagy can be stimulated in stress conditions such as nutrient deprivation or cell differentiation to remodel cytoplasmic content (Rubinsztein et al. 2012). Defects in the autophagy machinery have been reported in a number of pathological conditions such a neurodegenerative disorders, lysosomal storage dysfunctions and cancer (Rubinsztein 2006; Rubinsztein et al. 2012).

There are three currently identifiable types of autophagy: microautophagy, macroautophagy and chaperone-mediated autophagy (CMA). Microautophagy involves the direct uptake of portions of the cytoplasm through lysosomal membrane invagination (Rubinsztein 2006). The molecular mechanism, however, is still elusive in mammalian cells (Rubinsztein 2006). CMA is characterised by selective lysosomal degradation of short-lived cytosolic substrates containing a protein motif recognised by the HSC70 chaperone complex (Cuervo and Wong 2014; Cuervo et al. 2004). This complex moves the substrate proximal to the lysosomal membrane where binding with the cytosolic tail of the lysosomal receptor Lamp2a allows translocation of the complex into the lumen for degradation. One example of a substrate degraded via CMA are α-synuclein monomers (Cuervo et al. 2004), leading to the hypothesis of saturation of CMA in PD cases where α-synuclein aggregates and therefore is no longer degraded via CMA (Li et al. 2011).

Long-lived proteins and organelles are degraded via macroautophagy (also referred to as autophagy) (Nixon 2006). Autophagy is characterised by the phagocytosis of substrates and organelles into a newly formed structure called autophagosome which fuses with lysosomes. This process is regulated by the expression of autophagy-related genes (Atg), which products are sequentially recruited throughout the steps of phagophore formation or nucleation, membrane expansion, maturation and degradation (Beilina and Cookson 2016; Fougeray and Pallet 2014; Maday and Holzbaur 2014; Mizushima et al. 2010; Nixon 2013). In the presence of nutrients and trophic signals, mammalian Target of rapamycin (mTOR) is active and phosphorylates transcription factor EB (TFEB) which is retained in the cytoplasm and autophagy is inhibited (Ramírez-Valle et al. 2008; Rubinsztein et al. 2015). Starvation and environmental stress signals block

mTOR allowing TFEB nuclear translocation and transcription of autophagy genes. Activation of mTOR stimulates the complex Ulk1, which initiates the formation of the phagophore together with Vps34 and Beclin1 (Fougeray and Pallet 2014; Rubinsztein et al. 2012). Once the phagophore is formed, elongation is catalysed by a series of Atg proteins recruited on the phagophore membrane. One key step is the cleavage and lipidation of the cytosolic protein microtubule-associated protein 1 light chain 3 (LC3) I to form LC3II on the newly synthesised autophagosome membrane. The relative increase in LC3II is a common marker for measuring autophagy levels *in vivo* and *in vitro*. LC3 together with the p62 adaptors, another marker of autophagy, mediate cargo internalisation within the autophagosome. Once formed, the double-membrane autophagosome then fuses with the lysosome which contains hydrolytic enzymes responsible to cargo degradation.

A basal level of autophagy is constitutively maintained in cells in order to clear the cytoplasm from damaged organelles and protein aggregates. It is possible to monitor autophagy through measure of the initial step of autophagy such as autophagosome formation using LC3 or p62 levels as indicators (Fougeray and Pallet 2014; Mizushima et al. 2010). Interpreting autophagy, however, is not straightforward: increase in LC3II/LC3I ratio might be a result of accelerated autophagosomes generation, as well as reduced autophagosome clearance (Fougeray and Pallet 2014; Mizushima et al. 2010).

### 1.4.3 LRRK2 and autophagy

There is evidence of both increase and decrease of autophagy markers in LRRK2 knockout models *in vivo* depending on the age (Tong et al. 2012). Biphasic alterations in LC3II and p62 have been reported in kidneys from LRRK2-KO mice in independent cohorts (Tong et al. 2012). LC3II and p62 were reduced in 7

month-old LRRK2-KO kidneys and were instead increased at 20 months of age, suggesting a role for LRRK2 in the dynamic modulation of autophagy.

Upregulation of basal autophagy has been suggested upon LRRK2 knockdown (Alegre-Abarrategui et al. 2009). LRRK2 inhibition in combination with an inhibitor of lysosomal acidification, the last step of the autophagy pathway, results in higher autophagy rate, suggesting that loss of LRRK2 increases autophagosome formation rather than blocking autophagosome clearance (Manzoni et al. 2013). In addition, fibroblasts from patients carrying pathogenic mutations in LRRK2 enzymatic domains show altered turnover of membrane associated LC3 in response to starvation, supporting a pathogenic role of LRRK2 in autophagy (Manzoni et al. 2013).

### 1.4.4 The Ubiquitin-Proteasome System (UPS)

The UPS is a multi-step protein degradation system specialised in the degradation of short-lived and misfolded proteins (Cook and Petrucelli 2009; Goldberg 2003; Olanow and Mcnaught 2006). The proteasome is a cytosolic barrel containing several proteolytic enzymes in its core (Cook and Petrucelli 2009). Degradation via proteasome is generally a more rapid and restricted route compared to the less selective autophagy machinery (Giasson et al. 2003).

The first steps of this process involve a series of enzymes that link ubiquitin polypeptide chains to proteins (Cook and Petrucelli 2009; Giasson et al. 2003). The ubiquitin-activating enzyme (E1) binds to ubiquitin in an ATP-dependent process. Ubiquitin is then transferred to the ubiquitin-conjugation enzyme (E2) which forms a complex with the ubiquitin-protein ligase (E3). The E3 ubiquitin-ligase then links ubiquitin to the target protein (Giasson et al. 2003). The ubiquitin tag

marks the protein that will be digested by the proteasome complex. The selectivity of this system is ensured by a gate-mechanism which only allows ubiquitin-labelled proteins to undergo degradation (Giasson et al. 2003). In the final steps of the UPS, polyubiquitinated proteins are shuttled to the proteasome by chaperones (Olanow and Mcnaught 2006). Proteins are deubiquitinated and unfolded before translocation into the proteasome barrel (Olanow and Mcnaught 2006).

Proteasomal dysfunction has been reported in disease characterised by toxic protein accumulation, such AD and PD (Cook and Petrucelli 2009; Hong et al. 2014). Protein aggregates can inhibit proteasomal function and be redirected to the autophagy route (Webb et al. 2003). *In vitro* experiments suggests that α-synuclein aggregates are removed by both autophagy and proteasome (Webb et al. 2003), suggesting a link between the two degradation pathways.

### 1.4.5 LRRK2 and the proteasome degradation pathway

A role for LRRK2 in proteasomal degradation has been proposed (Lichtenberg et al. 2011). Overexpressing LRRK2 seems to impair proteasome function resulting in accumulation of proteins and of proteasome substrates independently of LRRK2 kinase activity (Lichtenberg et al. 2011). Conversely, accumulation of ubiquitinated proteins has been reported in LRRK2 knockout kidneys (Tong et al. 2010). This suggests that loss of LRRK2 could alter proteasomal degradation or transport of ubiquitinated proteins to the proteasome, although these findings will need to be confirmed by independent groups.

## 1.5 LRRK2 and microtubules

### 1.5.1 Microtubule structural overview

Microtubules are long, polarised cytoskeletal polymers composed of α/β-tubulin heterodimers (Fig.1.5). The alignment of α/β-heterodimers forms a protofilament and the lateral assembly of thirteen protofilaments generates a microtubule of generally 25nm diameter and highly variable length (Garnham and Roll-Mecak 2012). Microtubules cooperate with microtubule-associated proteins (MAPs) in order to provide a platform for intracellular transport or to form structural scaffolds for signalling complexes. Microtubules act as sensors of cellular conditions and form the cytoskeletal network together with actin to maintain cell architecture (Pellegrini et al. 2016).

Microtubules are fundamental in dynamic processes such as mitosis, as key elements in the formation of the mitotic spindle, and cell motility. To accomplish these functions, microtubules are constantly remodelled through a cyclic, stochastic addition and removal of GTP-tubulin heterodimers. Dynamic instability is the term used to describe the periodical and GTP-dependent alternation between shrinkage/catastrophe and growth/rescue occurring at their ends, observed both *in vitro* and *in vivo* (Gardner et al. 2013).

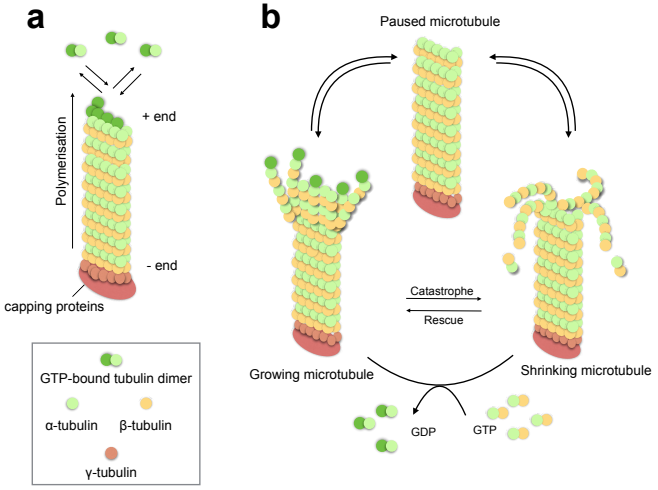


Figure 1.5: **Microtubule lattice composition and dynamic instability.** a) Assembly of α/β-tubulin heterodimers into a protofilament from the minus to the plus end. Capping proteins allow polymerisation of γ-tubulin that function as a template for the correct microtubule assembly. b) Cyclic exchange of GTP–tubulin defines microtubule dynamic instability. Microtubules stochastically alternate growing, paused and shrinking phases Image adapted from Conde and Cáceres 2009.

### 1.5.2 Post-translational acetylation of microtubules

Different post-translational modifications (PTMs) of tubulin regulate microtubule dynamics and function, helping the recruitment of specific protein complexes along the microtubule tracks. Notably, neuronal microtubules or motile structures such as cilia contain several microtubule subcellular populations modified for a specific function (Garnham and Roll-Mecak 2012). One of the earliest tubulin PTMs discovered is acetylation of α-tubulin (L'Hernault and Rosenbaum 1983).

Tubulin acetylation is a reversible modification and several deacetylases, such as histone deacetylase (HDAC) and sirtuins, have been identified (Garnham and Roll-Mecak 2012). Unlike the majority of tubulin PTMs that target the external surface of microtubules, acetylation occurs on the Lys40 predicted to be inside the luminal face of the protofilaments based on the electron crystal structure (Howes et al. 2014).

In mammalian cells, acetylation is mainly catalysed by the acetyltransferase MEC17/α-TAT or by the N-α-acetyltransferase A (NatA) (Dörfel and Lyon 2015). How the acetylation enzyme accesses its site and how this luminal modification influences microtubule function is still unclear (Hammond et al. 2008). One proposed model is that acetylation occurs from the microtubule ends, with the enzyme diffusing through the lumen (Akella et al. 2010; Ly et al. 2016). However, the presence of acetylated tubulin segments distal from *in vivo* microtubule ends might indicate an alternative lateral access of the acetyltransferase. Diaz and collaborators proposed a model where the acetyltransferase accesses its site via transient holes in the microtubule lattice (Díaz et al. 1998, 2003; Shida et al. 2010). This hypothesis was tested by another group which used mathematical modelling to prove that the uniform acetylation pattern observed in *in vitro* microtubules is due to defects along their shafts, rather then transient holes, therefore not recapitulating the properties of cellular microtubules (Ly et al. 2016). They suggest instead that α-TAT1 regulates the spreading of acetylation along the tubules from open microtubule ends and that multiple contacts between microtubules and α-TAT1-rich structures, would increase the chance of microtubule acetylation (Ly et al. 2016).

Acetylation stabilises microtubules and plays a role in neuron function by enhancing polarised protein trafficking as well as influencing binding and motility of motor

proteins (Falconer et al. 1989; Hubbert et al. 2002; Reed et al. 2006). A dramatic increase in α-tubulin acetylation occurs during axogenesis, implying a role of acetylation in stable axonal growth and neuronal plasticity (Falconer et al. 1989). Perhaps not surprisingly, several neurodegenerative diseases have been related to defects in tubulin acetylation (Perdiz et al. 2011). Intriguingly, promoting acetylation by inhibition of sirtuins in PD models decreased α-synuclein-mediated neurotoxicity (Outeiro et al. 2007). Increased acetylation also prevented axonal degeneration in a Wallerian degeneration mouse model (Suzuki and Koike 2007).

### 1.5.3 Microtubule-mediated intracellular transport

Microtubule-mediated transport is a highly dynamic intracellular process, essential for trafficking and recycle of cellular components. In particular, because of neuronal morphology comprising long axons and dendrites, these cells strictly rely on active transport, dependent on finely regulated microtubule organisation (Fig.1.6). Alteration of microtubule regulation is an early event associated with dopaminergic neuron degeneration preceding axonal transport impairment (Cartelli et al. 2013).

According to cargo speed and directionality, axonal transport is classified respectively into slow and fast, anterograde and retrograde (Maday et al. 2014). The speed of a certain cargo along microtubules depends on the interaction with molecular motors such as kinesins and dyneins (Jaarsma and Hoogenraad 2015; Okada et al. 1995), which dynamically associate and dissociate from cargos (Gibbs et al. 2015). These molecular motors travel along microtubules in a step-like process, coupled to constant ATP hydrolysis (Gibbs et al. 2015). Anterograde transport ensures directional movement of vesicles budding from the Golgi to the periphery of the cell and is mediated by kinesins. Retrograde transport is

responsible for the correct recycling of cargos and signals from the periphery back to the Golgi and is mediated by dyneins (Pellegrini et al. 2016) (Fig.1.6, a).

Recycling of signalling endosomes and autophagosomes is necessary in order to ensure constant replenishment and correct distribution of receptors and signalling components. Defects in microtubule structure or dynamics can affect microtubule transport resulting in impaired cargo delivery or fusion with other compartments. For example, defective microtubule transport results in incomplete fusion of autophagosomes with lysosomes causing accumulation of vesicles and undigested protein content (Arduíno et al. 2012; Köchl et al. 2006). In conclusion, microtubule-mediated transport is a key component of vesicular trafficking, tightly regulated by an array of cargo binding molecules with diverse specificity. To summarise, there is a delicate interplay between cytoskeletal components and abnormal cytoskeletal homoeostasis could lead to neurodegeneration (Pellegrini et al. 2016).

**The microtubule-associated protein tau**

A variety of microtubule-associated proteins (MAPs) transiently bind microtubules, contributing to their stability and orientation, and regulating transport directionality. Different neuronal compartments display specific subsets of MAPs (Pellegrini et al. 2016) (Fig.1.6, a).

Tau is the product of the *MAPT* gene (Neve et al. 1986), expressed in neurons, mainly decorating axonal microtubules to help maintain their stability (Lee et al. 2012; Mandelkow and Mandelkow 2011). Tau structure is composed of an N-terminal projection domain, a central proline-rich region and a C-terminal domain. The N-terminus interacts with other cytoskeletal elements and with the plasma membrane. The C-terminal domain is involved in microtubule

binding (Bussiere and Hof 2000). In particular, the tau KXGS motif, in the microtubule-binding domain, is important for interactions with microtubules, as well as for its folding and aggregation properties.

Tau has a role in axonal transport and neurite outgrowth (Vossel et al. 2010; Zhang et al. 2005). Tau can block organelle and cargo trafficking by competing with molecular motors for binding microtubules (Matenia and Mandelkow 2009). Phosphorylation of tau causes its detachment from microtubules resulting in increased transport flow. Studies from transgenic models expressing mutated tau show that deregulated tau phosphorylation may lead to microtubule destabilisation and abnormal tau aggregation (Denk and Wade-Martins 2009; Götz and Ittner 2008). Tau accumulation can create intracellular inclusions called paired helical filaments further assembled in neurofibrillary tangles in AD (Kosik et al. 1989; Shin et al. 1992).

Mutations and variants in the *MAPT* gene encoding tau have been linked to neurodegenerative diseases such as frontotemporal dementia with parkinsonism, progressive supranuclear palsy, AD and PD (Lee et al. 2001; Simón-Sánchez et al. 2009; Tobin et al. 2008). The *MAPT* gene has been nominated as a candidate gene for sporadic PD as well as a PD risk factor in GWAS (Simón-Sánchez et al. 2009; Zabetian et al. 2007). The H1 haplotype of the MAPT is significantly associated with an increased susceptibility to PD (Tobin et al. 2008; Zabetian et al. 2007). Several GWAS studies also indicate an association between SNCA and MAPT suggesting cooperation in PD pathomechanisms (Simón-Sánchez et al. 2009). Furthermore, tau pathology has been detected in post-mortem analysis of PD brains carrying Y1699C, G2019S, or I2020T LRRK2 mutations (Zimprich et al. 2004). In addition, one study suggested a functional interaction between LRRK2 and microtubule-associated tau (Kawakami et al. 2014).

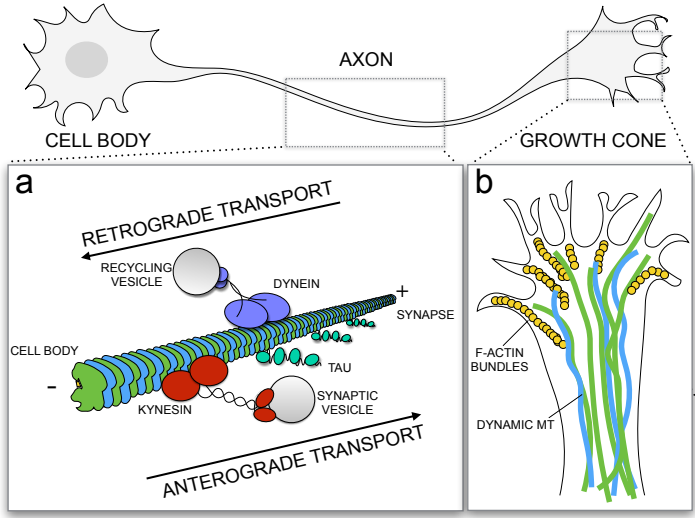


Figure 1.6: **Microtubule-mediated axonal transport and growth cone dynamics.** Schematic representation of a neuron segmented in cell body, axon and growth cone. (a) Axonal microtubule transport is regulated by molecular motors (such as kinesins and dyneins) and MAPs (such as tau). Kinesins transport vesicles to the synapse (anterograde transport) and dyneins deliver recycling vesicles to the cell body (retrograde transport). (b) At the neuronal growth cone F-actin bundles extend the plasma membrane and interact with polymerising microtubules to promote axon growth and remodeling.

### The axonal growth cone

Synaptic vesicles are transported to and from the axonal growth cone via microtubule transport (Fig.1.6, b). At the growth cone periphery, dynamic and polymerising microtubules are linked to F-actin bundles through several cross-linking proteins (Kalil and Dent 2005). This interaction between microtubules and actin helps to promote axonal growth (Kalil and Dent 2005). The central structure of a growth cone is composed of thick and more stable

microtubules and shows a dense distribution of synaptic vesicles (Fig.1.6, b). The cytoskeletal dynamics within the growth cone affects their morphology and movement. Impairments in growth cone dynamics have been observed in genetic PD models and will be discussed in the following section.

### 1.5.4 Microtubule dysfunction in PD

Abnormal cytoskeletal regulation has been described as a key process in neurodegenerative disorders (Cartelli et al. 2013; Esteves et al. 2010; Law et al. 2014; Min et al. 2015; Pellegrini et al. 2016). Disease-related proteins have been found to bind microtubules or influence microtubule dynamics. Mutations and variants in genes encoding cytoskeletal elements have been identified in genetic studies. Alterations of microtubules have been reported for at least five PD-linked proteins: parkin (PARK2), PINK1 (PARK6), DJ-1 (PARK7), LRRK2 (PARK8) and α-synuclein (SNCA) (Bonifati 2014; Pellegrini et al. 2016).

Mutations in the *parkin* gene, encoding for an E3 ubiquitin-ligase, segregate with early onset autosomal recessive PD (Shimura et al. 2000). Parkin decreases tubulin polymerisation and loss of parkin has been shown to block tubulin ubiquitination (Ren et al. 2003). Parkin has been reported to functionally interact with the serine-threonine kinase PINK1 and to regulate mitochondrial trafficking along microtubules (Kane and Youle 2011). It has been suggested that PD-linked mutations in parkin and PINK1 result in aberrant transport of mitochondria (Kazlauskaite and Muqit 2015). In addition, loss of DJ-1, although still poorly characterised, has also been implicated in mitochondrial fragmentation (Cookson 2012; Wang et al. 2012b).

The PD-linked protein α-synuclein (SNCA) has been proposed to functionally interact with tubulin (Zhou et al. 2010), however, the biological effects of this interaction are still unclear. α-synuclein promotes tubulin polymerisation and α-synuclein overexpression associates with axonal transport impairments (Lee et al. 2006). Interactions with kinesins and the microtubule-associated protein tau have also been reported, supporting the hypothesis of a key role for α-synuclein in microtubule-mediated transport (Koch et al. 2015; Lee et al. 2006; Pellegrini et al. 2016; Prots et al. 2013).

### 1.5.5 LRRK2 interaction with cytoskeletal proteins

Evidence for a cytoskeletal role of LRRK2 comes from several studies (Jaleel et al. 2007; Law et al. 2014; Parisiadou et al. 2009). Jaleel et al. suggested an association of LRRK2 with the actin cytoskeleton, in particular with the ERM (ezrin, radixin and moesin) complex (Jaleel et al. 2007). The ERM proteins connect transmembrane proteins with the cytoskeleton, providing a structural link and regulating signalling cascades. In 2009, Parisiadou and collaborators also reported an interaction between LRRK2 and the ERM (Parisiadou et al. 2009). Developing LRRK2-G2019S neurons displayed significant increased pERM and F-actin enriched filopodia, correlating with neurite growth defects (MacLeod et al. 2006). Interestingly, LRRK2-KO inversely decreased ERM phosphorylation (Parisiadou et al. 2009). Further studies on the LRRK2 interactome led to the identification of actin isoforms as well as actin-associated proteins involved in actin rearrangement and maintenance (Meixner et al. 2011). Together these findings strongly point out a role for LRRK2 in actin dynamics regulation.

Neuronal growth, survival and maintenance of plasticity rely on a finely regulated cytoskeletal homeostasis. It is therefore of interest that LRRK2 has been reported

to be associated with microtubules (Biskup et al. 2006; Kawakami et al. 2012; Law et al. 2014). LRRK2 interacts with microtubules through its Roc domain (Gandhi et al. 2009). Subsequently, LRRK2 was reported to mediate phosphorylation of β-tubulin 2C (Gillardon 2009). In 2014, Law et al. showed that LRRK2 interacts with specific neuronal tubulin isoforms (TUBB, TUBB4, TUBB6) (Law et al. 2014). The LRRK2 interaction site localises to the lumen of microtubules and the LRRK2 Roc domain was shown to interact with the C-terminus of β-tubulin. In particular, by using yeast two-hybrid assays and molecular modelling Lys362 and Ala364 on β-tubulin were shown to confer LRRK2 binding specificity (Law et al. 2014).

As LRRK2 is approximately five times the size of a tubulin heterodimer, it was suggested that LRRK2 can access its binding site, inside the microtubule lumen, only within a dynamic, open and flexible pool of microtubules (Law et al. 2014; Sancho et al. 2009). Moreover LRRK2 localisation within growth cones, where microtubules are dynamic to allow growth, is well established (Häbig et al. 2013; Sancho et al. 2009). This physical association might be relevant in the context of neurogenesis (Berwick and Harvey 2013). Taken together these observations point out that LRRK2 is likely to interact with a dynamic pool of microtubules where it may represent an essential scaffold providing a platform for intracellular signalling along the microtubule tracks.

### 1.5.6 LRRK2 affects microtubule stability

Defective PTMs of tubulins and MAPs cause alterations in the dynamic instability of microtubules, leading to aberrant axonal transport, synaptic dysfunction and axonal degeneration (Perdiz et al. 2011). In 2014, Law and collaborators shed light on LRRK2 modulation of tubulin acetylation (Law et al. 2014). The

tubulin-binding site for LRRK2 is in close proximity to Lys40, the acetylation site in α-tubulin. Since located inside of the microtubule lumen, this site is predicted to be accessible only within a dynamic population of microtubules. Interestingly, there was a significant increase in acetylated tubulin levels in LRRK2-KO immortalized mouse embryonic fibroblasts (MEFs) that could be partly rescued by over-expression of LRRK2, further supporting the idea that LRRK2 interferes with tubulin-acetylation *in vivo* (Law et al. 2014). Given its large size, LRRK2 might prevent the acetyltransferase to reach its site on Lys40, keeping tubulin in a non-acetylated state. Alternatively, microtubule over-stabilisation might be a compensatory mechanism following destabilisation, however, the precise role of LRRK2 is open to question.

A separate study conducted in *Drosophila* showed that LRRK2 Roc-COR mutations cause axonal transport defects in motor neurons *in vivo* (Godena et al. 2014). Interestingly, aberrant axonal transport leading to mitochondrial damage resulted in functional defects in locomotion, decreasing flies ability to climb and fly. Treatment with the deacetylase inhibitor trichostatin A (TSA) restored axonal transport and locomotion. Together these findings suggest that increase in tubulin acetylation may be able to restore LRRK2-induced transport defects, although the underlying mechanism by which LRRK2 affects microtubules is not clear.

## 1.6 LRRK2 pathological role

### 1.6.1 Overview

LRRK2 mutations cause parkinsonism with pleomorphic pathology including variable pathological features such as neuronal loss with or without LB, tau or ubiquitin-positive inclusions (Melrose 2008; Zimprich et al. 2004). How mutations affect LRRK2 function and how mutated LRRK2 results in PD neurodegeneration is still under debate. Since its discovery (Funayama et al. 2002), several studies using *in vivo* and *in vitro* models of LRRK2 mutations have characterised some of the pathogenic effects related to LRRK2 function. In this section, the toxic function of LRRK2 mutants and LRRK2 genetic models will be discussed.

### 1.6.2 LRRK2, α-synuclein and tau

Data from GWAS, biochemical studies and animal models support LRRK2 as an upstream regulator of α-synuclein and tau toxicity contributing to their aggregation in LB, the pathological hallmark of PD (Cookson 2010; Schapansky et al. 2014b; Taymans and Cookson 2010). Particularly, overexpressing LRRK2 seems to accelerate α-synuclein deposition in a mouse model overexpressing mutant α-synuclein (Lin et al. 2009). Furthermore, α-synuclein detrimental effects are attenuated after LRRK2 genetic ablation (Guerreiro et al. 2013; Lin et al. 2009). Recent data show that a direct phosphorylation of α-synuclein by LRRK2 seems unlikely (Khan et al. 2005; Taymans and Baekelandt 2014). There is some evidence of tau phosphorylation by LRRK2 (Kawakami et al. 2012; Lin et al. 2010), possibly via regulation of downstream tau kinases.

### 1.6.3 Toxic effects of pathogenic LRRK2 mutants

The most common LRRK2 mutation segregating with PD is the G2019S substitution located in the N-terminal boundary of the kinase activation segment (Lesage et al. 2006; Ozelius et al. 2006; West et al. 2005). This suggests that the catalytic activity of LRRK2 could be involved in PD pathophysiology (Wallings et al. 2015). In particular, the G2019S mutation leads to a significant increase in kinase activity relative to wild-type (West et al. 2005). As kinase-dead mutants are less toxic than kinase-active LRRK2, it has been proposed that the G2019S mutation leads to a toxic gain of function (Greggio et al. 2006). Several studies overexpressing G2019S-LRRK2 in cell lines and primary neuronal cultures reported reduced complexity of neurite processes and decreased cell viability (MacLeod et al. 2006; Winner et al. 2012).

The I2020T mutation, also localised in the kinase domain, was isolated from the Japanese family where the PARK8 locus was first identified (Funayama et al. 2005). The increase in kinase activity of this mutant, however, is less striking than the one observed in the G2019S-LRRK2 (Greggio et al. 2009). Interestingly, abnormal tau phosphorylation has been observed in models of both mutations (MacLeod et al. 2006; Ohta et al. 2015; Ujiie et al. 2012).

In conclusion, mutations may increase LRRK2 kinase activity or decrease its GTPase activity, but the real role of LRRK2 in neurodegeneration is not clear. LRRK2 mutations may display a toxic gain of function or a loss of function, affecting specific pathways. A toxic gain of function of the mutant protein is often associated with its propensity to aggregate. Most neurodegenerative diseases are characterised by formation of protein inclusions inside neurons, as in the case for PD and AD. LRRK2 may also function as a scaffold for signalling complexes.

The LRRK2 pathological role, therefore, may result from the destabilisation of LRRK2-mediated complexes leading to accumulation of downstream substrates. Together these observations lead to the hypothesis that LRRK2 pathological role involves deregulation of different pathways resulting in protein misfolding and aggregation prior to neurodegeneration.

### 1.6.4 LRRK2 in inflammation

As previously discussed, PD is a multisystem disorder with complex and largely unknown etiology where symptoms range from classical neuromotor defects to GI dysfunction (Caligiore et al. 2016). A key player in PD pathology is inflammation (Russo et al. 2014). According to Braak's *dual-hit* hypothesis, PD pathology begins in the peripheral nervous system, triggered by an external pathogenic source (i.e. a neurotropic virus), and immune response significantly contributes to disease progression (Braak et al. 2003; Hawkes et al. 2007; Visanji et al. 2013).

A number of studies show elevated LRRK2 mRNA and protein levels in a variety of immune cells including T and B cells, monocytes and microglia suggesting that LRRK2 might have an important role in immune response (Marker et al. 2012; Moehle et al. 2012; Speidel et al. 2016). LRRK2 expression is induced in LPS-activated microglia and inhibition of LRRK2 blocks microglia activation, supporting the LRRK2 role in regulating responses in brain immune cells (Moehle et al. 2012). Supporting these findings, LRRK2 mutants monocytes reveal deficits in migration capacity (Speidel et al. 2016). Another study reported a role for LRRK2 in ROS production and showed LRRK2 association to the phagocyte membrane during pathogens phagocytosis (Gardet et al. 2010; Schapansky et al. 2014a).

In addition, *LRRK2* is a susceptibility gene for Crohn's disease (Barrett et al. 2009; Franke et al. 2010), a chronic inflammatory intestinal disease, and loss of LRRK2 in mice confers higher risk to develop experimental colitis (Liu and Lenardo 2012). Collectively, these observations support a role for LRRK2 in immune response as a negative regulator of inflammation.

### 1.6.5 LRRK2 mouse models

A way to address scientific questions related to the normal function of a protein and how mutations may affect it, is to examine mice manipulated to have higher or lower expression of the target gene of interest. Mice have been extensively employed as a model organism as their genome significantly overlaps with the human genome (Waterston et al. 2002). The LRRK2 protein is highly conserved throughout species. Supporting this notion, expression and co-immunoprecipitation of human and mouse LRRK2 can result in cross-species heterodimers (Langston et al. 2016; Miyajima et al. 2015; West et al. 2014).

LRRK2 transgenic or knockout mouse models have been generated in the past years, but these animals do not recapitulate the primary PD symptoms or pathological features, i.e., locomotor dysfunctions, loss of dopamine neurons in the substantia nigra *pars compacta* or the formation of Lewy bodies (Herzig et al. 2011; Tong et al. 2010, 2012). Another study shows a LRRK2 knockout model with absence of neuronal loss but abnormal exploratory activity in the open-field test and longer resistance to rotarod testing (Hinkle et al. 2012). Together, these results indicate that loss of LRRK2 does not affect neurological functions consistently in mice.

Consistently reported features in LRRK2 genetically modified animals are pathological alterations in the kidneys of LRRK2 knockout rodents (Herzig et al.

2011; Kuwahara et al. 2016; Tong et al. 2010, 2012). The fact that kidneys are affected over other organs is perhaps not surprising since particularly high expression of LRRK2 relative to the homologous gene *LRRK1* is detected in kidneys (Herzig et al. 2011; Tong et al. 2010, 2012). Similar pathological alterations have also been reported in lungs from LRRK2-KO mice showing microvacuolation of type II pneumocytes (Herzig et al. 2011).

### 1.6.6 LRRK2 knockout kidney abnormalities

LRRK2-KO kidneys have altered color and texture, an increase in apoptotic cell death and inflammation (Tong et al. 2012), and accumulation of lipofuscin, an autofluorescent mixture of oxidised proteins and lipids resulting from altered degradative pathways (Herzig et al. 2011; Kuwahara et al. 2016; Tong et al. 2010, 2012). Tong and collaborators show a number of bi-phasic alterations in autophagy markers, indicating impaired protein degradation (Tong et al. 2012). Supporting the concept that altered protein degradation occurs in LRRK2-KO kidneys, the lysosomal protease cathepsin D accumulates in these tissues (Herzig et al. 2011; Tong et al. 2010, 2012).

Functional assays of LRRK2-KO kidneys compared to controls show no differences in levels of blood urea nitrogen (BUN) and serum creatinine, classic markers of renal function (Tong et al. 2012). The ratio between BUN and serum creatinine, a marker of acute kidney injury, was also not significantly different between genotypes (Tong et al. 2012). However, LRRK2-KO mice present significantly higher levels of the kidney injury molecule 1 (Kim1) starting from 1 month of age up to 20 months of age (Tong et al. 2012). Kim1 is a scavenger receptor expressed in epithelial cells from kidney proximal tubules and represents a measure of nephrotoxicity (Bonventre 2009). The function of Kim1 is to convert kidney

epithelial cells into phagocytes and its expression is increased in a number of kidney pathological conditions including acute kidney injury, tubulo-interstitial fibrosis and proteinuria (Bonventre 2009). Counterintuitively, loss of LRRK2 in kidney seems to protect rats against rhabdomyolysis, causing a specific form of acute-kidney injury, despite the accumulation of CD8+ macrophages, lysosomal proteins and lipids (Boddu et al. 2015).

Interestingly, some of the LRRK2-KO kidney phenotypes are reproduced in LRRK2 knockin mice expressing kinase dead mutations and wild-type mice exposed to kinase inhibitors, suggesting that intact kinase function is required for kidney proteostasis (Herzig et al. 2011). However, they are not present in kidneys from homozygous G2019S knockin mice, suggesting that kidney abnormalities specifically result from the loss of LRRK2 kinase activity (Herzig et al. 2011).

In conclusion, LRRK2-KO kidneys can be considered a reasonable model in which to study the normal function of this protein and to investigate the pathogenic effect of LRRK2 mutations.

# 2 Aims of the project

Mutations in LRRK2 are associated with late-onset familial and sporadic PD, but the normal physiological role of LRRK2 is not well understood. LRRK2 has been implicated in several cellular functions including endosomal trafficking, retrograde transport and autophagy (Beilina et al. 2014; Tong et al. 2012). Additionally, several pieces of evidence suggest that LRRK2 is involved in the regulation of cytoskeletal dynamics (Law et al. 2014; MacLeod et al. 2006, 2013; Sancho et al. 2009). Together these observations suggest that LRRK2 plays a central role in both vesicular trafficking and cytoskeletal function and it seems likely that these two aspects of LRRK2 are related (Boon et al. 2014; Esteves et al. 2014; Tsika and Moore 2012).

Pathogenic mutations in LRRK2 that segregate in families with PD are clustered in the enzymatic GTPase and kinase domains (Cookson 2010; Greggio and Cookson 2009; Steger et al. 2016; West et al. 2005) suggesting that LRRK2 catalytic activity could be involved in PD pathogenesis. Despite the evidence linking the G2019S mutation of LRRK2 with familial PD, there are a number of open questions concerning the function of LRRK2 mutations. Could the G2019S be a gain of normal function, resulting in alterations of gene dosage or could it harbor a different, toxic function? Alternatively, is the G2019S a dominant negative allele? It is crucial to distinguish whether mutant LRRK2 is pathogenic via higher or lower activity, given that kinase inhibitors, predicted to block normal function, are being developed as potential therapeutic agents for PD (Ray and Liu 2004).

One way to address these open questions might be to examine mice manipulated to have higher or lower LRRK2 function. Transgenic or knockout mouse models do not recapitulate the primary PD pathologies (Cookson 2010; Herzig et al.

2011; Tong et al. 2010, 2012). However, multiple groups have reported that loss of LRRK2 causes age-dependent pathological alterations in the kidneys (Herzig et al. 2011; Kuwahara et al. 2016; Tong et al. 2010, 2012). LRRK2-KO kidneys have altered texture, an increase in apoptotic cell death and inflammation (Tong et al. 2012), and accumulation of lipofuscin granules (Herzig et al. 2011; Kuwahara et al. 2016; Tong et al. 2010, 2012), supporting the concept that altered protein degradation occurs in LRRK2-KO kidneys. Nevertheless, the mechanism(s) by which phenotypes arise from loss of LRRK2 function are still uncertain. Specifically, whether accumulation of protein degradation defects is a primary or secondary event is unclear and it is not known if the reported effects of LRRK2 deficiency on lysosomal enzymes are specific or generalised to other vesicular organelles. Additionally, the hypothesis that pathogenic mutations may cause disease by dominant negative effects remains viable. To address these questions using relatively unbiased approaches, the initial aims of this thesis are the following:

## 2.1 Aim 1: To perform unbiased proteomic screening of LRRK2-KO and LRRK2-G2019S mutant kidneys

1. iTRAQ analysis on WT and LRRK2-KO kidney cytosolic and microsomal enriched fractions.
2. iTRAQ analysis on WT and LRRK2-G2019S kidney cytosolic and microsomal enriched fractions.
3. Comparative analysis of protein candidate hits between WT, LRRK2-KO and G2019S mutant.

## 2.2 Aim 2: To validate protein candidates with orthologous techniques

1. Candidate validation via immunoblot assays in WT, LRRK2-KO and G2019S mutant kidneys.
2. Comparative histopathological analysis in kidney sections by immunofluorescence staining.
3. Analysis of iTRAQ hits expression levels in LRRK2-KO and control brains

## 2.3 Aim 3: To examine biological changes across multiple cohorts of iTRAQ validated hits

1. Investigation of iTRAQ hits differences in LRRK2-KO and control mice at developmental stages by immunoblot
2. Investigation of iTRAQ hits differences in LRRK2-KO and control mice in ageing cohorts by immunoblot
3. Analysis of alterations in autophagy markers in LRRK2-KO and control mice independent cohorts by immunoblot

## 2.4 Aim 4: To investigate the molecular mechanisms affected by loss of LRRK2 *in vitro*

1. High content siRNA screen of proteomic candidates to identify potential modifiers of LRRK2 function.
2. Modelling of LRRK2-KO kidney pathology *in vitro* using primary kidney cells

# 3 Proteomic analysis of LRRK2 knockout and G2019S kidneys

## 3.1 Introduction

Genetic variations in the gene encoding LRRK2 have been linked to both familial and sporadic PD (Funayama et al. 2005; Nalls et al. 2014; Simón-Sánchez et al. 2009; Zimprich et al. 2004). However, the physiological role of LRRK2 remains elusive. LRRK2-KO or knockin mutant rodents do not display apparent signs of neuropathology that would mimic Parkinson's disease neurodegeneration. Loss of LRRK2, however, causes age-dependent defects in the autophagy-lysosomal pathway, including accumulation of lysosomal proteases and autophagy markers. These defects are accompanied by increase in oxidative stress, protein aggregation and inflammatory response markers in kidneys (Tong et al. 2010).

The most common LRRK2 pathological mutation associated with PD is the G2019S, which has been reported to increase LRRK2 kinase activity (Greggio et al. 2006; West et al. 2005). In experiments with LRRK2 G2019S mice, however, the aforementioned kidney phenotype was not observed (Herzig et al. 2011).

Despite that some of the pathological defects observed in LRRK2-KO kidneys have been characterised, a global understanding of the affected biological pathways is still lacking. One useful approach to investigate global changes in protein expression is to perform a proteomic analysis. Therefore, in an attempt to elucidate the biological role of LRRK2 *in vivo* and to investigate which pathways are perturbed in absence of LRRK2, I used a quantitative proteomic

approach to measure protein abundance changes in kidneys from LRRK2 knockout (LRRK2-KO) and control mice.

One modern quantitative proteomic approach is the isobaric tag labelling for Relative and Absolute Quantitation (iTRAQ). iTRAQ is a MS-based approach that allows multiple samples in the same experimental run reducing experimental variablity. Another advantange of this approach over other mass-spectrometry based techniques, is the availability of comprehensive databases of tryptic peptides, useful for unique peptide identification, and of reliable softwares for data analysis. A common disadvantage of these high-content screens is the high false positive rate (Reiter et al. 2009). iTRAQ analytical challenges can be minimised by sample enrichment or fractionation, to reduce complexity and improve coverage; and by result validation with orthologous techniques. Considering the problematic aspects of iTRAQ, sample enrichment in cytosolic and microsomal components was performed, followed by iTRAQ analysis and validation of the results with immunoblot (see section 8.3 for iTRAQ experimental design).

Cytosol and microsomal enriched fractions were collected, based on the expected association of LRRK2 with cytosolic/cytoskeletal and endosomal/vesicular compartments of cells (Alegre-Abarrategui et al. 2009; Beilina et al. 2014; Law et al. 2014). In the first screen I used cytosolic and microsomal enriched protein extracts from the kidneys of 5 LRRK2-KO and 5 wild-type (WT) control mice (12 months old). Significant changes in lysosomal proteases, cytoskeletal-associated proteins and regulators of protein translation were detected in LRRK2-KO fractions after iTRAQ analysis.

To examine the effects of pathogenic mutations in LRRK2, a second screen was performed, with same experimental design, using cytosolic and microsomal enriched

protein extracts from the kidneys of G2019S heterozygous knockin (G2019S-KI) and control mice (12 month old). In contrast to LRRK2-KO, mice expressing the G2019S pathogenic mutation of LRRK2 did not display significant alterations in protein abundance.

## 3.2 Results

### 3.2.1 LRRK2-KO kidney phenotype

To confirm the reported kidney phenotype, 5 controls, 5 LRRK2-KO and 5 LRRK2-G2019S homozygous kidneys from a 5-6 month-old cohort were compared (Fig. 3.1). LRRK2-KO kidneys were darker compared to both controls and G2019S mutant kidneys (Fig. 3.1, A). LRRK2-KO kidneys were larger and weighed significantly more compared to controls and G2019S kidneys ($p = 0.029$, WT *vs* LRRK2-KO; $p = 0.004$, LRRK2-KO *vs* G2019S Homo, Bonferroni post-hoc test from one-way ANOVA, n=5) (Fig. 3.1, B). With these observations it can be concluded that LRRK2-KO kidneys present similar abnormalities reported in the literature by other groups, and LRRK2-G2019S kidneys seem indistinguishable from control kidneys.

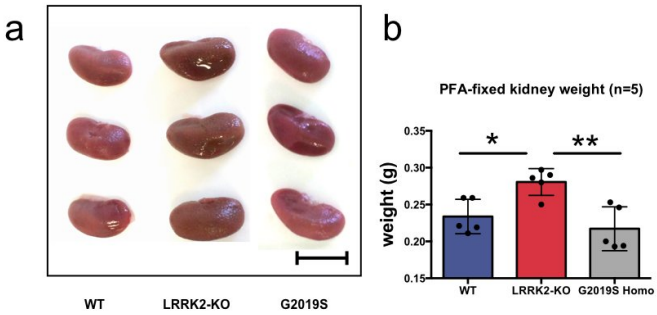


Figure 3.1: **Kidney phenotypes in LRRK2-KO and G2019S-KI animals.** Gross appearance of fresh frozen WT, KO and G2019S kidneys (a). Altered color, and texture are observed in LRRK2-KO kidneys (scale bar = 1cm). (b) Kidney size is significantly increased in LRRK2-KO compared to both controls and G2019S kidneys (males, 5-6 month-old, Bonferroni post-hoc test from one-way ANOVA, n=5). $*P<0.05$, $**P<0.01$
.

### 3.2.2 Proteomic screen of LRRK2-KO kidneys

To investigate changes in protein abundance in LRRK2-KO, kidneys from 1 year old LRRK2-KO and control mice (n=5) were dissected. Subcellular fractionation was performed in order to decrease sample complexity and improve proteome coverage. Sample fractionation into microsomal and cytosolic fractions was obtained using a multistep protocol with differential centrifugations and a final ultracentrifugation step to separate the cytosol enriched part from the microsomes (see Materials and Methods section for more details). To confirm sample enrichment after subcellular fractionation, immunoblots were used to detect the abundance of two widely used markers of the late-endosome and the lysosomal compartments, Rab7 ($p = 0.0018$, cytosol enriched *vs* microsome enriched, Student t test, n=4) and Lamp1 ($p =$

0.0004, cytosol enriched *vs* microsome enriched, Student t test, n=4) respectively. As expected, the levels of Rab7 and Lamp1 were significantly higher in the microsomal fractions, enriched in vesicular trafficking components, compared to the cytosolic fractions (Fig. 3.2). In addition, the cytosolic protein GAPDH was enriched in cytosolic fractions (Fig. 3.2). The presence of Rab7 in cytosolic fractions suggests partial enrichment. The goal of subcellular fractionation is to enrich samples in proteins from a certain intracellular compartment and not to produce pure fractions, therefore these samples were used for the following proteomic experiments.

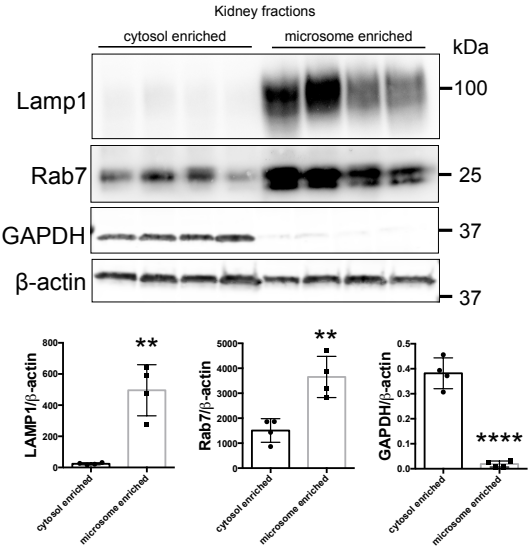


Figure 3.2: **Sample enrichment characterisation.** Immunoblots from kidney microsomal fractions show significant enrichment in endo-lysosomal markers Lamp1 and Rab7 compared to kidney cytosolic fractions which show increased abundance of the cytosolic protein GAPDH (12 month-old mice, Student t test, n=4). ∗P<0.05, ∗∗P<0.01, ∗∗∗ P<0.001, ∗∗∗∗ P<0.0001.

In the cytosol enriched samples, approximately 700 (Run 1) and 600 (Run 2) unique proteins were identified and quantified. There were 504 common hits between the two runs. In the microsomal enriched fractions, approximately 1500 (Run 1) and 1800 (Run 2) unique proteins were detected, with 1187 shared hits. There were 375 proteins detected in both fractions (Fig. 3.3, 3.4).

**Kidney cytosol enriched fractions**

In the cytosol enriched fractions, 23 proteins significantly different in abundance between LRRK2-KO and controls were identified (Fig. 3.3). Interestingly, most of these were higher in the KO compared to WT, with only two proteins, phosphopantothenoylcysteine synthetase (Ppcs), an enzyme involved in the biosynthesis of coenzyme A (Strauss et al. 2001), and glutathione peroxidase 1 (Gpx1), whose role is to protect the cells from oxidative stress (Higashi et al. 2013; Oelze et al. 2014), showing significantly lower expression (Fig. 3.3, Table 1). Among the proteins significantly increased in LRRK2-KO, six lysosomal proteases were detected, indicating a potential defect in lysosomal degradation (See 3.2.2 for full names and p values). An increase in the lysosomal protease cathepsin D (Ctsd), previously observed in LRRK2-KO kidneys (Tong et al. 2012), was also reported in this screen.

Interestingly, an increase in protein involved in membrane-recycling and vesicular transport was observed. In particular, the vesicle-associated membrane protein 1 (Vamp1), the synaptic vesicle membrane protein VAT1 homolog (Vat1) and the cytoplasmin dynein 1 heavy chain 1 (Dync1h1) were more abundant in LRRK2-KO the cytosolic fractions (Fig. 3.3). These observations strongly suggest the presence of a trafficking defect in LRRK2-KO kidneys.

Increase in cytoskeletal proteins, such as coronin 1C (Coro1c), septin 9 (Sept9) and protein kinase C and casein kinase substrate protein 2 (Pacsin2), was observed in LRRK2-KO cytosol enriched fractions (Fig. 3.3, see 3.2.2 for p values), supporting the idea that loss of LRRK2 results in cytoskeletal changes.

Another group of proteins differentially regulated in LRRK2-KO included regulators of protein synthesis such as heterogeneous nuclear ribonucleoprotein

K (Hnrnpk) and Elongation factor 1-gamma (Eef1g), which were higher in the cytosolic fractions of KO animals than wild type controls (Fig. 3.3, see 3.2.2 for p values).

Unsupervised hierarchical clustering was performed by plotting the proteomic dataset of significant hits in a heatmap which allows to observe global differences in protein levels across samples. The set of differential proteins was sufficient to identify group separation between genotypes in our cytosolic fractions (Fig. 3.3).

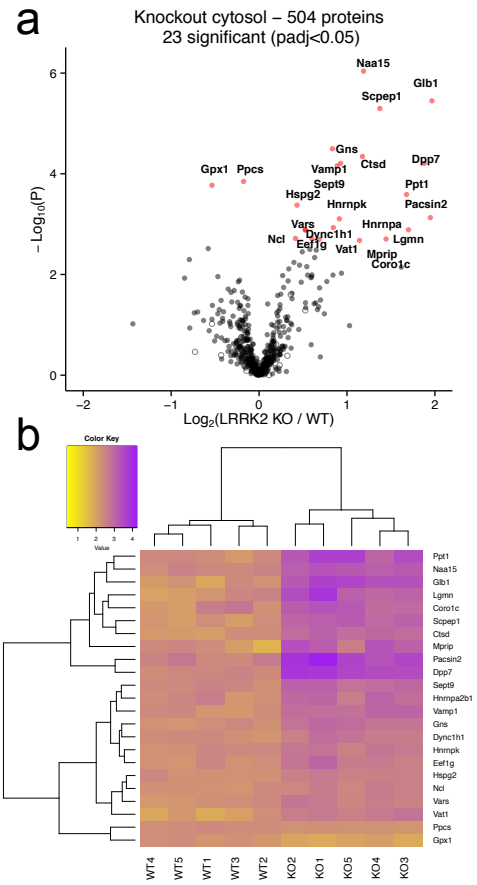


Figure 3.3: **iTRAQ proteomics of 12 month old LRRK2-KO kidneys cytosolic fractions.** (a) Volcano plot of the 504 proteins quantified in the cytosolic enriched fraction; y-axis shows p values (n=5, Welch T-test, p values corrected using Benjamini-Hochberg post hoc test), x-axis shows log2 of fold expression LRRK2-KO/WT. (b) Heat map of significant genes differently regulated in cytosolic fractions. Significant proteins are shown in the rows and individual samples in the columns. The darker the color the higher the protein abundance as indicated by the color scale.

| Full Protein Name | Gene | Accession | Adj p-value |
|---|---|---|---|
| N-alpha-acetyltransferase 15, NatA auxiliary subunit | Naa15 | NAA15 | 0.0005 |
| Beta-galactosidase | Glb1 | BGAL | 0.0008 |
| Retinoid-inducible serine carboxypeptidase | Scpep1 | RISC | 0.0008 |
| N-acetylglucosamine-6-sulfatase | Gns | GNS | 0.0040 |
| Cathepsin D | Ctsd | CATD | 0.0044 |
| Dipeptidyl peptidase | Dpp7 | DPP2 | 0.0044 |
| Septin-9 | Sept9 | SEPT9 | 0.0044 |
| Vesicle-associated membrane protein 1 | Vamp1 | VAMP1 | 0.0044 |
| Phosphopantothenate-cysteine ligase | Ppcs | PPCS | 0.0080 |
| Glutathione peroxidase 1 | Gpx1 | GPX1 | 0.0340 |
| 26S proteasome non-ATPase regulatory subunit 3 | Psmd3 | PSMD3 | 0.0340 |
| Valine tRNA ligase | Vars | SYVC | 0.0085 |
| Palmitoyl-protein thioesterase 1 | Ppt1 | PPT1 | 0.0118 |
| Basement membrane-specific heparan sulfate proteoglycan core protein | Hspg2 | PGBM | 0.0176 |
| Protein kinase C and casein kinase substrate in neurons protein 2 | Pacsin2 | PACN2 | 0.0282 |
| Synaptic vesicle membrane protein VAT-1 homolog | Vat1 | VAT1 | 0.0282 |
| Heterogeneous nuclear ribonucleoprotein K | Hnrnpk | HNRPK | 0.0369 |
| Legumain | Lgmn | LGMN | 0.0369 |
| Heterogeneous nuclear ribonucleoproteins A2/B1 | Hnrnpa2b1 | ROA2 | 0.0369 |
| Valine tRNA ligase | Vars | SYVC | 0.0369 |
| Cytoplasmic dynein 1 heavy chain 1 | Dync1h1 | DYHC1 | 0.0460 |
| Elongation factor 1-gamma | Eef1g | EF1G | 0.0460 |
| Myosin phosphatase Rho-interacting protein | Mprip | MPRIP | 0.0460 |
| Nucleolin | Ncl | NUCL | 0.0460 |
| Coronin-1C | Coro1c | COR1C | 0.0461 |

Table 3: **List of significant hits from iTRAQ cytosolic fraction analysis.**

**Kidney microsome enriched fractions**

Further analysis of the microsome enriched fractions identified 25 differentially abundant proteins (Fig. 3.4), of which 5 were also significantly different between genotypes in the cytosolic fractions (Fig. 3.3). The latter category included one protein, N(Alpha)-Acetyltransferase 15, NatA Auxiliary Subunit (Naa15), that was higher in the cytosol but lower in the microsomal fractions of KO animals compared to controls (Fig. 3.3, 3.4). The cytoskeletal protein Coro1c was also significantly increased in the cytosolic fractions (Fig. 3.3), but decreased in the microsomal fractions (Fig. 3.4).

Similarly to LRRK2-KO cytosol enriched fractions, four lysosomal proteases were identified as increased in LRRK2-KO microsome enriched fractions strongly suggesting the presence of lysosomal dysfunction in LRRK2-KO kidneys. In particular, the same lysosomal proteases Glb1, Lgmn and Dpp7 increased in the cytosolic fractions, were also more abundant in LRRK2-KO microsome enriched fractions compared to controls (Fig. 3.4).

Decrease in the transforming growth factor-beta receptor associated protein 1 (Tgfbrap1), a component of the CORVET complex involved in early endosome fusion, was observed in LRRK2-KO microsome enriched fractions. This result might indicate a defect in vesicle fusion events in absence of LRRK2.

Interestingly, where in the cytosolic fractions most of the significant hits were increased in abundance compared to controls, in the microsomal fractions the majority of the significant hits were lower in abundance compared to controls. A decrease in the tubulin isoform Tubb4b was detected in LRRK2-KO microsome enriched fractions (Fig. 3.4). Similarly, a decrease in the microtubule-binding

protein gephyrin (Gphn) was observed, suggesting the presence of cytoskeletal impairments in LRRK2-KO kidneys (Fig. 3.4).

A number of protein involved in protein synthesis initiation was differentially abundant in LRRK2-KO microsome enriched fractions (Fig. 3.4, see table 3.2.2 for full names and p values). These included proteins such as the eukaryotic translation initiation factor 3 subunit D (Eif3d) and the related proteins Eif4g3 and Eif5, all of which were lower in KO microsomal fractions compared to wild type animals (Fig. 3.4). These observations suggest a role for LRRK2 in protein synthesis regulation.

Again unsupervised hierarchical clustering using the dataset of proteomic hits from the microsomal fractions was performed. The results represented in the form of a heatmap indicate that the set of differential proteins was sufficient to identify group separation between genotypes (Fig. 3.4).

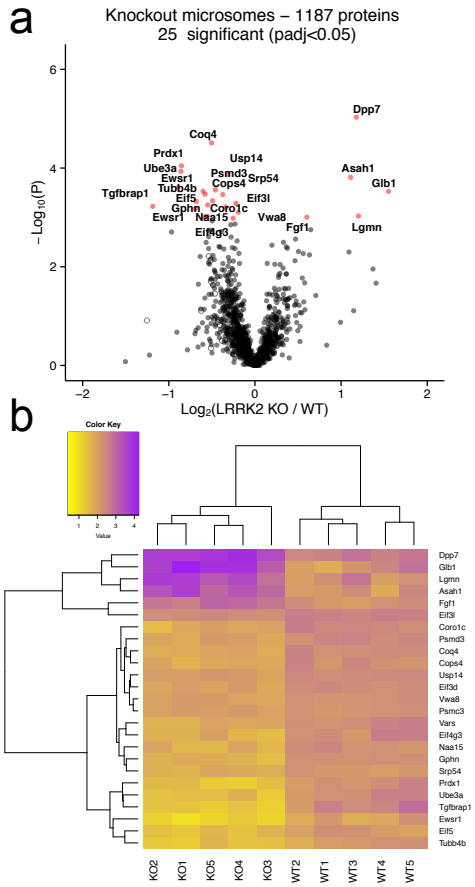


Figure 3.4: **iTRAQ proteomics of 12 month old LRRK2-KO kidneys microsomal fractions.** (a) Volcano plot of the 1187 proteins quantified in the microsomal enriched fraction (n=5, Welch T-test, p values corrected using Benjamini-Hochberg post hoc test). (b) Heat map of significant genes differently regulated in microsomal fractions. Significant proteins are shown in the rows and individual samples in the columns. Purple and yellow respectively indicate higher and lower protein abundance as indicated by the color scale.

| Full Protein Name | Gene | Accession Number | Adj p value |
|---|---|---|---|
| Dipeptidyl peptidase 2 | Dpp7 | DPP2 | 0.0110 |
| Ubiquinone biosynthesis protein COQ4 homolog | Coq4 | COQ4 | 0.018 |
| Acid ceramidase | Asah1 | ASAH1 | 0.0306 |
| Peroxiredoxin-1 | Prdx1 | PRDX1 | 0.0306 |
| Ubiquitin-protein ligase E3A | Ube3a | UBE3A | 0.0306 |
| Ubiquitin carboxyl-terminal hydrolase 14 | Usp14 | UBP14 | 0.0306 |
| Beta-galactosidase | Glb1 | BGAL | 0.0340 |
| Eukaryotic translation initiation factor 3 subunit D | Eif3d | EIF3D | 0.0340 |
| RNA-binding protein EWS | Ewsr1 | EWS | 0.0340 |
| Eukaryotic translation initiation factor 5 | Eif5 | IF5 | 0.0340 |
| 26S proteasome non-ATPase regulatory subunit 3 | Psmd3 | PSMD3 | 0.0340 |
| Valine tRNA ligase | Vars | SYVC | 0.0340 |
| COP9 signalosome complex subunit 4 | Cops4 | CSN4 | 0.0400 |
| Tubulin beta-4B chain | Tubb4b | TBB4B | 0.0400 |
| Eukaryotic translation initiation factor 3 subunit L | Eif3l | EIF3L | 0.0407 |
| Gephyrin | Gphn | GEPH | 0.0407 |
| Signal recognition particle 54 kDa protein | Srp54 | SRP54 | 0.0407 |
| Transforming growth factor-beta receptor-associated protein 1 | Tgfbrap1 | TGFA1 | 0.0407 |
| Eukaryotic translation initiation factor 4 gamma 3 | Eif4g3 | IF4G3 | 0.0418 |
| 26S protease regulatory subunit 6A | Psmc3 | PRS6A | 0.0468 |
| Coronin-1C | Coro1c | COR1C | 0.0490 |
| Fibroblast growth factor 1 | Fgf1 | FGF1 | 0.0490 |
| Legumain | Lgmn | LGMN | 0.0490 |
| N-alpha-acetyltransferase 15, NatA auxiliary subunit | Naa15 | NAA15 | 0.0490 |
| von Willebrand factor A domain-containing protein 8 | Vwa8 | VWA8 | 0.0494 |

Table 4: **List of significant hits from iTRAQ microsomal fraction analysis.**

### 3.2.3 Gene Ontology enrichment analysis

Gene ontology (GO) analysis helps to classify genes and their products with the goal to provide a common and controlled vocabulary enriched with functional data. GO analysis is classified into three main domains namely Cellular Component (CC), Biological Process (BP) and Molecular Function (MF). Here, the iTRAQ significant proteins whose abundance differed between genotypes were classified using GO analysis (Fig. 3.6).

Consistently with changes reported in the literature for the LRRK2-KO kidney phenotype, significant enrichment in several categories related to protein degradation was observed. The GO:Cellular compartment term lysosome was significantly enriched (Table 5), revealing changes in one of the major protein degradation systems of the cell (Fig. 3.5, A). Similarly, the GO:Molecular function category was enriched for serine-type carboxypeptidase complex. Underlying these categories, lysosomal enzymes including, cathepsin D (Ctsd), legumain (Lgmn), dipeptidyl peptidase 7 (Dpp7) and galactosidase beta 1 (Glb1) were at least 2-fold higher in LRRK2-KO compared to WT mice (Fig. 3.3, 3.4). An increase in Lgmn, Glb1 and Dpp7 was observed also in the microsomal enriched fraction (Fig. 3.3, 3.4).

A number of cytoskeletal proteins were differentially expressed between WT and KO kidneys (Table 6). Significantly lower levels of the tubulin isoform Tubb4b (previously known as Tubb2c, UniProt reference: P68372) and in the microtubule-associated protein gephyrin (Gphn) were noted in LRRK2-KO microsomal enriched fractions (Fig. 3.4). Other cytoskeletal-associated proteins, including coronin 1C (Coro1c), Protein kinase C and casein kinase substrate in neurons protein 1 (Pacsin2) and septin 9 (Sept9), were significantly higher in the

LRRK2-KO cytosolic enriched fractions compared to controls (Fig. 3.3). Many of these proteins were represented, along with some of the vesicular proteins listed above, in the GO:Cellular compartment term "extracellular exosome" ($p = 2.44 \times 10^{-10}$)(Fig. 3.5, A).

Interestingly, GO analysis identified enrichment in the GO:Cellular compartment term proteasome in the LRRK2-KO proteomic datasets. A decrease in six proteasome-related proteins was observed in LRRK2-KO microsome enriched fractions (Table 7). These findings support a role for LRRK2 in another intracellular pathway involved in protein degradation. In one study, LRRK2 seems to act upstream of proteasome activity (Lichtenberg et al. 2011). Dysfunctions in proteasome degradation could explain the accumulation of proteins in lipofuscin granules observed in LRRK2-KO kidneys (Sulzer et al. 2008; Tong et al. 2012).

An additional set of proteins that differed between WT and KO animals is related to the GO:biological process term "formation of translation preinitiation complex" and the GO:molecular function term "translational initiation factor activity" (Table 9, Fig. 3.5, B). These included proteins such as heterogeneous nuclear ribonucleoprotein K (Hnrnpk) and Elongation factor 1-gamma (Eef1g), which were higher in the cytosolic fractions of KO animals than WT controls and the eukaryotic translation initiation factor 3 subunit D (Eif3d) and the related proteins Eif4g3 and Eif5, all of which were lower in KO microsomal fractions compared to WT animals (Fig. 3.5, B).

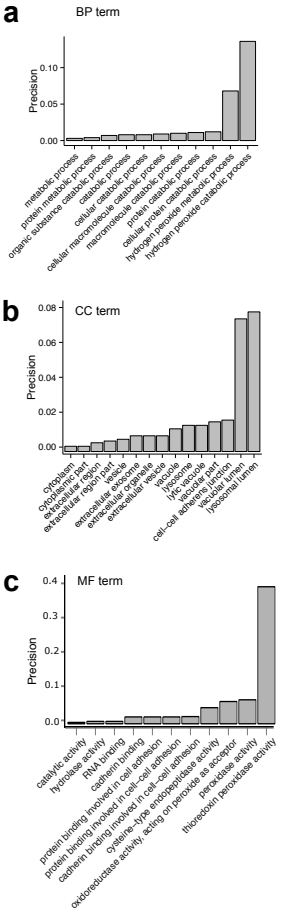


Figure 3.5: **Categorisation of proteins showing altered abundance in LRRK2-KO kidneys.** Significant ($p<0.01$) Gene Ontology (GO) enrichments for (a) biological processes (BP), (b) cellular compartment (CC) and (c) molecular function (MF). For each plot, the y-axes indicate precision, ie the number of proteins overlapping between the differentially abundant proteins in LRRK2-KO kidneys versus controls and the total number of proteins represented in that GO category.

| Protein | Function |
|---|---|
| ASAH1 | Hydrolase converting sphingolipid ceramide into sphingosine and free fatty acid. |
| CTSD | Lysosomal aspartyl protease active in intracellular protein breakdown and catalyzing alpha-synuclein degradation. CTSD levels increase with aging in human brain. |
| DPP7 | Lysosomal protease that cleaves dipeptides from the N-terminal of proteins. Expressed in cytoplasmic vesicles and lysosomes. |
| GLB1 | Exoglycosidase that hydrolyses β-galactosides into monosaccharides. Highly expressed in the cytoplasm and in lysosomes. |
| GNS | Lysosomal protease that hydrolyses 6-sulphate groups of the N-acetyl D-glucosamine 6-sulfate units of heparan and ketaran sulfate. |
| LGMN | Asparaginyl endopeptidase present in lysosomes. Involved in the processing of bacterial peptides or endogenous proteins for MHC class II presentation in the lysosomal/endosomal systems. |
| PPT1 | Glycoprotein involved in the catabolism of lipid-modified proteins in the lysosome. Mutations in *PPT1* are a cause of infantile neuronal ceroid lipofuscinosis 1. |
| SCPEP1 | Lysosomal matrix protein involved in kidney homeostasis. Expressed in kidney proximal convoluted tubules. |

Table 5: **List of iTRAQ candidates associated to the lysosomal compartment and their functions.** The open source Uniprot database (www.uniprot.org) was used for protein functional information.

| Protein | Function |
|---|---|
| CORO1C | Actin binding protein involved in cytokinesis, motility and signal transduction. Localised in cytosol and in F-actin-rich areas. |
| GPHN | Microtubule-associated protein involved in membrane protein-cytoskeleton interactions and in the glycine receptor clustering. |
| MPRIP | Actin-binding cytoskeletal protein which directs myosin phosphate to actin. Depletion of Mprip leads to increase of stress fibers. |
| PACSIN2 | Lipid-binding protein that promotes the tubulation of the membranes to which preferentially binds. Plays a role in intracellular vesicular transport and in the reorganisation of the actin cytoskeleton. |
| SEPT9 | Cytoskeletal GTPase with potential role in cytokinesis. Colocalises with actin stress fibers. |
| TUBB4B | Major constituent of microtubules, catalysing GTP-binding to allow its polymerisation. |

Table 6: **List of cytoskeletal iTRAQ candidates and their functions.**

| Protein | Function |
|---|---|
| COPS4 | Subunit of the COP9 signalosome that positively regulates the E3 ubiquitin ligase. |
| PSMC3 | 26S protease involved in the ATP-dependent degradation of ubiquitinated proteins. |
| PSMD3 | Regulatory subunit of 26S proteasome. |
| UBE3A | Ubiquitin protein ligase that functions as a cellular quality control by helping the degradation of the cytoplasmic misfolded proteins |
| USP14 | Proteasome-associated deubiquitinase which releases ubiquitin from ubiquitinated proteins ensuring regeneration of ubiquitin at the proteasome. |

Table 7: **List of iTRAQ candidates associated with the ubiquitin-proteasome system and their functions.**

| Protein | Function |
|---|---|
| DYNC1H1 | ATPase that serves as a molecular motor important in retrograde transport and protein trafficking. |
| TGFBRAP1 | Component of the CORVET complex involved in Rab5-Rab7 endosome conversion and in early endosome fusion. Plays a role in TGF-beta signaling. |
| VAMP1 | Vesicular protein involved in docking and/or fusion of transport vesicles to target membranes. |
| VAT1 | Membrane protein involved in the transport of synaptic vesicles. |

Table 8: **List of iTRAQ candidates associated to membrane recycling pathways and their functions.**

| Protein | Function |
|---|---|
| EEF1G | Subunit of the elongation factor complex 1 responsible for the enzymatic delivery of aminoacyl tRNAs to the ribosome. |
| EIF3D | Largest eukaryotic translation initiation factor that helps to dissociate ribosomal subunits 40S and 60S. |
| EIF3L | Component of the eukaryotic translation initiation complex (Eif3) required for initial steps of protein synthesis. |
| EIF5 | Translation initiation factor that interacts with the 40S initiation complex and link it, by GTP hydrolysis, with the 60S subunit. |
| EIF4G3 | Component of the protein complex eIF4F, involved in the recognition of the mRNA cap and recruitment of mRNA to the ribosome. |
| EWSR1 | RNA binding protein involved in RNA processing and transport. Mutations in EWSR1 gene cause Ewing sarcoma and ALS. |
| HNRNPA2 | Cytoplasmic ribonucleoprotein involved in pre-mRNA processing. |
| HNRNPK | Pre-mRNA binding protein. Plays important role in metabolism of hnRNAs and acts in p53 response to DNA damage. |
| HSPG2 | Large multidomain proteoglycan which binds extracellular matrix components in order to regulate endothelial barrier function. |
| NAA15 | Component of the N-terminal acetyltransferase A (NatA). NatA activity is important for development and neuronal growth. Mainly cytoplasmic and attached to ribosomes. |
| NCL | Major nucleolar protein in eukaryotic cells, associated with chromatin and pre-ribosomal particles. Induces chromatin decondensation via histone H1 binding. |
| SRP54 | Signal recognition protein involved in targeting nascent polypeptides to the endoplasmic reticulum. |
| VARS | Aminoacyl-tRNA synthetase localised in mitochondria. Important role in RNA translation. |

Table 9: **List of iTRAQ candidates associated with regulation of protein synthesis and their functions.**

| Protein | Function |
|---|---|
| FGF1 | Protein regulator of endothelial cell migration and proliferation and has important role in cell survival and cell division. |
| GPX1 | Cytoplasmic peroxidase that reduces lipid hydroperoxides to their corresponding alcohols and reduces free hydrogen peroxide to water. Protects erythrocytes from oxidative damage. |
| COQ4 | Component of ubiquinone and coenzyme Q biosynthetic pathways. |
| PRDX1 | Peroxidase eliminating peroxides generated during metabolism, involved in the response to oxidative stress. |
| PPCS | Cysteine ligase that catalyse the biosynthesis of coenzyme A from vitamin B5. |
| VWA8 | Coagulation factor with multiple roles in cell migration, basal membrane formation, malignant transformation and cell adhesion. |

Table 10: **List of iTRAQ candidates associated with oxidative stress response and cell survival with their functions.**

Given that there appeared to be common themes between subsets of proteins that were altered in abundance in response to Lrrk2 deficiency in vivo, the next question was whether some of the proteins might interact with each other physically. Probing publically available databases, I was able to reconstruct a network of protein interactions that included a subset of protein candidates (Fig. 3.6). Interestingly, two proteins in the network have previously been nominated as direct interactors of Lrrk2, Myosin Phosphatase Rho Interacting Protein (Mprip; (Meixner et al. 2011)) and tubulin beta 4b (Tubb4b; (Law et al. 2014)), the latter providing an indirect link to several other candidate responses to Lrrk2 deficiency.

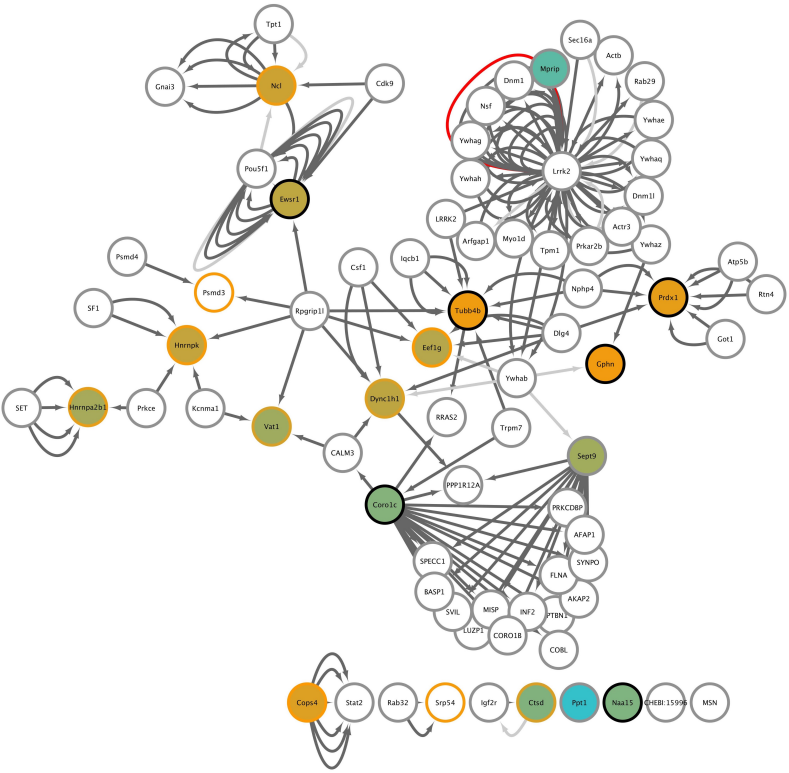


Figure 3.6: **iTRAQ Network Analysis.** Visualization of a candidate protein network generated from the Intact database queried using the list of differentially abundant proteins in LRRK2-KO kidneys versus controls. Colors indicate the relative fold change between genotypes from orange (lower in knockouts) to blue (higher in knockouts), with the center of the circles representing proteins recovered in the cytosol enriched fractions and the outside representing the microsomal enriched fractions. Grey symbols are proteins that were not represented in the iTRAQ datasets.

Collectively, these data nominate a series of novel candidates that respond to Lrrk2 deficiency in a physiological context. Prominent changes include alterations in protein synthesis and degradation, including several lysosomal proteases, and differential regulation of cytoskeletal-associated proteins.

### 3.2.4 Proteomic screen of LRRK2 G2019S mutant

To investigate the effect of LRRK2 most common pathogenic mutation, a second screen was performed. Given the utility of this approach in identifying underlying biological themes, the same technique with the same experimental design was next applied to G2019S-KI animals. If this allele had a dominant negative effect, as expected, then it would be possible to generate an overlapping list of protein alterations as in the knockout animals.

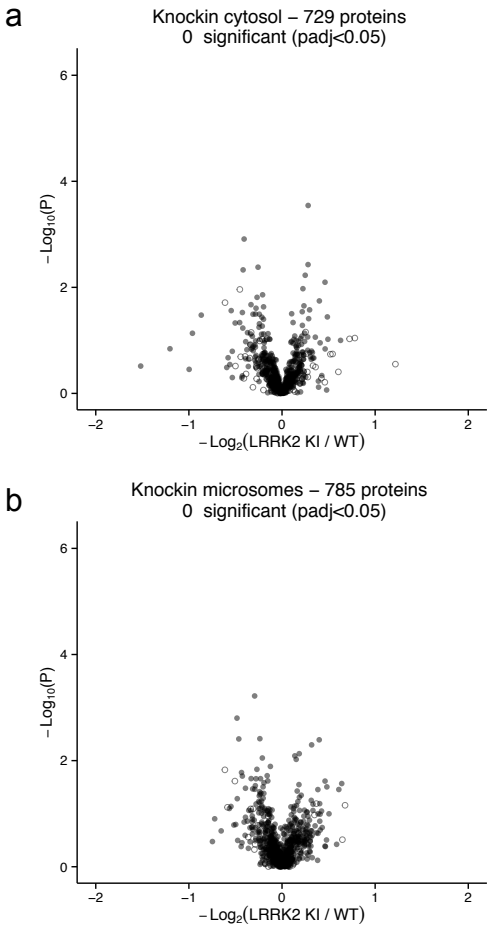


Figure 3.7: **iTRAQ proteomics of 12 month old LRRK2 G2019S kidneys cytosolic and microsomal fractions.** (a) Volcano plot of the 729 proteins quantified in the cytosol enriched fractions and (b) of the 785 proteins quantified in the microsome enriched fractions (n=5, Welch T-test, p values corrected using Benjamini-Hochberg post hoc test).

Kidney cytosolic and microsomal enriched fractions were obtained from 12 month-old LRRK2-G2019S heterozygous knockin and control mice. From two experimental runs for each fraction, I identified 729 unique proteins in the cytosolic enriched fractions and 785 unique proteins in the microsomal enriched fractions (Fig. 3.7). However, after multiple test correction, no significant differences in protein abundance between genotypes was detected in either fraction (Fig. 3.7).

Given that the number of proteins detected in each experiment varied and that iTRAQ ratios suffer from compression of dynamic range (Savitski et al. 2013) one concern was that the apparent negative result in the G2019S experiment was due to an underestimate of true differences. Therefore the KO and G2019S experiments were directly compared for those proteins detected in all experiments for each fraction. Using hierarchical clustering, I found that the KO samples separated from G2019S and the ten WT samples from two experiments, which were intermingled in the cytosol (Fig. 3.8, A) or microsomal fractions (Fig. 3.8, B). Plotting the log-2 fold differences in both iTRAQ experiments did not demonstrate any correlations between the differences in protein abundance related to genotype for cytosol (Fig. 3.9, A; Pearson's correlation between log2 fold differences, r= 0.0496, p=0.389, n=304 proteins) or microsomal (Fig. 3.9, B; Pearson's correlation between log2 fold differences, r= -0.0445, p=0.308, n=527 proteins) fractions.

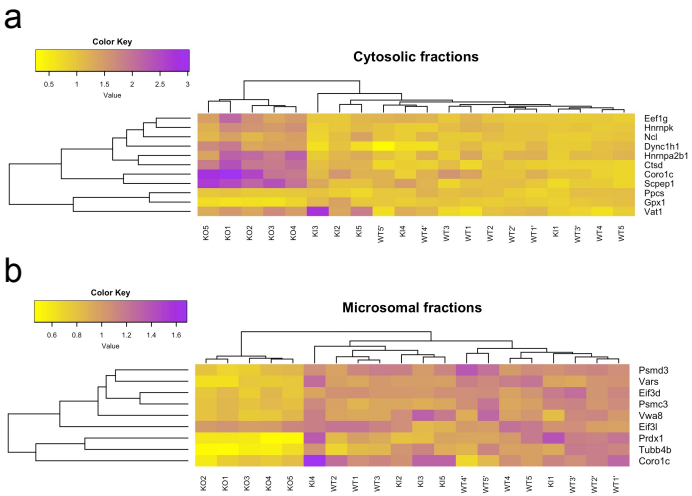


Figure 3.8: **Comparative analysis of LRRK2-KO and G2019S proteomic screens.** Heat maps of detected genes (nominal p <0.05) in cytosol enriched fractions (a) and microsome enriched fractions (b).

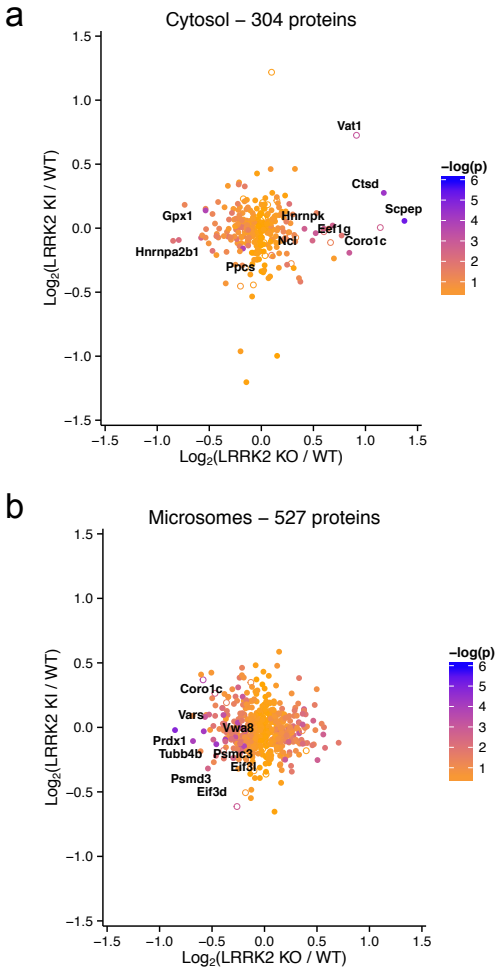


Figure 3.9: **Comparative analysis of LRRK2-KO and G2019S proteomic screens.** Correlation of fold-changes between G2019S-KI and LRRK2-KO, in cytosolic fractions (a) and microsomal fractions (b). P values represented by color scale corrected using Benjamini-Hochberg post hoc test.

### 3.2.5 Independent iTRAQ experiments in LRRK2-KO mice

I considered the hypothesis that the lack of effect of G2019S genotype might be due to the temporal separation between experiments. To address this, KO microsomal samples were re-run against WT controls as in the first iTRAQ experiment. Again, iTRAQ detected significant differences in genotype with an accumulation of several proteins in the microsomal fraction (Fig. 3.10, A) that was sufficient to separate genotypes using hierarchical clustering (Fig. 3.10, B).

Interestingly, in the second run of LRRK2-KO microsomal fractions, some of the hits previously observed as differentially regulated were reproducible. In particular, an increase in the lysosomal hydrolases Glb1 and Lgmn was detected. The lysosomal protease cathepsin A (Ctsa) was also increased in LRRK2-KO microsome enriched samples. As observed in the first screen, the protein peroxiredoxin 1 (Prdx1) was decreased in the second run of LRRK2-KO microsomal fractions.

In this independent iTRAQ run of LRRK2-KO microsomal fractions a significant increase in the protein galactosylceramidase (Galc) and prosaposin (Psap) was detected. Galc and Psap are two different lysosomal proteases involved in the catabolism of glicosphyngolipids (Lefrancois et al. 1999; Schulze and Sandhoff 2014). Increase in abundance in Galc and Psap might indicate an upstream role for LRRK2 in the regulation of this catabolic pathways.

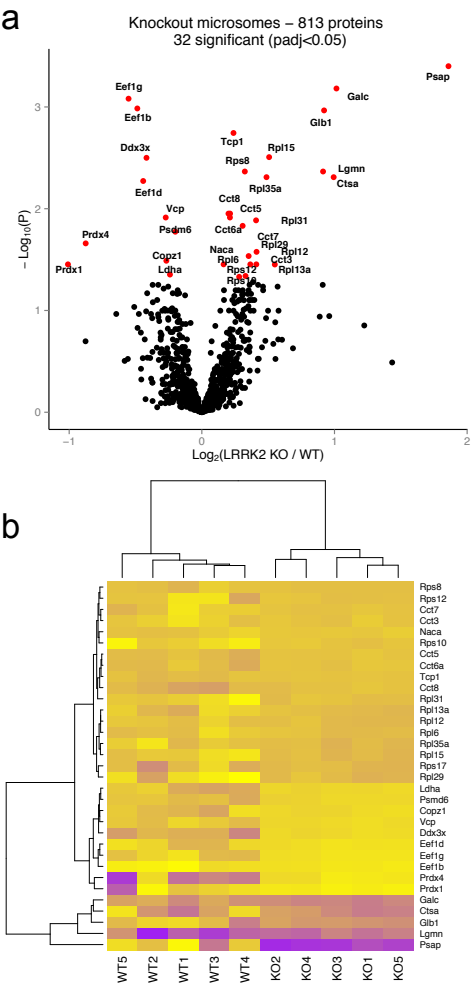


Figure 3.10: **Independent iTRAQ experiments in LRRK2-KO mice.** (a) Volcano plot and (b) heatmap of the microsomal fractions from LRRK2-KO and WT mice from the same samples as in Figure 4 and 5 but independently run on a temporally separate iTRAQ experiment.

Given the reproducibility of the results in the two LRRK2-KO screens, next the correlation between two proteomic datasets was performed. As expected, a positive correlation between the Log2 ratios of knockout to WT proteins was observed in the two runs (Fig. 3.11, a). However, again, no correlation was noted between knockout and knockin proteins (Fig. 3.11, b).

Overall, these results indicate that the G2019S allele in the heterozygous state in 12 month old mice kidneys do not cause proteome differences compared to the relatively strong effects of LRRK2 deficiency.

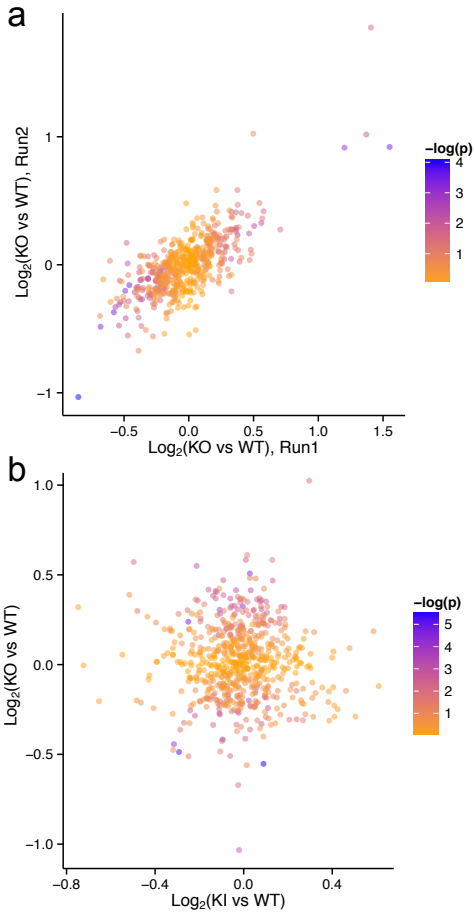


Figure 3.11: **Correlation between LRRK2-KO and G2019S proteomic screens.** There is a positive correlation of fold differences between genotypes for the second iTRAQ run of knockout kidneys against the first run (r = 0.7270) (a) but no correlation between fold differences for the second knockout run and the knockin animals (r = -0.0385) (b).

## 3.3 Discussion

### 3.3.1 iTRAQ proteomic screen reveals changes in protein abundance in LRRK2-KO kidneys compared to controls

Accumulating evidence supports a role for LRRK2 in vesicular trafficking and autophagy. Supporting this notion, LRRK2-KO mouse models display a severe kidney pathology characterised by a number of age-dependent phenotypic defects including impairments in protein degradation pathways resulting in accumulation of lysosomal proteases, increased oxidative stress and inflammation (Herzig et al. 2011; Tong et al. 2010). This phenotype is perhaps not surprising since, compared to brain, LRRK2 has the highest expression levels in kidneys. Moreover, the LRRK2 mammalian paralogue, LRRK1 is instead almost undetectable in kidneys (Biskup et al. 2007; Tong et al. 2010). As a result, functional redundancy between LRRK1 and LRRK2 is less likely in the kidney compared to other tissues. LRRK2-KO kidneys, therefore, represent a useful model to study LRRK2 biological function. In addition, the pathological features observed in this tissue mimic some aspects of proteinopathies such as PD and AD. In particular, defects in the autophagy-lysosomal pathway and cytoskeletal alterations are commonly implicated pathologies characterised by protein aggregate species. Therefore, to further investigate LRRK2 physiological function, two unbiased proteomic screens using knockout and knockin mutant were performed. LRRK2-KO proteomic screen revealed significant changes in different protein functional groups. These changes were not observed in the G2019S-KI screen.

It is likely that the lack of proteomic changes in the knockin screen is due to a lack of kidney phenotype in G2019S mice. This observation suggests that the G2019S mutant is not a loss of function, but also that the toxic gain of function associated

with the G2019S kinase activity increase might not affect LRRK2 function in the kidneys.

**LRRK2-KO increases lysosomal protease abundance**

A group of lysosomal proteins was significantly upregulated in LRRK2-KO fractions, consistent with phenotypes reported in the literature (Herzig et al. 2011; Tong et al. 2010). My results support changes in abundance of the lysosomal hydrolase cathepsin D previously reported in kidneys from LRRK2-KO mice (Tong et al. 2012). Cathepsin D deficiency has been correlated with α-synuclein accumulation in neurons, (Qiao et al. 2008). In line with multiple groups, the proteomic screen conducted in this project recovered a number of novel lysosomal proteins that accumulate in LRRK2 knockout kidneys. Among these proteases, mutations in CTSD, GNS, ASAH1 and in GLB1 are known to cause lysosomal storage disorders (Kaplan and Wolfe 1987; Koch et al. 1996; Kwak et al. 2015; Tyynelä et al. 2000; Zhou et al. 2012). Patients with lysosomal storage disorders e.g. Gaucher's disease or with homozygous mutations causing Gaucher's disease have a higher risk of PD (Beilina and Cookson 2016; Jose et al. 2008; Mielke et al. 2013; Schulze and Sandhoff 2014). Therefore, there is a clear correlation between lysosomal dysfunction and PD.

The observed accumulation of lysosomal enzymes might be a direct consequence of loss of LRRK2 or a compensatory mechanism. Lysosomal protease accumulation could be due to defective lysosomal function or to improper delivery to the lysosome. Alternatively, variations of vesicular pH can affect receptor-enzyme dissociation resulting in accumulation of enzyme precursors in pre-lysosomal compartments (Golabek et al. 2000). One possible interpretation of impaired lysosomal hydrolase turnover is a retromer misfunction leading to depletion or defective recycling of lysosomal enzyme receptors (Follett et al. 2014; Rojas et al.

2008). Collectively these results indicate that LRRK2 is important for lysosomal function and pathogenic LRRK2 mutations might cause lysosomal dysfunction contributing to PD pathogenesis.

**LRRK2-KO changes in vesicular proteins**

A number of vesicular-trafficking proteins was differentially regulated proteins in LRRK2-KO kidneys (3.2.2). Within this category, an increase in vesicle-associated membrane protein (Vamp1) and synaptic vesicle membrane protein (Vat1) was here reported. Vamp1 is important for the fusion of transport vesicles to their target membrane (Isenmann et al. 1998), and Vamp1 expression levels may modify AD risk (Sevlever et al. 2015). An increase in relative abundance of cytoplasmic dynein 1 heavy chain 1 (Dync1h1), the core subunit of the main retrograde motor dynein (Schiavo et al. 2013), was also detected in LRRK2-KO cyosolic fractions, perhaps indicating dysfunctional retrograde transport. Proteomic analysis of LRRK2-KO kidneys identified a significant decrease in Transforming Growth Factor Beta Receptor Associated Protein 1 (Tgfbrap1 or Vps3) which is a component of the CORVET complex, involved in membrane fusion and endo-lysosomal biogenesis in cooperation with Rab GTPases (Balderhaar et al. 2013; Peplowska et al. 2007). Depletion of CORVET complex subunits has been associated with early endosome accumulation. One possible hypothesis is that LRRK2 play a role in the conversion between early and late endosomes by regulating or stabilising the CORVET complex.

**LRRK2-KO cytoskeletal alterations**

LRRK2 has been reported to interact with multiple tubulin isoforms (Law et al. 2014). Proteomic data show major changes in cytoskeletal-associated proteins in LRRK2-KO fractions. In particular, alterations in Sept9, Pascin2, Coro1c, Gphn, Naa15 and tubulin were observed. A decrease in tubulin isoform Tubb2b abundance might indicate microtubules degradation, correlated with lower levels of the microtubule-bound protein Gphn. Microtubule stability is essential for organelles and vesicle transport, therefore, a logical consequence of LRRK2-KO loss of tubulin is a trafficking defect with missorting of cargos that are likely to accumulate or mislocalise. Actin cytoskeleton architecture is also of fundamental importance for vesicular trafficking dynamics and membrane fusion events (Jahraus et al. 2001). Interestingly, changes in actin cytoskeleton have also been reported in LRRK2-KO. Actin-binding protein Coro1c and cortactin-binding protein Naa15 (Paradis et al. 2008; Rybakin and Clemen 2005) are both increased in cytosolic LRRK2-KO fractions, but decreased in microsomal fractions. This differential expression might underlie changes in localisation of these proteins within signalling complexes.

**LRRK2-KO changes in UPS regulators**

An additional group of protein found modified in LRRK2-KO kidneys are ubiquitin-proteasome regulators (Cops4, Ube3a, Usp14). Cytoplasmic accumulation of ubiquitinated proteins is a common feature of PD. Deregulated proteasomal function is in agreement with the role of LRRK2 in protein homeostasis. In one study, LRRK2 overexpression seems to impair proteasome function resulting in accumulation of proteins and of proteasome substrates independently of LRRK2 kinase activity (Lichtenberg et al. 2011). This suggest that loss of LRRK2 could alter proteasomal degradation or transport of

ubiquitinated proteins to the proteasome, although these findings will need to be confirmed by independent groups.

**Alterations of protein translation regulators in LRRK2-KO**

Interestingly, proteomic analysis of LRRK2-KO kidneys resulted in significant changes in a subset of regulators of protein translation. Specifically, a decrease in a number of eukaryotic initiation factors, involved in the formation and stabilisation of the initiation complex (Eif5, Eif3l, Eif4g3) and an increase in ribosomal proteins RPs (Rpl12, Rpl15, Rpl29, Rpl31, Rpl35a, Rpl13a, Rpl6, Rps12, Rps8) was reported. Misregulation of protein translation can result in misfolding and subsequent protein aggregation, a common feature in neurodegenerative disease including PD.

Previous studies support a role for LRRK2 in transcriptional and translational control (Imai et al. 2008; Pons et al. 2012). Microarray analysis comparing fibroblasts carrying LRRK2 G2019S mutation with normal controls failed to report significant differences in basal gene expression (Devine et al. 2011). There is evidence linking LRRK2 with the TOR/4E-BP1 pathway (Imai et al. 2008). LRRK2 transient knockdown results in significant loss of 4E-BP1 protein and increased cell proliferation (Pons et al. 2012). These results are consistent with the proteomic data here described. One potential interpretation is that loss of LRRK2 could induce hyperplasia in kidneys, which appear significantly larger compared to controls at certain ages. Additionally, deregulation in protein synthesis pathways might correlate with accumulation of misfolded proteins observed in LRRK2-KO kidneys, resulting in the deposition of lipofuscin granules.

**LRRK2-KO, glycosphingolipids and ceramide metabolism**

Finally, increased levels of proteins involved in the catabolism of glycosphingolipids such as Galc and Psap, were reported. Higher levels of plasma ceramide and sphyngolipids metabolism defects have been documented in sporadic PD or in PD patients who carry mutations in the gene beta-glucosidase (GBA) and correlate with cognitive impairments (Mielke et al. 2013). One study, comparing different levels of brain extracted sphingolipids, showed a significant increase in GBA1 substrate ceramide and lower GBA1 expression levels in LRRK2-KO mice compared to controls (Ferrazza et al. 2016). Although further validation is needed to confirm these results, these data suggests that loss of LRRK2 may affect ceramide metabolism.

Together, these observations might support the hypothesis that LRRK2 is an essential scaffold acting upon multiple signalling pathways and affecting vesicle trafficking, membrane fusion, cytoskeletal dynamics, protein synthesis and degradation.

# 4 Validation of iTRAQ proteomic hits

## 4.1 Introduction

Despite mutations in LRRK2 being clearly associated with familial PD (Cookson 2010; Zimprich et al. 2004), genetically modified mouse models carrying LRRK2 pathological mutations do not have neurological symptoms (Tong et al. 2010). Similarly, the LRRK2-KO mouse models tested in these experiments do not develop neurodegeneration or neuropathological features. However, as previously discussed (See section 3), LRRK2-KO display gross morphological kidney abnormalities and undergo an age-dependent renal atrophy (Herzig et al. 2011; Tong et al. 2010, 2012). Therefore, LRRK2-KO kidneys represent a system in which the function of LRRK2 can be analysed.

In order to investigate the pathways affected by loss of LRRK2, a proteomic study of LRRK2-KO and LRRK2 G2019S knockin mouse kidneys was performed. This study revealed differences in protein abundance in several candidates representative of biological categories such as lysosomal proteases and cytoskeletal proteins in the LRRK2-KO kidneys. In contrast to LRRK2-KO, these changes were not observed in the mutant G2019S kidneys.

As with many techniques, proteomic screens are likely to contain a number of false positive hits due to the size of the data (Reiter et al. 2009). To provide validation using an orthologous technique to determine protein levels, immunoblots were performed for several proteins detected at different levels in the cytosol and microsome enriched fractions from LRRK2-KO and controls in iTRAQ. G2019S knockin animals were included to allow for a direct comparison to knockout.

Histological examination of LRRK2-KO kidney sections has previously identified the presence of autofluorescent aggregates in the epithelial cells of the proximal tubules of the cortical region (Tong et al. 2012). To characterise the histopathological changes in LRRK2-KO kidneys, immunohistochemical analysis of kidney sections was performed. Endo-lysosomal markers in combination with antibodies against candidate proteins were used to investigate changes in subcellular localisation. Additionally, superresolution imaging of histological sections was conducted to allow in depth characterisation of the identified vacuolated structures in LRRK2-KO kidneys.

Finally, to answer the question whether any of the identified protein candidates was significantly altered in the brain, immunoblots using multiple brain regions were conducted. Tissue samples of cerebral cortex, hippocampus and striatum were collected from the same mice tested in proteomics.

In summary, a proteomic study of LRRK2-KO kidney subcellular fractions identified a number of candidate proteins differentially abundant compared to controls. These proteins were not detected as significant in LRRK2 G2019S knockin kidneys. Immunoblot validation of iTRAQ candidates confirmed differences in lysosomal and cytoskeletal proteins in LRRK2-KO kidneys. These differences were absent in the brain of LRRK2-KO mice. By histological analysis of kidney sections, I identified enlarged structures positive for lysosomal markers, indicating the presence of a lysosomal trafficking defect in absence of LRRK2.

## 4.2 Results

### 4.2.1 LRRK2-KO kidney lysosomal changes

For technical validation of the detected protein hits, I performed immunoblots using cytosol enriched and microsome enriched fractions employed for iTRAQ proteomics. First, I confirmed the expected total absence of LRRK2 in both fractions in LRRK2-KO animals (Fig. 4.1, 4.2). Candidate selection for validation was based on availability of commercial antibodies for proteins nominated from the iTRAQ experiment as being significantly deregulated in LRRK2-KO fractions, compared to controls, namely lysosomal proteases and cytoskeletal-associated proteins. The endogenous control used in every experiment was β-actin, which was run in a separate blot and not reprobed.

The proteomic analysis predicted that cathepsin D, one of the most abundant lysosomal proteases (Banay-Schwartz et al. 1992; Qiao et al. 2008), was significantly higher in the LRRK2-KO cytosolic enriched fractions compared to the controls (p adjusted = 0.004, Welch's t-test with Benjamini-Hochberg FDR correction, n=5 animals); (Fig. 3.3). Immunoblot results confirmed higher levels for both mature (p = 0.0001, WT *vs* LRRK2-KO; p = 0.0001, LRRK2-KO *vs* G2019S-KI, Bonferroni post-hoc test from one-way ANOVA) and precursor (p = 0.0004, WT *vs* LRRK2-KO; p = 0.0003, LRRK2-KO *vs* G2019S-KI) forms of cathepsin D in LRRK2-KO samples compared to controls (Fig. 4.1). Consistent with the iTRAQ data, no differences in either form of cathepsin D was observed between WT and LRRK2-G2019S animals (Fig. 4.1).

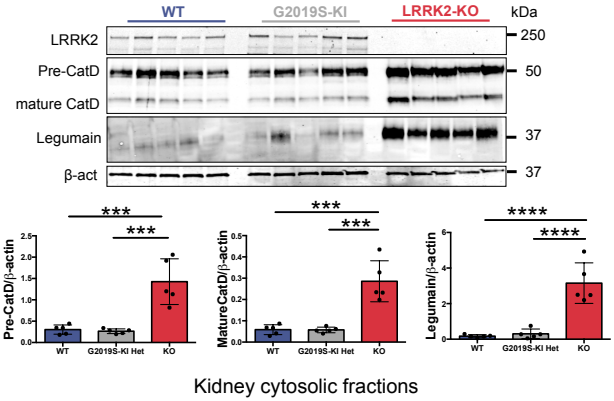


Figure 4.1: **Cathepsin D and Legumain are increased in LRRK2-KO cytosolic fractions**. Immunoblots for LRRK2 and the protein of interest cathepsin D and legumain normalised for the loading control β-actin in the cytosolic enriched fractions. Molecular weight markers are indicated on the left in kilodalton (kDa). Immunoblot quantifications are shown in the lower panels (Bonferroni post-hoc test from one-way ANOVA, n=5 animals). ∗P<0.05, ∗∗P<0.01, ∗∗∗ P<0.001, ∗∗∗∗ P<0.0001.

Although cathepsin D was not reliably detected in the microsomal enriched fractions using iTRAQ, the protein was visualised using western blotting. Both the mature (p = 0.0006, WT *vs* LRRK2-KO; p = 0.0003, LRRK2-KO *vs* G2019S-KI) and precursor forms (p = 0.0014, WT *vs* LRRK2-KO; p = 0.0014, LRRK2-KO *vs* G2019S-KI) of cathepsin D were higher in the LRRK2-KO, but not in LRRK2-G2019S, microsomal enriched fractions compared to wild-type controls (Fig. 4.2).

The lysosomal protease legumain (Lgmn) was more abundant in the cytosolic fraction of KO compared to controls by iTRAQ (p adjusted = 0.036). Legumain is an asparaginyl endopeptidase encoded by the gene LGMN and involved in MHC class II antigen presentation in the lysosomal/endosomal system (Dall and Brandstetter 2016). Immunoblots confirmed the increase in the mature form of legumain (37kDa) (p <0.0001, WT *vs* LRRK2-KO; p <0.0001, LRRK2-KO *vs* G2019S-KI; Fig. 4.1). Legumain was not detected in the G2019S iTRAQ screen and I did not detect any difference in legumain expression in immunoblot of LRRK2-G2019S cytosolic enriched fractions compared to controls (Fig. 4.1).

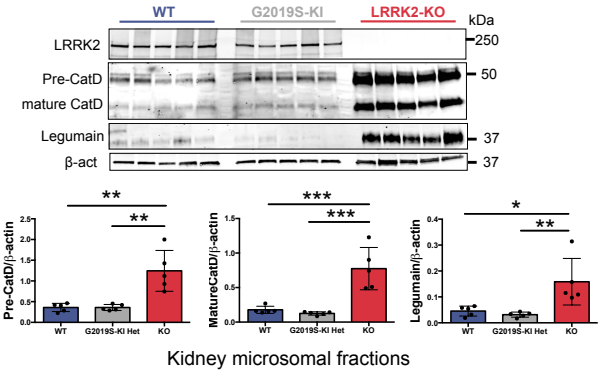


Figure 4.2: **Cathepsin D and Legumain are increased in LRRK2-KO microsomal fractions**. Immunoblots for LRRK2 and the protein of interest cathepsin D and legumain normalised for the loading control β-actin in the microsomal enriched fractions. Immunoblot quantifications are shown in the lower panels (Bonferroni post-hoc test from one-way ANOVA, n=5 animals). ∗P<0.05, ∗∗P<0.01, ∗∗∗ P<0.001, ∗∗∗∗ P<0.0001.

Legumain was shown to be as increased in LRRK2-KO microsomal enriched fractions by iTRAQ (p adjusted = 0.049), which was confirmed using immunoblotting in KO samples (p = 0.0173, WT *vs* LRRK2-KO; p = 0.0082, LRRK2-KO *vs* G2019S-KI). I did not observe any difference of these proteins in G2019S knockin samples (Fig. 4.2).

### 4.2.2 LRRK2-KO kidney cytoskeletal changes

Next, a series of cytoskeletal-associated proteins nominated by proteomic screen of LRRK2-KO kidneys were examined. iTRAQ results indicated that N(Alpha)-Acetyltransferase 15, (NatA Auxiliary Subunit, Naa15), which has been reported to interact with cortactin (Paradis et al. 2008) and is therefore potentially recruited to the cytoskeleton, was lower in LRRK2-KO microsomal fractions and higher in LRRK2-KO cytosolic fractions compared to controls. Lower protein levels of Naa15 were confirmed in microsomal fractions (p = 0.0003, WT *vs* LRRK2-KO; p = 0.0059, LRRK2-KO *vs* G2019S-KI) but, in contrast to the iTRAQ results, Naa15 expression was lower, not higher, in cytosolic enriched samples (p = 0.011, WT *vs* LRRK2-KO). Interestingly, Naa15 protein expression was significantly increased in G2019S cytosolic fractions, compared to LRRK2-KO or wild type samples (p<0.0001, LRRK2-KO *vs* G2019S-KI; p<0.0001, WT *vs* G2019S-KI) (Fig. 4.3).

The actin binding protein coronin-1C (Coro1c) was nominated in the iTRAQ experiments as more abundant in the LRRK2-KO mice compared to controls. The antibody against Coro1c detected two distinct bands by immunoblot. I observed a decrease of the upper band (53kDa in the LRRK2-KO kidneys). In addition, a lower molecular weight band (37kDa) was detected as significantly increased by LRRK2-KO (p<0.001, WT *vs* LRRK2-KO; p<0.001, LRRK2-KO *vs* G2019S-KI)

(Fig. 4.3). Possibly, the lower band is likely to correspond to the unique peptide detected as increased in the iTRAQ dataset and quantified from the immunoblots.

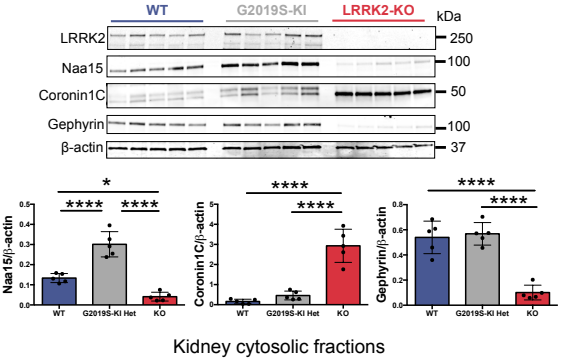


Figure 4.3: **Cytoskeletal alterations in LRRK2-KO kidney cytosolic fractions** Immunoblots for LRRK2 and the protein of interest Coro1c, Naa15 and Gphn normalised for the reference protein β-actin in the cytosolic enriched fractions. Immunoblot quantifications are shown in the lower panels (Bonferroni post-hoc test from one-way ANOVA, n=5 animals). ∗P<0.05, ∗∗P<0.01, ∗∗∗ P<0.001, ∗∗∗∗ P<0.0001.

The microtubule-associated protein gephyrin (Gphn) was found significantly decreased in LRRK2-KO microsomal enriched fractions in iTRAQ (p adjusted = 0.021), which I validated using immunoblotting in cytosolic enriched (p<0.0001, WT *vs* LRRK2-KO; p<0.0001, LRRK2-KO *vs* G2019S-KI) and microsomal enriched fractions (p = 0.0025, WT *vs* LRRK2-KO; p = 0.0073, LRRK2-KO *vs* G2019S-KI) (Fig. 4.3, 4.4). In the second iTRAQ screen of LRRK2-G2019S kidneys, gephyrin was detected only in cytosolic enriched fractions but was not

significantly different between mutant and controls. I did not observe a significant difference in immunoblot from both LRRK2-G2019S enriched fractions in gephyrin levels in either fraction (Fig. 4.3, 4.4).

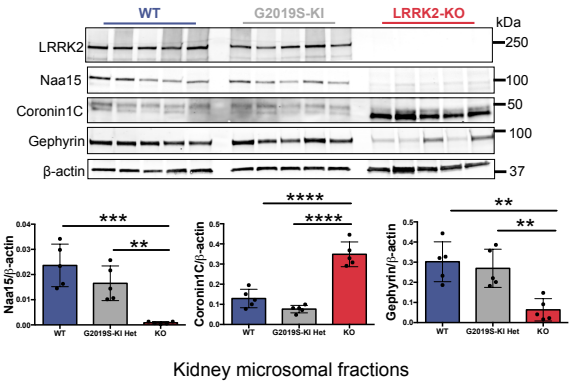


Figure 4.4: **Cytoskeletal alterations in LRRK2-KO kidney microsomal fractions** Immunoblots for LRRK2 and the protein of interest Coro1c, Naa15 and Gphn normalised for the reference protein β-actin in the microsomal enriched fractions. Immunoblot quantifications are shown in the lower panels (Bonferroni post-hoc test from one-way ANOVA, n=5 animals). ∗P<0.05, ∗∗P<0.01, ∗∗∗ P<0.001, ∗∗∗∗ P<0.0001.

A significant difference in acetylated-tubulin, a marker of microtubule stability, relative to α/β-tubulin was detected in cytosolic fractions from KO animals compared to wild type (p = 0.0171, WT *vs* LRRK2-KO; p = 0.0132, LRRK2-KO *vs* G2019S-KI). Additionally, α/β-tubulin normalised expression levels were significantly lower in LRRK2-KO cytosolic fractions compared to G2019S and controls (p = 0.0002, WT *vs* LRRK2-KO; p = 0.0001, LRRK2-KO *vs* G2019S-KI)

(Fig. 4.5). Similarly, in the microsomal fractions, α/β-tubulin normalised expression levels were lower in KO compared to G2019S, but this difference was not significant between KO and controls (p = 0.0096 LRRK2-KO *vs* G2019S-KI) (Fig. 4.6). I observed no significant differences between G2019S and wild type animals (Fig. 4.5, 4.6).

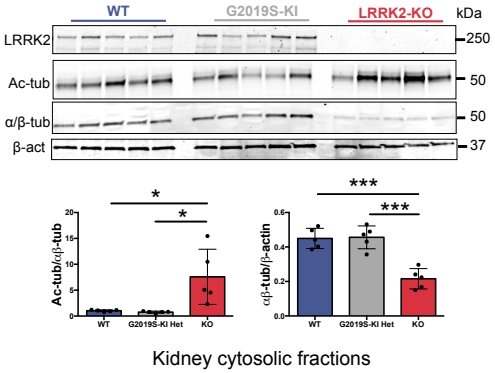


Figure 4.5: **Microtubule alterations in LRRK2-KO kidney cytosolic fractions** Immunoblots for LRRK2 and the protein of interest acetylated-tubulin and α/β-tubulin normalised for the loading control β-actin in the cytosolic enriched fractions. Immunoblot quantifications are shown in the lower panels (Bonferroni post-hoc test from one-way ANOVA, n=5 animals). ∗P<0.05, ∗∗P<0.01, ∗∗∗ P<0.001.

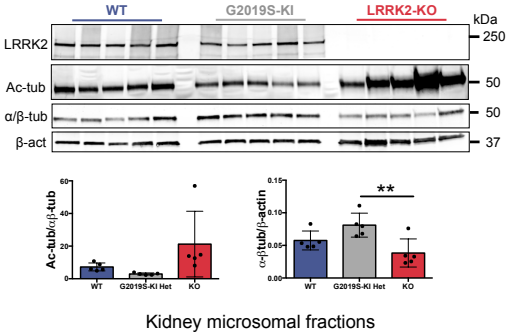


Figure 4.6: **Microtubule alterations in LRRK2-KO kidney microsomal fractions** Immunoblots for LRRK2 and the protein of interest acetylated-tubulin and α/β-tubulin normalised for the loading control β-actin in the microsomal enriched fractions. Immunoblot quantifications are shown in the lower panels (Bonferroni post-hoc test from one-way ANOVA, n=5 animals). $*P<0.05$, $**P<0.01$, $*** P<0.001$.

Proteomic approaches based on quantification with isobaric labelling can underestimate peptide abundance (Savitski et al. 2013). The presence of coeluting peptides contaminating the fractions, affecting the accuracy of iTRAQ quantifications, has been reported (Savitski et al. 2013). This issue is known as ratio compression (Savitski et al. 2013) and suggests that the initial proteomic screen may have underestimated some differences between genotypes (Fig. 4.7). Overall, by correlating fold differences between genotypes using immunoblotting *versus* iTRAQ, the differences were larger using immunoblot, consistent with the ratio compression phenomenon.

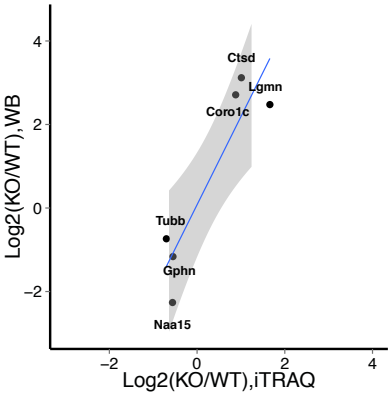


Figure 4.7: **Correlation between iTRAQ proteomics and immunoblot results.** Comparison of the log2 fold expression (KO/WT) using the iTRAQ data compared to the immunoblot data indicating larger differences detected via immunoblot compared to iTRAQ proteomics. Data were plotted in ggplot2 using the smooth (method = "lm") function of R (www.rstudio.com). X axis indicates the Log2 fold of KO/WT ratio measured by iTRAQ, the y axis indicates the Log2 fold of KO/WT ratio quantified by immunoblot (WB).

Collectively, I validated a subset of proteins differentially expressed between LRRK2-KO and wild type kidneys using an orthologous technique, with the exception being Naa15 in the cytosolic fraction. Consistent with the proteomic data, no differences between wild type and G2019S knockin animals was reported apart from Naa15 which is significantly increased in the cytosol, in contrast to knockout. These results strongly suggest that G2019S and LRRK2-KO have distinct effects on the proteome, and that in absence of LRRK2 there are several

changes in lysosomal and cytoskeletal protein abundance that suggest a defect in protein trafficking and degradation.

### 4.2.3 Histological analysis of kidneys

To provide a third independent method to validate the results obtained in the LRRK2-KO proteomic screen and to characterise the LRRK2-KO kidney alterations, I performed immunofluorescent staining of 5-6 month old kidney sections from wild-type and LRRK2-KO. In this independent cohort of animals, as expected, LRRK2-KO kidneys were abnormally larger and darker in colour than their wild type counterparts (Fig. 3.1).

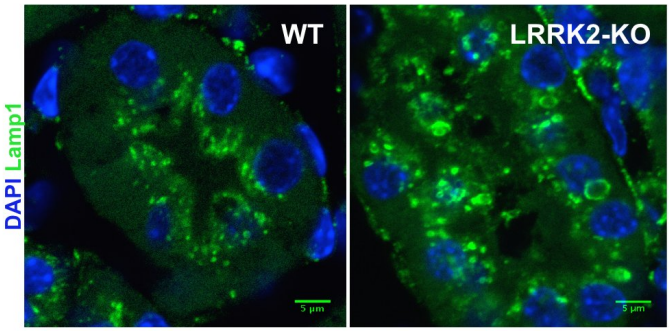


Figure 4.8: **Lamp1 positive structures in LRRK2-KO and control kidney sections.** Representative confocal images of wild-type and LRRK2-KO (5-6 month-old, n=3) kidney histological sections stained with the late-endosome/lysosomal marker Lamp1 (Lamp1 rat monoclonal antibody, AlexaFluor 488 secondary antibody and DAPI staining). Scale bar: 5µm.

Given the robust and consistent changes in lysosomal proteases in LRRK2-KO kidneys, I performed immunostaining of cortical kidney sections from LRRK2-KO

and control kidneys with the lysosomal marker Lamp1 (Fig. 4.8). As expected, LRRK2-KO sections are characterised by increased autofluorescence and the presence of larger Lamp1-positive intracellular structures indicating an abnormal accumulation of lysosomal content in LRRK2-KO kidneys (Fig. 4.8).

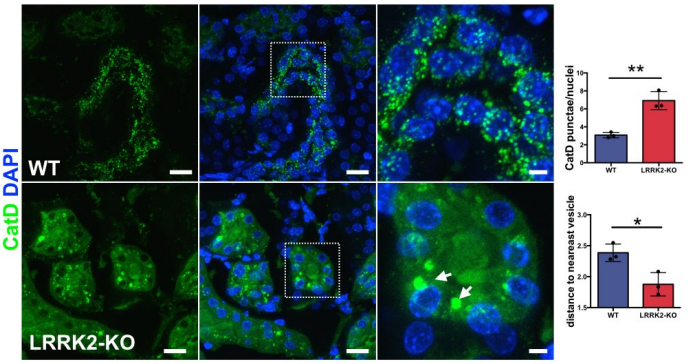


Figure 4.9: **Histological analysis of cathepsin D (CatD) in LRRK2 kidneys.** Confocal imaging of wild-type and LRRK2-KO (5-6 month-old, n=3 biological replicates) for CatD (CatD rabbit polyclonal antibody, AlexaFluor 488 secondary antibody and DAPI staining). Scale bar: 20µm (5µm for magnification). On the right, quantifications of number of CatD puntae per nuclei, and distance between the nearest vesicle (Student t test, n=3 mice, 15 images per genotype, data points represent averaged values of punctae from each blind quantification using a combination of custom algorithms in Fiji (NIH) and Imaris (Biplane, Inc.)). $*P<0.05$, $**P<0.01$.

Next, to investigate the alterations in lysosomal content in LRRK2-KO kidneys and to validate with an independent technique the iTRAQ results, I used the available cathepsin D antibody, previously employed for immunoblot, to stain LRRK2-KO and control kidney sections. The renal cortex, containing proximal and distal tubules, was visualised by confocal imaging. Cathepsin D was reliably detected in kidney sections (Fig. 4.9). Cathepsin D positive punctae were clearly

enlarged in LRRK2-KO kidney proximal tubules compared to WT (Fig. 4.9). The number of cathepsin D punctae was significantly higher in LRRK2-KO compared to WT (p = 0.0032, WT *vs* LRRK2-KO, Unpaired t test, n=3 animals) (Fig. 4.9). The distance between punctae was significantly lower between WT and LRRK2-KO, indicating a tendency to cluster in LRRK2-KO kidney cells (p= 0.0201, WT *vs* LRRK2-KO) (Fig. 4.9). Together these experimental observations indicate that LRRK2-KO kidneys have microscopic alterations in their morphology displaying endo-lysosomal clusters and increased autofluorescence compared to control kidneys.

### 4.2.4 Lamp1 and Cathepsin D vacuolated endosomes in LRRK2-KO kidneys

Cathepsin D is a major lysosomal protease that is transported, via the M6PR, from the trans-Golgi network (TGN) to the lysosome. As previously observed, cathepsin D is accumulating in LRRK2-KO kidneys, clustering in endo-lysosomal structures. However, the nature of these structures was still unclear. To address this question, I co-stained of LRRK2-KO and control kidney sections with Lamp1 (Fig. 4.10). As expected, Lamp1 partially colocalised with cathepsin D in control sections, highlighting a punctate pattern. In LRRK2-KO sections, as previously observed (Tong et al. 2012), cathepsin D was identified in vacuolated structures. In LRRK2-KO kidney sections, cathepsin D localises in the lumen of these structures and is visibly distinguishable from Lamp1, which highlights the membrane of the vesicle (Fig. 4.10).

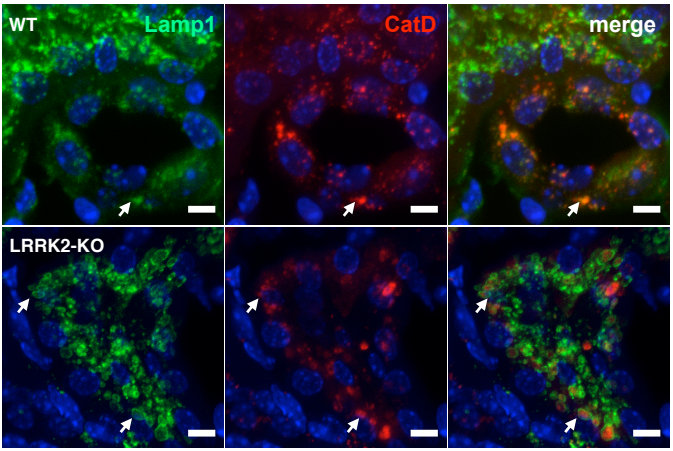


Figure 4.10: **Cathepsin D colocalisation with Lamp1 in vacuolated endosomes in LRRK2-KO kidneys.** Histological analysis of CatD and Lamp1 in LRRK2 kidneys. Confocal imaging of wild-type and LRRK2-KO kidney (5-6 month-old, n=3) for CatD (CatD rabbit polyclonal antibody, AlexaFluor 568 secondary antibody), Lamp1 (Lamp1 rat monoclonal, AlexaFluor 488 secondary antibody) and DAPI staining). Scale bar: 5µm.

### 4.2.5 Super-resolution imaging of kidney sections

To better discern cathepsin-D and Lamp1 positive vesicles, the cortical area of control and LRRK2-KO kidney sections was visualised using super-resolution microscopy (Fig. 4.11). I could observe that cathepsin D partially colocalised with Lamp1. Again, in the LRRK2-KO sections, I detected larger vacuolated lysosomes/late endosomes. At this resolution, the two markers are more distinguishable. Lamp1 decorates the membrane of these enlarged vesicles, whereas

cathepsin D localises in the lumen. By contrast, these vacuolated structures are absent in control sections of kidney cortical area (Fig.4.11).

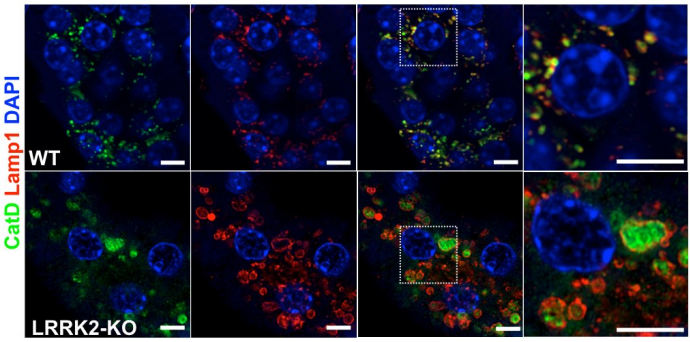


Figure 4.11: **Super-resolution imaging of LRRK2-KO and control kidneys.** Histological analysis of CatD and Lamp1 in LRRK2 kidneys. Representative Airy scan images of wild-type and LRRK2-KO kidney (5-6 month-old) for CatD (CatD rabbit polyclonal antibody, AlexaFluor 568 secondary antibody), Lamp1 (Lamp1 rat monoclonal, AlexaFluor 488 secondary antibody) and DAPI staining. Scale bar: 5µm.

Together, histological analysis of LRRK2-KO kidneys revealed the presence of a number of intracellular alterations including accumulation of lysosomal proteases and endo-lysosome clusters. These histopathological features indicate the presence of a trafficking defect of acid hydrolases in LRRK2-KO kidneys, which seem unable to recycle lysosomal enzymes resulting in protein accumulation in larger and vacuolated compartments.

### 4.2.6 No changes in iTRAQ hits in LRRK2-KO cerebral cortex

To investigate whether changes detected in the LRRK2-KO kidneys could also be observed in neural tissue, I performed immunoblots on cerebral cortex, hippocampus and striatum, brain regions usually affected in neurodegenerative diseases, from the same 12 month-old mice used for iTRAQ proteomics.

As previously mentioned, LRRK2 mouse models do not display any reproducible neurodegenerative feature or detectable brain pathology (Tong et al. 2012). LRRK2-KO brain morphology, colour and texture appear indistinguishable from controls (Tong et al. 2010). Only modest electrophysiological and cell signaling changes have been reported in brains from LRRK2-KO mice (Berwick and Harvey 2013; Hinkle et al. 2012; Maekawa et al. 2012; Paus et al. 2013). Given the absence of a neurological phenotype in LRRK2-KO mice, my initial hypothesis was to observe no significant differences in any of the iTRAQ candidates between knockout and controls in any brain region.

First, I analysed total homogenates from LRRK2-KO and control cerebral cortex by immunoblot (n=5). In these samples, I did not detect significant difference between genotypes for most of the proteins tested (Fig. 4.12). The immunoblots in figure 4.12 show 4 independent mice.

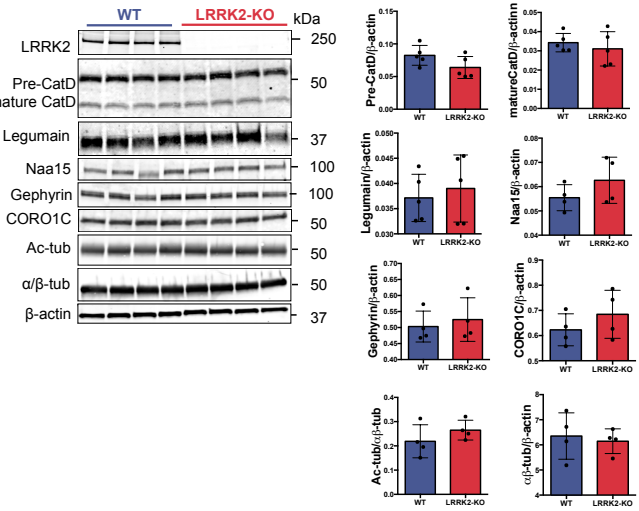


Figure 4.12: **Kidney proteomic hits in LRRK2-KO cerebral cortex.** Immunoblots for the iTRAQ candidate proteins in total homogenates from cerebral cortex and relative quantifications (Student t test, n=5 animals, P >0.05).

### 4.2.7 No changes in iTRAQ hits in LRRK2-KO striatum

Next, I analysed total homogenates from LRRK2-KO and control striatum by immunoblot (n=5). PD symptoms usually manifest where loss of dopaminergic neurons occurs in the striatum and LRRK2 is highly expressed in this tissue (Giesert et al. 2013). Again, I did not observe significant differences between genotypes for the proteins tested by immunoblots from striatal samples (Fig. 4.13).

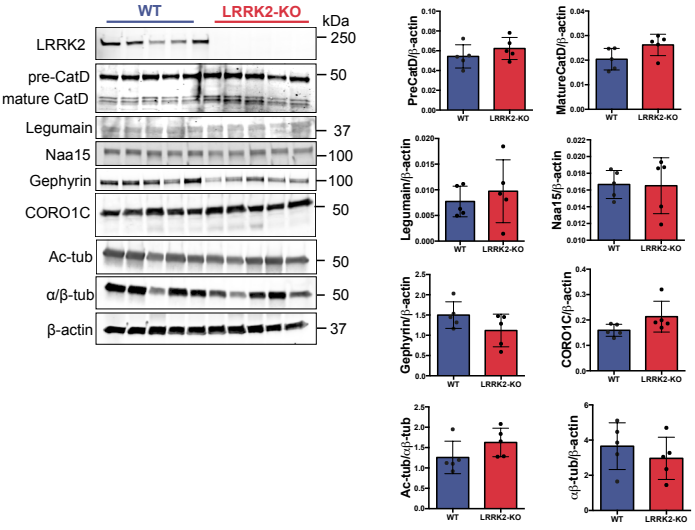


Figure 4.13: **Kidney proteomic hits in LRRK2-KO striatum.** Immunoblots for the iTRAQ candidate proteins in total homogenates from striatum and relative quantifications (Student t test, n=5 animals, P >0.05).

### 4.2.8 Gephyrin in LRRK2-KO hippocampus

Next, to test expression levels of iTRAQ hits in the hippocampus, I performed immunoblots from total homogenates of LRRK2-KO and control hippocampi. Hippocampal atrophy has been recognized as a biomarker of initial cognitive decline in PD, as well as AD (Henneman et al. 2009; Wiese et al. 2007). Here, no significant differences were detected in iTRAQ hits between genotypes, with the exception of gephyrin. In hippocampi from LRRK2-KO mice the levels of gephyrin were lower compared to wild type controls ($p = 0.0134$, WT *vs* LRRK2-KO, t-test,

n=5 animals). I observed this difference only in the hippocampus and not in other brain regions tested (Fig. 4.14). This result suggests a localised and specific role for LRRK2 in the hippocampus that might correlate with LRRK2 interaction with microtubules (Law et al. 2014). However, further validation is needed as it could represent a false positive.

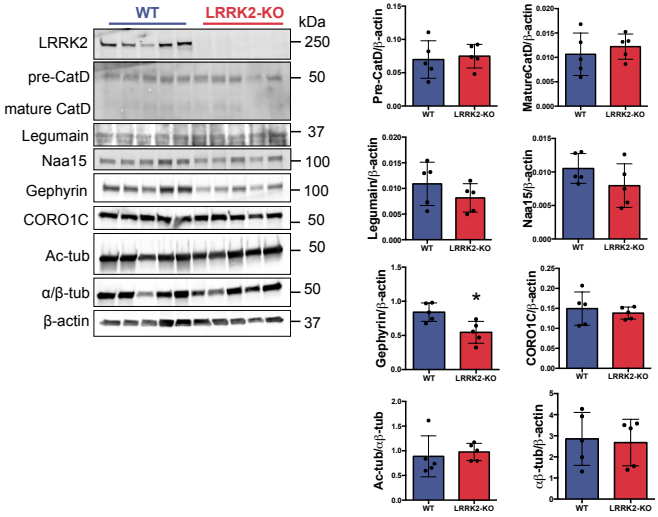


Figure 4.14: **Gephyrin downregulation in LRRK2-KO hippocampus.** Immunoblots for the iTRAQ candidate proteins in total homogenates from LRRK2-KO hippocampi and relative quantifications (Student t test, n=5 animals). $*P<0.05$.

In conclusion, taking these results together, the effects of LRRK2 deficiency in the brain seem more modest than those in the kidney. These observations might

indicate that the differences are too subtle to be detected. One way to address this problem is to increase the statistical power.

## 4.3 Discussion

Proteomic screens aim to characterise the proteome and changes in protein abundance. This screening approach generates large and complex datasets with a significant false positive rate (Reiter et al. 2009). Therefore, it is important to validate the set of candidate hits with orthologous techniques. In the LRRK2-KO proteomic screen, I observed differences in abundance in several categories of proteins (See GO analysis, Chapter 1). In particular, I detected differences in lysosomal proteases, cytoskeletal proteins and translational regulators. Considering the established role of LRRK2 in endo-lysosomal trafficking (Alegre-Abarrategui et al. 2009) and LRRK2 interaction with microtubules (Law et al. 2014), technical validation was focused on two major groups of proteins identified, namely lysosomal and cytoskeletal proteins, and a subset of proteomic hits was confirmed as differentially abundant in LRRK2-KO kidneys.

### 4.3.1 Loss of LRRK2 results in lysosomal protein alterations

Previous findings report an increase in the lysosomal protease cathepsin D in LRRK2-KO kidneys (Herzig et al. 2011; Tong et al. 2010, 2012). Consistent with these prior data, both precursor and mature form of cathepsin D were dramatically increased LRRK2-KO compared to controls and G2019S cytosolic and microsomal fractions. Similarly, the mature form of the lysosomal protease legumain was increased in both LRRK2-KO fractions. These observations suggest a role for LRRK2 in trafficking and/or maturation of these lysosomal proteases.

LRRK2 contains several protein interaction domains and has frequently been proposed as a scaffolding protein. In particular, LRRK2 is part of a multiprotein complex that promotes sorting of trans-Golgi-derived vesicles (Beilina et al. 2014).

Removal of LRRK2 from this complex might therefore impair the normal trafficking of these vesicles (Beilina et al. 2014). The observed accumulation of lysosomal proteases in LRRK2-KO kidneys could indicate that defective vesicle recycling leads to improper degradation of lysosomal content. Granular pigments called lipofuscin granules, composed of highly oxidised undigested proteins (Sulzer et al. 2008), precipitates in LRRK2-KO kidneys and in several neurodegenerative diseases with lysosomal storage dysfunction. Together, these findings suggest that absence of LRRK2 might alter the turnover of vesicular components leading to accumulation of undigested proteins.

Kidneys are highly specialised in secretion, and therefore, tight regulation of proteostasis is crucial for kidney health and function. In particular, one of the main cell mechanisms to maintain proteostasis is the autophagy pathway which has been suggested as a promising therapeutic target in acute kidney injury (Fougeray and Pallet 2014). Autophagy machinery dysfunction has been reported in LRRK2-KO and mutant forms (Alegre-Abarrategui et al. 2009; Herzig et al. 2011; Ramonet et al. 2011) and loss of LRRK2 has been reported to increase autophagosome formation (Manzoni et al. 2013). LRRK2-KO kidney sections show accumulation of vacuolated cathepsin D-positive structures. The observed structures, colocalising with Lamp1, are likely to be lysosomes or autophagosomes, clustering in LRRK2-KO kidney sections compared to controls. An increase in the early steps of autophagy, leading to autophagosome formation, coupled with impaired protein turnover, could explain the selective changes in lysosomal content and the accumulation of vesicles. The increase in lysosomal substrates, observed exclusively in LRRK2-KO kidneys, suggest that LRRK2 physiological function could be to suppress autophagosomes initiation and consequently monitor lysosomal function.

No changes in lysosomal proteases were observed in brain lysates, from cerebral cortex, striatum or hippocampus, dissected from the same animals employed for the proteomic screen. This difference might be due to the absence of a clear phenotypic effect in the LRRK2-KO brain. One possible explanation is the presence of compensatory mechanisms in neuronal cells such as the expression of comparable amount of LRRK1 and LRRK2 (Dachsel et al. 2010; Taylor et al. 2007). It is therefore tempting to speculate that the phenotype observed in kidneys is due to a lack of compensation by LRRK1. Cathepsin D has been proposed as a biomarker of ageing (Sato et al. 2006) since it is significantly increased in brains from aged rats compared to young and adult rats (Banay-Schwartz et al. 1992). The increase in cathepsin D in LRRK2-KO kidneys could therefore represent premature ageing of this tissue compared to controls. In addition, LRRK2 mutations have been shown to cause PD with age-related and high but incomplete penetrance (Funayama et al. 2002; Greggio et al. 2009). Ageing represents an accumulation of defects in a highly complex organisms. Perhaps, a simple explanation is that mice do not live long enough to develop neuropathological features typical of PD patients, or that additional stress factors might be needed to observe a difference in phenotype in the brain of LRRK2 deficient or mutant mice.

Collectively, these findings suggest a deficit in clearance or recycling of lysosomal content, reflecting the known role of LRRK2 in vesicular trafficking (Beilina and Cookson 2016; Beilina et al. 2014). Another interpretation could be that LRRK2 tightly controls autophagosome formation and loss of LRRK2 might lead to an increase in autophagy initiation. Importantly, autophagosomes are formed at multiple locations in the cytoplasm and need to be transported along microtubules to get into close proximity of lysosomes for their fusion (Rubinsztein et al. 2012). Therefore, it is possible that the observed vesicle and lysosomal

proteases accumulation represent a functional consequence of microtubular network alterations underlying a defect in microtubule transport.

### 4.3.2 Loss of LRRK2 results in cytoskeletal alterations

A direct interaction of LRRK2 with β-tubulin is supported by multiple experimental evidence (Caesar et al. 2013; Godena et al. 2014; Law et al. 2014). This interaction is specific to three β-tubulin isoforms and occurs at the luminal face of dynamic microtubule populations (Law et al. 2014). According to Law et al., LRRK2 interaction with microtubules is functionally relevant to microtubule tightly balanced dynamics since loss of LRRK2 results in increase in microtubule acetylation. In addition, a consistent effect of LRRK2 mutations on the cytoskeleton is reduced neurite outgrowth (MacLeod et al. 2006; Parisiadou et al. 2009). LRRK2 has also been reported to phosphorylate brain bovine β-tubulin (Gillardon 2009). Evidence from other groups support a functional interaction between LRRK2 and the MAP tau (Kawakami et al. 2012; Lin et al. 2010). These observations are in line with a key role of LRRK2 as a multidomain scaffold on microtubules potentially modulating microtubule stability and ensuring microtubule transport.

**Loss of α/β-tubulin in LRRK2-KO kidneys**

A differential regulation of cytoskeletal proteins was found in LRRK2-KO cytosolic and microsomal fractions after proteomic analysis. Immunoblot validation confirmed a significant downregulation in total levels of α/β-tubulin in both cytosolic and microsomal fractions. Decreased β-tubulin has been associated with renal damage in rats after bilateral ureteral obstruction (Stodkilde et al. 2014). These findings suggest an impairment in cytoskeletal dynamics, potentially associated with defects in microtubule transport, in turn affecting kidney

physiology. Defects in microtubule transport might also explain the progressive accumulation of lysosomal cargos that are not correctly delivered (Maday et al. 2014). Microtubules are also essential for secretory pathways to and from the Golgi such as retrograde transport (Fokin et al. 2014; Moughamian et al. 2013), receptor recycling and regulation of membrane fusion events (Maday et al. 2014). Therefore, microtubule dysfunction might be one of the earlier changes in LRRK2-KO kidneys, resulting in over time vesicle accumulation and mislocalisation. However, it is also possible that loss of LRRK2 causes an earlier defect in protein degradation pathways. The consequent accumulation of undigested proteins could then result in an excessive burden on microtubule transport, and therefore its dysfunction.

**Gephyrin decrease in LRRK2-KO kidneys**

Gephyrin decrease in LRRK2-KO kidneys was validated in both cytosolic and microsomal fractions by immunoblot. Gephryin is a microtubule-associated scaffolding protein involved in the clustering and localisation of inhibitory glycine and $GABA_A$ receptors to the postsynaptic membrane of neuronal and non-neuronal cells (Ramming et al. 2000; Rees et al. 2003; Ryzhikov and Bahr 2008; Smolinsky et al. 2008). Gephyrin mediates the interaction between membrane proteins and the cytoskeleton. Pharmacological disruption of microtubules and actin has been reported to decrease the amount of gephyrin in cultured spinal cord neurons (Charrier et al. 2006). Interestingly, a significant downregulation of gephyrin in hippocampal tissue from LRRK2-KO mice was reported (Fig. 4.14). This decrease might occur as a direct consequence of LRRK2 loss. Alternatively, the observed loss of tubulin in LRRK2-KO kidneys could result in lower stability of gephyrin, as an indirect effect of LRRK2 loss. In conclusion, hippocampi from LRRK2-KO mice show lower gephyrin protein levels compared to controls but no changes in tubulins.

**Coronin 1 C alterations in LRRK2-KO kidneys**

In LRRK2-KO proteomic screen analysis, I found the actin-binding protein Coro1c, involved in membrane-cytoskeleton interaction, significantly increased in the cytosolic fractions and decreased in microsomal fractions. By immunoblot, I observed an increase in abundance in Coro1c lower molecular weight form. It is unclear whether this form corresponds to a processed form or a degradation product of Coro1c. Coro1c is a ubiquitously expressed and highly conserved protein involved in cell motility, vesicular trafficking and actin regulation (Rybakin and Clemen 2005). Since actin and microtubules have overlapping functions (Etienne-Manneville 2004) and LRRK2 interacts with microtubules (Law et al. 2014), the capacity of Coro1c to link membrane to cytoskeleton may be impaired in the absence of LRRK2 leading to abnormal actin rearrangements. LRRK2 has been found to have a role in the guidance of actin cytoskeleton in neurons in collaboration with ARHGEF7 and tropomyosin 4 (Häbig et al. 2013). In addition, LRRK2-mediated phosphorylation of the ezrin, radixin, and moesin (ERM) family proteins has been reported (Jaleel et al. 2007; Parisiadou et al. 2009). ERM proteins link actin cytoskeleton with membranes and are involved in endosome maturation *via* interaction with the homotypic fusion and protein sorting (HOPS) complex (Chirivino et al. 2011).

**Naa15 and tubulin acetylation changes in LRRK2-KO kidneys**

The auxiliary subunit of the N-acetyltrasferase (Naa15) was differentially regulated in LRRK2-KO cytosolic and microsomal kidney fractions. A significant increase in Naa15 was reported in the LRRK2-KO cytosolic fractions, whereas Naa15 was decreased in the microsomal fractions. Naa15 localises mainly in the cytoplasm and forms the acetyltransferase complex NatA, together with the catalytic subunit Naa10, which assembles in translating ribosomes (Dörfel and Lyon 2015). Naa15

has also been reported to interact with the actin-binding protein cortactin and with F-actin in mouse (Paradis et al. 2008). Both Naa10 and Naa15 have been shown to colocalise with microtubules in dendrites and to acetylate purified α-tubulin (Ohkawa et al. 2008). Technical validation by immunoblot of Naa15 show a decrease in protein levels in both LRRK2-KO fractions (4.3). Interestingly, Naa15 was the only iTRAQ candidate which was differentially abundant in G2019S kidney cytosolic fractions, but not in the microsomal fractions (4.3, 4.4). One hypothesis might be that LRRK2 kinase activity, increased in the G2019S mutant (Greggio et al. 2006; West et al. 2005), is involved in the stabilisation of the NatA complex. It is possible that absence of LRRK2 leads to a differential regulation of the acetyltransferase complex resulting in changes in acetylated-tubulin. Interestingly, acetylated-tubulin was significantly higher in LRRK2-KO cytosolic and microsomal fractions compared to wild type animals (Fig. 4.5, 4.6). However, this hypothesis is not supported since no changes in tubulin acetylation were detected in G2019S cytosolic fractions despite Naa15 being differentially abundant (Fig. 4.5, 4.6). An increase in tubulin acetylation seems to enhance microtubule transport by promoting kinesin-1 binding and to change cargo directionality towards the neurite tips (Reed et al. 2006). Overall, the increase in tubulin acetylation in LRRK2-KO kidneys is consistent with previous findings (Law et al. 2014) and with the hypothesis that LRRK2 acts as a modulator of microtubule stability by maintaining microtubule in a dynamic state.

Collectively these results suggest a fundamental role of LRRK2 in cytoskeletal regulation and may provide insights into LRRK2 physiological function. LRRK2 might act as bridge between membrane and cytoskeletal proteins facilitating vesicle movement and fusion. It is clear that LRRK2 plays an essential role in regulation of protein homeostasis, the challenge now remains to understand

whether these changes are directly related to the absence of LRRK2 or if they represent a downstream consequence of the kidney phenotype.

# 5 Age-dependent biological changes of iTRAQ candidates in LRRK2-KO kidneys

## 5.1 Introduction

LRRK2-KO kidneys show complex, age-dependent differences compared to controls (Tong et al. 2012). The observed phenotypic changes are related to the two major protein degradation pathways of the cell: the autophagy machinery and the ubiquitin-proteasome system (UPS). Accumulation of ubiquitinated proteins has been reported in LRRK2-KO kidneys, suggesting dysfunctional proteasomal degradation (Tong et al. 2010). In addition, alterations in autophagy components and autophagy flux have been detected in the absence of LRRK2 (Alegre-Abarrategui et al. 2009; Ferree et al. 2012; Manzoni et al. 2013; Schapansky et al. 2014a; Tong et al. 2012).

Tong et al. reported that lack of LRRK2 results in biphasic changes of autophagy markers in kidney (Tong et al. 2012). The authors found accumulation of lysosomal substrates and autophagy markers in LRRK2-KO kidneys at 1, 4, 7 and 20 month of age. According to Tong et al. study, between 4 and 7 month of age, there is an induction in autophagy accompanied by increased protein degradation of autophagic substrates such as LC3I and p62. This initial increased digestion of these substrates is followed by an accumulation of autolysosomes. The observed imbalance in recycling of autophagic components then results in their functional depletion (Tong et al. 2012). As a result, at older ages, the autophagy machinery function is impaired causing accumulation of undigested lysosomal proteases, lipofuscin granules and autophagy markers (Tong et al. 2010, 2012).

Interestingly, in the experiments conducted by Tong et al. and validated in this work (see section 4), the lysosomal proteases cathepsin D is consistently more abundant in LRRK2-KO kidneys throughout the different tested ages (Tong et al. 2012). In particular, initial accumulation of pre-cathepsin D is detected in kidneys from LRRK2-KO at 1 month of age. At 7 month-old both cathepsin D forms are dramatically increased. In 20 month-old LRRK2-KO kidneys, lysosomal accumulation is less striking and replaced by large lipofuscin granules (Tong et al. 2012).

To test whether these age-dependent alterations were true for the proteins nominated in the previously described proteomic study, and to determine which proteins are most directly connected to LRRK2 deficiency, I examined a series of independent cohorts of LRRK2 knockout animals at different ages. I used kidney total protein homogenates for candidate proteins analysis via immunoblot. Then, to test alterations in the autophagy pathway, I probed the same lysates from different cohorts with the autophagy marker LC3.

## 5.2 Results

To investigate whether changes in proteomic candidates could be identified at early time points in development, total kidney lysates from newborn and 1 month-old LRRK2-KO and control mice were extracted and immunoblot analysis was performed. Antibodies against endogenous proteins identified as differentially abundant in the iTRAQ screen were used. Loss of LRRK2 was confirmed in LRRK2-KO samples and β-actin was used as endogenous control in each experiment. Full lenght LRRK2 was detected by immunoblot together with a truncated form of the protein, previously reported by mass spectrometry analysis to include the leucine-rich repeat (LRR) region and the kinase domain of LRRK2 (Herzig et al. 2011).

### 5.2.1 Biological validation of iTRAQ candidates in P0 and 1 month-old mice

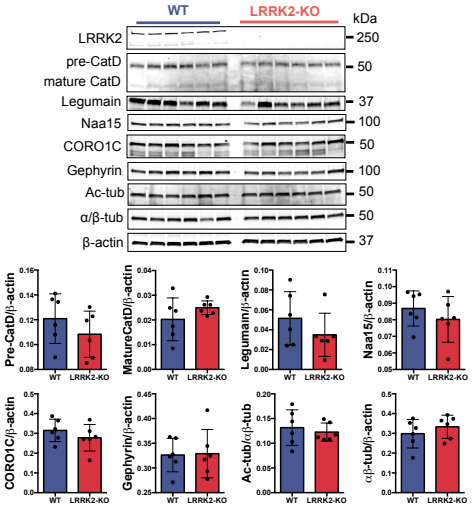


Figure 5.1: **No differences in iTRAQ candidates in LRRK2-KO kidneys from P0 mice.** Immunoblots for LRRK2 and the protein of interest detected via iTRAQ screen normalised for the loading control β-actin. Immunoblot quantifications are shown in the lower panels (n=6, Student t test, P >0.05).

Kidney lysates, extracted from a cohort of LRRK2-KO and control newborn (P0) mice, were probed for the following iTRAQ candidates: cathepsin D, legumain, Naa15, Coro1C, gephyrin, acetylated-tubulin and α/β-tubulin. No significant differences were observed between LRRK2-KO and controls in any of the markers examined (Student t test, n=6 animals per genotype) (Fig. 5.1).

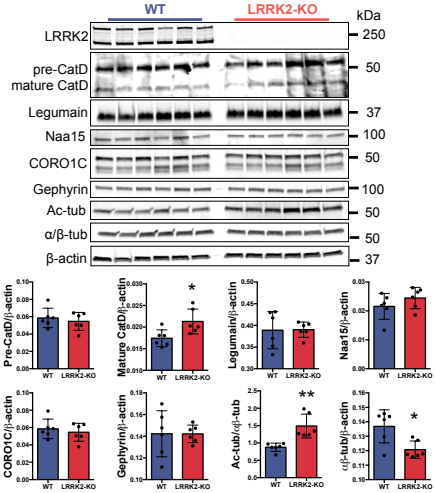


Figure 5.2: **LRRK2-KO 1 month-old kidneys display significant differences in proteins detected from iTRAQ as differentially abundant.** Immunoblots for LRRK2 and the protein of interest detected via iTRAQ screen normalised for the loading control β-actin. Immunoblot quantifications are shown in the lower panels (n=6, Student t test). ∗ P<0.05, ∗∗ P<0.01.

I then performed immunoblots using antibodies against the same iTRAQ candidates in 1 month old animals. In this cohort, a small but significant accumulation of the mature form of cathepsin D in LRRK2-KO animals compared to WT was observed (p = 0.0207, WT *vs* LRRK2-KO, Student t test, n=6 animals per genotype) (Fig. 5.2). In addition, significant differences in levels of α/β-tubulin (p = 0.0121, WT *vs* LRRK2-KO) and levels of acetylated-tubulin were reported (p = 0.0020, WT *vs* LRRK2-KO) (Fig. 5.2). No differences were detected for legumain, Naa15, Coro1c and gephyrin.

Together, these results indicate that the differences in iTRAQ candidates observed in the absence of LRRK2 *in vivo* occur at 1 month of age and include certain lysosomal enzymes, in particular the lysosomal protease cathepsin D, and two microtubule components, previously reported to interact with LRRK2 (Law et al. 2014).

### 5.2.2 Biological validation of iTRAQ candidates in 7 and 9 month-old mice

Two additional cohorts of 7 and 9 month-old mice were analysed to test whether the differences in abundance for the nominated iTRAQ candidates were more pronounced at these ages. These two age time points were chosen to replicate results from Tong et al. (7 month-old) and to test the progression of lysosomal protease alterations.

Immunoblots from total kidney lysates from 7 month-old mice (n=3), show a significant difference in mature ($p = 0.0005$, WT *vs* LRRK2-KO) and precursor forms of cathepsin D ($p = 0.0152$, WT *vs* LRRK2-KO) in LRRK2-KO compared to controls, as expected (Fig. 5.3). The legumain mature form was also significantly more abundant compared to WT ($p = 0.0133$, WT *vs* LRRK2-KO). However, there were no significant differences detected in other candidate proteins, Coro1c, gephyrin, Naa15 and α/β-tubulin or acetylated-tubulin in LRRK2-KO kidneys compared to controls (Fig. 5.3).

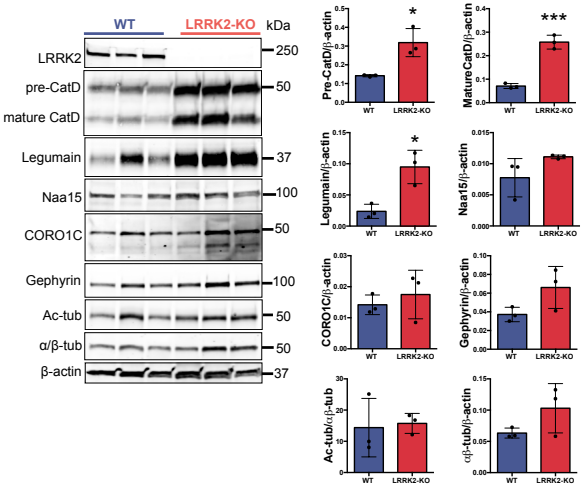


Figure 5.3: **LRRK2-KO 7 month-old kidneys display significant differences in iTRAQ candidates.** Immunoblots for LRRK2 and the proteins of interest detected via iTRAQ screen normalised for the loading control β-actin. Immunoblot quantifications are shown in the right panels (n=3, Student t test). ∗ P<0.05, ∗∗ P<0.01, ∗∗∗ P<0.001.

In an independent cohort of adult mice (n=3, 9 month old), significant higher levels of precursor (p = 0.0043, WT *vs* LRRK2-KO) and mature (p = 0.0004, WT *vs* LRRK2-KO) forms of cathepsin D were detected in LRRK2-KO kidney homogenates compared to wild-type animals (Fig. 5.4). Legumain was also more abundant in LRRK2-KO kidney homogenates (p<0.0001, WT *vs* LRRK2-KO). Naa15 protein levels were significantly different in the LRRK2-KO samples (p = 0.0051, WT *vs* LRRK2-KO) and Coro1c was differentially abundant as previously reported in the initial cohort used for proteomics (lower Coro1c band, p = 0.0002, WT *vs* LRRK2-KO). Significantly lower levels of α/β-tubulin (p = 0.0148, WT *vs*

LRRK2-KO), together with higher levels of tubulin-acetylation were detected (p = 0.0080, WT *vs* LRRK2-KO) (Fig. 5.4).

Collectively, these results show more prominent changes at 7 and 9 months compared to younger ages. Proteomic candidates were validated in the 9-month-old cohort and the most consistent changes appear to be related to the lysosomal proteases cathepsin D and legumain.

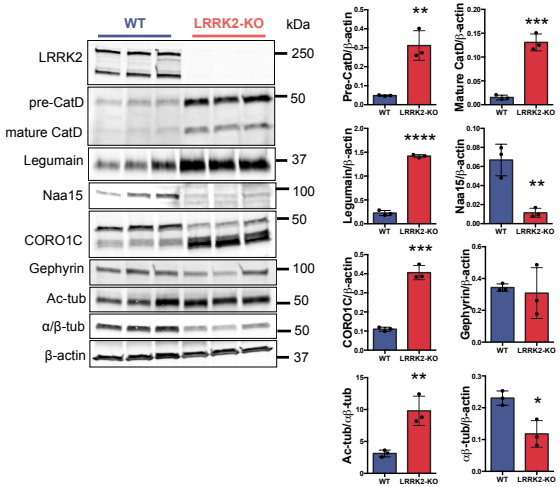


Figure 5.4: **LRRK2-KO 9 month-old kidneys display significant differences in iTRAQ candidates.** Immunoblots for LRRK2 and the protein of interest detected via iTRAQ screen normalised for the loading control β-actin. Immunoblot quantifications are shown in the right panels (n=3, Student t test). ∗ P<0.05, ∗∗ P<0.01, ∗∗∗ P<0.001, ∗∗∗∗ P <0.0001.

### 5.2.3 Biological validation of iTRAQ candidates in 12-15 month-old mice

Kidney total homogenates from the 12 month old mouse cohort (n=5) previously tested for iTRAQ proteomics were analysed to confirm changes previously reported in microsomal and cytosolic fractions (Fig. 5.5). Here, as expected, all protein candidates were validated with the exception of gephyrin, which was not significantly different between LRRK2-KO and controls in kidney total homogenates.

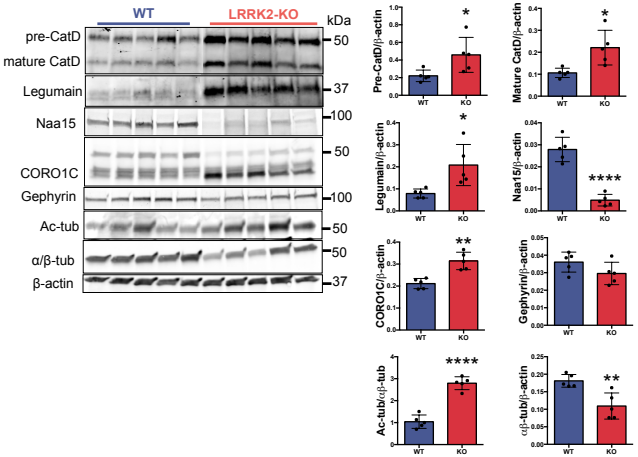


Figure 5.5: **LRRK2-KO 12 month-old kidneys display significant differences in iTRAQ candidates.** Immunoblots for LRRK2 and the protein of interest detected via iTRAQ screen normalised for the loading control β-actin. Immunoblot quantifications are shown in the right panels (n=5, Student t test). ∗ P<0.05, ∗∗ P<0.01, ∗∗∗ P<0.001, ∗∗∗∗ P <0.0001.

To explore protein changes at older ages, immunoblots in an additional cohort of 15 month old (n=3) animals were performed. Subtler changes in these protein levels were observed, with only the accumulation of mature cathepsin D being statistically significant (p = 0.0012, WT *vs* LRRK2-KO) (Fig. 5.6).

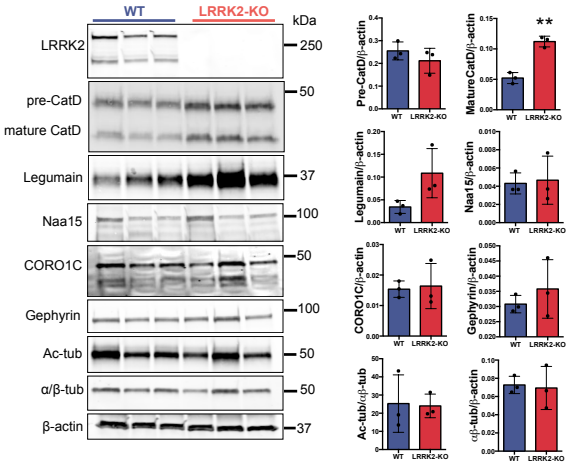


Figure 5.6: **LRRK2-KO 15 month-old kidneys display significant differences in iTRAQ candidates.** Immunoblots for LRRK2 and the proteins of interest detected via iTRAQ screen normalised for the loading control β-actin. Immunoblot quantifications are shown in the right panels (n=3, Student t test). ∗ P<0.05, ∗∗ P<0.01, ∗∗∗ P<0.001.

Overall, this biological validation of iTRAQ protein candidates confirms that in LRRK2-KO kidneys there is an age-dependent accumulation of the lysosomal protease cathepsin D. This accumulation is first observed in 1 month-old mice, then progressively increases with a maximum peak at 7-9 months and less strikingly at 15 month of age. These results overlap with the previously published analysis

from Tong et al. and support the hypothesis of a role for LRRK2 in lysosomal function (Tong et al. 2012). In contrast to the lysosomal changes observed in LRRK2-KO kidneys, differences detected in the cytoskeletal proteins were more variable between cohorts.

### 5.2.4 Age dependent changes in LRRK2-KO kidneys

Collectively, these results show that the earliest changes are detectable approximately at 1-month of age and that these changes progressively increase up to 9 month of age but then appear to decline (Fig. 5.7), consistent with prior suggestions that the effects of Lrrk2 deficiency are age-dependent (Tong et al. 2012).

The changes of loss of α/β-tubulin and increase in acetylated-tubulin were consistent throughout different cohorts and seem to recover at older ages. Similarly, differences in Naa15 and Coro1c observed in two independent cohorts at 9 and 12 months of age, are no longer observed in the older 15 month-old cohort, despite the presence of lyosomal changes in LRRK2-KO kidneys (Fig. 5.6). These results show that the cytoskeletal alterations observed in LRRK2-KO kidneys are age-dependent and more variable between different cohorts.

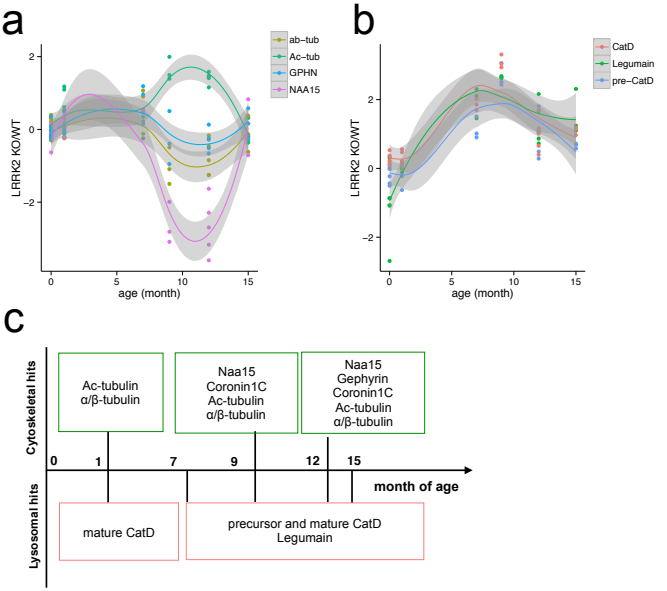


Figure 5.7: **Age-dependent alterations in LRRK2-KO kidneys.** Plot indicating the differences in the iTRAQ cytoskeletal (a) and lysosomal (b) candidates of interest, data points represent each individual immunoblot band quantification of LRRK2-KO normalised for the average of the controls for each cohort. (c) Timeline displaying lysosomal and cytoskeletal protein changes in LRRK2-KO kidneys at different ages.

These results suggest that the primary responses to LRRK2 deficiency in the kidney include lysosomal and cytoskeletal changes. The consistent increase in lysosomal proteases suggest a primary defect in endo-lysosomal trafficking, alone or in combination with cytoskeletal alterations. Endo-lysosomal trafficking relies on a fine regulation of microtubule transport and parallel changes occur in lysosomal and cytoskeletal proteins. However, whether the primary defect is related to lysosomal accumulation or to microtubule impairments is still unclear.

### 5.2.5 Alterations of autophagy markers in LRRK2-KO kidneys

Dysfunction of the autophagy-lysosome system has been previously reported in LRRK2-KO models (Herzig et al. 2011; Tong et al. 2010, 2012). To investigate autophagy levels in absence of LRRK2, I probed the previously tested kidney homogenates (Fig. 5.1 and 5.6) from different cohorts of LRRK2-KO and control mice for the marker of autophagosome LC3. The antibody used for these experiments recognises both forms of LC3: LC3I and LC3II. The ratio between the membrane-associated LC3II and β-actin was used as a measure of autophagy steady-state, endogenous levels (Barth et al. 2010).

Immunoblot analysis of P0 kidney lysates show a subtle difference in the steady-state levels of LC3I in LRRK2-KO ($p = 0.027$, WT *vs* LRRK2-KO) (Fig. 5.8). No differences in LC3II and LC3II/I ratio was observed.

Next, I performed immunoblot analyis of 1 month-old LRRK2-KO and control kidney lysates. At 1 month of age, no difference in LC3I and LC3II was detected (Fig. 5.9).

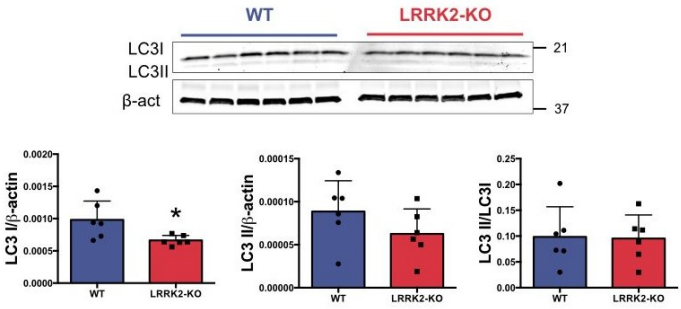


Figure 5.8: **LC3 levels in LRRK2-KO kidneys from P0 mice** Immunoblots from the autophagy marker LC3 normalised for the loading control β-actin. Immunoblot quantifications are reported below (n=6, Student t test). $*$ P<0.05.

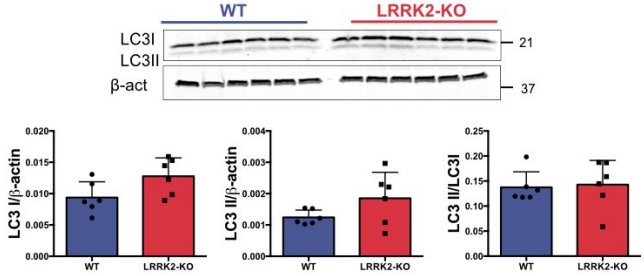


Figure 5.9: **No differences in the autophagy marker LC3 in LRRK2-KO kidneys from 1 month-old mice.** Immunoblots from the autophagy marker LC3 normalised for the loading control β-actin. Immunoblot quantifications are reported below (n=6, Student t test).

To explore changes at older ages, LRRK2-KO and control kidney lysates from 9 month-old mice were examined. I observed an increase in LC3I levels normalised

to β-actin (p = 0.0093, WT *vs* LRRK2-KO). Again, no difference in LC3II were detected. A subtle difference in LC3II to LC3I ratio was observed in these samples (p = 0.0429, WT *vs* LRRK2-KO).

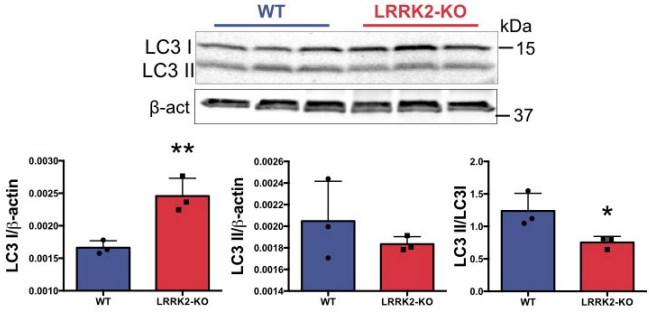


Figure 5.10: **Accumulation of LC3I in LRRK2-KO kidneys from 9 month-old mice.** Immunoblots from the autophagy marker LC3 normalised for the loading control β-actin. Immunoblot quantifications are reported below (n=3, Student t test). ∗ P<0.05, ∗∗ P<0.01.

Two additional older cohorts at 12 and 15 months of age were next probed for LC3 (Fig. 5.12). The 12 month-old kidney lysates from LRRK2-KO, G2019S heterozygous knockin and controls previously employed for the initial iTRAQ proteomic screens were tested. Consistently with Tong et al., I observed an increase in LC3I levels (p = 0.0008, WT *vs* LRRK2-KO, Bonferroni post-hoc test from one-way ANOVA). I also detected a subtle increase in LC3II in LRRK2-KO kidneys (p = 0.0127, WT *vs* LRRK2-KO). No changes in LC3 forms were detected in the G2019S samples.

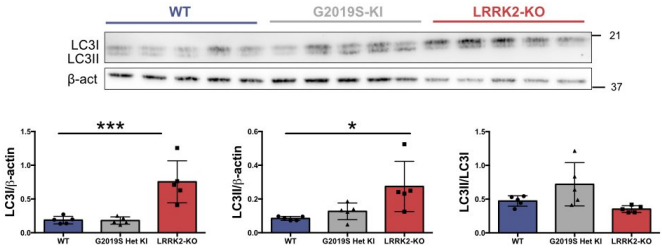


Figure 5.11: **Accumulation of LC3I and LC3II in LRRK2-KO kidneys at 12 month of age.** Immunoblots from the autophagy marker LC3 normalised for the loading control β-actin. Memrbanes were developed by ECL. Immunoblot quantifications are reported below (n=5, Bonferroni post-hoc test from one-way ANOVA). ∗ P<0.05, ∗∗ P<0.01, ∗∗∗ P<0.001.

Similarly to 12 month-old LRRK2-KO kidneys, immunoblots from 15 month-old kidney show an accumulation of LC3I ($p = 0.036$, WT *vs* LRRK2-KO, n=3, Student t test). No differences in LC3II or in LC3II to LC3I ratio were detected (Fig 5.12).

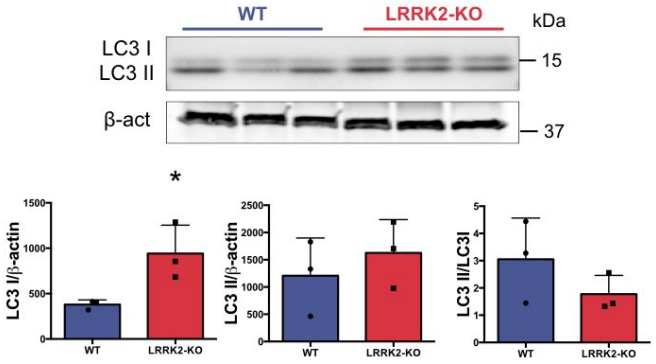


Figure 5.12: **Accumulation of LC3I in LRRK2-KO kidneys at 15 month of age.** Immunoblots from the autophagy marker LC3 normalised for the loading control β-actin. Immunoblot quantifications are reported below (n=3, Student t test). $*$ $P<0.05$.

Collectively, these results indicate that loss of LRRK2 result in *in vivo* alterations of autophagic components.

## 5.3 Discussion

### 5.3.1 Cathepsin D age-dependent accumulation in LRRK2-KO kidneys

Previous findings (Tong et al. 2012) report a biphasic accumulation of autophagy markers and of the lysosomal protease cathepsin D in LRRK2-KO kidneys. This accumulation was observed for cathepsin D in every tested cohort excluding P0 kidneys, whereas increase in the other lysosomal protease validated from iTRAQ screen, legumain, was detected at 7, 9 and 12 months but not at 1 month. These results collectively indicate a defect in lysosomal sorting starting at 1 month of age, exacerbating over-time up to 9 month of age and reaching a plateau around 12-15 month of age.

One possible hypothesis is that LRRK2 affects the sorting of cathepsin D receptor, the M6PR, causing impaired cathepsin D trafficking and accumulation in pre-lysosomal compartments. This accumulation would lead to a decrease in the content of acid proteases in the lysosome (Mcmillan et al. 2017). The consequence of an impaired delivery of hydrolytic enzymes to the lysosome is likely to be a less efficient lysosome, with a decreased ability to digest its content. It seems reasonable to conclude that, over time, impairment of lysosomal function due to alteration in enzymatic content results in accumulation of undigested proteins and lipofuscin granules in LRRK2-KO kidneys. One problematic aspect to consider, however, is the difficulty to capture this dynamic process with static measurements on tissue lysates.

LRRK2-KO kidneys appear larger at 5-7 months of age and then tend to shrink in size, becoming smaller than controls at 15-18 months (Tong et al. 2012).

It is possible that the observed kidney hypertrophy at the age of 5-6 months is accompanied by specific changes in protein levels and the biphasic trend might correlate with the functional state of the kidney. Another explanation for the variations in cathepsin D accumulation throughout different stages of mouse development could be the attempt to compensate cathepsin D defective sorting. Cathepsin D is an important enzyme for extracellular matrix degradation and remodelling, cell motility (Berchem et al. 2002). It has been suggested that cathepsin D stimulates tumor growth of both cancer and epithelial cells independently of its catalytic activity (Berchem et al. 2002; Tan et al. 2013). Perhaps the observed alterations in kidney size and morphology are correlated to changes in cathepsin D protein levels.

### 5.3.2 Biological validation of cytoskeletal changes in LRRK2-KO kidneys

As previously suggested, loss of LRRK2 seems to affect the dynamic instability of microtubules, resulting in an increase of microtubule acetylation (Law et al. 2014). The unbiased proteomic study conducted on LRRK2-KO kidneys identified a number of differentially abundant cytoskeletal proteins, as shown in the previous chapters. Among these proteins, I validated α/β-tubulin, the microtubule-binding protein gephyrin (Gphn), the subunit of the acetyl-transferase complex, Naa15 and the actin-bindin protein coronin 1C. Changes in other proteins involved in cytoskeletal regulation have also been reported. In particular the cytoskeletal GTPase septin-9 (Sept9), the myosin phosphatase Rho-interacting protein (Mprip) and the protein kinase C and casein kinase substrate protein 2 (Pacsin2) were all significantly increased in LRRK2-KO cytosolic fractions (Table. 6). Together,

these results suggest the presence of cytoskeletal deregulation in LRRK2-KO kidney.

Biological validation of cytoskeletal changes in LRRK2-KO kidneys seem less consistent throughout aging cohorts, compared to the lysosomal changes, suggesting no obvious correlation between accumulation of lysosomal hydrolases and changes in cytoskeleton. In this study, an initial increase in acetylated-tubulin in combination with a decrease in total tubulin was detected at 1 month of age. LRRK2 expression seems to inversely correlate with tubulin acetylation and an increase in acetylated tubulin was previously reported in LRRK2-KO mouse embryonic fibroblasts (Law et al. 2014). The LRRK2 interaction site on α-tubulin is in close proximity to the luminal Lys40 acetylation site, an important PTM modulating microtubule stability (Law et al. 2014). The authors hypothesised a mechanism by which LRRK2, localising to the lumen of flexible and dynamic microtubules, regulates microtubule acetylation by preventing the access of the tubulin acetyltransferase enzyme (Law et al. 2014). Fine regulation of microtubule dynamic instability is crucial for cell survival as demonstrated by chemotherapeutic agents such as taxol and vincristine that induce cell death by dramatically increasing or decreasing microtubule stability (Law et al. 2014). Therefore, microtubule impairments could lead to increase of apoptotic cell death observed in LRRK2-KO kidneys (Tong et al. 2010). Additionally, an increase in tubulin acetylation could result in redirection of kinesin-1 transport on microtubules (Godena et al. 2014; Reed et al. 2006). Redirection of transport might lead to accumulation or misplacement of cargos such as cathepsins. In conclusion, cytoskeletal impairments may aggravate lysosomal trafficking defects over time. Biological differences between independent cohorts or compensatory

changes due to microtubule dynamic regulation are both plausible explanations of this variability.

### 5.3.3 Significant changes in the autophagy marker LC3 in absence of LRRK2

LRRK2 has been localised with different intracellular compartments, including TGN and autophagosomes (Alegre-Abarrategui et al. 2009). A role for LRRK2 in autophagy has been suggested (Alegre-Abarrategui et al. 2009; Ferree et al. 2012; Manzoni et al. 2013; Schapansky et al. 2014a; Tong et al. 2012). Autophagy is characterised by dynamic regulation and different environmental stressors such as starvation and oxidative stress can induce alterations in the autophagy flux (Mizushima et al. 2010). Biphasic changes in autophagy markers LC3 and p62 have been reported in LRRK2-KO kidneys (Tong et al. 2012). To investigate whether these changes could be reproduced in LRRK2-KO kidneys for the previously tested cohorts, the levels of LC3 were analysed in the previously tested kidney lysates. In P0 kidney lysates, an initial decrease in LC3I but no changes in LC3II were observed. This result could suggest a lower synthesis of LC3I or a higher degradation, but it does not provide a definite answer on the levels of autophagy flux. At 1 month of age no differences were detected in LC3. At the older ages of 9, 12 and 15 months, however, an accumulation in LC3I was consistently detected. One interpretation of this result could be a slower or impaired LC3I to LC3II conversion in absence of LRRK2, as suggested by decrease in LC3II to LC3I ratio in the 9 month-old cohort. The observation that alterations in autophagy markers may variate *in vivo* depending on the age of the animal might indicate a direct consequence downstream of loss of LRRK2. However, it is likely that the altered lysosomal function, observed in LRRK2-KO kidneys, has an impact on

the turnover of autophagy markers. Together, I was not able to fully reproduce the biphasic alterations of LC3 in LRRK2-KO kidneys reported by Tong et al.

Studies in iPSc-derived neurons carrying G2019S mutation in LRRK2 revealed an increase in LC3II protein levels compared to controls (Sánchez-Danés et al. 2012). Conversely, fibroblasts from patients with LRRK2 mutations show a decrease in LC3II to LC3I ratio in response to starvation (Manzoni et al. 2013). These discrepancies might be due to cell type variability and different experimental conditions (Beilina and Cookson 2016). Here, however, no changes in LC3 forms were detected in LRRK2 G2019S mutant kidneys. LRRK2 G2019S mutation might have a tissue-dependent function and altered kinase function might not affect protein degradation pathways in kidneys. Additionally, since no difference in other iTRAQ candidates was observed and no alterations in kidneys have been reported for this mutant, it seems likely that LRRK2 increase in kinase activity, reported for this mutation, does not alter kidney physiology.

Autophagosomes traffick along microtubules to fuse with lysosomes (Xie et al. 2010). Defects in LC3I to LC3II conversion have been reported in the presence of microtubule impairments (Xie et al. 2010). Microtubule stabilisation or destabilisation causes defects in autophagosome biogenesis and increase LC3I but not LC3II protein levels (Xie et al. 2010). Interestingly, microtubule changes, i.e. loss of α/β-tubulin and increase of acetylated-tubulin, have been consistently reported in independent LRRK2-KO cohorts. LRRK2-KO cytoskeletal impairments could lead to altered LC3I to LC3II conversion. However, it is important to point out that autophagy is a dynamic process and caution is needed to avoid overinterpretation of protein steady-state levels. In conclusion, static measurements of autophagy markers *in vivo* could indicate both a primary

consequence of loss of LRRK2 or a compensatory redirection of the autophagy flux.

# 6 High Content siRNA Screen to identify possible modifiers of LRRK2 localisation at the Golgi

## 6.1 Introduction

Genome Wide Association studies (GWAS) represents a useful strategy to analyse DNA sequence variants across the whole genome with the goal to identify genetic risk factors for complex diseases, such as PD, that are common in the population (Bush and Moore 2012). GWAS studies, conducted in several cohorts of PD patients and healthy controls, identified large chromosomal regions containing genes known to be mutated in rare, monogenetic forms of PD, such as SNCA, MAPT, LRRK2 (Satake et al. 2009; Simón-Sánchez et al. 2009); as well chromosomal regions containing genes such as Rab7L1 and GAK, associated with sporadic PD (Nalls et al. 2014; Satake et al. 2009; Simón-Sánchez et al. 2009). These observations suggest that these genes are also relevant for the etiology of sporadic PD and support the concept of a common molecular pathway for familial and sporadic PD (Beilina et al. 2014; Simón-Sánchez et al. 2009).

Recent efforts to dissect molecular pathways for familial and sporadic PD come from protein array studies that identified a network of LRRK2 interactors (Beilina et al. 2014; Chia et al. 2014; MacLeod et al. 2013; Meixner et al. 2011). Among these interactors, BAG5, GAK and Rab7L1 were validated by co-immunoprecipitation (Beilina et al. 2014). These experiments helped to identify a multiprotein complex composed of LRRK2, GAK, Rab7L1, BAG5 and Hsp70 (Beilina et al. 2014). Rab7L1 is a Rab GTPase that localises at the TGN in a

GTP-bound form (Aoki et al. 2017). GAK contains a a serine-threonine kinase domain and is functionally homologous to the neuronal-specific protein auxilin (Beilina et al. 2014; Greener et al. 2000). The ubiquitous protein GAK is essential for the Hsc70-dependent uncoating of clathrin-coated vesicles (Greener et al. 2000; Lee et al. 2005b). Similarly to Rab7L1, GAK localises to the TGN where it seems to have a role in M6PR trafficking (Lee et al. 2005b). This co-complex requires both LRRK2 and Rab7L1 enzymatic activities and assembles at the TGN (Beilina et al. 2014; MacLeod et al. 2013). When LRRK2 and Rab7L1 are coexpressed, LRRK2 seems to be recruited to the Golgi by Rab7L1 and to subsequently promote the clustering and removal of TGN-derived vesicles (Beilina et al. 2014; MacLeod et al. 2013). TGN turnover is influenced by the autophagy-lysosomal pathway, as showed in experiments blocking lysosomal function with bafilomycin (Beilina et al. 2014). According to this model, mutations of LRRK2 impair turnover of Golgi-derived vesicles resulting in alterations in autophagy function over time.

Interestingly, another study shows a relationship between the phosphorylation state of LRRK2 and Rab7L1-dependent Golgi clustering, adding another level of complexity to the model (Chia et al. 2014). First, the casein kinase 1 α (CK1α), which directly phosphorylates LRRK2, was identified as an upstream regulator (Chia et al. 2014). Second, depending on LRRK2 phosphorylation state, LRRK2 interacts and phosphorylates the guanine exchange factor ARHGEF7 (Chia et al. 2014). Transient siRNA knockdown of CK1α increases the proportion of cells with clustered TGN, whereas knockdown of ARHGEF7 has opposite effects, suggesting physiologically relevant modulation dependent on two LRRK2 interactors (Chia et al. 2014).

In the previously discussed proteomic screen of LRRK2-KO kidneys (see section 4), a number of proteins was confirmed as differentially abundant in absence of

LRRK2. To investigate whether any of the validated proteomic candidates is part of the LRRK2-Rab7L1 network of interactors, a siRNA screen against iTRAQ significant proteins was performed in HEK293FT cells. In addition, this screen has the goal to identify potential modifiers of LRRK2 function at the Golgi. In collaboration with Dr. Ravindran Kumaran (LNG, National Institute of Health), two identical siRNA screens were performed and LRRK2 localisation at the TGN was measured using an automated microscopy platform (see section 8, Automated cellomic assay). Next, validation of the most significant candidates was performed by immunoblot. Together, the results from the screen show that knockdown of cathepsin D significantly increased LRRK2 localisation with TGN. However, validation of individual siRNAs suggests that this result is an off-target effect of the pooled siRNAs rather than a cathepsin D specific event.

## 6.2 Results

### 6.2.1 siRNA functional screen of iTRAQ candidates

To test whether any of the previously identified iTRAQ candidates is involved in LRRK2 function at the Golgi, two independent siRNA screens followed by an unbiased morphological assay were employed to quantify LRRK2/Rab7L1 colocalisation spots at the TGN in HEK293FT cells.

The positive control of the assay was tested by coexpressing LRRK2 and Rab7L1 in HEK293FT cells. Cells were stained for LRRK2, Rab7L1 and the TGN marker, TGN46, to highlight the presence of the LRRK2-Rab7L1 co-complex (Fig. 6.1). These structures represent the Cellomics readout automatically recognised by the biodetector application and quantified in each screen.

The Q67L variant of Rab7L1, shown to lack GTP binding and unable to hydrolyse GTP (Beilina et al. 2014), was used as a negative control for the assay. When Rab7L1-Q67L mutant is coexpressed with LRRK2 in HEK293FT cells, the complex is no longer formed and Rab7L1-Q67L is no longer membrane-bound (Fig. 6.2).

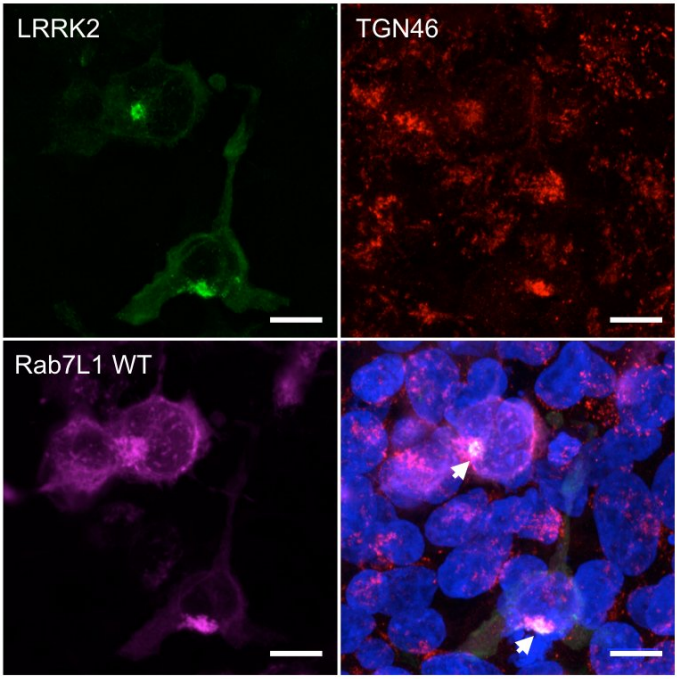


Figure 6.1: **Rab7L1-dependent localisation of LRRK2 at the Golgi.** Confocal images of HEK293FT cells co-expressed with FLAG-LRRK2 and myc-Rab7L1. Cells were stained for FLAG (green), TGN46 (red), myc (magenta) and nuclei (blue). Arrows indicate the LRRK2-Rab7L1 Golgi clusters quantified via automated cellomic assay. Scale bar: 10µm

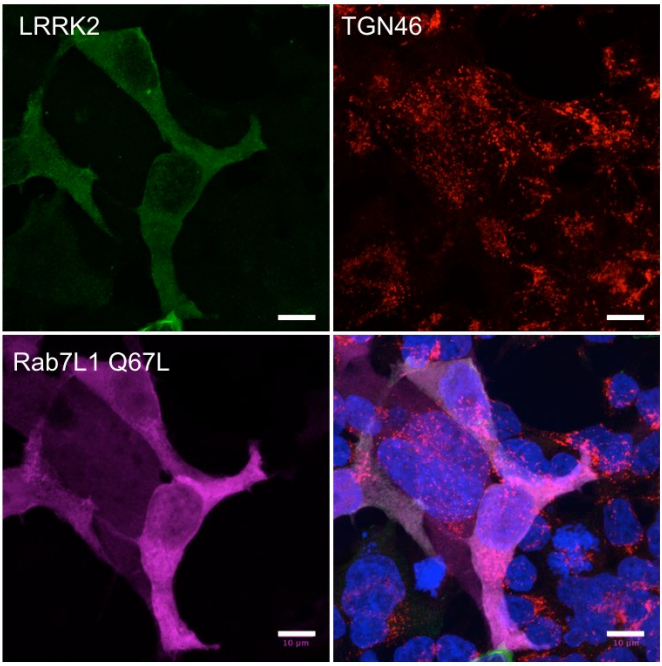


Figure 6.2: **Abolished Golgi localisation of Rab7L1 Q67L mutant.** Confocal images of HEK293FT cells co-expressed with FLAG-LRRK2 and myc-Rab7L1 Q67L (loss of function variant). Cells were stained for FLAG (green), TGN46 (red), myc (magenta) and nuclei (blue). Scale bar: 10µm

For the siRNA functional screen of iTRAQ candidates, cells were transfected with a customised library of pooled siRNA against iTRAQ proteins previously detected as differentially abundant in LRRK2-KO (Fig. 6.3, 6.4). To test the validity of the assay, siRNA constructs against Rab7L1, ARHGEF7 and CK1α (CSNK1A1) were included. As expected, siRNA knockdown of CSNK1A1 increases the number of cells with LRRK2-Rab7L1-TGN punctae, whereas knockdown of ARHGEF7

decreases it (Chia et al. 2014). 24 hours post siRNA transfection, cells were co-expressed with FLAG-LRRK2 and either myc-GUS, as a negative control for transfection, Rab7L1 WT or Q67L Rab7L1 mutant as a negative control for the assay.

In both screens, LRRK2/TGN46 clustering was promoted by WT Rab7L1 (NTC WT) but not by the Q67L mutant (NTC QL) (Chia et al. 2014) (Fig. 6.3, 6.4). Decreased clustering of TGN46 was observed also with knockdown of Rab7L1 and ARHGEF7, as expected. Knockdown of CK1$\alpha$, positive control for the assay, increased the proportion of cells with LRRK2 and Rab7L1 colocalised at the TGN46 (Fig. 6.3, 6.4). Together these observations confirm the validity and reproducibility of the assay (Fig. 6.3, 6.4).

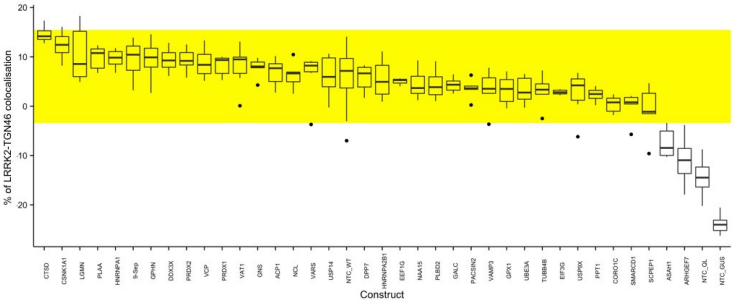


Figure 6.3: **Initial siRNA screen of iTRAQ candidates using Cellomic automated assay.** Box plot representing candidates of interest ranked from highest to lowest percentage of co-localised spots. The yellow bar indicates the 95% confidence interval for the standard normal distribution. Values outside of the bar are considered of interest; x axis display individual siRNA constructs and y axis display the % of cells with LRRK2 and TGN46 colocalisation spots relative to WT (NTC WT).

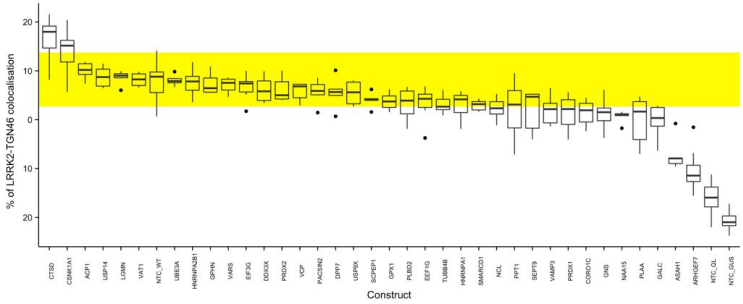


Figure 6.4: **Second siRNA screen of iTRAQ candidates using Cellomic automated assay.** Box plot representing candidates of interest ranked from highest to lowest percentage of co-localised spots. The yellow bar indicates the 95% confidence interval, values outside of the bar are considered of interest; x axis display individual siRNA constructs and y axis display the % of cells with LRRK2 and TGN46 colocalisation spots relative to WT.

The candidates that show a significant effect in LRRK2/TGN46 clustering in both screens are two lysosomal enzymes namely ASAH1 and CTSD, with respectively decreased and increased relocalisation of LRRK2 at the Golgi (Fig.6.3, 6.4). When CTSD is knocked down, 10-20% more cells have co-localised spots than in control cells (Bonferroni post-hoc test from one-way ANOVA, screen 1: $P < 0.001$ - screen 2: $P < 0.0001$); whereas 10% less cells have co-localised spots than control cells when ASAH1 is knocked down.

Correlation was performed by plotting the percentages of colocalisation obtained from the two screens. As expected, a positive correlation was found between the two screens comparing the adjusted percentages of cells with colocalisation spots, confirming the reproducibility of the assay (Pearson's correlation coefficient: $R = 0.875$).

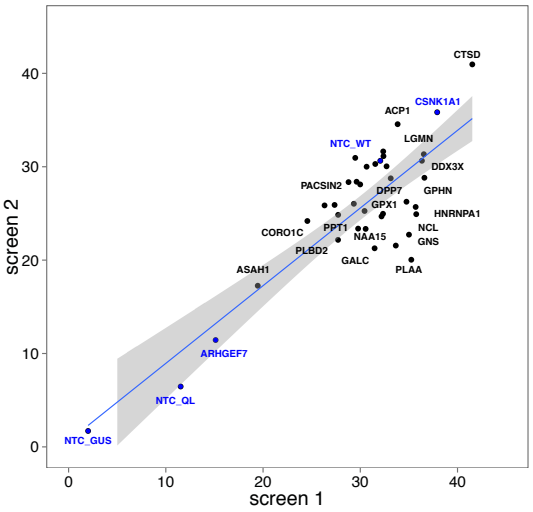


Figure 6.5: **Correlation of siRNA screens.** Comparison of the percentages of colocalisation from the two siRNA screens using the cor(test) function of the R software (www.rstudio.com). Controls are indicated in blue.

Transfection reagents that deliver nucleid acids such as siRNAs to the cytosplasm often generate cytotoxicity (Wittrup and Lieberman 2015). Therefore, in order to determine cell viability, both nuclear intensity and cell count analysis were automatically performed in both screens. Interestingly, based on cell count and nuclear staining, ASAH1 knockdown appears to be toxic to the cells. Similarly, VCP and EIF3G knockdown also show an effect on cell viability (Fig.6.6).

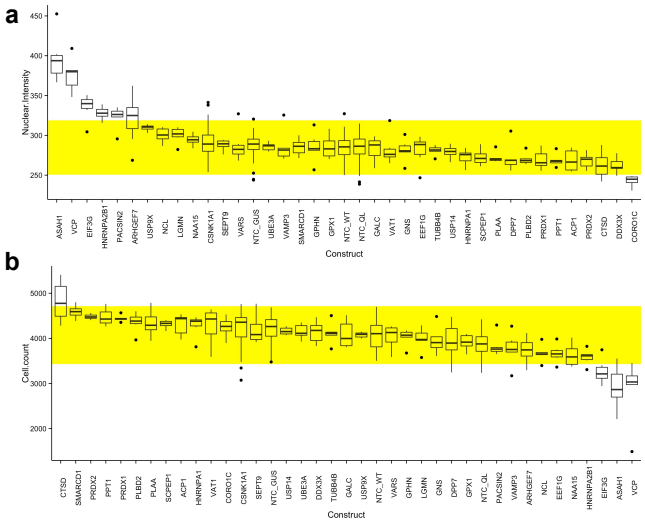


Figure 6.6: **TGN screen effects on cell viability.** Representative box plots from the initial siRNA screen against iTRAQ candidates. (a) Box plot displaying siRNA effects on Hoechst staining intensities ranked from higher to lower. (b) Box plot showing siRNA cytotoxic effects on nuclear count ranked from higher to lower.

Together, these data suggest that loss of CTSD significantly increases the formation of LRRK2-Rab7L1 complexes at the TGN.

### 6.2.2 Cathepsin D siRNA validation

The results obtained via two independent siRNA screens of iTRAQ candidates show that knockdown of two candidate proteins, CTSD and ASAH1, significantly alter LRRK2 localisation at the Golgi. Given the observed toxic effects due to ASAH1 knockdown, this protein was not selected for following validation. Validation

was focused on cathepsin D which represents an interesting candidate since, as previously shown in this thesis (see sections 3 and 4), loss of LRRK2 causes increase in cathepsin D. To investigate whether cathepsin D directly influenced the previously described LRRK2 function at the Golgi, individual cathepsin D siRNAs were analysed. Individual siRNAs were also compared to cathepsin D siRNA Smart Pool, employed in the siRNA screens and containing a combination of targeting siRNAs. Finally changes in LRRK2 colocalisation with the Golgi marker TGN46 were measured via Cellomics quantitative analysis.

First, the different tested siRNAs and non-targeting control (NTC) were validated using immunoblot against cathepsin D. No changes in precursor form of cathepsin D were detected with siRNAs. However, as observed in fig. 6.7, the expression levels of cathepin D mature form were significantly decreased with cathepsin D siRNA Pool and with the individual cathepsin D targeting siRNAs C1, C2 and C3 compared to the NTC and normalised by the endogenous control β-actin. The individual siRNA C4 failed to reduce cathepsin D expression (Fig.6.7).

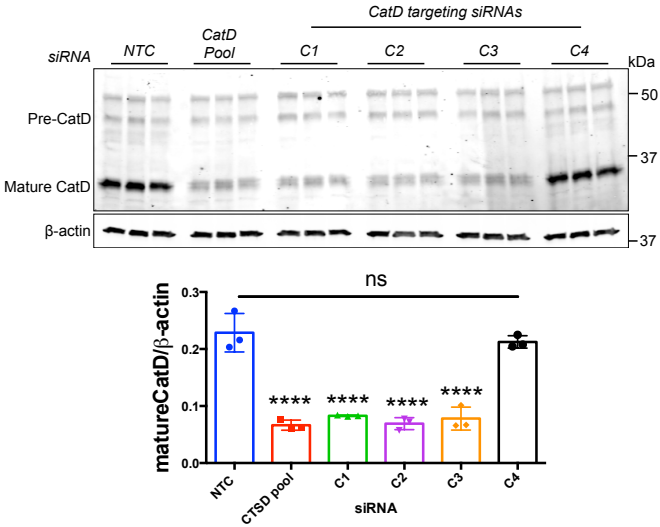


Figure 6.7: **Immunoblot validation of cathepsin D siRNAs.** Immunoblots for cathepsin D normalised for the loading control β-actin in HEK293FT lysates transfected for 48h with individual cathepsin D targeting siRNA (C1-C4), cathepsin D siRNA Pool and non-targeting control (NTC). Molecular weight markers are indicated on the left in kilodalton (kDa). Immunoblot quantifications are shown in the lower panel (Bonferroni post-hoc test from one-way ANOVA). $*P<0.05$, $**P<0.01$, $***$ $P<0.001$.

After siRNA validation, the TGN functional screen was conducted to test whether cathepsin D expression influences LRRK2 translocation to the Golgi. As expected, the negative control with Rab7L1-QL mutant and ARHGEF7 both decreased colocalisation of LRRK2 with TGN marker, where the positive control with CK1 increased it. Cathepsin D downregulation with CTSD siRNA Pool and with the individual C1 targeting siRNA significantly increased LRRK2 localisation with the TGN46. Surprisingly, this effect was not observed for C2 and C3 siRNA, despite

being validated by immunoblot (Fig.6.9). Representative Cellomics images are shown in Fig. 6.8. These results suggest that the observed increased localisation of LRRK2 with TGN46 is likely due to an off-target effect of cathepsin D siRNA (Fedorov et al. 2006).

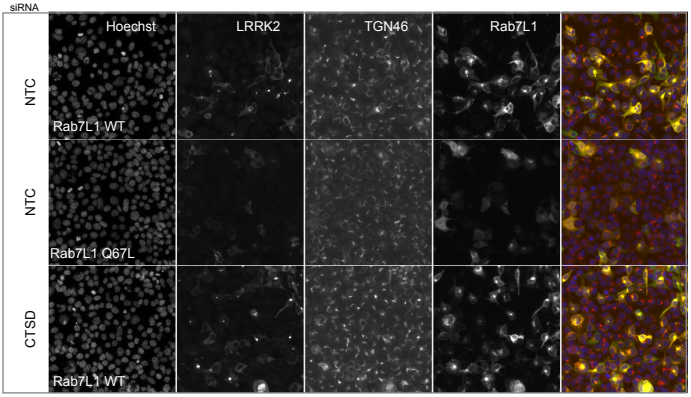


Figure 6.8: **Colocalisation of LRRK2, Rab7L1 co-complex at the Golgi** Representative images of HEK293FT cells transfected with cathepsin D (CTSD) siRNA or NTC and coexpressed with FLAG-LRRK2 and either with myc-Rab7L1 WT or Q67L. Cells were stained for FLAG (green), TGN46 (red), myc (yellow) and nucleus (blue).

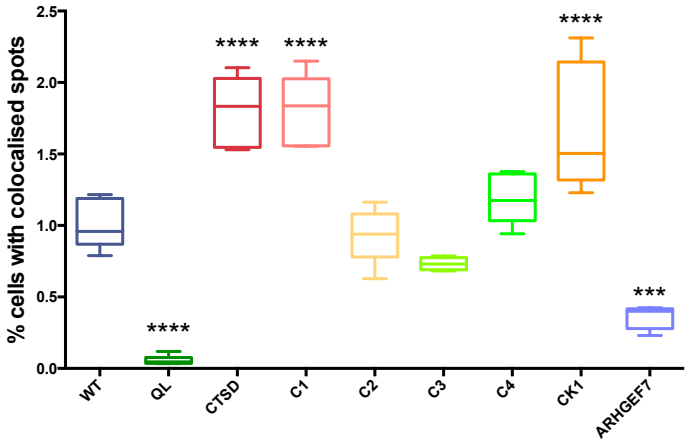


Figure 6.9: **Automated cellomic analysis.** Quantification of percentage of cells with Golgi clusters in figure 6.8. The assay was performed in a 96-well plate and Golgi clusters were imaged and counted using the spot detector bioapplication of the Cellomics arrayscan. Results are from three independent experimental replicates with six wells per condition. Statistical significance tested with Bonferroni post-hoc test from two-way ANOVA. ∗P<0.05, ∗∗P<0.01, ∗∗∗ P<0.001, ∗∗∗∗ P<0.0001.

### 6.2.3 Pharmacological inhibition of Cathepsin D

Another way to test the null hypothesis that cathepsin D does not influence LRRK2, is to use pharmacological inhibitors of cathepsin D. Pepstatin A is a commercially available inhibitor of aspartic proteases such as cathepsin D, renin and pepsin (Yoshida et al. 2006). For this experiment, HEK293FT cells were treated for 24 hours with different concentrations of pepstatin A and its solvent, and a negative control without cell sample was included. To assess the efficacy of pepstatin A, cathepsin D enzymatic activity was measured using a fluorimetric assay (see section Materials and Methods). As expected, increasing

concentrations of pepstatin A progressively decrease cathepsin D activity, where the same concentration of solvent does not alter cathepsin D activity (Fig.6.10).

The functional TGN morphology assay was next performed in HEK293FT. As previously described, when co-expressed with Rab7L1, LRRK2 colocalises with TGN46 and forms a complex that can be visualised as spots and the number of spots normalised per cell can be quantified by confocal microscopy or Cellomics. HEK293FT cells were transfected with LRRK2 and either Rab7L1 or inactive Rab7L1-QL plasmids. 6 hours post-transfection, cells were treated with 5 and 10µM of pepstatin A and respective concentrations of solvent for 24 hours. The results in fig. 6.10 show that cells transfected with Rab7L1 displayed an increased number of spots compared to cells transfected with Rab7L1-QL, as expected. However, there were no differences between controls and pepstatin A treated samples after Cellomics quantification.

This result supports the hypothesis that loss of cathepsin D or inhibition of cathepsin D activity does not alter LRRK2 localisation at the TGN and that the previously reported increase in percentage of LRRK2-TGN46 spots is likely to be an siRNA off-target effect.

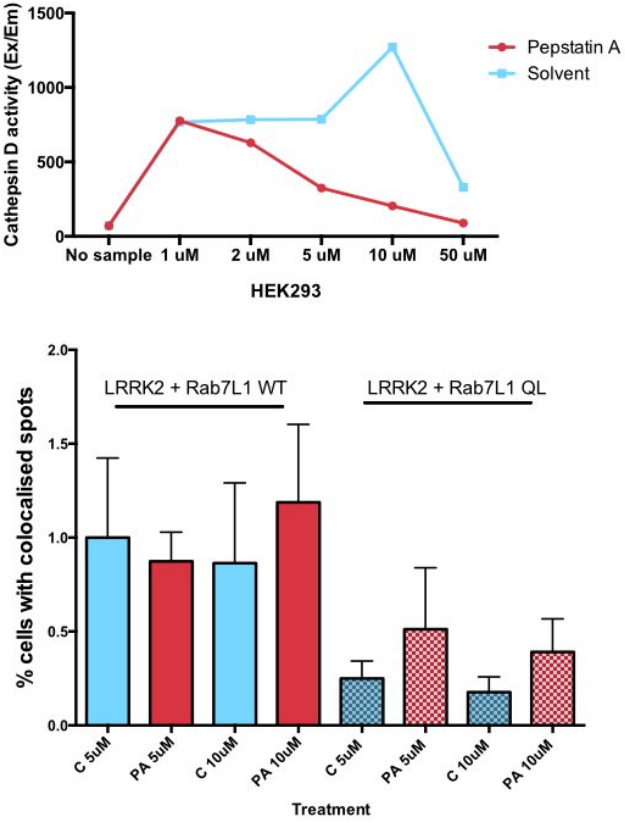


Figure 6.10: **Pharmacological inhibition of cathepsin D with pepstatin A.** (a) Pepstatin A (PA) titration in HEK293FT. Cathepsin D activity (Ex/Em) progressively decreases with increasing concentration of pepstatin A (5-50µM) compared to controls (C). (b) LRRK2-TGN46 functional screen performed in HEK293FT using 5µM and 10µM concentrations of pepstatin A.

## 6.3 Discussion

### 6.3.1 Evaluation of potential off-target effects of the siRNA screen

To test the hypothesis that the previously identified and validated proteomic candidates, differentially abundant in LRRK2-KO kidneys, are functionally involved in the LRRK2-Rab7L1 network of interactors, a siRNA screen against iTRAQ candidates was performed in HEK293FT cells.

Combined results from two independent siRNA screens revealed that knockdown of cathepsin D significantly increased the formation of LRRK2-Rab7L1 punctae at the TGN (Fig. 6.3, 6.4). In both screens, siRNA Smart Pools were used to perform genetic knockdown. The design of siRNA Smart Pools allows to target all gene transcripts, including potential splice variants to maximise knockdown efficiency. To test the validity of the results, individual siRNAs contained in the Smart Pool were examined. The immunoblot analysis of cathepsin D siRNAs revealed that three out of four siRNAs contained in the Smart pool significantly lowered protein levels of cathepsin D. However, despite the efficiency of these three cathepsin D siRNAs, only one siRNA contained in the pool was able to reproduce the phenotype observed with the pool, suggesting the presence of an off-target effect.

Off-target effects occur when siRNA constructs downregulate unintended targets resulting in a phenotype identifiable as false-positive (Fedorov et al. 2006). These effects might be caused by similarity in the target gene sequence with other genes (Fedorov et al. 2006). One possible way to reduce unwanted off-target effects is to maximise sequence specificity for target genes or to lower siRNA final concentration (Caffrey et al. 2011). In addition, in the experimental condition

that only one siRNA in the Smart Pool is effectively targeting the gene, the transcript knockdown might be diluted resulting in subsignificant or false negative results, which can be avoided by immunoblot validation of individual siRNAs and appropriate statistical power.

Another way to interpret the result observed with knockdown of cathepsin D, is that LRRK2 affects cathepsin D but not vice versa. A direct interaction between cathepsin D and LRRK2 is unlikely since they are separated by the membrane of Golgi-derived endosomes, therefore the energy required for a direct interaction would be too high (McGlinchey and Lee 2015; Perrett et al. 2015; Schapansky et al. 2014a). However, an indirect interaction between LRRK2 and cathepsin D could be mediated by the clathrin binding protein GAK (Greener et al. 2000; Lee et al. 2005b). GAK has been suggested to induce clathrin polymerisation and is directly involved in the uncoating of the clathrin vesicle, containing cathepsin D, budding from the Golgi (Greener et al. 2000; Lee et al. 2005b). Perhaps the LRRK2-GAK-Rab7L1 complex participates in the uncoating of clathrin-coated vesicles containing cathepsin D. Interestingly, expression levels of the cathepsin D receptor, the M6PR, regulate the recruitment of clathrin adaptors and determine the number of clathrin-coated vesicles formed at the Golgi (Le Borgne and Hoflack 1997).

The pharmacological inhibition of cathepsin D via pepstatin A did not significantly alter the formation of the LRRK2-Rab7L1 complex at the Golgi (Fig. 6.10). This result supports the hypothesis that the previously observed increase of LRRK2-Rab7L1 punctae at the TGN is an siRNA off target effect. However, it can be argued that cathepsin D is not active at the Golgi, as the pH is not acidic enough to allow cathepsin D maturation and enzymatic activity (Hu et al. 2015;

McGlinchey and Lee 2015). Therefore, the enzymatic inhibition via pepstatin A is more likely to affect mature, lysosomal cathepsin D.

Further experiments are needed to dissect which genes are potentially involved in the LRRK2-Rab7L1 network at the Golgi and to test the hypothesis of an indirect interaction between LRRK2 and cathepsin D.

### 6.3.2 Evaluation of cytotoxic effects of the siRNA screen

In order to investigate whether siRNA knockdown of iTRAQ candidates results in changes of cell viability, analysis of nuclear staining intensity and nuclear count were performed. Nuclear condensation and chromatin rearrangements correlate both with necrosis and apoptosis (Cummings et al. 2004). Toxic effects have been observed after transient knockdown of some of the iTRAQ candidates, perhaps indicating an essential role for these proteins in cell survival or cell cycle regulation. Off-target effects and toxicity due to transfection reagents are common problematic aspects of these screens and need to be considered. In this screen, siRNA knockdown of three genes of interest, ASAH1, EIF3G and VCP, resulted in cytotoxic effects with cell loss and increased nuclear staining intensity (Fig. 6.6).

The enzyme acid ceramidase 1 (ASAH1) is a lysosomal enzyme involved in the regulation of steroidogenesis (Lucki et al. 2012). Aberrant overexpression of ASAH1 has been previously found in malignant cells (Berndt et al. 2013). ASAH1 knockdown by siRNA or pharmacological inhibition have both been reported to decrease cell proliferation and viability, accompanied by reduction of β-catenin levels (Berndt et al. 2013; Camacho et al. 2013; Lucki et al. 2012). These data

are consistent with the cytotoxic effects observed in the siRNA screen described in this chapter.

The transitional endoplasmic reticulum ATPase or valosin containing protein (VCP) is involved in DNA damage response and is part of a complex that regulates disassembly of the mitotic spindle in the last step of mitosis, to ensure correct formation of the nuclear envelope (Acs et al. 2011; Nowis et al. 2006; Schuberth and Buchberger 2008). Similarly to ASAH1, siRNA knockdown of VCP in colorectal cancer cells was shown to arrest cell proliferation and induce apoptosis (Fu et al. 2016). These observations are in line with the cell loss observed in the presence of VCP siRNA in this screen.

Increased cell death and nuclear staining intensity were also detected in the presence of siRNA against EIF3G. Knockdown of EIF3G and of other components of the translation initiation complex have been reported to decrease cell viability and induce apopotosis (Chen et al. 2015; Sudo et al. 2010). Together these results suggest that expression levels of ASAH1, EIF3G and VCP are crucial for cell survival.

Future work to investigate subsignificant results observed in the two independent siRNA screens performed here will help to identify modifiers of LRRK2 function at the Golgi. Due to the intrinsic experimental variability of these siRNA screens, a third independent screen could help to reveal potential target genes involved in the LRRK2-Rab7L1 network.

# 7 Establishment of an *in vitro* model of lysosomal dysfunction

## 7.1 Introduction

In order to further investigate the functional role for LRRK2 in the endo-lysosomal pathway, primary kidney cells from LRRK2-KO and WT adult mice were prepared for this project. This cell model, partially reproducing the phenotypic defects observed *in vivo*, has successfully been employed to investigate the biological role of LRRK2. Characterisation of LRRK2-KO kidney cells revealed that, as *in vivo*, cells lacking LRRK2 show higher abundance of cathepsin D compared to controls. I therefore examined whether differences that might explain lysosomal accumulation could be detected in these cells. The hypothesis that cathepsin D accumulation observed in LRRK2-KO kidneys is due to an increase of protein synthesis was tested. This hypothesis is supported by the detected changes in abundance of several proteins involved in translation control indicating alterations in the protein synthesis machinery (see 3, Table 9). However, experiments performed in this chapter suggest that cathepsin D accumulation is not due to increased protein synthesis.

Cathepsin D, as other lysosomal proteases, is recognised and delivered to the lysosomal compartment by the mannose-6-phosphate receptor (M6PR) (Braulke and Bonifacino 2009; Young et al. 1991). The M6PR is recycled back to the Golgi via retromer transport (Attar and Cullen 2010; Farias et al. 2014; Lucas et al. 2016; Seaman 2012). To investigate whether accumulation of cathepsin D is due to impaired trafficking of its receptor, LRRK2-KO and control kidney cells were probed for the cation-independent M6PR (CI-M6PR). Differences in the

distribution of cathepsin D receptor were observed in LRRK2-KO cells, showing a more dispersed localisation compared to WT cells. A significant difference in colocalisation between cathepsin D and CI-M6PR was observed in LRRK2-KO primary kidney cells.

Similarly, mutants of retromer complex display altered M6PR distribution (Follett et al. 2014; Rojas et al. 2008). LRRK2 has been reported to functionally interact with part of the retromer complex (Beilina and Cookson 2016; Cookson 2016; Linhart et al. 2014; MacLeod et al. 2013). Therefore, I next tested whether loss of retromer components would result in further cathepsin D accumulation in LRRK2-KO cells. For this purpose, siRNA knockdown of the retromer subunit Vps35 was then performed. Preliminary results show no cumulative phenotype in LRRK2-KO cells treated with Vps35 siRNA. Together these data suggest that LRRK2 might have a role in retrograde transport affecting trafficking of lysosomal enzymes.

## 7.2 Results

### 7.2.1 Phenotypic reproducibility in primary kidney cells from LRRK2-KO mice

To further investigate the role of LRRK2 in vesicular trafficking, primary kidney cells from WT and LRRK2-KO mice were generated in order to provide a tractable platform for understanding mechanism(s) involved in LRRK2 regulation of lysosomal pathways.

I examined expression levels of LRRK2 in control cells and confirmed absence of LRRK2 in knockout kidney cells (Fig. 7.1). To test the presence of lysosomal protease accumulation, observed in LRRK2-KO kidney tissue, I probed LRRK2-KO and control kidney cells for the previosuly validated hits cathepsin D and legumain found to be differentially expressed in KO versus WT tissue (Fig. 4.1). I was able to reproduce the accumulation of cathepsin D in LRRK2-KO cells compared to control kidney cells, consistently with the phenotype observed in kidney tissue (Fig. 7.1). The precursor form of cathepsin D was significantly increased in LRRK2-KO kidney cells in three independent preparations ($P < 0.0001$, Student T test, kidney extracted from n=3 mice, 8-9 month of age). LRRK2-KO primary kidney cells, however, did not have the same increase in mature form of cathepsin D observed in kidney tissue at the same age. This discrepancy could be due to intrinsic differences between *in vivo* and *in vitro* models. In one out of three independent LRRK2-KO kidney cell preparations, the lysosomal protease legumain was also more abundant.

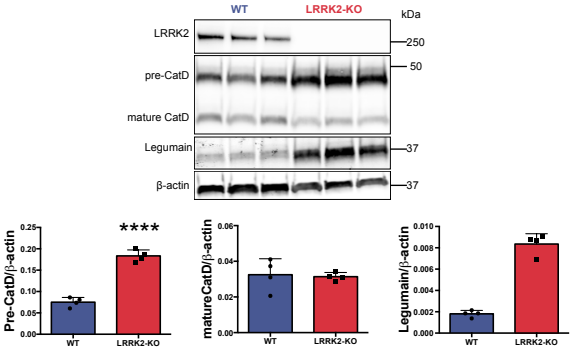


Figure 7.1: **LRRK2-KO primary kidney cells reproduce endogenous cathepsin D accumulation.** Immunoblots for the lysosomal proteases cathepsin D and legumain in total homogenates from LRRK2-KO and control primary kidney cells (Student T test, each band represents a repeat from the same kidney preparation. ∗P<0.05, ∗∗P<0.01, ∗∗∗ P<0.001.)

To assess whether LRRK2-KO kidney cells showed the differences in cytoskeletal proteins reported in tissue (Fig. 4.3, 4.4), I probed one of the tested kidney cell preparations that displayed significantly different levels of cathepsin D in LRRK2-KO, for the cytoskeletal candidates identified by proteomic screen: Naa15, coronin 1C, acetylated-tubulin, α-β-tubulin and gephyrin (Fig. 7.2). In this preparation, no significant differences in gephyrin, coronin 1C, acetylated-tubulin or α/β-tubulin were observed. However, an increase in Naa15 was detected in LRRK2-KO kidney cells compared to controls in this preparation (Fig. 7.2).

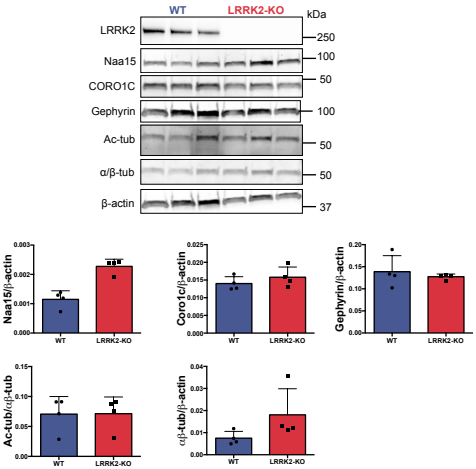


Figure 7.2: **LRRK2-KO primary kidney cells do not reproduce endogenous changes in cytoskeletal proteins.** Immunoblots for the cytoskeletal proteins of interest in total homogenates from LRRK2-KO and control primary kidney cells (Student t test, each band represent a repeat from the same kidney preparation, n=2 biological replicates, $*P<0.05$, $**P<0.01$, $***$ $P<0.001$.)

To test whether the larger, vacuolated structures observed in LRRK2-KO kidney histological sections (Fig. 4.9, 4), were identifiable in LRRK2-KO kidney cells. Cellomics high content imaging was performed using two independent kidney cell cultures stained with cathepsin D antibody. Representative cellomic images show larger cathepsin D punctae in LRRK2-KO cells compared to controls (Fig. 7.3).

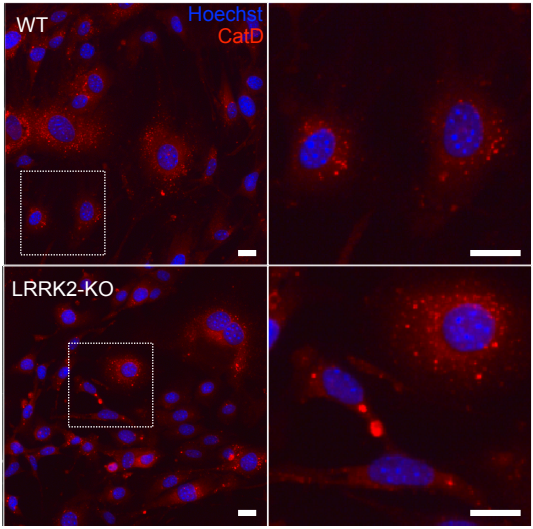


Figure 7.3: **LRRK2-KO primary kidney cells display enlarged cathepsin D-positive structures.** Representative Cellomics images of LRRK2-KO and control primary kidney cells stained in red for cathepsin D (anti-rabbit, Alexa-568) and in blue for nulcei (Hoechst). Scale bar = 10µm.

Unbiased quantification detected a significant increase in number and intensity of cathepsin D positive spots in LRRK2-KO kidney cells compared to controls in both kidney cell preparations (Fig. 7.4). This result indicates that one of the earlier detectable intracellular defects in LRRK2-KO primary kidney cells is accumulation of cathepsin D and formation of enlarged cathepsin D-containing structures.

Together, these results suggest that LRRK2-KO primary kidney cells are a valuable tool to study pathways affected by loss of LRRK2. Control WT cells express

significant levels of LRRK2 and knockout cells reproduce some of the phenotypic changes observed in kidney tissue.

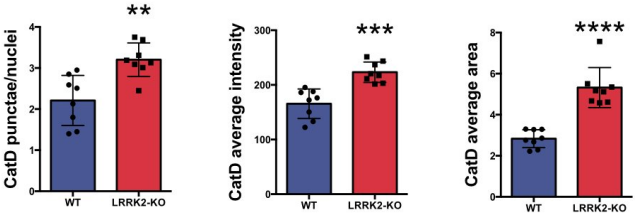


Figure 7.4: **Cellomics quantification of cathepsin D structures.** Quantification of average intensity, area and number of cathepsin D-positive punctae per cell in LRRK2-KO and control cells. The experiment was performed in a 96-well plate and cathepsin D was imaged and counted using the spot detector bioapplication of the Cellomics arrayscan. Statistical significance tested with Student T test, data points represent the average measures from 8 wells of a 96 well plate. The experiment was repeated 3 times. $*P<0.05$, $**P<0.01$, $***P<0.001$, $****P<0.0001$.

### 7.2.2 Loss of LRRK2 decreases protein turnover in primary kidney cells

To answer the question whether cathepsin D accumulation is due to an increase in protein synthesis or to a decrease in turnover, I treated control and LRRK2-KO kidney cells with the lysosomal inhibitor bafilomycin. Bafilomycin is a compound that blocks the vacuolar-type $H^+$-ATPase, preventing lysosomal acidification, therefore inhibiting protein degradation. The hypothesis tested was that loss of LRRK2 causes an increase in synthesis of lysosomal hydrolases, therefore, by blocking protein degradation, a higher accumulation of cathepsin D precursor forms will be detected (Fig. 7.5).

To validate the effect of bafilomycin treatment, kidney cell lysates were probed for the autophagy marker LC3. LC3II accumulation indicates lysosomal blockage and impaired protein degradation. Interestingly, the previously observed cathepsin D accumulation in LRRK2-KO cells was significantly reduced to the control level in cells treated with bafilomycin, compared to controls (Fig. 7.5).

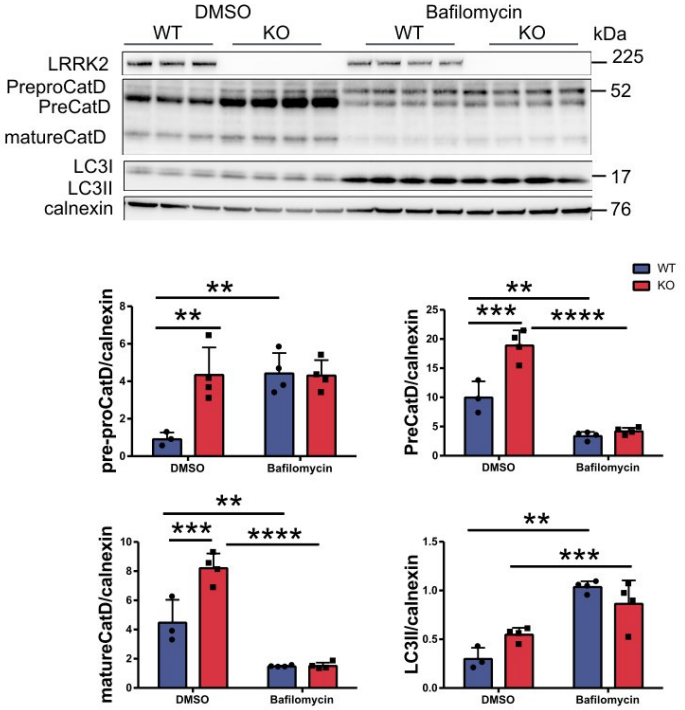


Figure 7.5: **Lysosomal inhibition blocks cathepsin D accumulation in primary kidney cells.** Immunoblots for LRRK2, cathepsin D, LC3 and endogenous control calnexin in LRRK2-KO and control primary kidney cells treated with the lysosomal inhibitor bafilomycin (40µM, 24h) and DMSO control. Immunoblots were developed by ECL. (Bonferroni post-hoc test from two-way ANOVA, representative immunoblots from one of three independent experiments). $*P<0.05$, $**P<0.01$, $***$ $P<0.001$.

This result suggests that, in LRRK2-KO kidney cells, accumulation of cathepsin D is likely due to a decrease in protein turnover rather than an increase in protein synthesis. In particular, translation of cathepsin D seems not affected by loss of

LRRK2. Alternatively, normalisation of cathepsin D protein levels in LRRK2-KO after bafilomycin treatment could indicate lysosomal exocitosis to eliminate the excess of lysosomal substrates building up in the cell.

Another way to further investigate the potential involvement of LRRK2 in cathepsin D protein synthesis, is to test whether mRNA transcription levels are altered. In collaboration with Dr. Andrea Wetzel (UCL, School of Pharmacy), analysis by quantitative RT-PCR analysis of LRRK2-KO and control mRNA, extracted either from cells or from tissue, was performed (Fig. 7.6). No significant changes were detectable for CTSD expression levels in LRRK2 KO compared to wild type samples in kidney cells or tissue (Fig. 7.6). This result strongly suggests that loss of LRRK2 does not affect CTSD expression.

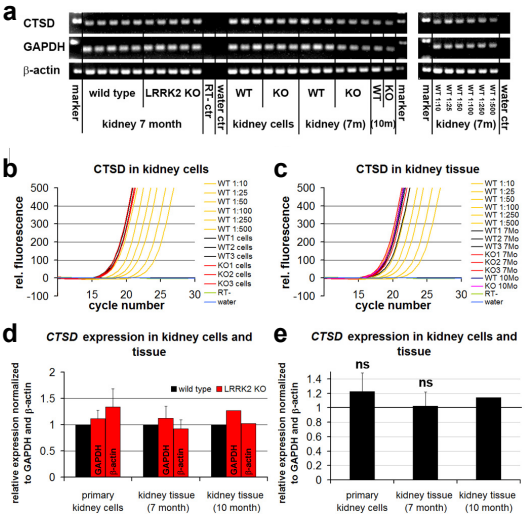


Figure 7.6: **CTSD expression in primary cultured kidney cells and kidney tissue from wild type and LRRK2 knockout mice.** (a) Gel electrophoresis of representative amplification products after quantitative RT-PCR showing the specific expression of transcripts coding for cathepsin D (CTSD) as gene of interest and for GAPDH and β-actin as reference genes in primary mouse kidney cells (n=3 per genotype), 7 month old kidney tissue (n=8 per genotype) and 10 month old kidney tissue as control. A serial dilution of 7 month old kidney tissue from wild type mice has been used as external control. Fluorescence emission of SYBR Green during real time PCR amplification of CTSD in (b) primary mouse kidney cells and (c) kidney tissue of wild type (black lines, standard in yellow) and LRRK2 KO (red lines) mice. (d and e) Relative expression levels of CTSD in primary kidney cells and tissue of wild type and LRRK2 KO mice, normalised to GAPDH and β-actin expression. Values represent the mean ± SD.

### 7.2.3 Mannose-6 phosphate missorting in LRRK2-KO kidney cells

The M6PR plays a key role in cathepsin D sorting to the early endosome (Campbell et al. 1983; Le Borgne and Hoflack 1997). Acidification of the endosomal pH causes the release of cathepsin D from the receptor which is then recycled to the

TGN via retromer tubules for a new round of cargo sorting (Holliday 2014; Hu et al. 2015).

To test the hypothesis that accumulation of cathepsin D is due to impaired recycling of its receptor, I examined M6PR distribution in primary epithelial kidney cells by immunofluorescence. I observed that the receptor changes from juxtanuclear clusters in WT to more disperse localization in KO (Fig. 7.7). This result indicates an impairment in receptor recycling and is reminiscent of experiments with the Vps35 mutant D620N (Follett et al. 2014), which, despite retaining the ability to bind M6PR, results in abnormal secretion of the immature pro-cathepsin D form from the cells.

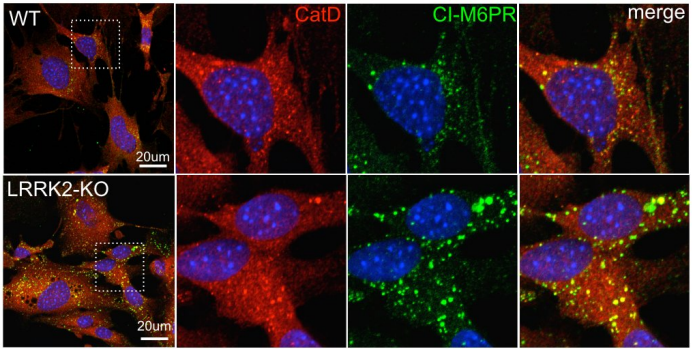


Figure 7.7: **Dispersed distribution of mannose-6-phosphate receptor in LRRK2-KO kidney cells.** Representative confocal images of LRRK2-KO and control primary kidney cells stained in red for cathepsin D (anti-rabbit, Alexa-568), in green for M6PR (anti-mouse, Alexa-488). Nuclei in blue were stained with Hoechst. Scale bar = 20µm

Quantification of M6PR punctae via Cellomics automated detection, identified a significant difference in M6PR punctae per cell between LRRK2-KO and control

primary kidney cells (Fig. 7.8). The intensity and area of M6PR punctae was also significantly higher compared to control cells, indicating the presence of M6PR-containing endosomes in the absence of LRRK2 (Fig. 7.8).

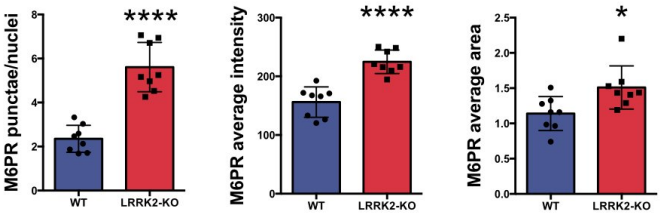


Figure 7.8: **Cellomics quantification of mannose-6-phosphate receptor in LRRK2-KO kidney cells.** Quantification of percentage of cells with M6PR punctae. The experiment was performed in a 96-well plate and M6PR were imaged and counted using the spot detector bioapplication of the Cellomics arrayscan. Statistical significance tested with Student T test. $*P<0.05$, $**P<0.01$, $***P<0.001$, $****P<0.0001$.

To test the hypothesis of M6PR recycling impairment in the absence of LRRK2, I measured colocalisation between cathepsin D and M6PR markers both via manual confocal quantification and via Cellomics automated quantitation (Fig. 7.10). Both preliminary results show a significant difference in colocalisation represented by Pearson's coefficient (P = 0.0002, confocal measure, fig. 7.10, panel a) and by overlap area (P <0.0001, cellomics measure, fig. 7.10, panel b) between M6PR and cathepsin D stainings. Representative confocal images are shown in figure 7.9.

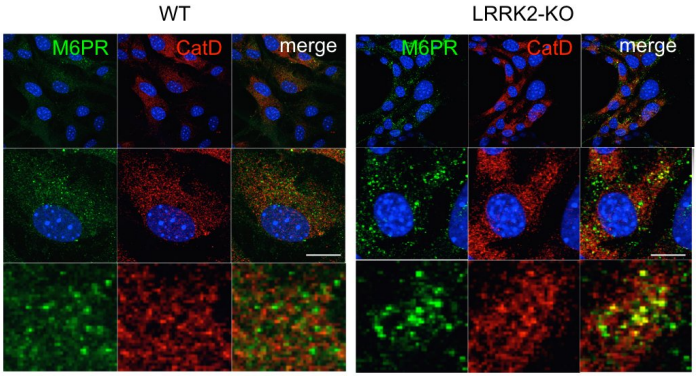


Figure 7.9: **Colocalisation of cathepsin D with mannose-6-phosphate receptor in LRRK2-KO kidney cells.** Representative confocal images of LRRK2-KO and control primary kidney cells stained in red for cathepsin D (anti-rabbit, Alexa-568), in green for M6PR (anti-mouse, Alexa-488). Nuclei in blue were stained with Hoechst. Scale bar = 10µm

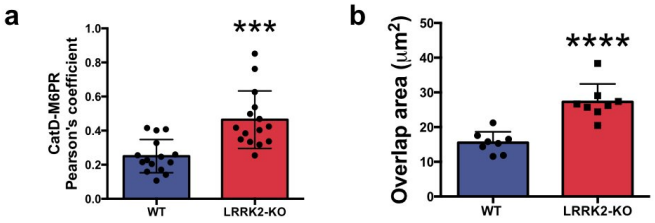


Figure 7.10: **Quantification of mannose-6-phosphate receptor colocalisation with cathepsin D in primary kidney cells.** (a) Pearson's correlation coefficient measured by manually quantifying 15 cells after confocal imaging. (b) Overlap area ($\mu m^2$) measured by automated cellomics analysis, data points represent the average area of overlap between the two channels measured from 8 wells of a 96 well plate. Statistical significance tested with Student T test. $*P<0.05$, $**P<0.01$, $***$ $P<0.001$.

Together these results support the hypothesis that in the absence of LRRK2, there is an impairment of M6PR trafficking, resulting in enlarged endosomes positive for both cathepsin D and its receptor, unable to recycle and deliver cathepsin D to the lysosome. Additional experiments in independent kidney cell preparation are needed to confirm these results.

### 7.2.4 Retromer misfunction in LRRK2-KO primary kidney cells

Accumulation of cathepsin D has been reported in mutants of retromer complex (Follett et al. 2014; Rojas et al. 2008). This phenotype is observed in mutants and after knockdown of the retromer subunit Vps26 (Rojas et al. 2008). Defects in retrograde transport impair the trafficking of the M6PR (Rojas et al. 2008). In particular, the M6PR seems trapped in early endosomes resulting in its depletion from the TGN and, consequently, in accumulation of acid hydrolase

precursors (Rojas et al. 2008). Similarly, abnormal secretion and accumulation of pro-cathepsin D has been observed in the *VPS35* mutant D620N (Follett et al. 2014).

Therefore, I next investigated whether cathepsin D accumulation in LRRK2-KO cells is a consequence of retromer misfunction, suggesting that LRRK2 is in the same functional pathway as retromer. To test this hypothesis, knockdown of the Vps35 subunit of retromer in the LRRK2-KO cells was performed. If LRRK2 is in a different pathway from retromer, the expected result should be an additive, exacerbated phenotype of pre-cathepsin D accumulation. If, however, the phenotype observed in LRRK2-KO cells is not worsened this would suggest that LRRK2 acts in the same recycling pathway.

In this preliminary experiment, I observed that knockdown of *VPS35* reproduced the cathepsin D precursor accumulation in control primary kidney cells, indicating the validity of the siRNA. Depletion of retromer, however, did not worsen the LRRK2-KO accumulation of cathepsin D, suggesting that LRRK2 acts in the same functional pathway as retromer and that cathepsin D accumulation is likely due to defective sorting of its receptor.

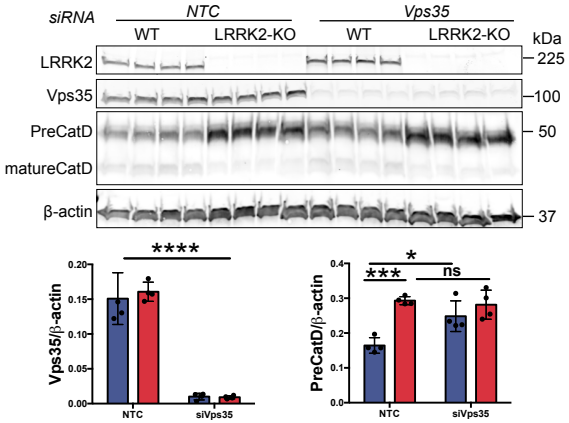


Figure 7.11: **Loss of Vps35 does not worsen Cathepsin D accumulation in LRRK2-KO primary kidney cells.** Immunoblots from LRRK2, Vps35, cathepsin D and β-actin endogenous control in LRRK2-KO and control primary kidney cells. Cells were transfected for 48h with *VPS35* siRNA and non-targeting control siRNA. (Bonferroni post-hoc test from two-way ANOVA). ∗P<0.05, ∗∗P<0.01, ∗∗∗ P<0.001.

## 7.3 Discussion

### 7.3.1 A platform to study lysosomal accumulation

In order to provide a platform to investigate the molecular mechanisms underlying LRRK2-KO pathology in kidneys, primary cells extracted from the cortical region of LRRK2-KO and control mouse kidneys were cultured and passaged *in vitro*. The purpose of these experiments was also to validate a cell model that can then be used for functional analysis, not possible to explore in tissue. I first obtained immunocytochemistry and immunoblot data. A difference in cathepsin D protein levels and staining was observed in LRRK2-KO primary kidney cells compared to control cells. Primary kidney cells from LRRK2-KO mice started to accumulate cathepsin D after several passages. Similarly to kidney histological sections, LRRK2-KO kidney cells display a higher number of cathepsin D positive punctae and enlarged endosomes.

I did not observe differences in cytoskeletal proteins, previously detected as differentially abundant in LRRK2-KO kidneys *in vivo*, with the exception of Naa15. One possible interpretation could be that the cytoskeletal impairments reported in LRRK2-KO kidney tissue indicate a compensatory effect, whereas lysosomal dysfunction represents a primary consequence of loss of LRRK2 in kidney cells. Another possibility is that certain differences are only detectable *in vivo*. Cells cultured *in vitro* lack tissue architecture and extracellular matrix. This may result in the lack of compensatory changes in cytoskeletal morphology and function in cultures.

### 7.3.2 Intrinsic variability of the model

Cathepsin D accumulation was reproducible in LRRK2-KO kidney cells, however, the previously validated lysosomal protease legumain, was not consistently different in LRRK2-KO kidney cells between cell preparations. Primary cells present intrinsic animal to animal variability. One possible explanation for the discrepancy between primary kidney cell preparations are selection artefacts. Primary kidney cells are mixed cultures and it is possible that one cell type prevails over others since cells are continuously passaged in culture and subpopulations of cells can be selected.

A phenotypic difference between LRRK2-KO and control cells may be present but could be too subtle to observe or quantify. Future experiments will require a higher number of kidney cell preparations or use isogenic models to determine whether the tissue phenotype can be reproduced.

Variability between passages was also observed. Accumulation of cathepsin D in LRRK2-KO kidney cells was detectable between passage 6-8 in most preparations but in other preparations cathepsin D started to accumulate earlier (passage 2-4). Primary kidney cells from LRRK2-KO mice could represent a valuable cell model to study lysosomal dysfunction that partially reproduces the pathology observed *in vivo*.

### 7.3.3 Loss of LRRK2 does not alter cathepsin D transcription or translation

The proteomic screen performed in this study reported a number of candidates involved in protein synthesis as significantly more abundant in LRRK2-KO kidneys (3, 4). To test the hypothesis that accumulation of the lysosomal protease

cathepsin D was due to enhanced mRNA transcription, quantification of cathepsin D mRNA expression was obtained via quantitative RT-PCR in collaboration with Dr. Andrea Wetzel (UCL, School of Pharmacy). The results obtained both in primary kidney cells and tissue strongly argue against a transcriptional effect on cathepsin D in LRRK2-KO models as they show no significant difference in the expression levels of cathepsin D between LRRK2-KO and control samples.

To investigate whether accumulation of cathepsin D represents a consequence of increased protein translation, I treated LRRK2-KO and control kidney cells with bafilomycin to block lysosomal degradation. After treatment, precursor forms of cathepsin D were no longer different between LRRK2-KO and control cells, indicating that an increase in cathepsin D synthesis is unlikely. Another possible explanation of this normalisation could be that LRRK2-KO cells undergo lysosomal exocytosis, in attempt to reduce the excess of accumulated undigested materials in the cell (Medina et al. 2011). Induction of lysosomal exocytosis via transcription factor TFEB overexpression has been shown to rescue pathological storage of intracellular lysosomes both *in vivo* and *in vitro*, suggesting that this could be a physiological mechanism of repair (Medina et al. 2011).

Together these results support the hypothesis of a trafficking defect of cathepsin D, rather than a protein expression abnormality, in the absence of LRRK2. LRRK2 might function as a scaffold on microtubules, helping the transport to the lysosome of newly formed endosomes containing lysosomal hydrolases. An important question remains whether the trafficking defects observed in the absence of LRRK2 are related to anterograde or retrograde vesicle transport.

### 7.3.4 Mannose 6 phosphate trafficking defect in LRRK2-KO kidney cells

In the endosomal network, cargo can either be sorted towards the lysosome for degradation or can be recycled back and reused (Mcmillan et al. 2017). The cathepsin D receptor, the M6PR, represents one of the most common examples of cargo recycled via retromer (Braulke and Bonifacino 2009; Karcher et al. 2002; Lucas et al. 2016). Therefore, I next asked whether cathepsin D accumulation in the absence of LRRK2 was a consequence of impaired receptor trafficking. A significant difference in M6PR distribution was observed in LRRK2-KO kidney cells compared to controls. Unbiased analysis of M6PR positive structures reported a significant increase in area, intensity and punctae per cell in LRRK2-KO kidney culture.

A significant difference in colocalisation between cathepsin D and M6PR was also observed in LRRK2-KO kidney cells. This result can be interpreted as a slower recycling of the M6PR. A decrease in cyclic rounds of M6PR and lysosomal hydrolase trafficking could result in a less efficient delivery of these enzymes to the lysosome. As a consequence, reduced lysosomal activity results in an accumulation of non-degraded proteins (Mcmillan et al. 2017).

Alterations in M6PR distribution with impaired lysosomal hydrolase delivery were previously reported in mutants of the retromer subunit Vps35 (Follett et al. 2014), indicating that alterations in retrograde transport affect cathepsin D sorting. To investigate whether retromer defects were contributing to cathepsin D accumulation in LRRK2-KO kidney cells, I performed siRNA knockdown of *VPS35*. Preliminary results show a significant difference in abundance of cathepsin D precursor in control cells treated with siRNA against *VPS35*. This difference

was not detected in LRRK2-KO cells treated with *VPS35* siRNA which were not significantly different from LRRK2-KO cells treated with non-targeting control siRNA. This result, although it needs to be validated, supports the previously reported notion that LRRK2 and retromer are in the same functional pathway (Linhart et al. 2014).

To conclude, the establishment of a cellular model to study lysosomal dysfunction has allowed to reproduce and investigate the functional defects observed in LRRK2-KO kidney tissue such as cathepsin D accumulation. Loss of LRRK2 does not affect cathepsin D synthesis but it is likely to affect cathepsin D receptor recycling via retromer. Further experiments to investigate the potential role of LRRK2 in retrograde transport are needed to dissect this molecular mechanism.

# 8 Materials and Methods

## 8.1 Animals

Experiments using animals were conducted in compliance with the Guide for the Care and Use of Laboratory Animals of the National Institutes of Health. The specific experiments performed in this study were approved by the Institutional Animal Care and Use Committees of the US National Institute on Aging (Animal study protocol number 463-LNG-2018). Animal experiments performed at UCL were approved by the UCL Ethics Committee and by the home office as detailed in the relevant project licence (KH). LRRK2 KO mice (Lin et al. 2009) were generously provided by Dr. Huaibin Cai, NIA. LRRK2 G2019S knock-in mice were a gift from Dr. Heather Melrose (Majo Clinic, Jacksonville).

## 8.2 Organ Dissection and Protein Extraction

For proteomics experiments and for validation by western blotting, age-matched wild-type, LRRK2-KO, homozygous and heterozygous knock-in mice, each bred on a C57BL/6J background, were euthanised by cervical dislocation. From each animal, one kidney was immediately frozen in dry ice while the other was fixed in 4% PFA in PBS for histological analysis. Brain hemispheres were separated and cortex, striatum and hippocampus were dissected and frozen in dry ice. For experiments where G2019S heterozygous animals were used, littermate wild type animals were used as controls in the proteomics screens and for validation experiments. In these experiments, the knockout animals were from separate litters from homozygous breeding pairs in the same facility.

Tissue samples were placed in pre-chilled Eppendorf tubes and kept at -80°C prior to protein extraction where required. The lyisis buffer used was Tris HCl 20mM, 1% of Surfact-Amps NP40, (Thermo Scientific), 1mM EDTA, 10% glycerol, NaCl 150mM. 1% Complete Protease inhibitor cocktail tablet (Roche) and 1% HALT phosphatase inhibitor (Thermo Scientific) were added immediately before use. Tissue was weighed and mixed with 5 volumes of extraction buffer. Total protein concentration of each lysate was measured using a Protein Reagent 660nm assay (Thermo Scientific Pierce, #22660), carried out in a 96-well plate according to the manufacturer's instruction.

## 8.3 iTRAQ Proteomics

### 8.3.1 Cytosol and Microsome Enriched Fractions Preparation

Frozen kidneys dissected from one-year-old mice were homogenised in Mito isolation buffer (0.225M mannitol, 0.05M sucrose, 0.0005M HEPES, 1mM EDTA). The homogenate was centrifuged at 2000×g for 3min at 4°C. The supernatant was collected in a separate tube and the pellet, containing the nuclei, was resuspended in isolation buffer, and the centrifugation step repeated. The supernatant was combined with the previous supernatant collected and centrifuged to clear lysates at 12000×g for 8min at 4°C. This step allows the separation of a pellet enriched in mitochondria, which was subsequently washed in isolation buffer and centrifuged at 12000×g for 8min at 4°C. Ultracentrifugation of the supernatant from the last step was employed to allow the separation between cytosolic and microsomal fractions. Backman Centrifuge tubes (11×34mm) were loaded with the exact same amount of the supernatant collected from the previous steps. The ultracentrifugation was carried out at 55,000×g for 30min at 4°C. The pellet was resuspended in iTRAQ

compatible buffer (0.3M HEPES, 2% CHAPS, 1mM EDTA). Both fractions were used in iTRAQ and immunoblotting experiments. Protein concentration was determined using 660nm protein assay reagent (Pierce #22660) using bovine serum albumin as a standard reference.

### 8.3.2 Isobaric Tag for Relative and Absolute Quantitation (iTRAQ) Labelling

Kidney cytosolic and microsomal fractions from five wild type and five LRRK2-KO samples were analysed in two separate experiments for a total of four iTRAQ runs (Fig. 8.1). A pooled control, used as a reference sample, was made by combining 40µg of each wild type sample. The concentration of each sample was adjusted to 1µg/µl with iTRAQ buffer (0.3M HEPES, 2% CHAPS, 1mM EDTA). Samples were treated with 2µl of Reducing Reagent (TCEP solution) for 60min at 60°C, subsequently alkylated with 1µl of methyl methanethiosulfonate for 20min at RT. Digestion with sequence grade modified trypsin (Promega, Madison, WI) diluted 1:50 (v/v) with sample was then carried out overnight at 37°C. Before addition to samples, iTRAQ 8-plex reagents were dissolved in 150µl of isopropanol and vortexed. Each sample mixture was labelled for 3h at room temperaturewith the appropriate iTRAQ reagent and labelled peptide mixtures were combined. Samples were desalted using an Oasis HLB 200mg cartridge (Waters, Milford, MA). Fractionation of iTRAQ labelled peptides by liquid chromatography (LC) and subsequent tandem mass spectrometry (MS/MS) analysis of the fractions were carried out by Dr. Yan Li (Protein/Peptide Sequencing Facility, NINDS, NIH) and performed according to (Hauser et al. 2014).

cytosolic fractions

| Experiment 1 | |
|---|---|
| *Run1* | *Run2* |
| WC Pool | WC Pool |
| WC1 | WC4 |
| WC2 | WC5 |
| WC3 | KC3 |
| KC1 | KC4 |
| KC2 | KC5 |

microsomal fractions

| Experiment 2 | |
|---|---|
| *Run1* | *Run2* |
| WM Pool | WM Pool |
| WM1 | WM4 |
| WM2 | WM5 |
| WM3 | KM3 |
| KM1 | KM4 |
| KM2 | KM5 |

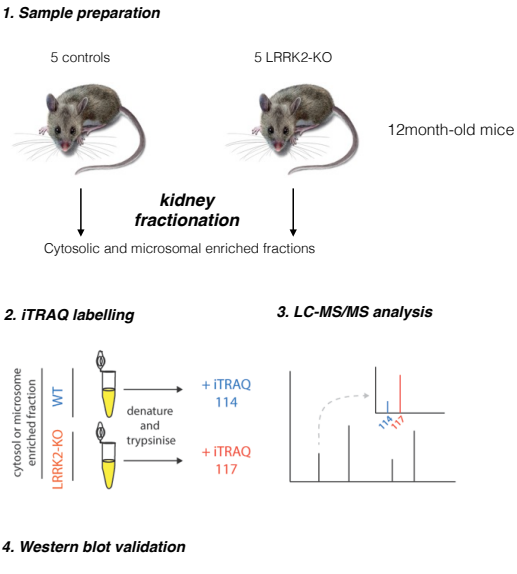


Figure 8.1: **iTRAQ experimental design** W = Wild type, K = LRRK2-KO, C = cytosolic enriched fractions, M = microsomal enriched fractions. On the left, tables of the iTRAQ runs: cytosolic fractions for the experiment 1 and microsomal fractions for experiment 2. On the right, schematic experimental plan including sample preparation, representative iTRAQ labelling, peptide fractionation via LC followed by tandem MS and western blot validation of the significant hits.

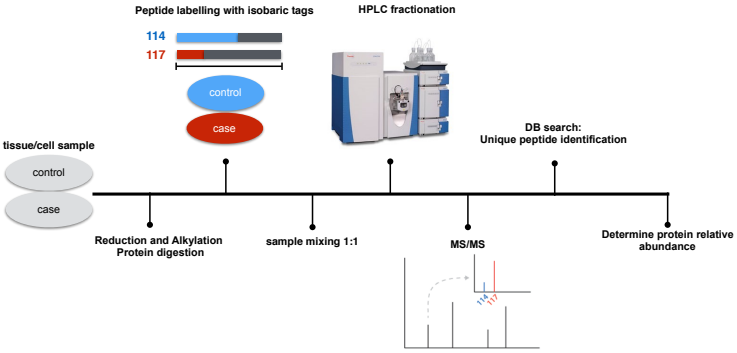


Figure 8.2: **iTRAQ technology workflow.** iTRAQ sample preparation includes reduction and alkylation of the protein samples before digestion with trypsin. Samples are then differentially labelled with isobaric tags and mixed in a 1:1 ratio. HPLC fractionation and tandem mass spec MS/MS are then performed to allow peptide separation. Database research is conducted to identify unique peptides and determine relative abundance.

## 8.4 Polyacrylamide Gel Electrophoresis

Samples containing approximately 10µg total protein were treated with NuPAGE LDS Sample Buffer 4× (Novex) and NuPAGE Sample Reducing agent 10× (Thermo Fisher), then heated for 3min at 95°C. NuPAGE LDS Sample buffer contains SDS, Tris-Hcl pH6.8, glycerol and bromophenol blue.

Protein samples were loaded into consecutive lanes with one additional lane containing Full-range Amersham Rainbow Marker (BioLabs). Pre-cast gels

were run at a voltage of 90mV for 1h and 30min using BIORAD Modular Mini-PROTEAN II Electrophoresis System. Running buffer (Novex) was Tris-glycine-SDS (0.1% SDS, 25mM Tris, 192mM glycine, pH8.3).

The same technique was carried out in the NIH Laboratory of Neurogenetics. In this laboratory protein samples and markers (Precision Plus Protein All Blue Standards) were loaded in a pre-cast gel (Criterion TGX, Biorad) and a voltage of 250V for 30min was applied.

## 8.5 Western Blot

Samples were transferred to a polyvinylidene fluoride (PVDF) membrane (Merck Millipore) requilibrated in methanol, at 20V for 1h utilizing a Trans Blot SD Semi-Dry Transfer Cell machine. Blocking of the membrane was then performed by placing the membrane in a dilute solution of non-fat dry milk 5%, Tris-buffered saline supplemented with 0.1% (v/v) Tween 20 and incubating for 1h at room temperatureunder gentle agitation. After blocking, membranes were washed 3 times, 5min each, with TBS-Tween 20 0.1%. Detection involved two main steps: incubation with primary antibody and incubation with secondary antibody, both diluted in TBS-Tween 20 0.1%, with either 5% non-fat dry milk or 5% BSA for phospho-specific antibodies.

The quantified amount of each target protein was normalised to the amount of β-actin, as a reference protein. Incubation with primary antibody took place at 4°C overnight under gentle agitation. Membranes were then rinsed 3 times at 5min intervals, with TBS-Tween 20 0.1%. Incubation with secondary antibody took place at RT, for 1h under gentle agitation. The secondary antibody is directed at a species-specific portion of the primary antibody and is linked to a reporter enzyme

called horseradish peroxidase (HRP). This reporter enzyme-linked antibody is used to cleave a chemiluminescent agent, and the reaction produces luminescence in proportion to the amount of protein. The secondary antibodies, purchased from Santa Cruz, are goat anti-mouse IgG-HRP (sc-516102), goat anti-rabbit IgG-HRP (sc-2357) and goat anti-rat IgG-HRP (sc-2006).

Before imaging, membranes were then rinsed 3 times at 5min intervals, with TBS-Tween 20 0.1%. SuperSignal West Pico and Femto Chemiluminescent Substrate (Pierce ECL Western Blotting system kit), containing luminol were both used to image the bound antibody complexes. After 1min incubation, membranes were placed into the chamber center of the chemiluminescence detection device. GeneGNOME software was used for analysis and quantification of blot images (High quantum efficiency camera - Syngene).

### 8.5.1 Western Blot Using Li-COR Technology

In the NIH Laboratory of Neurogenetics, Western blot technique was carried out using Li-COR (Lambda Instruments Corporation, Biosciences, Lincoln, NE). Lysates were resolved using Biorad gels and transferred on PVDF membranes using the Trans-Turbo Transfer System (Biorad). Membranes were blocked with Odyssey®Blocking Buffer (Bioscience). Primary antibody incubation was carried out using the previously listed antibodies following the optimised protocol described above. After 3 washes each of 10min with TBS-Tween 20 0,1%, PVDF membranes were probed with IRDye®800CW Goat anti-Mouse IgG (1:15,000, Li-COR) or 800CW Goat anti-Rabbit secondary antibody (1:15,000, Li-COR) for 1h at room temperaturewith shaking. Finally, membranes were washed as previously described, and imaged using a Li-COR Odyssey CLx Infrared Imaging System. Quantification was performed using Li-COR Image Studio software. The

majority of immunoblots presented in this thesis were imaged using Li-COR Odyssey CLx Infrared Imaging System unless alternatively specified.

## 8.6 Antibodies and Chemicals

The following antibodies used for immunoblot were diluted in a 1:1 mix of Odyssey Blocking Buffer (LI-COR) and TBS containing 0.1% (v/v) Tween 20: rabbit polyclonal antibody to cathepsin D (Millipore, # 219361, 1:2000), goat polyclonal antibody to cathepsin D C-20 (Santa Cruz, # sc-6486, 1:200), rabbit polyclonal antibody to legumain (Abcam, # ab125286, 1:1000), mouse monoclonal antibody to gephyrin (Synaptic System, #147 111, 1:2000), mouse monoclonal antibody to β-actin (Sigma, #A5316, 1:10,000), rabbit polyclonal antibody to α/β-tubulin (Cell Signaling, #2148, 1:1000), mouse monoclonal antibody to acetylated-tubulin (Sigma, #T7451, 1:1000), rabbit polyclonal antibody to coronin 1C (Proteintech, #14749-1-AP, 1:1000), mouse monoclonal antibody to NAA15 (LSBio, #LS-C342562, 1:1000), rabbit monoclonal antibody to Rab7 (Abcam, #ab137029, 1:1000), rat monoclonal antibody to LAMP1 (1D4B) (Abcam, #ab25245, 1:1000), mouse monoclonal to GAPDH (Abcam, #ab8245, 1:5000). Bafilomycin (Sigma, #B1793-2UG) dissolved in dimethyl sulphoxide (DMSO) was used at a concentration of 40µM for 24h incubation at 37°C. Pepstatin A (Sigma, #P5318) was dissolved in a solution of methanol and acetic acid (9:1 v/v) to obtain a 1mM stock solution. Cathepsin D Fluorimetric Assay Kit (Abcam, #ab65302) was employed, according to manufacturer's instructions, to test cathepsin D enzymatic activity in HEK293FT cells.

## 8.7 Immunohistochemistry

Frozen kidneys were post-fixed by immersion in 4% PFA overnight. This solution helps to maintain tissue organization and facilitates subsequent sectioning. Whole kidneys were stored in PBS with 30% sucrose and 0.05% sodium azide to prevent any bacterial infections. Tissues were then frozen and 40µm thick sections were collected using the Leica CM1900 Cryostate. Kidney sections were then washed in PBS 3 times for 10min. Antigen retrieval was performed for 20min at 80°C in sodium citrate buffer solution (10mM sodium citrate, 0.05% Tween20, pH 6.0). Following three 5min washes in PBS, non specific sites were blocked by incubating the sections for 1h at room temperatureunder gentle shaking with blocking buffer (0.3% Triton, 1% BSA, 1% donkey serum). Incubation with primary antibody, diluted in blocking buffer, took place at 4°C overnight under gentle agitation. Sections were then washed 3 times for 10min in PBS and incubated with Alexa Fluor secondary antibodies (donkey anti-rabbit and donkey anti-goat 1:500) for 1h at RT, covered with foil, on the shaker. Before imaging, sections were washed again 3 times for 10min in PBS and mounted on slides using Prolong Gold mounting media (Life Technologies).

Kidneys were post-fixed by immersion in 4% PFA overnight and then transferred to PBS with 30% sucrose and 0.05% sodium azide for 24h. Tissues were then frozen and 40µm sections cut using a Leica CM1900 cryostat. After three 5min washes in PBS, sections were blocked at room temperature for 1h in blocking buffer (0.3% Triton, 1% BSA, 1% donkey serum in PBS). The same buffer was used for the primary antibody incubation overnight at 4°C with gentle shaking. Sections were then washed 3 times in PBS for 10min and incubated with Alexa Fluor secondary antibodies (donkey anti-rabbit and donkey anti-goat, 1:500) for

2h at room temperature. After three 10min washes in PBS, sections were mounted on glass slides using ProLong Gold Antifade Mountant.

## 8.8 Cell Culture

### 8.8.1 Primary Kidney Cells

For the preparation of primary kidney cells, kidneys from 8-9 month-old mice, euthanatised by $CO_2$, were collected. Kidneys were washed in cold Hank's buffered saline solution (HBSS, Gibco, #24020117) to remove residual blood. Renal fibrous capsule, connective tissue and renal medulla were removed under sterile conditions. Kidney cortical tissue was dissected in order to obtain 1 $mm^3$ fragments. The fragments were washed in HBSS and then mechanically minced using clean scalpels. Tissue homogenates were then transferred into 50ml falcon tubes containing HBSS with 1mg/mL collagenase IV (enzymatic activity: 200 U/mL) (Thermo Fisher) to allow digestion at 37°C for 30min, shaking the tubes every 10min. Digested kidney fragments were then passed through a 100µm sieve in another falcon tube to remove fibrous tissue. The sieve was carefully washed in HBSS and the cell suspension centrifuged at 1200rpm for 5min. This step was repeated twice. Finally, cell pellet was resuspended in complete culture media: DMEM/F12 1:1 media (Thermo Fisher, Cergy Pontoise, France) containing 5% fetal bovine serum (FBS, #16J365, Sigma), 10 ng/mL Epidermal Growth Factor (EGF, #PHG0311L, Thermo Fisher), 1% penicillin/streptomycin (#15140122, Thermo Fisher), 1% L-glutamine (Thermo Fisher), 50mM hydrocortisone (#H0888, Sigma Aldrich), 5µg/mL insulin, 5µg/mL transferrin and 50nM sodium selenite (ITS-G, #41400045, Thermo Fisher). Cells were cultured in 75$cm^2$ plastic flasks with complete culture medium at 37°C under 5% $CO_2$ in a humidified atmosphere. The culture medium

was changed after 24h in order to eliminate non-adherent cells and residual cellular fragments. Cells were allowed to grow to 80% confluence and then subcultured or frozen.

### 8.8.2 Quantitative real-time polymerase chain reaction (qRT-PCR)

Isolation of total RNA, reverse transcription and qRT-PCR were performed as previously described with few changes (Subramanian et al. 2012). Total RNA from primary cultured mouse kidney cells and mouse kidney tissue was isolated and purified with the RNeasy Mini Kit (QIAGEN). RNA was reverse transcribed with the SuperScript®III First-Strand Synthesis System (Invitrogen) and qPCR of diluted cDNA was carried out on an AriaMx Realtime PCR System (Agilent Technologies) using iTaq™ Universal SYBR®Green Supermix (Bio-Rad Laboratories) for a total reaction volume of 20µl. Oligo 6.0 software (MedProbe) served as program to select intron-spanning primers targeting the mus musculus Ctsd gene (NM_009983.2; 330-forward 5'-GCCGCAGTGTTTCACAG-3'; 479-reverse 5'-TGAGCCGTAGTGGATGTCAA-3'; amplification product: 169bp). Optimized primers for the two housekeeping reference genes, GAPDH and β-actin, have been used as published earlier (Subramanian et al. 2012): GAPDH: NM_008084; 205-forward 5'-GCAAATTCAACGGCACA-3'; 337-reverse 5'-CACCAGTAGACTCCACGAC-3'; amplification product: 141 bp; β-actin: NM_007393; forward 5'-GCCAACCGTGAAAAGATGAC-3'; reverse 5'GGCGTGAGGGAGAGCATAG-3'. In order to verify the specificity of the PCR products gel electrophoresis, melting curve analysis and '-RT' (reverse transcriptase) as well as water control PCR reactions were conducted. Calculation of relative expression levels for Ctsd in LRRK2 knockout versus wild type samples

was determined with the ΔΔCt method. Statistical analysis was done using nonparametric Mann-Whitney test.

### 8.8.3 Vectors and Cell Lines

Human Embryonic Kidney 293 (HEK293) cells FT (Thermo Fisher), an immortalised cell line derived from human embryonic kidney, were maintained in DMEM (Lonza) containing 4.5g/l glucose, 2mM l-glutamine, and 10% fetal bovine serum (Lonza) 37°C under 5% $CO_2$. Cells were allowed to grow in a 75 $cm^2$ flask and passaged every two to three days to avoid over-confluency. Passaging consisted of washing the cells in 10ml of phosphate buffered saline (PBS, #10010023, Thermo Fisher) prior to incubation with 2ml of TrypLE Express Enzyme (1X), phenol red solution (#12605010; Thermo Fisher) at RT for 2-3min with occasional gentle agitation until cell detachment. Cell suspensions were subsequently diluted in DMEM and plated at a suitable density for experiments and/or continued culture. When growing HEK293FT cells achieved 50-70% confluency, cells were transfected with DNA constructs. Plasmids employed for the siRNA screen (previously described in Beilina et al. 2014) are 3x FLAG-LRRK2, myc-Rab7L1 and myc-Rab7L1 Q67L. Transfection was performed using Lipofectamine 2000 (#11668019, Thermo Fisher), according to manufacturer's protocol.

### 8.8.4 siRNA Transfection and Protein Extraction

For siRNA knockdown experiments, primary kidney cells were grown in 6-well plates, each transfected with 2µg of siRNA in Opti-MEM media using RNAiMax (#13778500, Thermo Fisher) according to the manufacturer's protocol. Cells were harvested 48 hours post-transfection in a lysis buffer containing: 50mM Tris pH 7.5, 150mM NaCl, 1% Triton TX-100, 1× complete protease inhibitor

cocktail (Roche) and 1× Halt phosphatase inhibitor cocktail (Pierce). Lysates were clarified by centrifugation at 14000g for 10 min at 4°C, and supernatants collected for Western blot.

## 8.9 Immunocytochemistry

For immunocytochemistry, primary kidney cells or HEK293 FT cells were seeded in 24-well plates containing coverslips previously treated with 0.5ml poly-D lysine per well for 1h at RT. Cells were fixed in 4% paraformaldehyde (PFA) for 15min, washed with PBS and permeabilised with a solution of 0.1% Triton-X in PBS for 10min. Blocking was performed using a solution of 3% BSA in PBS for 1h under gentle shaking. Cells were incubated with the appropriate dilution for 2h at RT. Subsequent washes with PBS and 1h secondary antibody incubation at room temperaturewere carried out. Alexa Fluor antibodies diluted 1:500 in 3% BSA/PBS blocking solution were used. Both cell lines were also stained for DAPI (1:500), which strongly binds A-T rich regions in DNA allowing nuclei identification. Each coverslip was then mounted on a microscope slide (usually 2 coverslips per slide) using ProLong Gold Antifade Mountant (#P36934, Thermo Fisher) and left to dry overnight at room temperature, covered with a foil lid. Slides were subsequently analysed using confocal microscopy as described below.

## 8.10 RNA Interference Screen

### 8.10.1 Automated Cellomic Assay

For the automated cellomic assay, HEK293FT cells (Chia et al. 2014) were seeded at $12.5\times10^3$ cells per well in a 96-well Matrigel-coated plate. Cells were transfected with pooled ON-TARGETplus siRNA (GE Dharmacon) against ARHGEF7,

CK1α, Non-Targeting siRNA Control (NTC) and individual target genes of interest at a final concentration of 25nM. Transfection was carried out using DharmaFECT 1 transfection reagent (GE Dharmacon). Twenty-four hours after siRNA transfection, cells were further transfected with 3×FLAG-LRRK2 and 2×myc- GUS or 2×myc-Rab7L1 WT or 2×myc-Rab7L1 Q67L mutant plasmids using Lipofectamine 2000 (#11668019, Thermo Fisher) reagent. 48h after siRNA transfection and 24h after plasmid transfection cells were fixed with 4% PFA for 15min at RT. Cells were then washed once with PBS and blocked for 1h with a solution containing 0.1% triton, 5% FBS in PBS. After blocking, primary antibody incubation with TGN46 (AbD Serotec), FLAG (Sigma) and myc (Roche) antibodies was carried out for 2h at RT. Cells were then washed 3 times with PBS and incubated for 1h at room temperaturewith Alexa Fluor secondary antibodies (goat anti-rabbit 488, goat anti-mouse 647 and goat anti-sheep 568, 1:500) and Hoechst (1:10,000). Finally, cells were washes 3 times with PBS and left in the fridge overnight before imaging.

Cells that were fixed and immunostained for confocal analysis, as previously described, were subsequently analysed using Thermo Scientific Cellomics ArrayScan VTI HCS Reader. This is a modular High Content Screening instrument designed for high capacity automated fluorescence imaging and quantitative analysis of fixed and live cells. This instrument features optics by Carl Zeiss, broad white-light source, scientific grade digital camera and integrated acquisition and analysis software. Plates were imaged at 20× objective on high-throughput Cellomics VTI arrayScanner and analysed using Spot Detector bioapplication for % of cells with LRRK2 and TGN46-positive spots from total number of LRRK2-transfected cells. Three independent experiments were performed with six wells per sample with the minimum of 1,000 cells per well. siRNAs samples

for CK1α, Rab7L1 or ARHGEF7 were compared with NTC within families (GUS, Rab7L1 WT or Rab7L1 Q67L) by two-way analysis of variance (ANOVA), Tukey's multiple comparison test. The same Spot Detector bioapplication was used to count cathepsin D-positive spots in primary kidney cells.

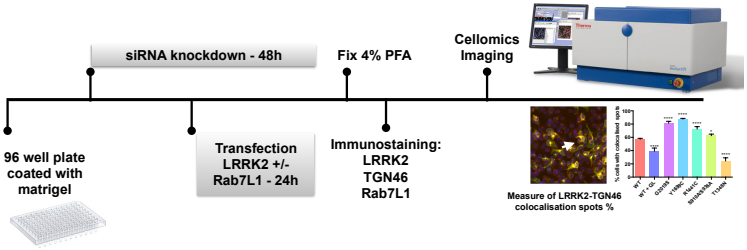


Figure 8.3: **Cellomics automated assay workflow.** Knockdown of detected hits of interest in HEK293FT cells using siRNA (24h). Double-DNA transfection of LRRK2, Rab7L1 WT/QL (24-30h). Fixation with 4% PFA and staining for LRRK2, Rab7L1 and TGN46. Quantification of LRRK2-TGN46-Rab7L1 colocalisation spot percentage via Cellomics quantitative analysis.

## 8.11 Microscopy

### 8.11.1 Confocal Microscopy

Confocal microscopy was performed using a Zeiss LSM 710 (Carl Zeiss). Fluorescence was excited by the 405nm, 488nm and 595nm laser lines of Argon,

diode and Helium/Neon lasers. Images were taken with a 40×1.3 numerical aperture (NA) or 63×1.4 NA oil objective. Images were collected using Zen software (Carl Zeiss) and prepared using Fiji (NIH) .

### 8.11.2 Super-resolution Microscopy

Super-resolution imaging was performed using a Zeiss 880 outfitted with an Airyscan module. Data was collected using a 63×1.4 NA objective and immersion oil optimised for 30°C (Carl Zeiss). Colours were collected sequentially to minimise crosstalk, and Airyscan processing was performed using the Airyscan module in the commercial ZEN software package (Carl Zeiss).

### 8.11.3 Image Quantification

Quantification was performed blinded using a combination of custom algorithms in Fiji (NIH) and Imaris (Biplane, Inc.) (Fig. 8.4). To assist the algorithm in correctly identifying the structures, background subtraction was performed by subtracting a flat numerical value from all channels in all images. The number of cathepsin D-positive vesicles was quantified using a spot detection algorithm in Imaris, thresholds were decided from several images and then applied to all images simultaneously. The algorithm was quality checked by eye, and confirmed to be specific and complete. To normalize the number of cathepsin D-positive vesicles to the number of cells in the tissue section, the nuclei were quantified using a surface detection algorithm using the method of marching squares. Thresholds were again applied universally and quality checked by eye.

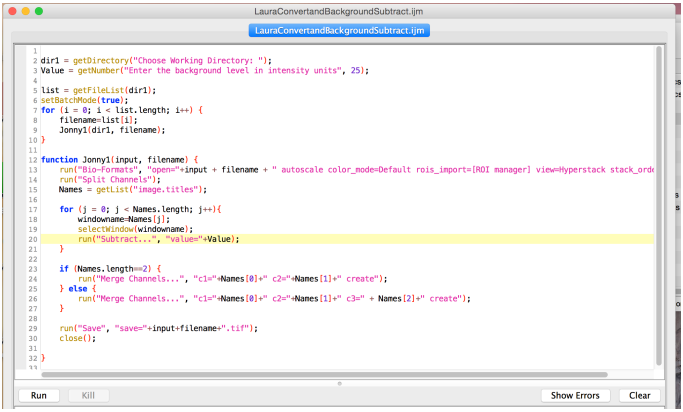


Figure 8.4: **Custom algorithm for image unbiased quantifications.** Screenshot of custom algorithm in Fiji and Imaris used to identify cathepsin D structures and background correction (collaboration with Dr. Jonathon Nixon-Abell).

## 8.12 Bioinformatics and Statistical Analyses

In all experiments, n represents the number of individual animals included in an experiment. Both male and female mice were used. Although animals were not treated and therefore not randomized into treatment groups, iTRAQ proteomics experiments were performed with animals of both genotypes included across different proteomics runs. In all statistical analyses, a preset value of $\alpha$=0.05 was used, with multiple test correction as appropriate.

iTRAQ labelled peptide identification and quantitation was performed using Mascot (Cottrell and London 1999) from Xcalibur RAW files with parameters and thresholds for peak picking as previously described (Hauser et al. 2014). Peptide identification was performed using the Mascot Server (version 2.5) to identify homologous peptides in the Sprot Mouse Database (Uniprot Proteome ID: UP000000589) with iTRAQ8plex (N-term) and iTRAQ8plex (K) set as fixed modifications and Methylthio (C), Oxidation (M) and iTRAQ8plex (Y) set as variable modifications. Only unique peptides were used to identify and calculate protein ratios. The iTRAQ label intensity for each sample was divided by the intensity of the pooled reference to obtain peptide ratios, and subsequently normalized so that the median ratio for each peptide was 1 for the wild type animals. Missing data points were imputed using k-nearest neighbours in the "impute" package in R within each sample type and series only where the number of missing values was less than five (Hastie et al. 2017). Statistical inferences were assessed by Welch's t-test, allowing for unequal variance between groups, followed by the Benjamini-Hochberg false-discovery rate correction for multiple testing (Benjamini and Hochberg 1995). Graphs are plotted as raw p values, but reported as significant only if the adjusted $p<0.05$. Evaluation of Gene Ontology term enrichments was performed using gProfileR within R (Reimand et al. 2011). Protein interaction networks were acquired from the IntAct database (http://www.ebi.ac.uk/intact/) and visualized using Cytoscape.

Data was plotted using Prism 6 (Graphpad) or R (https://www.rstudio.com/) and displayed as means and standard error of the mean (SEM). For validation experiments, student's t-test was used to determine differences between data consisting of two groups and Analysis of Variance (ANOVA) with Bonferroni post-hoc tests for multiple group comparisons. Differences between groups were

considered significant if $P<0.05$ and plotted on graphs using the following codes: $*P<0.05$, $**P<0.01$, $***$ $P<0.001$, $****$ $P<0.0001$.

# 9 General Discussion

Since the discovery of LRRK2 in 2002, and first publication in 2004 (Di Fonzo et al. 2005; Funayama et al. 2002, 2005; Paisan-Ruiz et al. 2004), innumerable studies have been performed to unravel the biological role of this protein and the pathological processes associated with LRRK2 mutations that lead to PD. However, the lack of a reproducible neurological phenotype in rodents, and the still limited tools to study this complex protein have represented a challenge in the research field of LRRK2 (Garcia-Miralles et al. 2015; Hinkle et al. 2012). In this study, I focused on understanding the biological role of LRRK2 using LRRK2-KO and G2019S mouse models. I have reported that loss of LRRK2 results in significant differences in protein abundance *in vivo*. Using an extensively validated proteomic screens, I detected several novel candidates that shed light on some of the mechanisms in which LRRK2 might be involved. This approach revealead that, overall, three key integrated biological mechanisms seem to be affected: vesicular trafficking, cytoskeletal alterations and protein turnover. An analogous study for the LRRK2 kinase mutant G2019S was also reported here. The G2019S mutant showed only minimal changes in protein expression levels compared to knockout, countering the hypothesis of a dominant-negative role for this mutation (Hindle et al. 2013; West et al. 2005). These results overall support a key physiological role for LRRK2 in endo-lysosomal and cytoskeletal pathways, both commonly impaired in early stages of Parkinson's disease (Pellegrini et al. 2016; Rivero-Ríos et al. 2015). Finally, a functional role for LRRK2 in endo-lysosomal pathways was further confirmed in primary kidney cells from LRRK2-KO and control mice, a novel *in vitro* cell model to study the biological role of LRRK2.

## 9.1 Key Findings

### 9.1.1 Loss of LRRK2 results in dysfunctional protein trafficking with accumulation of lysosomal proteases

Mounting evidence supports a role for LRRK2 in vesicular trafficking (Beilina et al. 2014; Kuwahara et al. 2016; Rivero-Ríos et al. 2015; Steger et al. 2016; Tong et al. 2012). Abnormalities in protein degradation pathways have been reported in LRRK2-KO mouse models which develop a severe kidney pathology (Herzig et al. 2011; Tong et al. 2012). By contrast, LRRK2 G2019S mutant mice do not display any overt phenotypic difference from control mice. Consistently with these previous findings (Tong et al. 2012), here I reported that loss of LRRK2 results in accumulation of lysosomal proteases.

How does loss LRRK2 result in protein accumulation? Defects in protein degradation pathways might represent the primary cause (Tong et al. 2010, 2012). In this proteomic study, significant differences in two major protein degradation pathways have been observed: the ubiquitin-proteasome system (UPS) and the autophagy-lysosomal pathway. A crosstalk between the UPS and autophagy-lysosome system has been reported (Korolchuk et al. 2009). In LRRK2-KO tissue, proteins involved in the degradation of ubiquitinated proteins (Psmc3 and Psmd3, 7) were significantly lower in abundance compared to controls. The ubiquitin protein ligase Ube3a and the deubiquitinase Usp14 were also lower in abundance in LRRK2-KO samples compared to controls. Together these data suggest that the UPS system, which regulates the quality control of proteins in the cytoplams, is altered in the absence of LRRK2.

Evidence indicating alteration of the autophagy-lysosome pathway in the absence of LRRK2 was provided in multiple studies (Herzig et al. 2011; Rivero-Ríos et al. 2015; Tong et al. 2010, 2012) and in this work. Lysosomal protease dysfunction was first observed in 1-month-old mice with significant accumulation of the mature form of cathepsin D. Precursor and mature forms of cathepsin D accumulate throughout different ages, with a maximum peak in protein levels at 9 months and reaching a plateau around 12-15 month of age. Similarly, I reported a significant accumulation of other lysosomal proteases including Lgmn, Scpep1, Asah1, Gns and Glb1 in LRRK2-KO kidneys.

The interaction network of LRRK2 at the Golgi suggests a role for LRRK2 as a scaffold involved in sorting of trans-Golgi-derived vesicles (Beilina et al. 2014; MacLeod et al. 2013). Disruption of protein interactions within this network might result in defective vesicle recycling. Since LRRK2 has been reported to phosphorylate and interact with several Rab GTPases (Cookson 2016; Shin et al. 2008; Steger et al. 2016), loss of LRRK2 might result in altered Rab signalling leading to differential regulation of the autophagy-lysosome pathway.

A correlation between lysosomal dysfunction and PD has been reported in several studies and mutations in genes encoding lysosomal proteases such as CTSD, GNS, ASAH1 and in GLB1 are known to cause lysosomal storage disorders (Kaplan and Wolfe 1987; Koch et al. 1996; Kwak et al. 2015; Tyynelä et al. 2000; Zhou et al. 2012). Patients with lysosomal storage disorders have a higher risk to develop PD and psychomotor symptoms (Beilina and Cookson 2016; Jose et al. 2008; Mielke et al. 2013; Schulze and Sandhoff 2014). Therefore understanding LRRK2 biology might provide new insights into the pathogenesis of lysosomal storage dysfunctions.

### 9.1.2 Altered lysosomal trafficking is a primary consequence of LRRK2 deficiency

Given the complexity of the results obtained via proteomic screen, I focused on two major biological themes, lysosomal and cytoskeletal proteins, to dissect which alterations are first observed in the absence of LRRK2. I generated primary kidney cells from WT and LRRK2-KO mice. Consistently with the phenotype observed in kidney tissue, I first observed accumulation of the precursor form of cathepsin D in LRRK2-KO cells. Results from this work suggest that this accumulation is not due to increased protein synthesis of cathepsin D, but rather altered trafficking resulting in a decrease of lysosomal degradation.

One possible mechanism for accumulation of the cathepsin D precursor is via impaired recycling of its receptor, the M6PR. The M6PR is recycled from endosomes to the Golgi via the retromer complex. The importance of retromer function in the recycling of M6PR is demonstrated by mutants of retromer subunits, resulting in more dispersed receptor localisation and accumulation of lysosomal enzyme precursors (Collins 2008; Farias et al. 2014; Follett et al. 2014; Lucas et al. 2016; Mcmillan et al. 2017; Seaman 2012; Zhang et al. 2015). Loss of LRRK2 results in enlarged endosomes, positive for cathepsin D and M6PR. This phenotype resembles mutants of retromer (Follett et al. 2014) and indicates a defect in sorting and maturation of cathepsin D to the lysosome.

Supporting the hypothesis of a dysfunction in retrograde transport, proteomic data reported an increase in relative abundance of cytoplasmic dynein 1 heavy chain 1 (Dync1h1), the core subunit of the main retrograde motor dynein (Schiavo et al. 2013), in LRRK2-KO cytosolic fractions. LRRK2 might therefore affect the movement of recycling endosomes back to the TGN.

Significant differences in the abundance of the vesicular protein involved in docking/fusion of vesicles to target membranes (Vamp1) and in the component of the CORVET complex Transforming Growth Factor Beta Receptor Associated Protein 1 (Tgfbrap1 or Vps3) were also detected. The CORVET complex is involved in membrane fusion events in cooperation with Rab GTPases (Balderhaar and Ungermann 2013; Peplowska et al. 2007). LRRK2 has been found to phosphorylate and interact with several small GTPases and to localise to endosomes (MacLeod et al. 2013; Roosen and Cookson 2016; Schreij et al. 2015; Steger et al. 2016). LRRK2 might therefore play a role in early to late endosome conversion or mediate fusion events via the CORVET complex, linking endosomal membranes to the cytoskeleton. Misfusion might also lead to impaired acidification, resulting in inefficient lysosomal activity and incomplete cathepsin D maturation.

### 9.1.3 Loss of LRRK2 causes alterations in cytoskeletal structure and function *in vivo*

LRRK2 has been reported to interact with multiple tubulin isoforms and to help maintaining microtubules in a dynamic state (Law et al. 2014). Significant changes in the abundance of cytoskeletal components were detected in absence of LRRK2. I showed differences in the abundance of Sept9, Pacsin2, Coro1c, Gphn, Naa15, Mprip and tubulin as well as changes in α-tubulin acetylation. Previous studies also showed that LRRK2 might interfere with tubulin acetylation (Law et al. 2014). The reported differences could also represent a secondary effect to overcompensate the lysosomal trafficking impairments observed in knockout kidneys. LRRK2-knockout might affect microtubule function by altering the binding of proteins to the luminal surface, where the α-tubulin acetylation site resides (Garvalov et al. 2006; Howes et al. 2014). Observed cytoskeletal changes

might also result in defective microtubule transport. Disruption of microtubule transport may be responsible or exacerbate the observed accumulation of lysosomal vesicles over time. Together with microtubules, the actin cytoskeleton is involved in vesicular trafficking and membrane fusion events (Jahraus et al. 2001). In this study, I reported differences in abundance in cortactin and actin binding proteins (Naa15 and Coro1c) in LRRK2-KO samples compared to controls. Together, these findings support the idea that LRRK2 modulates cytoskeletal stability possibly acting as a scaffold.

### 9.1.4 Loss of LRRK2 results in changes in abundance of translational regulators

Deregulation of protein translation can result in protein misfolding and subsequent aggregation (Dorval and Hébert 2012; Hindle 2010). Proteomic analysis of LRRK2-KO kidneys showed significant changes in a subset of regulators of protein translation (Ncl, Hnrnpk, Hnrnpa, Eef1g, Vars, Eif5). A decrease in several eukaryotic initiation factors (eIFs), involved in the formation and stabilisation of the initiation complex (Eif5, Eif3l, Eif4g3) and an increase in ribosomal proteins (RPs) (Rpl12, Rpl15, Rpl29, Rpl31, Rpl35a, Rpl13a, Rpl6, Rps12, Rps8) was also reported here. Therefore, loss of LRRK2 seems to correlate with abnormal regulation of protein synthesis mechanisms, although this could be a secondary mechanism. Abnormal regulation of protein synthesis could result in accumulation of misfolded proteins and deposition of lipofuscin granules as observed in LRRK2-KO kidneys.

LRRK2-KO kidneys usually show an increase in size starting from 4 months to older ages (Tong et al. 2012). This is often accompanied by deregulation in protein transcription and translation, autophagy and actin organisation under the

regulation of mTOR (Schmelzle and Hall 2000). In addition, proteins detected in the proteomic screen as differentially abundant, such as Ctsd (Berchem et al. 2002; Radisky 2010; Tan et al. 2013) and Asah1 (Berndt et al. 2013; Camacho et al. 2013), are expressed at high levels in several types of tumors. Although LRRK2-KO mice have not been reported to have an higher incidence of cancer, loss of LRRK2 might predispose to the development of benign kidney tumors.

### 9.1.5 LRRK2 kinase activity is not responsible for the pathological alterations in kidneys

The G2019S substitution is caused by the most common LRRK2 mutation that segregates with PD (Khan et al. 2005; Lesage et al. 2006; Ozelius et al. 2006). This mutation is located in the kinase loop and it is proposed to cause a toxic gain of function since it increases LRRK2 kinase activity relative to controls (Greggio 2012; Greggio et al. 2006; Imai et al. 2008; West et al. 2005). However, mice expressing the G2019S pathogenic mutation do not display any overt phenotypic difference compared to control mice and kidneys from mutant G2019S mice are almost indistinguishable from control kidneys. Since no significant differences were observed in any of the listed protein candidates, I conclude that the effects of LRRK2 on cytoskeletal and endo-lysosomal pathways are unlikely to be dependent on LRRK2 kinase signaling. The toxic gain of function reported in the literature for this mutation in cellular assays might not affect LRRK2 function in kidneys. In addition, as the LRRK2 G2019S and KO phenotypes are clearly different my results might indicate that the kinase mutant G2019S does not act as a dominant negative mutation.

In conclusion, my observations suggest that LRRK2 acts as a multidomain scaffold on microtubules ensuring the correct trafficking of signaling components that are essential for the recycling of acid hydrolases.

## 9.2 Future Perspectives

The work of this thesis could be continued with several different approaches in order to further understand the biological role of LRRK2, to dissect the molecular mechanism underlying the pathological accumulation of lysosomal substrates in LRRK2-KO models and to understand which pathways are affected by LRRK2 mutants.

### 9.2.1 Modelling lysosomal dysfunction

In this work, primary epithelial kidney cells have been generated to understand and model *in vitro* LRRK2-KO kidney pathology. This model expressing LRRK2 at higher levels compared to other primary culture models such as neuronal cells and microglia, has been useful for phenotypic characterisation and for functional studies. To further characterise the endo-lysosomal pathway in LRRK2-KO and control primary kidney cells, internalisation assays coupled with live-cell imaging technique could be employed. One example is to test the differences in M6PR trafficking by transfecting kidney cells with CD8-M6PR and monitoring its internalisation (Seaman 2004). Another possible approach is to dissect cathepsin D trafficking from the ER to the endosomes using a technique called retention using selective hooks (RUSH) (Boncompain et al. 2012) in LRRK2-KO and control cells. This technology allows spatio-temporal resolution of protein trafficking from the ER to the destination compartment. The protein-of-interest, fused with streptavidin-binding-peptide (SBP), is retained in the ER because of its interaction with streptavidin fused to an endoplasmic reticulum localisation signal. Addition of biotin, out-competes the streptavidin-SBP interaction and releases the protein,

which has accumulated in the ER, now free to traffick to its cellular compartment (Boncompain et al. 2012).

### 9.2.2 Alternative tools for modelling LRRK2-dependent pathology

As previously discussed, LRRK2 mouse models do not consistently develop overt neurological phenotypes and modelling neurodegeneration using genetically modified rodents has been challenging. The simplest explanations are perhaps related to the organism itself. Mice do not age as humans and are not exposed to the same environmental stressors as humans are. One solution could be to use fibroblasts from PD patients carrying LRRK2 mutations to derive cerebral organoids, an innovative research tool with basic and translational potential (Camp et al. 2015; Lancaster et al. 2013; Schwarz et al. 2015). Generating LRRK2 mutant cerebral organoids would provide an essential tool to perform disease modelling allowing the study of different brain regions. Even though the current scale of production of organoids is still limited, organoids could be used in future for drug discovery and therefore could represent a therapeutic resourse for screening of LRRK2 pharmacological inhibitors and of novel compounds.

### 9.2.3 Rescuing LRRK2-KO kidney cells

The dramatic changes observed in LRRK2-KO kidneys reveal multiple pathways affected by the absence of LRRK2. To determine which processes and pathways are directly affected by LRRK2, one possible approach would be to rescue the phenotype by reintroducing LRRK2 in primary LRRK2-KO kidney cells. Questions that would to be answered are whether the phenotype could be rescued with mutant forms of LRRK2 and which enzymatic activity is important for kidney physiology. These questions could be investigated by overexpressing the LRRK2

mutant G2019S, kinase-dead LRRK2, GTP-binding-deficient LRRK2, or truncated forms of LRRK2. Examination of protein interactions via coimmunoprecipitations with the validated proteomic candidates in kidney cells or tissue would also reveal associations with LRRK2, directly or indirectly through known LRRK2 interactors.

### 9.2.4 *In vivo* future approaches

*In vivo* strategies to investigate the LRRK2-KO kidney pathology could be to generate double LRRK2/CTSD knockout mice, and test whether loss of cathepsin D ameliorates the kidney phenotype.

The lack of a phenotypic effect in LRRK2-KO mouse brain represent a challenge in the understanding of LRRK2 pathogenic effects. Compensatory mechanisms provided by LRRK1 might be only one of the logical explanations for the lack of a neurological phenotype. LRRK2 and LRRK1 double knockout cells or animals using CRISPR/Cas9 technology might help us to answer these questions.

## 9.3 Conclusions and Open Questions

LRRK2 mutations represent a well-established common genetic cause of PD. After almost 15 years from its discovery, the LRRK2 physiological role and involvement in PD pathogenesis are still elusive. Genetic analysis, molecular biology technologies and large proteomic screens have greatly accelerated the understanding of the mechanisms underlying PD pathology and have provided us with a large amount of information. However, there are many open questions. How does loss of LRRK2 affect lysosomal trafficking? What are the signalling pathways primarily altered by loss of LRRK2? How do LRRK2 mutations alter protein function? Will reduction of LRRK2 kinase activity lead to clinical improvements in PD and are potential long-term side effects tolerable?

Although it is not clear whether PD patients carrying LRRK2 mutations develop kidney abnormalities, LRRK2 is expressed at the highest levels in kidneys and lungs (Atashrazm and Dzamko 2016), therefore future therapeutic strategies using LRRK2 inhibitors could result in peripheral side effects.

In summary, in this study I only discussed some of the multiple aspects related to LRRK2 biology. I reported co-ordinated changes in vesicular trafficking, cytoskeletal networks and protein degradation pathways in LRRK2-KO mouse kidneys. Although these changes were only observed in the kidneys but not in brain, they strikingly correlate with an aged phenotype and they resemble some of the pathogenic changes observed in brains from PD patients. Together these observations suggest that LRRK2-KO kidneys represent a relevant *in vivo* model to further investigate LRRK2 cellular pathways. Future work to dissect the interaction networks altered in the absence of LRRK2 and to understand the

biology of LRRK2 will build evidence for therapeutic avenues and will provide the basis for potential clinical trials.

# 10 References

Aasly, J. O., C. Vilariño-Güell, J. C. Dachsel, P. J. Webber, A. B. West, K. Haugarvoll, K. K. Johansen, M. Toft, J. G. Nutt, H. Payami, J. Kachergus, S. J. Lincoln, A. Felic, C. Wider, A. I. Soto-Ortolaza, S. A. Cobb, L. R. White, O. A. Ross, and M. J. Farrer (2010). "Novel pathogenic LRRK2 p.Asn1437His substitution in familial Parkinson's disease". In: *Movement Disorders* 25.13, pp. 2156–2163

Acs, K., M. S. Luijsterburg, L. Ackermann, F. A. Salomons, T. Hoppe, and N. P. Dantuma (2011). "The AAA-ATPase VCP/p97 promotes 53BP1 recruitment by removing L3MBTL1 from DNA double-strand breaks". In: *Nature Structural & Molecular Biology* 18.12, pp. 1345–1350

Akella, J. S., D. Wloga, J. Kim, N. G. Starostina, S. Lyons-Abbott, N. S. Morrissette, S. T. Dougan, E. T. Kipreos, and J. Gaertig (2010). "MEC-17 is an alpha-tubulin acetyltransferase." In: *Nature* 467.7312, pp. 218–222

AlDakheel, A., L. V. Kalia, and A. E. Lang (2014). "Pathogenesis-Targeted, Disease-Modifying Therapies in Parkinson Disease". In: *Neurotherapeutics* 11.1, pp. 6–23

Alegre-Abarrategui, J., H. Christian, M. M. P. Lufino, R. Mutihac, L. L. Venda, O. Ansorge, and R. Wade-Martins (2009). "LRRK2 regulates autophagic activity and localizes to specific membrane microdomains in a novel human genomic reporter cellular model". In: *Human Molecular Genetics* 18.21, pp. 4022–4034

Aoki, Y., R. Manzano, Y. Lee, R. Dafinca, M. Aoki, A. G. L. Douglas, M. A. Varela, C. Sathyaprakash, J. Scaber, P. Barbagallo, P. Vader, I. Mäger, K. Ezzat, M. R. Turner, N. Ito, S. Gasco, N. Ohbayashi, S. El Andaloussi, S. Takeda, M. Fukuda, K. Talbot, and M. J. A. Wood (2017). "C9orf72 and RAB7L1 regulate vesicle trafficking in amyotrophic lateral sclerosis and frontotemporal dementia". In: *Brain* 1, pp. 1–11

Arduíno, D. M., A. R. Esteves, L. Cortes, D. F. Silva, B. Patel, M. Grazina, R. H. Swerdlow, C. R. Oliveira, and S. M. Cardoso (2012). "Mitochondrial metabolism in Parkinson's disease impairs quality control autophagy by hampering microtubule-dependent traffic". In: *Human Molecular Genetics* 21.21, pp. 4680–4702

Atashrazm, F. and N. Dzamko (2016). "LRRK2 inhibitors and their potential in the treatment of Parkinson's disease: Current perspectives". In: *Clinical Pharmacology: Advances and Applications* 8, pp. 177–189

Attar, N. and P. J. Cullen (2010). "The retromer complex". In: *Advances in Enzyme Regulation* 50.1, pp. 216–236

Balderhaar, H. J. K. and C. Ungermann (2013). "CORVET and HOPS tethering complexes - coordinators of endosome and lysosome fusion." In: *Journal of cell science* 126.Pt 6, pp. 1307–16

Balderhaar, H. J. K., J. Lachmann, E. Yavavli, C. Bröcker, A. Lürick, and C. Ungermann (2013). "The CORVET complex promotes tethering and fusion of Rab5/Vps21-positive membranes." In: *Proceedings of the National Academy of Sciences of the United States of America* 110.10, pp. 3823–8

Banay-Schwartz, M., T. DeGuzman, A. Kenessey, M. Palkovits, and A. Lajtha (1992). "The distribution of cathepsin D activity in adult and aging human brain regions." In: *Journal of neurochemistry* 58.6, pp. 2207–2211

Baptista, M. A. S., K. D. Dave, M. a. Frasier, T. Sherer, M. Greeley, M. J. Beck, J. S. Varsho, G. a. Parker, C. Moore, M. J. Churchill, C. K. Meshul, and B. K. Fiske (2013). "Loss of leucine-rich repeat kinase 2 (LRRK2) in rats leads to progressive abnormal phenotypes in peripheral organs". In: *PLoS ONE* 8.11, pp. 1–16

Barbeau, A. (1961). "Dopamine and Basal Ganglia Diseases". In: *Archives of Neurology*

Barlowe, C., L. Orci, T. Yeung, M. Hosobuchi, S. Hamamoto, N. Salama, M. Rexach, M. Ravazzola, M. Amherdt, and R. Schekman (2017). "COPII: A membrane coat formed by Sec proteins that drive vesicle budding from the endoplasmic reticulum". In: *Cell* 77.6, pp. 895–907

Barrett, J. C., S. Hansoul, D. L. Nicolae, J. H. Cho, R. H. Duerr, J. D. Rioux, S. R. Brant, M. S. Silverberg, K. D. Taylor, M. Michael, A. Bitton, T. Dassopoulos, L. W. Datta, T. Green, M. Griffiths, E. O. Kistner, M. T. Murtha, M. D. Regueiro, I. Jerome, L. P. Schumm, A. H. Steinhart, S. R. Targan, J. Ramnik, J. Prescott, C. M. Onnie, S. A. Fisher, J. Marchini, and J. Ghori (2009). "Genome-wide association defines more than thirty distinct susceptibility loci for Crohn's disease". In: *Nat Genet.* 40.8, pp. 955–962

Barth, S., D. Glick, and K. F. Macleod (2010). "Autophagy: Assays and artifacts". In: *Journal of Pathology* 221.2, pp. 117–124

Beilina, A. and M. R. Cookson (2016). "Genes associated with Parkinson's disease: regulation of autophagy and beyond". In: *Journal of Neurochemistry* 139, pp. 91–107

Beilina, A., I. N. Rudenko, A. Kaganovich, L. Civiero, H. Chau, S. K. Kalia, L. V. Kalia, E. Lobbestael, R. Chia, K. Ndukwe, J. Ding, M. A. Nalls, M. Olszewski, D. N. Hauser, R. Kumaran, A. M. Lozano, V. Baekelandt, L. E. Greene, J.-M. Taymans, E. Greggio, and M. R. Cookson (2014). "Unbiased screen for interactors of leucine-rich repeat kinase 2 supports a common pathway for sporadic and familial Parkinson disease." In: *Proceedings of the National Academy of Sciences of the United States of America* 111.7, pp. 2626–31

Ben-Shlomo, Y. and M. G. Marmot (1995). "Survival and cause of death in a cohort of patients with parkinsonism: possible clues to aetiology?" In: *Journal of neurology, neurosurgery, and psychiatry* 58.3, pp. 293–299

Benjamini, Y. and Y. Hochberg (1995). *Controlling the false discovery rate: a practical and powerful approach to multiple testing*

Berchem, G., M. Glondu, M. Gleizes, J.-P. Brouillet, F. Vignon, M. Garcia, and E. Liaudet-Coopman (2002). "Cathepsin-D affects multiple tumor progression

steps in vivo: proliferation, angiogenesis and apoptosis." In: *Oncogene* 21.38, pp. 5951–5

Bernard, A. and D. J. Klionsky (2015). "Toward an understanding of autophagosomelysosome fusion: The unsuspected role of ATG14". In: *Autophagy* 11.4, pp. 583–584

Berndt, N., R. Patel, H. Yang, M. E. Balasis, and S. M. Sebti (2013). "Akt2 and acid ceramidase cooperate to induce cell invasion and resistance to apoptosis". In: *Cell Cycle* 12.13, pp. 2024–2032

Berwick, D. C. and K. Harvey (2011). "LRRK2 signaling pathways: the key to unlocking neurodegeneration?" In: *Trends in cell biology* 21.5, pp. 257–65

– (2012). "LRRK2 functions as a Wnt signaling scaffold, bridging cytosolic proteins and membrane-localized LRP6." In: *Human molecular genetics* 21.22, pp. 4966–79

– (2013). "LRRK2: an éminence grise of Wnt-mediated neurogenesis?" In: *Frontiers in cellular neuroscience* 7.82, pp. 1–13

– (2014). "The regulation and deregulation of Wnt signaling by PARK genes in health and disease". In: *Journal of Molecular Cell Biology* 6.1, pp. 3–12

Biskup, S., D. J. Moore, F. Celsi, S. Higashi, A. B. West, S. A. Andrabi, K. Kurkinen, S.-W. Yu, J. M. Savitt, H. J. Waldvogel, R. L. M. Faull, P. C. Emson, R. Torp, O. P. Ottersen, T. M. Dawson, and V. L. Dawson (2006). "Localization of LRRK2 to membranous and vesicular structures in mammalian brain." In: *Annals of neurology* 60.5, pp. 557–69

Biskup, S., D. J. Moore, A. Rea, B. Lorenz-Deperieux, C. E. Coombes, V. L. Dawson, T. M. Dawson, and A. B. West (2007). "Dynamic and redundant regulation of LRRK2 and LRRK1 expression." In: *BMC neuroscience* 8, p. 102

Boddu, R., T. D. Hull, S. Bolisetty, X. Hu, M. S. Moehle, J. P. L. Daher, A. I. Kamal, R. Joseph, J. F. George, A. Agarwal, L. M. Curtis, and A. B. West (2015). "Leucine-rich repeat kinase 2 deficiency is protective in rhabdomyolysis-induced kidney injury." In: *Human molecular genetics* 24.14, pp. 4078–4093

Boehm, M. and J. S. Bonifacino (2001). "Adaptins: the final recount." In: *Molecular biology of the cell* 12.10, pp. 2907–2920

Boncompain, G., S. Divoux, N. Gareil, H. de Forges, A. Lescure, L. Latreche, V. Mercanti, F. Jollivet, G. Raposo, and F. Perez (2012). "Synchronization of secretory protein traffic in populations of cells". In: *Nature Methods* 9.5, pp. 493–498

Bonifacino, J. S. and B. Glick (2004). "The Mechanisms of Vesicle Budding and Fusion". In: *Cell* 116.2, pp. 153–166

Bonifati, V. (2006). "Parkinson's disease: the LRRK2-G2019S mutation: opening a novel era in Parkinson's disease genetics." In: *European journal of human genetics : EJHG* 14.10, pp. 1061–1062

– (2014). "Genetics of Parkinson's disease – state of the art, 2013". In: *Parkinsonism & Related Disorders* 20.2014, S23–S28

Bonventre, J. V. (2009). "Kidney injury molecule-1 (KIM-1): A urinary biomarker and much more". In: *Nephrology Dialysis Transplantation* 24.11, pp. 3265–3268

Boon, J. Y., J. Dusonchet, C. Trengrove, and B. Wolozin (2014). "Interaction of LRRK2 with kinase and GTPase signaling cascades". In: *Frontiers in Molecular Neuroscience* 7.64, pp. 1–8

Braak, H., U. Rüb, W. P. Gai, and K. Del Tredici (2003). "Idiopathic Parkinson's disease: Possible routes by which vulnerable neuronal types may be subject to neuroinvasion by an unknown pathogen". In: *Journal of Neural Transmission* 110.5, pp. 517–536

Braulke, T. and J. S. Bonifacino (2009). "Sorting of lysosomal proteins". In: *Biochimica et Biophysica Acta - Molecular Cell Research* 1793.4, pp. 605–614

Bush, W. S. and J. H. Moore (2012). "Chapter 11: Genome-Wide Association Studies". In: *PLoS Computational Biology* 8.12

Bussiere, T. and P. R. Hof (2000). "Tau protein isoforms , phosphorylation and role in neurodegenerative". In: 33, pp. 95–130

Caesar, M., S. Zach, C. B. Carlson, K. Brockmann, T. Gasser, and F. Gillardon (2013). "Leucine-rich repeat kinase 2 functionally interacts with microtubules and kinase-dependently modulates cell migration." In: *Neurobiology of disease* 54, pp. 280–8

Caffrey, D. R., J. Zhao, Z. Song, M. E. Schaffer, S. A. Haney, R. R. Subramanian, A. B. Seymour, and J. D. Hughes (2011). "Sirna off-target effects can be reduced at concentrations that match their individual potency". In: *PLoS ONE* 6.7

Caligiore, D., R. C. Helmich, M. Hallett, A. A. Moustafa, L. Timmermann, I. Toni, and G. Baldassarre (2016). "Parkinson's disease as a system-level disorder". In: *npj Parkinson's Disease* 2.October, p. 16025

Camacho, L., O. Meca-Cortés, J. L. Abad, S. García, N. Rubio, A. Díaz, T. Celià-Terrassa, F. Cingolani, R. Bermudo, P. L. Fernández, J. Blanco, A. Delgado, J. Casas, G. Fabriàs, and T. M. Thomson (2013). "Acid ceramidase as a therapeutic target in metastatic prostate cancer.-suppl". In: *Journal of lipid research* 54.5, pp. 1207–20

Camp, J. G., F. Badsha, M. Florio, S. Kanton, T. Gerber, M. Wilsch-Bräuninger, E. Lewitus, A. Sykes, W. Hevers, M. Lancaster, J. A. Knoblich, R. Lachmann, S. Pääbo, W. B. Huttner, and B. Treutlein (2015). "Human cerebral organoids recapitulate gene expression programs of fetal neocortex development." In: *Proceedings of the National Academy of Sciences of the United States of America* 112.51, pp. 15672–7

Campbell, C. H., R. E. Fine, J. Squicciarini, and L. H. Rome (1983). "Coated vesicles from rat liver and calf brain contain cryptic mannose 6-phosphate receptors." In: *Journal of Biological Chemistry* 258.4, pp. 2628–2633

Cartelli, D., F. Casagrande, C. L. Busceti, D. Bucci, G. Molinaro, A. Traficante, D. Passarella, E. Giavini, G. Pezzoli, G. Battaglia, and G. Cappelletti (2013). "Microtubule alterations occur early in experimental parkinsonism and the microtubule stabilizer epothilone D is neuroprotective." In: *Scientific reports* 3, p. 1837

Charrier, C., M.-V. Ehrensperger, M. Dahan, S. Lévi, and A. Triller (2006). "Cytoskeleton regulation of glycine receptor number at synapses and diffusion

in the plasma membrane." In: *The Journal of neuroscience : the official journal of the Society for Neuroscience* 26.33, pp. 8502–8511

Chen, B., B. Zhang, L. Xia, J. Zhang, Y. Chen, Q. Hu, and C. Zhu (2015). "Knockdown of eukaryotic translation initiation factor 4E suppresses cell growth and invasion, and induces apoptosis and cell cycle arrest in a human lung adenocarcinoma cell line". In: *Molecular Medicine Reports*, pp. 7971–7978

Chia, R., S. Haddock, A. Beilina, I. N. Rudenko, A. Mamais, A. Kaganovich, Y. Li, R. Kumaran, M. A. Nalls, and M. R. Cookson (2014). "Phosphorylation of LRRK2 by casein kinase 1$\alpha$ regulates trans-Golgi clustering via differential interaction with ARHGEF7". In: *Nature Communications* 5, p. 5827

Chinta, S. J. and J. K. Andersen (2005). "Dopaminergic neurons". In: *The International Journal of Biochemistry & Cell Biology* 37.5, pp. 942–946

Chirivino, D, L Del Maestro, E Formstecher, P Hupe, G Raposo, D Louvard, and M Arpin (2011). "The ERM proteins interact with the HOPS complex to regulate the maturation of endosomes". In: *Mol Biol Cell* 22.3, pp. 375–385

Cho, H. J., J. Yu, C. Xie, P. Rudrabhatla, X. Chen, J. Wu, L. Parisiadou, G. Liu, L. Sun, B. Ma, J. Ding, Z. Liu, and H. Cai (2014). "Leucine-rich repeat kinase 2 regulates Sec16A at ER exit sites to allow ER-Golgi export." In: *The EMBO journal* 33.20, pp. 2314–31

Civiero, L., R. Vancraenenbroeck, E. Belluzzi, A. Beilina, E. Lobbestael, L. Reyniers, F. Gao, I. Micetic, M. de Maeyer, L. Bubacco, V. Baekelandt, M. R. Cookson, E. Greggio, and J.-M. Taymans (2012). "Biochemical Characterization of Highly Purified Leucine-Rich Repeat Kinases 1 and 2 Demonstrates Formation of Homodimers". In: *PLoS ONE* 7.8

Collins, B. M. (2008). "The structure and function of the retromer protein complex". In: *Traffic* 9.11, pp. 1811–1822

Conde, C. and A. Cáceres (2009). "Microtubule assembly, organization and dynamics in axons and dendrites." In: *Nature reviews. Neuroscience* 10.5, pp. 319–32

Cook, C. and L. Petrucelli (2009). "A critical evaluation of the ubiquitin-proteasome system in Parkinson's disease". In: *Biochimica et Biophysica Acta - Molecular Basis of Disease* 1792.7, pp. 664–675

Cookson, M. R. (2010). "The role of leucine-rich repeat kinase 2 (LRRK2) in Parkinson's disease." In: *Nature reviews. Neuroscience* 11.12, pp. 791–7

– (2012). "Parkinsonism due to mutations in PINK1, Parkin, and DJ-1 and oxidative stress and mitochondrial pathways". In: *Cold Spring Harbor Perspectives in Medicine* 2.9, pp. 1–11

– (2016). "Cellular functions of LRRK2 implicate vesicular trafficking pathways in Parkinson's disease." In: *Biochemical Society transactions* 44.6, pp. 1603–1610

Cottrell, J. S. and U. London (1999). "Probability-based protein identification by searching sequence databases using mass spectrometry data". In: *Electrophoresis* 20.18, pp. 3551–3567

Cuervo, A. M. and E. Wong (2014). "Chaperone-mediated autophagy: roles in disease and aging." In: *Cell research* 24.1, pp. 92–104

Cuervo, A. M., L. Stefanis, F. Ross, T. L. Peter, and D. Sulzer (2004). "Impaired Degradation of Mutant Alpha-Synuclein by Chaperone-Mediated Autophagy". In: *Science* 305.5688, pp. 1292–1295

Cummings, B. S., L. P. Wills, and R. G. Schnellmann (2004). "Measurement of Cell Death in Mammalian Cells Brian". In: 69.7, pp. 442–463

Dachsel, J. C., K. Nishioka, C. Vilariño-Güell, S. J. Lincoln, A. I. Soto-Ortolaza, J. Kachergus, K. M. Hinkle, M. G. Heckman, B. Jasinska-Myga, J. P. Taylor, D. W. Dickson, R. A. Gibson, F. Hentati, O. A. Ross, and M. J. Farrer (2010). "Heterodimerization of Lrrk1-Lrrk2: Implications for LRRK2-associated Parkinson disease". In: *Mechanisms of Ageing and Development* 131.3, pp. 210–214

Daher, J. P. L., H. A. Abdelmotilib, X. Hu, L. A. Volpicelli-Daley, M. S. Moehle, K. B. Faser, E. Needle, Y. Chen, S. J. Steyn, P. Galatsis, W. D. Hirst, and A. B. West (2015). "LRRK2 Pharmacological Inhibition Abates $\alpha$-Synuclein Induced Neurodegeneration". In: *Journal of Biological Chemistry* 290.32, pp. 19433–19444

Dall, E. and H. Brandstetter (2016). "Structure and function of legumain in health and disease". In: *Biochimie* 122.2016, pp. 126–150

Dasuri, K., L. Zhang, and J. N. Keller (2013). "Oxidative stress, neurodegeneration, and the balance of protein degradation and protein synthesis". In: *Free Radical Biology and Medicine* 62.2013, pp. 170–185

Deinhardt, K., S. Salinas, C. Verastegui, R. Watson, D. Worth, S. Hanrahan, C. Bucci, and G. Schiavo (2006). "Rab5 and Rab7 Control Endocytic Sorting along the Axonal Retrograde Transport Pathway". In: *Neuron* 52.2, pp. 293–305

Denk, F. and R. Wade-Martins (2009). "Knock-out and transgenic mouse models of tauopathies". In: *Neurobiology of Aging* 30.1, pp. 1–13

Dever, T. E. and R. Green (2012). "The elongation, termination, and recycling phases of translation in eukaryotes". In: *Cold Spring Harbor Perspectives in Biology* 4.7, pp. 1–16

Devine, M. J., A. Kaganovich, M. Ryten, A. Mamais, D. Trabzuni, C. Manzoni, P. McGoldrick, D. Chan, A. Dillman, J. Zerle, S. Horan, J. W. Taanman, J. Hardy, J. F. Marti-Masso, D. Healey, A. H. V. Schapira, B. Wolozin, R. Bandopadhyay, M. R. Cookson, M. P. Van Der Brug, and P. Lewis (2011). "Pathogenic LRRK2 mutations do not alter gene expression in cell model systems or human brain tissue". In: *PLoS ONE* 6.7, pp. 3–8

Di Fonzo, A., C. F. Rohé, J. Ferreira, H. F. Chien, L. Vacca, F. Stocchi, L. Guedes, E. Fabrizio, M. Manfredi, N. Vanacore, S. Goldwurm, G. Breedveld, C. Sampaio, G. Meco, E. Barbosa, B. A. Oostra, and V. Bonifati (2005). "A frequent LRRK2 gene mutation associated with autosomal dominant Parkinson's disease". In: *The Lancet* 365.9457, pp. 412–415

Díaz, J. F., J. M. Valpuesta, P. Chacón, G. Diakun, and J. M. Andreu (1998). "Changes in microtubule protofilament number induced by taxol binding to an easily accessible site: Internal microtubule dynamics". In: *Journal of Biological Chemistry* 273.50, pp. 33803–33810

Díaz, J. F., I. Barasoain, and J. M. Andreu (2003). "Fast kinetics of Taxol binding to microtubules: Effects of solution variables and microtubule-associated proteins". In: *Journal of Biological Chemistry* 278.10, pp. 8407–8419

Dörfel, M. J. and G. J. Lyon (2015). "The biological functions of Naa10 — From amino-terminal acetylation to human disease". In: *Gene* 567.2, pp. 103–131

Dorval, V. and S. S. Hébert (2012). "LRRK2 in transcription and translation regulation: Relevance for Parkinson's disease". In: *Frontiers in Neurology* FEB.February, pp. 2–7

Edvardson, S., Y. Cinnamon, A. Ta-Shma, A. Shaag, Y. I. Yim, S. Zenvirt, C. Jalas, S. Lesage, A. Brice, A. Taraboulos, K. H. Kaestner, L. E. Greene, and O. Elpeleg (2012). "A deleterious mutation in DNAJC6 encoding the neuronal-specific clathrin-uncoating Co-chaperone auxilin, is associated with juvenile parkinsonism". In: *PLoS ONE* 7.5, pp. 4–8

Ehringer, H. and O. Hornykiewicz (1998). "Distribution of noradrenaline and dopamine (3-hydroxytyramine) in the human brain and their behavior in diseases of the extrapyramidal system". In: *Parkinsonism and Related Disorders* 4.2, pp. 53–57

Esteves, A. R., D. M. Arduíno, R. H. Swerdlow, C. R. Oliveira, and S. M. Cardoso (2010). "Microtubule depolymerization potentiates alpha-synuclein oligomerization." In: *Frontiers in aging neuroscience* 1.January, p. 5

Esteves, A. R., R. H. Swerdlow, and S. M. Cardoso (2014). "LRRK2, a puzzling protein: Insights into Parkinson's disease pathogenesis." In: *Experimental neurology* 261C, pp. 206–216

Etienne-Manneville, S. (2004). "Actin and microtubules in cell motility: which one is in control?" In: *Traffic (Copenhagen, Denmark)* 5.7, pp. 470–7

Falconer, M. M., U. Vielkind, and D. L. Brown (1989). "Establishment of a stable, acetylated microtubule bundle during neuronal commitment." In: *Cell motility and the cytoskeleton* 12.3, pp. 169–180

Farias, G. G., D. C. Gershlick, and J. S. Bonifacino (2014). "Going Forward with Retromer". In: *Developmental Cell* 29.1, pp. 3–4

Farrer, M. J., J. T. Stone, C. H. Lin, J. C. Dächsel, M. Hulihan, K. Haugarvoll, O. A. Ross, and R. M. Wu (2007). "Lrrk2 G2385R is an ancestral risk factor for Parkinson's disease in Asia". In: *Parkinsonism and Related Disorders* 13.2, pp. 89–92

Fedorov, Y., E. M. Anderson, A. Birmingham, A. Reynolds, J. Karpilow, K. Robinson, D. Leake, W. S. Marshall, and A. Khvorova (2006). "Off-target effects by siRNA can induce toxic phenotype." In: *RNA (New York, N.Y.)* 12.7, pp. 1188–96

Ferrazza, R., S. Cogo, H. L. Melrose, L. Bubacco, E. Greggio, G. Guella, L. Civiero, and N. Plotegher (2016). "LRRK2 deficiency impacts ceramide metabolism in brain". In: *Biochemical and Biophysical Research Communications* 478.3, pp. 1141–1146

Ferree, A., M. D. Guillily, H. Li, K. Smith, A. Takashima, R. Squillace, M. Weigele, J. J. Collins, and B. Wolozin (2012). "Regulation of physiologic actions

of LRRK2: Focus on autophagy". In: *Neurodegenerative Diseases* 10.1-4, pp. 238–241

Fjorback, A. W., M. N. J. Seaman, C. Gustafsen, A. Mehmedbasic, S. Gokool, C. Wu, D. Militz, V. Schmidt, P. Madsen, J. R. Nyengaard, T. E. Willnow, E. I. Christensen, W. B. Mobley, A. Nykjær, and O. M. Andersen (2012). "Retromer binds the FANSHY sorting motif in SorLA to regulate amyloid precursor protein sorting and processing." In: *The Journal of neuroscience : the official journal of the Society for Neuroscience* 32.4, pp. 1467–80

Fokin, A. I., I. B. Brodsky, A. V. Burakov, and E. S. Nadezhdina (2014). "Interaction of early secretory pathway and Golgi membranes with microtubules and microtubule motors." In: *Biochemistry. Biokhimiia* 79.9, pp. 879–93

Follett, J., S. J. Norwood, N. A. Hamilton, M. Mohan, O. Kovtun, S. Tay, Y. Zhe, S. A. Wood, G. D. Mellick, P. A. Silburn, B. M. Collins, A. Bugarcic, and R. D. Teasdale (2014). "The Vps35 D620N Mutation Linked to Parkinson's Disease Disrupts the Cargo Sorting Function of Retromer". In: *Traffic* 15.2, pp. 230–244

Fougeray, S. and N. Pallet (2014). "Mechanisms and biological functions of autophagy in diseased and ageing kidneys". In: *Nature Reviews Nephrology* 11.1, pp. 34–45

Franke, A., D. P. B. McGovern, J. C. Barrett, K. Wang, G. L. Radford-Smith, T. Ahmad, C. W. Lees, T. Balschun, J. Lee, R. Roberts, C. A. Anderson, J. C. Bis, S. Bumpstead, D. Ellinghaus, E. M. Festen, M. Georges, T. Green, T. Haritunians, L. Jostins, A. Latiano, C. G. Mathew, G. W. Montgomery, N. J. Prescott, S. Raychaudhuri, J. I. Rotter, L. P. Schumm, Y. Sharma, L. A. Simms, K. D. Taylor, D. Whiteman, C. Wijmenga, R. N. Baldassano, M. Barclay, T. M. Bayless, S. Brand, C. Büning, A. Cohen, J.-F. Colombel, M. Cottone, L. Stronati, T. Denson, M. De Vos, R. D'Inca, M. Dubinsky, C. Edwards, T. Florin, D. Franchimont, R. Gearry, J. Glas, A. Van Gossum, S. L. Guthery, J. Halfvarson, H. W. Verspaget, J.-P. Hugot, A. Karban, D. Laukens, I. Lawrance, M. Lemann, A. Levine, C. Libioulle, E. Louis, C. Mowat, W. Newman, J. Panés, A. Phillips, D. D. Proctor, M. Regueiro, R. Russell, P. Rutgeerts, J. Sanderson, M. Sans, F. Seibold, A. H. Steinhart, P. C. F. Stokkers, L. Torkvist, G. Kullak-Ublick, D. Wilson, T. Walters, S. R. Targan, S. R. Brant, J. D. Rioux, M. D'Amato, R. K. Weersma, S. Kugathasan, A. M. Griffiths, J. C. Mansfield, S. Vermeire, R. H. Duerr, M. S. Silverberg, J. Satsangi, S. Schreiber, J. H. Cho, V. Annese, H. Hakonarson, M. J. Daly, and M. Parkes (2010). "Genome-wide meta-analysis increases to 71 the number of confirmed Crohn's disease susceptibility loci." In: *Nature genetics* 42.12, pp. 1118–25

Fu, Q., Y. Jiang, D. Zhang, X. Liu, J. Guo, and J. Zhao (2016). "Valosin-containing protein (VCP) promotes the growth, invasion, and metastasis of colorectal cancer through activation of STAT3 signaling". In: *Molecular and Cellular Biochemistry* 418.1-2, pp. 189–198

Fujiwara, T., S. Ye, T. Castro-Gomes, C. G. Winchell, N. Andrews, D. E. Voth, K. I. Varughese, S. G. Mackintosh, Y. Feng, N. Pavlos, T. Nakamura, S. C.

Manolagas, and H. Zhao (2016). "PLEKHM1/DEF8/RAB7 complex regulates lysosome positioning and bone homeostasis". In: *JCI Insight* 1.17, pp. 1–19

Funayama, M., K. Hasegawa, H. Kowa, M. Saito, S. Tsuji, and F. Obata (2002). "A new locus for Parkinson's disease (PARK8) maps to chromosome 12p11.2-q13.1." In: *Annals of neurology* 51.3, pp. 296–301

Funayama, M., K. Hasegawa, E. Ohta, N. Kawashima, M. Komiyama, H. Kowa, S. Tsuji, and F. Obata (2005). "An LRRK2 mutation as a cause for the Parkinsonism in the original PARK8 family". In: *Annals of Neurology* 57.6, pp. 918–921

Gandhi, S. and N. W. Wood (2005). "Molecular pathogenesis of Parkinson's disease". In: *Human Molecular Genetics* 14.18, pp. 2749–2755

Gandhi, S., S. G. Chen, and A. L. Wilson-Delfosse (2009). "Leucine-rich repeat kinase 2 (LRRK2): a key player in the pathogenesis of Parkinson's disease." In: *Journal of neuroscience research* 87.6, pp. 1283–95

Garcia-Miralles, M., J. Coomaraswamy, K. Häbig, M. C. Herzig, N. Funk, F. Gillardon, M. Maisel, M. Jucker, T. Gasser, D. Galter, and S. Biskup (2015). "No Dopamine Cell Loss or Changes in Cytoskeleton Function in Transgenic Mice Expressing Physiological Levels of Wild Type or G2019S Mutant LRRK2 and in Human Fibroblasts". In: *Plos One* 10.4, e0118947

Gardet, A., Y. Benita, C. Li, B. E. Sands, I. Ballester, C. Stevens, J. R. Korzenik, J. D. Rioux, M. J. Daly, X. J. Ramnik, and D. K. Podolsky (2010). "LRRK2 Is Involved in the IFN-$\gamma$ Response and Host Response to Pathogens". In: 185.9, pp. 5577–5585

Gardner, M. K., M. Zanic, and J. Howard (2013). "Microtubule catastrophe and rescue". In: *Current Opinion in Cell Biology* 25.1, pp. 1–9

Garnham, C. P. and A. Roll-Mecak (2012). "The chemical complexity of cellular microtubules: Tubulin post-translational modification enzymes and their roles in tuning microtubule functions". In: *Cytoskeleton* 69.7, pp. 442–463. arXiv: NIHMS150003

Garvalov, B. K., B. Zuber, C. Bouchet-Marquis, M. Kudryashev, M. Gruska, M. Beck, A. Leis, F. Frischknecht, F. Bradke, W. Baumeister, J. Dubochet, and M. Cyrklaff (2006). "Luminal particles within cellular microtubules". In: *Journal of Cell Biology* 174.6, pp. 759–765

Gebauer, F. and M. W. Hentze (2004). "Molecular mechanisms of translational control". In: *Nat.Rev.Mol.Cell Biol.* 5.1471-0072 (Print), pp. 827–835

Gershlick, D. C., C. Schindler, Y. Chen, and J. S. Bonifacino (2016). "TSSC1 is novel component of the endosomal retrieval machinery". In: *Molecular Biology of the Cell* 27.18, pp. 2867–2878

Ghoshal, N., F. García-Sierra, J. Wuu, S. Leurgans, D. A. Bennett, R. W. Berry, and L. I. Binder (2002). "Tau conformational changes correspond to impairments of episodic memory in mild cognitive impairment and Alzheimer's disease." In: *Experimental neurology* 177.2, pp. 475–493

Giasson, B. I., M. S. Forman, M. Higuchi, L. I. Golbe, C. L. Graves, P. T. Kotzbauer, J. Q. Trojanowski, and V. M. Lee (2003). "Initiation and synergistic fibrillization of tau and alpha-synuclein". In: *Science* 300.5619, pp. 636–640

Giasson, B. I., J. P. Covy, N. M. Bonini, H. I. Hurtig, M. J. Farrer, J. Q. Trojanowski, and V. M. Van Deerlin (2006). "Biochemical and pathological characterization of Lrrk2." In: *Annals of neurology* 59.2, pp. 315–22

Gibbs, K. L., L. Greensmith, and G. Schiavo (2015). "Regulation of Axonal Transport by Protein Kinases". In: *Trends in Biochemical Sciences* 40.10, pp. 597–610

Giesert, F., A. Hofmann, A. Bürger, J. Zerle, K. Kloos, U. Hafen, L. Ernst, J. Zhang, D. M. Vogt-Weisenhorn, and W. Wurst (2013). "Expression Analysis of Lrrk1, Lrrk2 and Lrrk2 Splice Variants in Mice". In: *PLoS ONE* 8.5

Gillardon, F. (2009). "Leucine-rich repeat kinase 2 phosphorylates brain tubulin-beta isoforms and modulates microtubule stability - A point of convergence in Parkinsonian neurodegeneration?" In: *Journal of Neurochemistry* 110.5, pp. 1514–1522

Gilsbach, B. K. and A. Kortholt (2014). "Structural biology of the LRRK2 GTPase and kinase domains: implications for regulation." In: *Frontiers in molecular neuroscience* 7.May, p. 32

Gingras, A.-C., S. G. Kennedy, M. A. O. Leary, N. Sonenberg, and N. Hay (1998). "is phosphorylated and inactivated by the Akt ( PKB ) signaling pathway". In: *Genes & Development*, pp. 502–513

Gloeckner, C. J., N. Kinkl, A. Schumacher, R. J. Braun, E. O'Neill, T. Meitinger, W. Kolch, H. Prokisch, and M. Ueffing (2006). "The Parkinson disease causing LRRK2 mutation I2020T is associated with increased kinase activity". In: *Human Molecular Genetics* 15.2, pp. 223–232

Godena, V. K., N. Brookes-Hocking, A. T. Moller, G. Shaw, M. Oswald, R. M. Sancho, C. C. J. Miller, A. J. Whitworth, and K. J. De Vos (2014). "Increasing microtubule acetylation rescues axonal transport and locomotor deficits caused by LRRK2 Roc-COR domain mutations." In: *Nature communications* 5, p. 5245

Golabek, A. A., E. Kida, M. Walus, W. Kaczmarski, M. Michalewski, and K. E. Wisniewski (2000). "CLN3 Protein Regulates Lysosomal pH and Alters Intracellular Processing of Alzheimer's Amyloid-$\beta$ Protein Precursor and Cathepsin D in Human Cells". In: *Molecular Genetics and Metabolism* 70.3, pp. 203–213

Goldberg, A. L. (2003). "Protein degradation and protection against misfolded or damaged proteins". In: *Nature* 426.6968, pp. 895–899

Gómez-Suaga, P., P. Rivero-Ríos, E. Fdez, M. Blanca Ramírez, I. Ferrer, A. Aiastui, A. López De Munain, and S. Hilfiker (2014). "LRRK2 delays degradative receptor trafficking by impeding late endosomal budding through decreasing Rab7 activity." In: *Human molecular genetics* 23.25, pp. 6779–96

Götz, J. and L. M. Ittner (2008). "Animal models of Alzheimer's disease and frontotemporal dementia." In: *Nature reviews. Neuroscience* 9.7, pp. 532–544

Greener, T., X. Zhao, H. Nojima, E. Eisenberg, and L. E. Greene (2000). "Role of cyclin G-associated kinase in uncoating clathrin-coated vesicles from non-neuronal cells". In: *Journal of Biological Chemistry* 275.2, pp. 1365–1370

Greggio, E. (2012). "Role of LRRK2 kinase activity in the pathogenesis of Parkinson's disease." In: *Biochemical Society transactions* 40.5, pp. 1058–62

Greggio, E. and M. R. Cookson (2009). "Leucine-rich repeat kinase 2 mutations and Parkinson ' s disease : three questions". In: 1.1, pp. 13–24

Greggio, E., S. Jain, A. Kingsbury, R. Bandopadhyay, P. Lewis, A. Kaganovich, M. P. Van Der Brug, A. Beilina, J. Blackinton, K. J. Thomas, R. Ahmad, D. Miller, S. Kesavapany, A. B. Singleton, A. J. Lees, R. J. Harvey, K. Harvey, and M. R. Cookson (2006). "Kinase activity is required for the toxic effects of mutant LRRK2/dardarin". In: *Neurobiology of Disease* 23.2, pp. 329–341

Greggio, E., P. Lewis, M. P. Van Der Brug, R. Ahmad, A. Kaganovich, J. Ding, A. Beilina, A. K. Baker, and M. R. Cookson (2007). "Mutations in LRRK2/dardarin associated with Parkinson disease are more toxic than equivalent mutations in the homologous kinase LRRK1". In: *Journal of Neurochemistry* 102.1, pp. 93–102

Greggio, E., I. Zambrano, A. Kaganovich, A. Beilina, J.-M. Taymans, V. Daniëls, P. Lewis, S. Jain, J. Ding, A. Syed, K. J. Thomas, V. Baekelandt, and M. R. Cookson (2008). "The Parkinson disease-associated leucine-rich repeat kinase 2 (LRRK2) is a dimer that undergoes intramolecular autophosphorylation". In: *Journal of Biological Chemistry* 283.24, pp. 16906–16914

Greggio, E., J.-M. Taymans, E. Y. Zhen, J. Ryder, R. Vancraenenbroeck, A. Beilina, P. Sun, J. Deng, H. Jaffe, V. Baekelandt, K. Merchant, and M. R. Cookson (2009). "The Parkinson's disease kinase LRRK2 autophosphorylates its GTPase domain at multiple sites". In: *Biochemical and Biophysical Research Communications* 389.3, pp. 449–454

Guerreiro, P. S., Y. Huang, A. Gysbers, D. Cheng, W. P. Gai, T. F. Outeiro, and G. M. Halliday (2013). "LRRK2 interactions with $\alpha$ -synuclein in Parkinson ' s disease brains and in cell models". In: pp. 513–522

Häbig, K., M. Walter, S. Poths, O. Riess, and M. Bonin (2008). "RNA interference of LRRK2-microarray expression analysis of a Parkinson's disease key player." In: *Neurogenetics* 9.2, pp. 83–94

Häbig, K., S. Gellhaar, B. Heim, V. Djuric, F. Giesert, W. Wurst, C. Walter, T. Hentrich, O. Riess, and M. Bonin (2013). "LRRK2 guides the actin cytoskeleton at growth cones together with ARHGEF7 and Tropomyosin 4". In: *Biochimica et Biophysica Acta - Molecular Basis of Disease* 1832.12, pp. 2352–2367

Halliday, G. M., H. McCann, and C. Shepherd (2012). "Evaluation of the Braak hypothesis: how far can it explain the pathogenesis of Parkinson's disease?" In: *Expert review of neurotherapeutics* 12.6, pp. 673–86

Halliday, G. M., H. Radford, Y. Sekine, J. Moreno, N. Verity, J. le Quesne, C. A. Ortori, D. A. Barrett, C. Fromont, P. M. Fischer, H. P. Harding, D. Ron, and G. R. Mallucci (2015). "Partial restoration of protein synthesis rates by the

small molecule ISRIB prevents neurodegeneration without pancreatic toxicity". In: *Cell Death and Disease* 6.3, e1672

Hammond, J. W., D. Cai, and K. J. Verhey (2008). "Tubulin modifications and their cellular functions". In: *Current Opinion in Cell Biology* 20.1, pp. 71–76

Han, B. S., L. Iacovitti, T. Katano, N. Hattori, W. Seol, and K.-S. Kim (2008). "Expression of the LRRK2 gene in the midbrain dopaminergic neurons of the substantia nigra." In: *Neuroscience letters* 442.3, pp. 190–194

Hanafusa, H., K. Ishikawa, S. Kedashiro, T. Saigo, S.-I. Iemura, T. Natsume, M. Komada, H. Shibuya, A. Nara, and K. Matsumoto (2011). "Leucine-rich repeat kinase LRRK1 regulates endosomal trafficking of the EGF receptor." In: *Nature communications* 2, p. 158

Hardy, J., P. Lewis, T. Revesz, A. J. Lees, and C. Paisan-Ruiz (2009). "The genetics of Parkinson's syndromes: a critical review." In: *Current opinion in genetics & development* 19.3, pp. 254–65

Hastie, T., R. Tibshirani, B. Narasimhan, and G. Chu (2017). "Package 'impute'". In: pp. 1–5

Hauser, D. N., A. Dillman, J. Ding, Y. Li, and M. R. Cookson (2014). "Post-translational decrease in respiratory chain proteins in the polg mutator mouse brain". In: *PLoS ONE* 9.4, pp. 1–10

Hawkes, C. H., K. Del Tredici, and H. Braak (2007). "Parkinson's disease: a dual-hit hypothesis". In: *Neuropathology and Applied Neurobiology* 33.6, pp. 599–614

Healy, D. G., M. Falchi, S. S. O'Sullivan, V. Bonifati, A. Durr, S. B. Bressman, A. Brice, J. O. Aasly, C. P. Zabetian, S. Goldwurm, J. Ferreira, E. Tolosa, D. M. Kay, C. Klein, D. Willey, C. Marras, A. E. Lang, Z. K. Wszolek, J. Berciano, A. H. V. Schapira, T. Lynch, K. P. Bhatia, T. Gasser, A. J. Lees, and N. W. Wood (2008). "Phenotype, genotype, and worldwide genetic penetrance of LRRK2-associated Parkinson's disease: a case-control study." In: *The Lancet. Neurology* 7.7, pp. 583–90

Henneman, W. J. P., J. D. Sluimer, J. Barnes, W. M. Van Der Flier, I. C. Sluimer, N. C. Fox, P. Scheltens, H. Vrenken, and F. Barkhof (2009). "Hippocampal atrophy rates in Alzheimer disease: Added value over whole brain volume measures". In: *Neurology* 72.11, pp. 999–1007

Herzig, M. C., C. Kolly, E. Persohn, D. Theil, T. Schweizer, T. Hafner, C. Stemmelen, T. J. Troxler, P. Schmid, S. Danner, C. R. Schnell, M. Mueller, B. Kinzel, A. Grevot, F. Bolognani, M. Stirn, R. R. Kuhn, K. Kaupmann, P. H. Van der putten, G. Rovelli, and D. R. Shimshek (2011). "LRRK2 protein levels are determined by kinase function and are crucial for kidney and lung homeostasis in mice". In: *Human Molecular Genetics* 20.21, pp. 4209–4223

Higashi, S., D. J. Moore, R. E. Colebrooke, S. Biskup, V. L. Dawson, H. Arai, T. M. Dawson, and P. C. Emson (2007). "Expression and localization of Parkinson's disease-associated leucine-rich repeat kinase 2 in the mouse brain". In: *Journal of Neurochemistry* 100.2, pp. 368–381

Higashi, Y., A. Pandey, B. Goodwin, and P. Delafontaine (2013). "Insulin-like growth factor-1 regulates glutathione peroxidase expression and activity in

vascular endothelial cells: Implications for atheroprotective actions of insulin-like growth factor-1." In: *Biochimica et biophysica acta* 1832.3, pp. 391–9

Hindle, J. V. (2010). "Ageing, neurodegeneration and Parkinson's disease". In: *Age and Ageing* 39.2, pp. 156–161

Hindle, S., F. Afsari, M. Stark, C. A. Middleton, G. J. O. Evans, S. T. Sweeney, and C. J. H. Elliott (2013). "Dopaminergic expression of the Parkinsonian gene LRRK2-G2019S leads to non-autonomous visual neurodegeneration, accelerated by increased neural demands for energy." In: *Human molecular genetics* 22.11, pp. 2129–40

Hinkle, K. M., M. Yue, B. Behrouz, J. C. Dächsel, S. J. Lincoln, E. Bowles, J. E. Beevers, B. N. Dugger, B. Winner, I. Prots, C. B. Kent, K. Nishioka, W.-L. Lin, D. W. Dickson, C. J. Janus, M. J. Farrer, and H. L. Melrose (2012). "LRRK2 knockout mice have an intact dopaminergic system but display alterations in exploratory and motor co-ordination behaviors". In: *Molecular Neurodegeneration* 7.1, p. 25

Holliday, L. S. (2014). "Vacuolar H+-ATPase: an essential multitasking enzyme in physiology and pathophysiology". In: *New Journal of Science* 2014, pp. 1–21

Hong, L., H.-C. Huang, and Z.-F. Jiang (2014). "Relationship between amyloid-beta and the ubiquitin–proteasome system in Alzheimer's disease". In: *Neurological Research* 36.3, pp. 276–282

Howes, S. C., G. M. Alushin, T. Shida, M. V. Nachury, and E. Nogales (2014). "Effects of tubulin acetylation and tubulin acetyltransferase binding on microtubule structure." In: *Molecular biology of the cell* 25.2, pp. 257–266

Hu, Y.-B., E. B. Dammer, R.-J. Ren, and G. Wang (2015). "The endosomal-lysosomal system: from acidification and cargo sorting to neurodegeneration". In: *Translational Neurodegeneration* 4.1, p. 18

Hubbert, C., A. Guardiola, R. Shao, Y. Kawaguchi, A. Ito, R. A. Nixon, M. Yoshida, X. Wang, and T. Yao (2002). "HDAC6 is a microtubule-associated deacetylase." In: *Nature* 417.6887, pp. 455–8

Imai, Y., S. Gehrke, H.-Q. Wang, R. Takahashi, K. Hasegawa, E. Oota, and B. Lu (2008). "Phosphorylation of 4E-BP by LRRK2 affects the maintenance of dopaminergic neurons in Drosophila." In: *The EMBO journal* 27.18, pp. 2432–43

Isenmann, S., Y. Khew-Goodall, J. Gamble, M. Vadas, and B. W. Wattenberg (1998). "A splice-isoform of vesicle-associated membrane protein-1 (VAMP-1) contains a mitochondrial targeting signal." In: *Molecular biology of the cell* 9.7, pp. 1649–1660

Ishihara, L., R. A. Gibson, L. Warren, R. Amouri, K. Lyons, C. Wielinski, C. Hunter, J. E. Swartz, R. Elango, P. A. Akkari, D. Leppert, L. Surh, K. H. Reeves, S. Thomas, L. Ragone, N. Hattori, R. Pahwa, J. Jankovic, M. Nance, A. Freeman, N. Gouider-Khouja, M. Kefi, M. Zouari, S. B. Sassi, S. B. Yahmed, G. El Euch-Fayeche, L. Middleton, D. J. Burn, R. Watts, and F. Hentati (2007). "Screening for Lrrk2 G2019S and clinical comparison of Tunisian and North American Caucasian Parkinson's disease families". In: *Movement Disorders* 22.1, pp. 55–61

Ito, G., T. Okai, G. Fujino, K. Takeda, H. Ichijo, T. Katada, and T. Iwatsubo (2007). "GTP binding is essential to the protein kinase activity of LRRK2, a causative gene product for familial Parkinson's disease". In: *Biochemistry* 46.5, pp. 1380–1388

Jaarsma, D. and C. C. Hoogenraad (2015). "Cytoplasmic dynein and its regulatory proteins in Golgi pathology in nervous system disorders". In: *Frontiers in Neuroscience* 9.October, pp. 1–9

Jackson, R. J., C. U. T. Hellen, and T. V. Pestova (2010). "The mechanism of eukaryotic translation initiation and principles of its regulation." In: *Nature reviews. Molecular cell biology* 11.2, pp. 113–127

Jahn, R. and R. H. Scheller (2006). "SNAREs — engines for membrane fusion". In: *Nature Reviews Molecular Cell Biology* 7.9, pp. 631–643

Jahraus, A., M. Egeberg, B. Hinner, A. Habermann, E. Sackman, A. Pralle, H. Faulstich, V. Rybin, H. Defacque, and G. Griffiths (2001). "ATP-dependent membrane assembly of F-actin facilitates membrane fusion." In: *Molecular biology of the cell* 12.1, pp. 155–170

Jaleel, M., R. J. Nichols, M. Deak, D. G. Campbell, F. Gillardon, A. Knebel, and D. R. Alessi (2007). "LRRK2 phosphorylates moesin at threonine-558: characterization of how Parkinson's disease mutants affect kinase activity." In: *The Biochemical journal* 405.2, pp. 307–317

Jankovic, J. (2008). "Parkinson's disease: clinical features and diagnosis." In: *Journal of neurology, neurosurgery, and psychiatry* 79.4, pp. 368–376

Jellinger, K. (2012). "Neuropathology of sporadic Parkinson's disease: Evaluation and changes of concepts". In: *Movement Disorders* 27.1, pp. 8–30

Jensen, P. H., H. Hager, M. S. Nielsen, P. Højrup, J. Gliemann, and R. Jakes (1999). "Alpha-Synuclein Binds to Tau and Stimulates the Protein Kinase A-catalyzed Tau Phosphorylation of Serine Residues 262 and 356". In: 274.36, pp. 25481–25489

Jose, B., A. B. Singleton, M. R. Cookson, and J. Hardy (2008). "Potential Role of Ceramide Metabolism in Lewy Body Disease". In: *FEBS Journal* 275.23, pp. 5767–5773

Kalil, K. and E. W. Dent (2005). "Touch and go: Guidance cues signal to the growth cone cytoskeleton". In: *Current Opinion in Neurobiology* 15.5, pp. 521–526

Kane, L. A. and R. J. Youle (2011). "PINK1 and Parkin flag miro to direct mitochondrial traffic". In: *Cell* 147.4, pp. 721–723

Kaplan, P. and L. S. Wolfe (1987). "Sanfilippo syndrome type D." In: *The Journal of pediatrics* 110.2, pp. 267–271

Karcher, R. L., S. W. Deacon, V. I. Gelfand, R. L. Karcher, S. W. Deacon, and V. I. Gelfand (2002). "Motor – cargo interactions : the key to transport specificity". In: 8924.January, pp. 21–27

Kawakami, F., T. Yabata, E. Ohta, T. Maekawa, N. Shimada, M. Suzuki, H. Maruyama, T. Ichikawa, and F. Obata (2012). "LRRK2 phosphorylates tubulin-associated tau but not the free molecule: LRRK2-mediated regulation of the tau-tubulin association and neurite outgrowth". In: *PLoS ONE* 7.1, pp. 1–9

Kawakami, F., N. Shimada, E. Ohta, G. Kagiya, R. Kawashima, T. Maekawa, H. Maruyama, and T. Ichikawa (2014). "Leucine-rich repeat kinase 2 regulates tau phosphorylation through direct activation of glycogen synthase kinase-3$\beta$." In: *The FEBS journal* 281.1, pp. 3–13

Kazlauskaite, A. and M. M. K. Muqit (2015). "PINK1 and Parkin - Mitochondrial interplay between phosphorylation and ubiquitylation in Parkinson's disease". In: *FEBS Journal* 282.2, pp. 215–223

Khan, N. L., S. Jain, J. M. Lynch, N. Pavese, P. M. Abou-Sleiman, J. L. Holton, D. G. Healy, W. P. Gilks, M. G. Sweeney, M. Ganguly, V. Gibbons, S. Gandhi, J. Vaughan, L. H. Eunson, R. Katzenschlager, J. Gayton, G. Lennox, T. Revesz, D. Nicholl, K. P. Bhatia, N. Quinn, D. Brooks, A. J. Lees, M. B. Davis, P. Piccini, A. B. Singleton, and N. W. Wood (2005). "Mutations in the gene LRRK2 encoding dardarin (PARK8) cause familial Parkinson's disease: Clinical, pathological, olfactory and functional imaging and genetic data". In: *Brain* 128.12, pp. 2786–2796

Kim, J.-S. and H.-Y. Sung (2015). "Gastrointestinal Autonomic Dysfunction in Patients with Parkinson's Disease." In: *Journal of movement disorders* 8.2, pp. 76–82

Kobe, B. and J. Deisenhofer (1995). *A structural basis of the interactions between leucine-rich repeats and protein ligands.*

Koch, J. C., S. Ga, C.-M. Li, L. E. Quintern, K. Bernardo, O. Levran, D. Schnabel, R. J. Desnick, E. H. Schuchman, and K. Sandhoff (1996). "Molecular Cloning and Characterization of a Full-length Complementary DNA Encoding Human Acid Ceramidase". In: *The Journal of Biological Chemistry* 271, pp. 33110–33115

Koch, J. C., F. Bitow, J. Haack, Z. D'Hedouville, J.-N. Zhang, L. Tonges, U. Michel, L. M. A. Oliveira, T. M. Jovin, J. Liman, L. Tatenhorst, M. Bahr, and P. Lingor (2015). "Alpha-Synuclein affects neurite morphology, autophagy, vesicle transport and axonal degeneration in CNS neurons". In: *Cell Death Dis* 6.2015, e1811

Köchl, R., X. W. Hu, E. Y. W. Chan, and S. Tooze (2006). "Microtubules facilitate autophagosome formation and fusion of autophagosomes with endosomes". In: *Traffic* 7.2, pp. 129–145

Korolchuk, V. I., A. Mansilla, F. M. Menzies, and D. C. Rubinsztein (2009). "Autophagy Inhibition Compromises Degradation of Ubiquitin-Proteasome Pathway Substrates". In: *Molecular Cell* 33.4, pp. 517–527

Korr, D., L. Toschi, P. Donner, H.-D. Pohlenz, B. Kreft, and B. Weiss (2006). "LRRK1 protein kinase activity is stimulated upon binding of GTP to its Roc domain". In: *Cellular Signalling* 18.6, pp. 910–920

Kosik, K. S., L. D. Orecchio, S. Bakalis, and R. L. Neve (1989). "Developmentally regulated expression of specific tau sequences." In: *Neuron* 2.4, pp. 1389–1397

Kumar, A., E. Greggio, A. Beilina, A. Kaganovich, D. Chan, J.-M. Taymans, B. Wolozin, and M. R. Cookson (2010). "The Parkinson's disease associated LRRK2 exhibits weaker in vitro phosphorylation of 4E-BP compared to autophosphorylation". In: *PLoS ONE* 5.1

Kumaran, R. and M. R. Cookson (2015). "Pathways to Parkinsonism Redux: convergent pathobiological mechanisms in genetics of Parkinson's disease". In: *Human Molecular Genetics*, pp. 1–13

Kuwahara, T., K. Inoue, V. D. D'Agati, T. Fujimoto, T. Eguchi, S. Saha, B. Wolozin, T. Iwatsubo, and A. Abeliovich (2016). "LRRK2 and RAB7L1 coordinately regulate axonal morphology and lysosome integrity in diverse cellular contexts". In: *Scientific Reports* 6, p. 29945

Kwak, J. E., M.-Y. Son, Y. S. Son, M. J. Son, and Y. S. Cho (2015). "Biochemical and molecular characterization of novel mutations in GLB1 and NEU1 in patient cells with lysosomal storage disorders". In: *Biochemical and Biophysical Research Communications* 457.4, pp. 554–560

Lancaster, M., M. Renner, C.-a. Martin, D. Wenzel, S. Bicknell, M. E. Hurles, T. Homfray, J. M. Penninger, and P. Andrew (2013). "Cerebral organoids model human brain development and microcephaly". In: *Nature* 501.7467, pp. 373–379

Langston, J., P Ballard, J. Tetrud, and I Irwin (1983). "Chronic Parkinsonism in humans due to a product of meperidine-analog synthesis". In: *Science* 219.4587, pp. 979–980

Langston, R. G., I. N. Rudenko, and M. R. Cookson (2016). "The function of orthologues of the human Parkinson's disease gene LRRK2 across species: implications for disease modelling in preclinical research." In: *The Biochemical journal* 473.3, pp. 221–32

Law, B. M. H., V. A. Spain, V. H. L. Leinster, R. Chia, A. Beilina, H. J. Cho, J.-M. Taymans, M. K. Urban, R. M. Sancho, M. B. Ramírez, S. Biskup, V. Baekelandt, H. Cai, M. R. Cookson, D. C. Berwick, and K. Harvey (2014). "A direct interaction between leucine-rich repeat kinase 2 and specific $\beta$-Tubulin isoforms regulates tubulin acetylation". In: *Journal of Biological Chemistry* 289.2, pp. 895–908

Le Borgne, R. and B. Hoflack (1997). "Mannose 6-phosphate receptors regulate the formation of clathrin-coated vesicles in the TGN". In: *Journal of Cell Biology* 137.2, pp. 335–345

Lee, B. D., J.-H. Shin, J. VanKampen, L. Petrucelli, A. B. West, H. S. Ko, Y.-I. Lee, K. A. Maguire-Zeiss, W. J. Bowers, H. J. Federoff, V. L. Dawson, and T. M. Dawson (2010). "Inhibitors of leucine-rich repeat kinase-2 protect against models of Parkinson's disease." In: *Nature medicine* 16.9, pp. 998–1000

Lee, D. W., X. Zhao, F. Zhang, E. Eisenberg, and L. E. Greene (2005a). "Depletion of GAK/auxilin 2 inhibits receptor-mediated endocytosis and recruitment of both clathrin and clathrin adaptors." In: *Journal of cell science* 118, pp. 4311–4321

Lee, H.-J., F. Khoshaghideh, and S. J. S. Lee (2006). "Impairment of microtubule-dependent trafficking by overexpression of alpha-synuclein". In: *European Journal of Neuroscience* 24.11, pp. 3153–3162

Lee, M. C. S., L. Orci, S. Hamamoto, E. Futai, M. Ravazzola, and R. Schekman (2005b). "Sar1p N-terminal helix initiates membrane curvature and completes the fission of a COPII vesicle". In: *Cell* 122.4, pp. 605–617

Lee, S., Y. Imai, S. Gehrke, S. Liu, and B. Lu (2012). "The synaptic function of LRRK2." In: *Biochemical Society transactions* 40.5, pp. 1047–51

Lee, V. M., M. Goedert, and J. Q. Trojanowski (2001). "Neurodegenerative Tauopathies". In: *Annual Review of Neuroscience* 24, pp. 1121–59.

Lees, A. J., J. Hardy, and T. Revesz (2009). "Parkinson's disease." In: *Lancet* 373.9680, pp. 2055–66

Lefrancois, S., L. Michaud, M. Potier, S. Igdoura, and C. R. Morales (1999). "Role of sphingolipids in the transport of prosaposin to the lysosomes." In: *Journal of lipid research* 40.9, pp. 1593–1603

Lesage, S., A. Dürr, M. Tazir, E. Lohmann, A.-L. Leutenegger, S. Janin, P. Pollak, and A. Brice (2006). "G2019S as a Cause of Parkinson's Disease in North African Arabs". In: *New England Journal of Medicine* 354.4, pp. 422–423

Lewin, D. A. and I. Mellman (1998). "Sorting out adaptors". In: *Biochimica et Biophysica Acta - Molecular Cell Research* 1401.2, pp. 129–145

L'Hernault, S. W. and J. L. Rosenbaum (1983). "Chlamydomonas alpha-tubulin is posttranslationally modified in the flagella during flagellar assembly". In: *Journal of Cell Biology* 97.1, pp. 258–263

Li, B., Y. Zhang, Y. Yuan, and N. Chen (2011). "A new perspective in Parkinson's disease, chaperone-mediated autophagy." In: *Parkinsonism & related disorders* 17.4, pp. 231–5

Lichtenberg, M., A. Mansilla, V. R. Zecchini, A. Fleming, and D. C. Rubinsztein (2011). "The Parkinson's disease protein LRRK2 impairs proteasome substrate clearance without affecting proteasome catalytic activity." In: *Cell death & disease* 2.8, e196

Lin, C. H., P.-I. Tsai, R. M. Wu, and C.-T. Chien (2010). "LRRK2 G2019S mutation induces dendrite degeneration through mislocalization and phosphorylation of tau by recruiting autoactivated GSK3ß." In: *The Journal of Neuroscience* 30.39, pp. 13138–49

Lin, X., L. Parisiadou, X. L. Gu, L. Wang, H. Shim, L. Sun, C. Xie, C. X. Long, W. J. Yang, J. Ding, Z. Chen, P. E. Gallant, J. H. Tao-Cheng, G. Rudow, J. C. Troncoso, Z. Liu, Z. Li, and H. Cai (2009). "Leucine-Rich Repeat Kinase 2 Regulates the Progression of Neuropathology Induced by Parkinson's-Disease-Related Mutant $\alpha$-synuclein". In: *Neuron* 64.6, pp. 807–827

Linhart, R., S. A. Wong, J. Cao, M. Tran, A. Huynh, C. Ardrey, J. M. Park, C. Hsu, S. Taha, R. Peterson, S. Shea, J. Kurian, and K. Venderova (2014). "Vacuolar protein sorting 35 (Vps35) rescues locomotor deficits and shortened lifespan in Drosophila expressing a Parkinson's disease mutant of Leucine-rich repeat kinase 2 (LRRK2)." In: *Molecular neurodegeneration* 9.1, p. 23

Liu, Z. and M. J. Lenardo (2012). "The role of LRRK2 in inflammatory bowel disease". In: *Cell Research* 22.7, pp. 1092–1094

Liu, Z., S. Hamamichi, B. D. Lee, D. Yang, A. Ray, G. A. Caldwell, K. A. Caldwell, T. M. Dawson, W. W. Smith, and V. L. Dawson (2011). "Inhibitors of LRRK2 kinase attenuate neurodegeneration and Parkinson-like phenotypes in

Caenorhabditis elegans and Drosophila Parkinson's disease models." In: *Human molecular genetics* 20.20, pp. 3933–42

Liu-Yesucevitz, L., G. J. Bassell, A. D. Gitler, A. C. Hart, E. Klann, J. D. Richter, S. T. Warren, and B. Wolozin (2011). "Local RNA Translation at the Synapse and in Disease". In: *Journal of Neuroscience* 31.45, pp. 16086–16093

Lucas, M., D. C. Gershlick, A. Vidaurrazaga, A. L. Rojas, J. S. Bonifacino, and A. Hierro (2016). "Structural Mechanism for Cargo Recognition by the Retromer Complex". In: *Cell*, pp. 1–13

Lucki, N. C., S. Bandyopadhyay, E. Wang, A. H. Merrill, and M. B. Sewer (2012). "Acid ceramidase (ASAH1) is a global regulator of steroidogenic capacity and adrenocortical gene expression." In: *Molecular endocrinology (Baltimore, Md.)* 26.2, pp. 228–43

Ly, N., N. Elkhatib, E. Bresteau, O. Piétrement, M. Khaled, M. M. Magiera, C. Janke, E. Le Cam, A. D. Rutenberg, and G. Montagnac (2016). "$\alpha$TAT1 controls longitudinal spreading of acetylation marks from open microtubules extremities". In: *Scientific Reports* 6.35624, pp. 1–10

MacLeod, D., J. Dowman, R. Hammond, T. Leete, K. Inoue, and A. Abeliovich (2006). "The Familial Parkinsonism Gene LRRK2 Regulates Neurite Process Morphology". In: *Neuron* 52.4, pp. 587–593

MacLeod, D., H. Rhinn, T. Kuwahara, A. Zolin, G. D. Paolo, B. D. McCabe, K. S. Marder, L. S. Honig, L. N. Clark, S. A. Small, and A. Abeliovich (2013). "RAB7L1 interacts with LRRK2 to modify intraneuronal protein sorting and Parkinson's disease risk." In: *Neuron* 77.3, pp. 425–39

Maday, S. and E. L. F. Holzbaur (2014). "Autophagosome biogenesis in primary neurons follows an ordered and spatially regulated pathway". In: *Developmental Cell* 30.1, pp. 71–85

Maday, S., A. E. Twelvetrees, A. J. Moughamian, and E. L. F. Holzbaur (2014). "Axonal Transport: Cargo-Specific Mechanisms of Motility and Regulation". In: *Neuron* 84.2, pp. 292–309

Maekawa, T., S. Mori, Y. Sasaki, T. Miyajima, S. Azuma, E. Ohta, and F. Obata (2012). "The I2020T Leucine-rich repeat kinase 2 transgenic mouse exhibits impaired locomotive ability accompanied by dopaminergic neuron abnormalities". In: *Molecular Neurodegeneration* 7.1, p. 15

Mandelkow, E.-M. and E. Mandelkow (2011). "Biochemistry and cell biology of Tau protein in neurofibrillary degeneration". In: *Cold Spring Harbor Perspectives in Biology* 3.10, pp. 1–25

Manzoni, C., A. Mamais, S. Dihanich, P. McGoldrick, M. J. Devine, J. Zerle, E. Kara, J. W. Taanman, D. G. Healy, J. F. Marti-Masso, A. H. V. Schapira, H. Plun-Favreau, S. Tooze, J. Hardy, R. Bandopadhyay, and P. Lewis (2013). "Pathogenic parkinson's disease mutations across the functional domains of LRRK2 alter the autophagic/lysosomal response to starvation". In: *Biochemical and Biophysical Research Communications* 441.4, pp. 862–866

Marín, I., W. N. van Egmond, and P. J. M. van Haastert (2008). "The Roco protein family: a functional perspective." In: *The FASEB journal : official*

*publication of the Federation of American Societies for Experimental Biology* 22.9, pp. 3103–3110

Marker, D. F., J. M. Puccini, T. E. Mockus, J. Barbieri, S.-M. Lu, and H. A. Gelbard (2012). "LRRK2 kinase inhibition prevents pathological microglial phagocytosis in response to HIV-1 Tat protein." In: *Journal of neuroinflammation* 9.1, p. 261

Martin, I., J. W. Kim, B. D. Lee, H. C. Kang, J. C. Xu, H. Jia, J. Stankowski, M. S. Kim, J. Zhong, M. Kumar, S. A. Andrabi, Y. Xiong, D. W. Dickson, Z. K. Wszolek, A. Pandey, T. M. Dawson, and V. L. Dawson (2014). "Ribosomal protein s15 phosphorylation mediates LRRK2 neurodegeneration in parkinson's disease". In: *Cell* 157.2

Mata, I. F., J. Kachergus, J. P. Taylor, S. J. Lincoln, J. O. Aasly, T. Lynch, M. Hulihan, S. A. Cobb, R. M. Wu, C.-S. Lu, C. Lahoz, Z. K. Wszolek, and M. J. Farrer (2005). "Lrrk2 pathogenic substitutions in Parkinson's disease". In: *Neurogenetics* 6.4, pp. 171–177

Matenia, D. and E.-M. Mandelkow (2009). "The tau of MARK: a polarized view of the cytoskeleton." In: *Trends in biochemical sciences* 34.7, pp. 332–42

Matenia, D., C. Hempp, T. Timm, A. Eikhof, and E.-M. Mandelkow (2012). "Microtubule affinity-regulating kinase 2 (MARK2) turns on phosphatase and tensin homolog (PTEN)-induced kinase 1 (PINK1) at Thr-313, a mutation site in Parkinson disease: effects on mitochondrial transport." In: *The Journal of biological chemistry* 287.11, pp. 8174–86

McGlinchey, R. P. and J. C. Lee (2015). "Cysteine cathepsins are essential in lysosomal degradation of $\alpha$-synuclein". In: *Proceedings of the National Academy of Sciences* 112.30, p. 201500937

McGough, I. J., F. Steinberg, D. Jia, P. A. Barbuti, K. J. Mcmillan, K. J. Heesom, A. L. Whone, M. A. Caldwell, D. D. Billadeau, M. K. Rosen, and P. J. Cullen (2014). "Retromer binding to FAM21 and the WASH complex is perturbed by the Parkinson disease-linked VPS35(D620N) mutation". In: *Current Biology* 24.14, pp. 1670–1676

Mcmillan, K. J., H. C. Korswagen, and P. J. Cullen (2017). "The emerging role of retromer in neuroprotection". In: *Current Opinion in Cell Biology* 47.Figure 1, pp. 72–82

Medina, D. L., A. Fraldi, V. Bouche, F. Annunziata, G. Mansueto, C. Spampanato, C. Puri, A. Pignata, J. A. Martina, M. Sardiello, M. Palmieri, R. Polishchuk, R. Puertollano, and A. Ballabio (2011). "Transcriptional activation of lysosomal exocytosis promotes cellular clearance". In: *Developmental Cell* 21.3, pp. 421–430

Meixner, A., K. Boldt, M. Van Troys, M. Askenazi, C. J. Gloeckner, M. Bauer, J. A. Marto, C. Ampe, N. Kinkl, and M. Ueffing (2011). "A QUICK screen for Lrrk2 interaction partners–leucine-rich repeat kinase 2 is involved in actin cytoskeleton dynamics." In: *Molecular & cellular proteomics : MCP* 10.1, p. M110.001172

Melrose, H. L. (2008). "Update on the functional biology of Lrrk2." In: *Future neurology* 3.6, pp. 669–681

Metcalf, P. and M. Fusek (1993). "Two crystal structures for cathepsin D: the lysosomal targeting signal and active site". In: *The EMBO Journal* 12.4, pp. 1293–1302

Mettlen, M., T. Pucadyil, R. Ramachandran, and S. L. Schmid (2009). "Dissecting dynamin's role in clathrin-mediated endocytosis." In: *Biochemical Society transactions* 37, pp. 1022–1026

Mielke, M. M., W. Maetzler, N. J. Haughey, V. V. R. Bandaru, R. Savica, C. Deuschle, T. Gasser, A. K. Hauser, S. Gräber-Sultan, E. Schleicher, D. Berg, and I. Liepelt-Scarfone (2013). "Plasma Ceramide and Glucosylceramide Metabolism Is Altered in Sporadic Parkinson's Disease and Associated with Cognitive Impairment: A Pilot Study". In: *PLoS ONE* 8.9, pp. 1–6

Min, S.-W., X. Chen, T. E. Tracy, Y. Li, Y. Zhou, C. Wang, K. Shirakawa, S. S. Minami, E. Defensor, S. A. Mok, P. D. Sohn, B. Schilling, X. Cong, L. Ellerby, B. W. Gibson, J. Johnson, N. Krogan, M. Shamloo, J. Gestwicki, E. Masliah, E. Verdin, and L. Gan (2015). "Critical role of acetylation in tau-mediated neurodegeneration and cognitive deficits". In: *Nature Medicine* 21.April 2014, pp. 1–12

Minarowska, A., M. Gacko, A. Karwowska, and L. Minarowski (2008). "Human cathepsin D". In: *Folia Histochemica et Cytobiologica* 46.1, pp. 23–38

Miyajima, T., E. Ohta, H. Kawada, T. Maekawa, and F. Obata (2015). "The mouse/human cross-species heterodimer of leucine-rich repeat kinase 2: Possible significance in the transgenic model mouse of Parkinson's disease"

Mizushima, N., T. Yoshimori, and B. Levine (2010). "Methods in Mammalian Autophagy Research". In: *Cell* 140.3, pp. 313–326

Moehle, M. S., P. J. Webber, T. Tse, N. Sukar, D. G. Standaert, T. M. Desilva, R. M. Cowell, A. B. West, and G. David (2012). "LRRK2 Inhibition Attenuates Microglial Inflammatory Responses". In: *Journal of Neursocience* 32.5, pp. 1602–1611

Montagu, K. A. (1957). "Catechol compounds in rat tissues and in brains of different animals". In: *Nature* 180.4579, pp. 244–245

Moughamian, A. J., G. E. Osborn, J. E. Lazarus, S. Maday, and E. L. F. Holzbaur (2013). "Ordered recruitment of dynactin to the microtubule plus-end is required for efficient initiation of retrograde axonal transport." In: *The Journal of neuroscience : the official journal of the Society for Neuroscience* 33.32, pp. 13190–203

Moussaud, S., D. R. Jones, E. L. Moussaud-Lamodière, M. Delenclos, O. A. Ross, and P. J. McLean (2014). "Alpha-synuclein and tau: teammates in neurodegeneration?" In: *Molecular Neurodegeneration* 9.1, p. 43

Muhammad, A., I. Flores, H. Zhang, R. Yu, A. Staniszewski, E. Planel, M. Herman, L. Ho, R. Kreber, L. S. Honig, B. Ganetzky, K. E. Duff, O. Arancio, and S. Small (2008). "Retromer deficiency observed in Alzheimer's disease causes hippocampal dysfunction, neurodegeneration, and Abeta accumulation." In: *Proceedings of the National Academy of Sciences of the United States of America* 105.20, pp. 7327–32

Mukherjee, A., A. Biswas, and S. K. Das (2016). "Gut dysfunction in Parkinson's disease". In: *World Journal of Gastroenterology* 22.25, pp. 5742–5752

Murphy, D. D., S. M. Rueter, J. Q. Trojanowski, and V. M. Lee (2000). "Synucleins are developmentally expressed, and alpha-synuclein regulates the size of the presynaptic vesicular pool in primary hippocampal neurons." In: *The Journal of neuroscience : the official journal of the Society for Neuroscience* 20.9, pp. 3214–3220

Musa, J., M. F. Orth, M. Dallmayer, M. Baldauf, C. Pardo, B. Rotblat, T. Kirchner, G. Leprivier, and T. G. P. Grünewald (2016). "Eukaryotic initiation factor 4E-binding protein 1 (4E-BP1): a master regulator of mRNA translation involved in tumorigenesis". In: *Nature Publishing Group* 1.October 2015, pp. 1–14

Nalls, M. A., V. Plagnol, D. G. Hernandez, M. Sharma, U.-M. Sheerin, M. Saad, J. Simón-Sánchez, C. Schulte, S. Lesage, S. Sveinbjörnsdóttir, K. Stefánsson, M. Martinez, J. Hardy, P. Heutink, A. Brice, T. Gasser, A. B. Singleton, and N. W. Wood (2011). "Imputation of sequence variants for identification of genetic risks for Parkinson's disease: a meta-analysis of genome-wide association studies." In: *Lancet* 377.9766, pp. 641–9

Nalls, M. A., N. Pankratz, C. M. Lill, C. B. Do, D. G. Hernandez, M. Saad, A. L. DeStefano, E. Kara, J. Bras, M. Sharma, C. Schulte, M. F. Keller, S. Arepalli, C. Letson, C. Edsall, H. Stefansson, X. Liu, H. Pliner, J. H. Lee, R. Cheng, M. A. Ikram, J. P. A. Ioannidis, G. M. Hadjigeorgiou, J. C. Bis, M. Martinez, J. S. Perlmutter, A. Goate, K. Marder, B. K. Fiske, M. Sutherland, G. Xiromerisiou, R. H. Myers, L. N. Clark, K. Stefansson, J. Hardy, P. Heutink, H. Chen, N. W. Wood, H. Houlden, H. Payami, A. Brice, W. K. Scott, T. Gasser, L. Bertram, N. Eriksson, T. Foroud, and A. B. Singleton (2014). "Large-scale meta-analysis of genome-wide association data identifies six new risk loci for Parkinson's disease." In: *Nature genetics* 056.9, pp. 1–7

Neve, R. L., P. Harris, K. S. Kosik, D. M. Kurnit, and T. A. Donlon (1986). "Identification of cDNA clones for the human microtubule-associated protein tau and chromosomal localization of the genes for tau and microtubule-associated protein 2." In: *Brain research* 387.3, pp. 271–280

Nichols, R. J., N. Dzamko, N. A. Morrice, D. G. Campbell, M. Deak, A. Ordureau, T. Macartney, Y. Tong, J. Shen, A. R. Prescott, and D. R. Alessi (2010). "14-3-3 binding to LRRK2 is disrupted by multiple Parkinson's disease-associated mutations and regulates cytoplasmic localization." In: *The Biochemical journal* 430.3, pp. 393–404

Nixon, R. A. (2006). "Autophagy in neurodegenerative disease: friend, foe or turncoat?" In: *Trends in Neurosciences* 29.9, pp. 528–535

– (2013). "The role of autophagy in neurodegenerative disease." In: *Nature medicine* 19.8, pp. 983–997

Nowis, D., E. McConnell, and C. Wójcik (2006). "Destabilization of the VCP-Ufd1-Npl4 complex is associated with decreased levels of ERAD substrates". In: *Experimental Cell Research* 312.15, pp. 2921–2932

Oelze, M., S. Kröller-Schön, S. Steven, E. Lubos, C. Doppler, M. Hausding, S. Tobias, C. Brochhausen, H. Li, M. Torzewski, P. Wenzel, M. Bachschmid, K. J. Lackner, E. Schulz, T. Münzel, and A. Daiber (2014). "Glutathione peroxidase-1 deficiency potentiates dysregulatory modifications of endothelial nitric oxide synthase and vascular dysfunction in aging". In: *Hypertension* 63.2, pp. 390–396

Ohkawa, N., S. Sugisaki, E. Tokunaga, K. Fujitani, T. Hayasaka, M. Setou, and K. Inokuchi (2008). "N-acetyltransferase ARD1-NAT1 regulates neuronal dendritic development". In: *Genes to Cells* 13.11, pp. 1171–1183

Ohta, E., T. Nihira, A. Uchino, Y. Imaizumi, Y. Okada, W. Akamatsu, K. Takahashi, H. Hayakawa, M. Nagai, M. Ohyama, M. Ryo, M. Ogino, S. Murayama, A. Takashima, K. Nishiyama, Y. Mizuno, H. Mochizuki, F. Obata, and H. Okano (2015). "I2020T mutant LRRK2 iPSC-derived neurons in the Sagamihara family exhibit increased Tau phosphorylation through the AKT/GSK-3$\beta$ signaling pathway". In: *Human Molecular Genetics* 24.17, pp. 4879–4900

Okada, Y., H. Yamazaki, Y. Sekine-Aizawa, and N. Hirokawa (1995). "The neuron-specific kinesin superfamily protein KIF1A is a unique monomeric motor for anterograde axonal transport of synaptic vesicle precursors". In: *Cell* 81.5, pp. 769–780

Olanow, C. W. and K. S. P. Mcnaught (2006). "Ubiquitin – Proteasome System and Parkinson ' s Disease". In: 21.11, pp. 1806–1823

Orci, L., B. Glick, and J. E. Rothman (1986). "A new type of coated vesicular carrier that appears not to contain clathrin: its possible role in protein transport within the Golgi stack." In: *Cell* 46.2, pp. 171–184

Outeiro, T. F., E. Kontopoulos, S. M. Altmann, I. Kufareva, K. E. Strathearn, A. M. Amore, C. B. Volk, M. M. Maxwell, J.-C. Rochet, P. J. Mclean, A. B. Young, R. Abagyan, M. B. Feany, B. T. Hyman, and A. G. Kazantsev (2007). "Sirtuin 2 Inhibitors Rescue alpha-synuclein-Mediated Toxicity in Models of Parkinson' s Disease". In: 1968.August 2006

Ozelius, L. J., G. Senthil, R. Saunders-Pullman, E. Ohmann, A. Deligtisch, M. Tagliati, A. L. Hunt, C. Klein, B. Henick, S. M. Hailpern, R. B. Lipton, J. Soto-Valencia, N. Risch, and S. B. Bressman (2006). "LRRK2 G2019S as a cause of Parkinson's disease in Ashkenazi Jews". In: *The New England journal of medicine* 354.4, pp. 424–425

Paisan-Ruiz, C., S. Jain, E. W. Evans, W. P. Gilks, J. Simón, M. P. Van Der Brug, A. López de Munain, S. Aparicio, A. M. Gil, N. L. Khan, J. O. Johnson, J. R. Martinez, D. Nicholl, I. M. Carrera, A. S. Pena, R. de Silva, A. J. Lees, J. F. Martí-Massó, J. Pérez-Tur, N. W. Wood, and A. B. Singleton (2004). "Cloning of the gene containing mutations that cause PARK8-linked Parkinson's disease." In: *Neuron* 44.4, pp. 595–600

Paradis, H., T. Islam, S. Tucker, L. Tao, S. Koubi, and R. L. Gendron (2008). "Tubedown associates with cortactin and controls permeability of retinal endothelial cells to albumin." In: *Journal of cell science* 121.Pt 12, pp. 1965–1972

Parisiadou, L., C. Xie, H. J. Cho, X. Lin, X. L. Gu, C. X. Long, E. Lobbestael, V. Baekelandt, J.-M. Taymans, L. Sun, and H. Cai (2009). "Phosphorylation of ezrin/radixin/moesin proteins by LRRK2 promotes the rearrangement of actin cytoskeleton in neuronal morphogenesis." In: *The Journal of neuroscience : the official journal of the Society for Neuroscience* 29.44, pp. 13971–13980

Paus, M., Z. Kohl, N. M.-B. Ben Abdallah, D. Galter, F. Gillardon, and J. Winkler (2013). "Enhanced dendritogenesis and axogenesis in hippocampal neuroblasts of LRRK2 knockout mice." In: *Brain research* 1497, pp. 85–100

Pearse, B. M. (1976). "Clathrin: a unique protein associated with intracellular transfer of membrane by coated vesicles." In: *Proceedings of the National Academy of Sciences of the United States of America* 73.4, pp. 1255–1259

Pellegrini, L., A. Wetzel, S. Grannó, G. Heaton, and K. Harvey (2016). "Back to the tubule: microtubule dynamics in Parkinson's disease". In: *Cellular and Molecular Life Sciences*, pp. 1–26

Peplowska, K., D. F. Markgraf, C. W. Ostrowicz, G. Bange, and C. Ungermann (2007). "The CORVET Tethering Complex Interacts with the Yeast Rab5 Homolog Vps21 and Is Involved in Endo-Lysosomal Biogenesis". In: *Developmental Cell* 12.5, pp. 739–750

Perdiz, D., R. Mackeh, C. Poüs, and A. Baillet (2011). "The ins and outs of tubulin acetylation: More than just a post-translational modification?" In: *Cellular Signalling* 23.5, pp. 763–771. arXiv: 183

Perrett, R. M., Z. Alexopoulou, and G. K. Tofaris (2015). "The endosomal pathway in Parkinson's disease". In: *Molecular and Cellular Neuroscience* 66, pp. 21–28

Polito, L., A. Greco, and D. Seripa (2016). "Genetic Profile , Environmental Exposure , and Their Interaction in Parkinson ' s Disease". In: 2016

Polymeropoulos, M. H., C. Lavedan, E. Leroy, S. E. Ide, A. Dehejia, A. Dutra, B. Pike, H. Root, J. Rubenstein, R. Boyer, E. S. Stenroos, S. Chandrasekharappa, A. Athanassiadou, T. Papapetropoulos, W. G. Johnson, A. M. Lazzarini, R. C. Duvoisin, G. D. Iorio, L. I. Golbe, and R. L. Nussbaum (1997). "Mutation in the $\alpha$ -Synuclein Gene Identified in Families with Parkinson ' s Disease Mutation in the ␣-Synuclein Gene Identified in Families with Parkinson ' s Disease". In: *Science* 276.June, pp. 2045–2047. arXiv: arXiv:1411.6330v1

Pons, B., G. Armengol, M. Livingstone, L. López, L. Coch, N. Sonenberg, and S. Ramón Y Cajal (2012). "Association between LRRK2 and 4E-BP1 protein levels in normal and malignant cells". In: *Oncology Reports* 27.1, pp. 225–231

Prots, I., V. Veber, S. Brey, S. Campioni, K. Buder, R. Riek, K. J. Böhm, and B. Winner (2013). "Alpha-Synuclein Oligomers Impair Neuronal Microtubule-Kinesin Interplay". In: *Journal of Biological Chemistry* 288.30, pp. 21742–21754

Qian, L. and P. M. Flood (2008). "Microglial cells and Parkinson's disease." In: *Immunologic research* 41.3, pp. 155–64

Qiao, L., S. Hamamichi, K. A. Caldwell, G. A. Caldwell, T. A. Yacoubian, S. Wilson, Z.-L. Xie, L. D. Speake, R. Parks, D. Crabtree, Q. Liang, S. Crimmins, L. Schneider, Y. Uchiyama, T. Iwatsubo, Y. Zhou, L. Peng, Y. Lu, D. G. Standaert,

K. C. Walls, J. J. Shacka, K. A. Roth, and J. Zhang (2008). "Lysosomal enzyme cathepsin D protects against alpha-synuclein aggregation and toxicity." In: *Molecular brain* 1.Cl, p. 17

Radisky, E. S. (2010). "Cathepsin D Cathepsin D Regulation in mammary gland remodeling , misregulation in breast cancer". In: *Cancer Biology & Therapy* 10.5, pp. 467–470

Ramírez-Valle, F., S. Braunstein, J. Zavadil, S. C. Formenti, and R. J. Schneider (2008). "eIF4GI links nutrient sensing by mTOR to cell proliferation and inhibition of autophagy". In: *Journal of Cell Biology* 181.2, pp. 293–307

Ramming, M., S. Kins, N. Werner, A. Hermann, H. Betz, and J. Kirsch (2000). "Diversity and phylogeny of gephyrin: tissue-specific splice variants, gene structure, and sequence similarities to molybdenum cofactor-synthesizing and cytoskeleton-associated proteins." In: *Proceedings of the National Academy of Sciences of the United States of America* 97, pp. 10266–10271

Ramonet, D., J. P. L. Daher, B. M. Lin, K. Stafa, J. Kim, R. Banerjee, M. Westerlund, O. Pletnikova, L. Glauser, L. Yang, Y. Liu, D. A. Swing, M. F. Beal, J. C. Troncoso, J. M. McCaffery, N. A. Jenkins, N. G. Copeland, D. Galter, B. Thomas, M. K. Lee, T. M. Dawson, V. L. Dawson, and D. J. Moore (2011). "Dopaminergic Neuronal loss, Reduced Neurite Complexity and Autophagic Abnormalities in Transgenic Mice Expressing G2019S Mutant LRRK2". In: *PLoS ONE* 6.4, pp. 13–19

Ray, S. and M. Liu (2004). "Current understanding of LRRK2 in Parkinson's disease : biochemical and structural features and inhibitor design". In: pp. 1701–1713

Redecker, B., B. Heckendorf, H.-W. Grosch, G. Mersmann, and A. Hasilik (1991). "Molecular organization of the human cathepsin D gene". In: *DNA and Cell Biology* 10.6, pp. 423–431

Reed, N. A., D. Cai, T. L. Blasius, G. T. Jih, E. Meyhofer, J. Gaertig, and K. J. Verhey (2006). "Microtubule Acetylation Promotes Kinesin-1 Binding and Transport". In: *Current Biology* 16.21, pp. 2166–2172

Rees, M. I., K. Harvey, H. Ward, J. H. White, L. Evans, I. C. Duguid, C. H. Hsu, S. L. Coleman, J. Miller, K. Baer, H. J. Waldvogel, F. Gibbon, T. G. Smart, M. J. Owen, R. J. Harvey, and R. G. Snell (2003). "Isoform Heterogeneity of the Human Gephyrin Gene (GPHN), Binding Domains to the Glycine Receptor, and Mutation Analysis in Hyperekplexia". In: *Journal of Biological Chemistry* 278.27, pp. 24688–24696

Reeve, A., E. Simcox, and D. Turnbull (2014). "Ageing and Parkinson's disease: Why is advancing age the biggest risk factor?" In: *Ageing Research Reviews* 14.1, pp. 19–30

Reimand, J., T. Arak, and J. Vilo (2011). "G:Profiler - A web server for functional interpretation of gene lists (2011 update)". In: *Nucleic Acids Research* 39.SUPPL. 2, pp. 307–315

Reiter, L., M. Claassen, S. P. Schrimpf, M. Jovanovic, A. Schmidt, J. M. Buhmann, M. O. Hengartner, and R. Aebersold (2009). "Protein Identification False

Discovery Rates for Very Large Proteomics Data Sets Generated by Tandem Mass Spectrometry". In: *Molecular & Cellular Proteomics* 8.11, pp. 2405–2417

Ren, Y., J. Zhao, and J. J. Feng (2003). "Parkin binds to alpha/beta tubulin and increases their ubiquitination and degradation." In: *The Journal of neuroscience : the official journal of the Society for Neuroscience* 23.8, pp. 3316–24

Reyniers, L., M. G. Del Giudice, L. Civiero, E. Belluzzi, E. Lobbestael, A. Beilina, G. Arrigoni, R. Derua, E. Waelkens, Y. Li, C. Crosio, C. Iaccarino, M. R. Cookson, V. Baekelandt, E. Greggio, and J.-M. Taymans (2014). "Differential protein-protein interactions of LRRK1 and LRRK2 indicate roles in distinct cellular signaling pathways". In: *Journal of Neurochemistry*, pp. 239–250

Rivero-Ríos, P., P. Gómez-Suaga, B. Fernández, J. Madero-Pérez, A. J. Schwab, A. D. Ebert, and S. Hilfiker (2015). "Alterations in late endocytic trafficking related to the pathobiology of LRRK2-linked Parkinson's disease." In: *Biochemical Society transactions* 43.3, pp. 390–5

Robinson, M. S. and J. S. Bonifacino (2001). "Adaptor-related proteins". In: *Current Opinion in Cell Biology* 13.4, pp. 444–453

Rojas, R., T. Van Vlijmen, G. A. Mardones, Y. Prabhu, A. L. Rojas, S. Mohammed, A. J. R. Heck, G. Raposo, P. Van Der Sluijs, and J. S. Bonifacino (2008). "Regulation of retromer recruitment to endosomes by sequential action of Rab5 and Rab7". In: *Journal of Cell Biology* 183.3, pp. 513–526

Roosen, D. A. and M. R. Cookson (2016). "LRRK2 at the interface of autophagosomes , endosomes and lysosomes". In: *Molecular Neurodegeneration*, pp. 1–10

Rubinsztein, D. C. (2006). "The roles of intracellular protein-degradation pathways in neurodegeneration". In: *Nature* 443.7113, pp. 780–786

Rubinsztein, D. C., P. Codogno, and B. Levine (2012). "Autophagy modulation as a potential therapeutic target for diverse diseases". In: *Nature Reviews Drug Discovery* 11.9, pp. 709–730. arXiv: `NIHMS150003`

Rubinsztein, D. C., C. F. Bento, and V. Deretic (2015). "Therapeutic targeting of autophagy in neurodegenerative and infectious diseases." In: *The Journal of experimental medicine* 212.7, pp. 979–90

Rudenko, I. N., A. Kaganovich, D. N. Hauser, A. Beilina, R. Chia, J. Ding, D. Maric, H. Jaffe, and M. R. Cookson (2012). "The G2385R variant of leucine-rich repeat kinase 2 associated with Parkinson's disease is a partial loss-of-function mutation". In: *Biochemical Journal* 446.1, pp. 99–111

Russo, I., L. Bubacco, and E. Greggio (2014). "LRRK2 and neuroinflammation: partners in crime in Parkinson's disease?" In: *Journal of neuroinflammation* 11.1, p. 52

Ryan, B. J., S. Hoek, E. A. Fon, and R. Wade-Martins (2015). "Mitochondrial dysfunction and mitophagy in Parkinson's: from familial to sporadic disease". In: *Trends in Biochemical Sciences* 40.4, pp. 200–210

Rybakin, V. and C. S. Clemen (2005). "Coronin proteins as multifunctional regulators of the cytoskeleton and membrane trafficking". In: *BioEssays* 27.6, pp. 625–632

Ryzhikov, S. and B. A. Bahr (2008). "Gephyrin alterations due to protein accumulation stress are reduced by the lysosomal modulator Z-Phe-Ala-diazomethylketone." In: *Journal of molecular neuroscience : MN* 34.2, pp. 131–139

Saha, S., M. D. Guillily, A. Ferree, J. Lanceta, D. Chan, J. Ghosh, C. H. Hsu, L. Segal, K. Raghavan, K. Matsumoto, N. Hisamoto, T. Kuwahara, T. Iwatsubo, L. Moore, L. Goldstein, M. R. Cookson, and B. Wolozin (2009). "LRRK2 modulates vulnerability to mitochondrial dysfunction in Caenorhabditis elegans." In: *The Journal of neuroscience : the official journal of the Society for Neuroscience* 29.29, pp. 9210–9218

Sánchez-Danés, A., Y. Richaud-Patin, I. Carballo-Carbajal, S. Jiménez-Delgado, C. Caig, S. Mora, C. Di Guglielmo, M. Ezquerra, B. Patel, A. Giralt, J. M. Canals, M. Memo, J. Alberch, J. López-Barneo, M. Vila, A. M. Cuervo, E. Tolosa, A. Consiglio, and A. Raya (2012). "Disease-specific phenotypes in dopamine neurons from human iPS-based models of genetic and sporadic Parkinson's disease". In: *EMBO Molecular Medicine* 4.5, pp. 380–395

Sancho, R. M., B. M. H. Law, and K. Harvey (2009). "Mutations in the LRRK2 Roc-COR tandem domain link Parkinson's disease to Wnt signalling pathways." In: *Human molecular genetics* 18.20, pp. 3955–68

Satake, W., Y. Nakabayashi, I. Mizuta, Y. Hirota, C. Ito, M. Kubo, T. Kawaguchi, T. Tsunoda, M. Watanabe, A. Takeda, H. Tomiyama, K. Nakashima, K. Hasegawa, F. Obata, T. Yoshikawa, H. Kawakami, S. Sakoda, M. Yamamoto, N. Hattori, M. Murata, Y. Nakamura, and T. Toda (2009). "Genome-wide association study identifies common variants at four loci as genetic risk factors for Parkinson's disease." In: *Nature genetics* 41.12, pp. 1303–1307

Sato, Y., Y. Suzuki, E. Ito, S. Shimazaki, M. Ishida, T. Yamamoto, H. Yamamoto, T. Toda, M. Suzuki, A. Suzuki, and T. Endo (2006). "Identification and characterization of an increased glycoprotein in aging: Age-associated translocation of cathepsin D". In: *Mechanisms of Ageing and Development* 127.10, pp. 771–778

Savitski, M. M., T. Mathieson, N. Zinn, G. Sweetman, C. Doce, I. Becher, F. Pachl, B. Kuster, and M. Bantscheff (2013). "Measuring and managing ratio compression for accurate iTRAQ/TMT quantification". In: *Journal of Proteome Research* 12.8, pp. 3586–3598

Schapansky, J., J. D. Nardozzi, F. Felizia, and M. J. LaVoie (2014a). "Membrane recruitment of endogenous LRRK2 precedes its potent regulation of autophagy". In: 14, pp. 4201–4214

Schapansky, J., J. D. Nardozzi, and M. J. LaVoie (2014b). "The Complex Relationships between Microglia, Alpha-Synuclein, and LRRK2 in Parkinson's Disease." In: *Neuroscience*

Schiavo, G., L. Greensmith, M. Hafezparast, and E. M. C. Fisher (2013). "Cytoplasmic dynein heavy chain: The servant of many masters". In: *Trends in Neurosciences* 36.11, pp. 641–651

Schmelzle, T. and M. N. Hall (2000). "TOR, a Central Controller of Cell Growth". In: *Cell* 103.2, pp. 253–262

Schmid, E. M., M. G. J. Ford, A. Burtey, G. J. K. Praefcke, S. Y. Peak-Chew, I. G. Mills, A. Benmerah, and H. T. McMahon (2006). "Role of the AP2 Beta-appendage hub in recruiting partners for clathrin-coated vesicle assembly". In: *PLoS Biology* 4.9, pp. 1532–1548

Schneider, J. A., J.-L. Li, Y. Li, R. S. Wilson, J. H. Kordower, and D. A. Bennett (2006). "Substantia nigra tangles are related to gait impairment in older persons." In: *Annals of neurology* 59.1, pp. 166–73

Schreij, A. M. A., M. Chaineau, W. Ruan, S. Lin, P. A. Barker, E. A. Fon, and P. S. Mcpherson (2015). "LRRK 2 localizes to endosomes and interacts with clathrin-light chains to limit Rac 1 activation". In: pp. 79–86

Schuberth, C. and A. Buchberger (2008). "UBX domain proteins: Major regulators of the AAA ATPase Cdc48/p97". In: *Cellular and Molecular Life Sciences* 65.15, pp. 2360–2371

Schulz, C., M. Paus, K. Frey, R. Schmid, Z. Kohl, D. Mennerich, J. Winkler, and F. Gillardon (2011). "Leucine-rich repeat kinase 2 modulates retinoic acid-induced neuronal differentiation of murine embryonic stem cells". In: *PLoS ONE* 6.6

Schulze, H. and K. Sandhoff (2014). "Sphingolipids and lysosomal pathologies". In: *Biochimica et Biophysica Acta - Molecular and Cell Biology of Lipids* 1841.5, pp. 799–810

Schwarz, J. S., H. R. De Jonge, and J. N. Forrest (2015). "Value of organoids from comparative epithelia models". In: *Yale Journal of Biology and Medicine* 88.4, pp. 367–374

Seaman, M. N. J. (2004). "Cargo-selective endosomal sorting for retrieval to the Golgi requires retromer". In: *Journal of Cell Biology* 165.1, pp. 111–122

– (2012). "The retromer complex - endosomal protein recycling and beyond". In: *Journal of Cell Science* 125.20, pp. 4693–4702

Seaman, M. N. J., E. G. Marcusson, J. L. Cereghino, and S. D. Emr (1997). "Endosome to Golgi retrieval of the vacuolar protein sorting receptor, Vps10p, requires the function of the VPS29, VPS30, and VPS35 gene products". In: *Journal of Cell Biology* 137.1, pp. 79–92

Sen, S., P. J. Webber, and A. B. West (2009). "Dependence of leucine-rich repeat kinase 2 (LRRK2) kinase activity on dimerization". In: *Journal of Biological Chemistry* 284.52, pp. 36346–36356

Sevlever, D., P. Jiang, and S. H. C. Yen (2008). "Cathepsin D is the main lysosomal enzyme involved in the degradation of alpha-synuclein and generation of its carboxy-terminally truncated species". In: *Biochemistry* 47.36, pp. 9678–9687

Sevlever, D., F. Zou, L. Ma, S. Carrasquillo, M. G. Crump, O. J. Culley, T. Hunter, G. D. Bisceglio, L. Younkin, M. Allen, M. M. Carrasquillo, S. B. Sando, J. O. Aasly, D. W. Dickson, N. R. Graff-Radford, R. C. Petersen, and O. Belbin (2015). "Genetically-controlled Vesicle-Associated Membrane Protein 1 expression may

contribute to Alzheimer's pathophysiology and susceptibility". In: *Molecular Neurodegeneration* 10.1, pp. 1–12

Shannon, K. M., A. Keshavarzian, H. B. Dodiya, S. Jakate, and J. H. Kordower (2012). "Is alpha-synuclein in the colon a biomarker for premotor Parkinson's Disease? Evidence from 3 cases". In: *Movement Disorders* 27.6, pp. 716–719

Shida, T., J. G. Cueva, Z. Xu, M. B. Goodman, and M. V. Nachury (2010). "The major alpha-tubulin K40 acetyltransferase alphaTAT1 promotes rapid ciliogenesis and efficient mechanosensation." In: *Proceedings of the National Academy of Sciences of the United States of America* 107.50, pp. 21517–21522

Shimura, H., N. Hattori, S. I. Kubo, Y. Mizuno, S. Asakawa, S. Minoshima, N. Shimizu, K. Iwai, T. Chiba, K. Tanaka, and T. Suzuki (2000). "Familial Parkinson disease gene product, parkin, is a ubiquitin-protein ligase." In: *Nature genetics* 25.3, pp. 302–305

Shin, N., H. Jeong, J. Kwon, H. Y. Heo, J. J. Kwon, H. J. Yun, C.-H. Kim, B. S. Han, Y. Tong, J. Shen, T. Hatano, N. Hattori, K.-S. Kim, S. Chang, and W. Seol (2008). "LRRK2 regulates synaptic vesicle endocytosis." In: *Experimental cell research* 314.10, pp. 2055–65

Shin, R. W., T. Iwaki, T. Kitamoto, Y. Sato, and J. Tateishi (1992). "Massive accumulation of modified tau and severe depletion of normal tau characterize the cerebral cortex and white matter of Alzheimer's disease. Demonstration using the hydrated autoclaving method." In: *The American journal of pathology* 140.4, pp. 937–945

Simón-Sánchez, J., C. Schulte, J. Bras, M. Sharma, J. R. Gibbs, D. Berg, C. Paisan-Ruiz, P. Lichtner, S. W. Scholz, D. G. Hernandez, R. Krüger, M. Federoff, C. Klein, A. Goate, J. S. Perlmutter, M. Bonin, M. A. Nalls, T. Illig, C. Gieger, H. Houlden, M. Steffens, M. S. Okun, B. A. Racette, M. R. Cookson, K. D. Foote, H. H. Fernandez, B. J. Traynor, S. Schreiber, S. Arepalli, R. Zonozi, K. Gwinn, M. P. Van Der Brug, G. Lopez, S. J. Chanock, A. Schatzkin, Y. Park, A. Hollenbeck, J. Gao, X. Huang, N. W. Wood, D. Lorenz, G. Deuschl, H. Chen, O. Riess, J. Hardy, A. B. Singleton, and T. Gasser (2009). "Genome-wide association study reveals genetic risk underlying Parkinson's disease." In: *Nature genetics* 41.12, pp. 1308–12

Singleton, A. B., M. J. Farrer, J. O. Johnson, S. Hague, J. Kachergus, M. Hulihan, T. Peuralinna, A. Dutra, R. Nussbaum, S. J. Lincoln, A. Crawley, M. Hanson, D. M. Maraganore, C. Adler, M. R. Cookson, M. Muenter, M. A. S. Baptista, D. Miller, J. Blancato, J. Hardy, and K. Gwinn-Hardy (2003). "alpha-Synuclein locus triplication causes Parkinson's disease." In: *Science* 302.5646, p. 841

Smolinsky, B., S. A. Eichler, S. Buchmeier, J. C. Meier, and G. Schwarz (2008). "Splice-specific functions of gephyrin in molybdenum cofactor biosynthesis". In: *Journal of Biological Chemistry* 283.25, pp. 17370–17379

Speidel, A., S. Felk, P. Reinhardt, J. Sterneckert, and F. Gillardon (2016). "Leucine-rich repeat kinase 2 influences fate decision of human monocytes differentiated from induced pluripotent stem cells". In: *PLoS ONE* 11.11, pp. 1–19

Spillantini, M. G., R. A. Crowther, R. Jakes, M. Hasegawa, and M. Goedert (1998). "Alpha-Synuclein in filamentous inclusions of Lewy bodies from Parkinson's disease and dementia with Lewy bodies". In: *Proceedings of the National Academy of Sciences* 95.11, pp. 6469–6473

Stefanis, L. (2012). "Alpha-Synuclein in Parkinson's disease". In: *Cold Spring Harbor Perspectives in Medicine* 2.2, pp. 1–23

Steger, M., F. Tonelli, G. Ito, P. Davies, M. Trost, M. Vetter, S. Wachter, E. Lorentzen, G. Duddy, S. Wilson, M. A. S. Baptista, B. K. Fiske, M. J. Fell, J. A. Morrow, A. D. Reith, D. R. Alessi, M. Mann, and I. Genta (2016). "Phosphoproteomics reveals that Parkinson's disease kinase LRRK2 regulates a subset of Rab GTPases". In: *eLife* 5, pp. 1–28

Stodkilde, L., J. Palmfeldt, L. Nilsson, I. Carlsen, Y. Wang, R. Norregaard, and J. Frokiaer (2014). "Proteomic identification of early changes in the renal cytoskeleton in obstructive uropathy". In: *AJP: Renal Physiology* 306.12, F1429–F1441

Strauss, E., C. Kinsland, Y. Ge, F. W. McLafferty, and T. P. Begley (2001). "Phosphopantothenoylcysteine Synthetase from Escherichia coli. Identification and characterization of the last unidentified coenzyme A biosynthetic enzyme in bacteria". In: *Journal of Biological Chemistry* 276.17, pp. 13513–13516

Subramanian, N., A. Wetzel, B. Dombert, P. Yadav, S. Havlicek, S. Jablonka, M. A. Nassar, R. Blum, and M. Sendtner (2012). "Role of nav1.9 in activity-dependent axon growth in motoneurons". In: *Human Molecular Genetics* 21.16, pp. 3655–3667

Sudo, H., A. B. Tsuji, A. Sugyo, M. Kohda, C. Sogawa, C. Yoshida, Y. N. Harada, O. Hino, and T. Saga (2010). "Knockdown of copa, identified by loss-of-function screen, induces apoptosis and suppresses tumor growth in mesothelioma mouse model". In: *Genomics* 95.4, pp. 210–216

Sulzer, D., E. Mosharov, Z. Talloczy, F. A. Zucca, J. D. Simon, and L. Zecca (2008). "Neuronal pigmented autophagic vacuoles: Lipofuscin, neuromelanin, and ceroid as macroautophagic responses during aging and disease". In: *Journal of Neurochemistry* 106.1, pp. 24–36

Suzuki, K. and T. Koike (2007). "Mammalian Sir2-related protein (SIRT) 2-mediated modulation of resistance to axonal degeneration in slow Wallerian degeneration mice: A crucial role of tubulin deacetylation". In: *Neuroscience* 147.3, pp. 599–612

Tan, G.-J., Z.-K. Peng, J.-P. Lu, and F.-Q. Tang (2013). "Cathepsins mediate tumor metastasis." In: *World journal of biological chemistry* 4.4, pp. 91–101

Taylor, J. P., M. Hulihan, J. Kachergus, H. L. Melrose, S. J. Lincoln, K. M. Hinkle, J. T. Stone, O. A. Ross, R. Hauser, J. O. Aasly, T. Gasser, H. Payami, Z. K. Wszolek, and M. J. Farrer (2007). "Leucine-rich repeat kinase 1: A paralog of LRRK2 and a candidate gene for Parkinson's disease". In: *Neurogenetics* 8.2, pp. 95–102

Taymans, J.-M. and V. Baekelandt (2014). "Phosphatases of alpha-synuclein, LRRK2, and tau: important players in the phosphorylation-dependent pathology of Parkinsonism". In: *Frontiers in Genetics* 5.November, pp. 1–12

Taymans, J.-M. and M. R. Cookson (2010). "Mechanisms in dominant parkinsonism: The toxic triangle of LRRK2, alpha-synuclein, and tau". In: *BioEssays* 32.3, pp. 227–235

Titz, B., T. Y. Low, E. Komisopoulou, S. S. Chen, L. Rubbi, and T. G. Graeber (2010). "The proximal signaling network of the BCR-ABL1 oncogene shows a modular organization." In: *Oncogene* 29.44, pp. 5895–5910

Tobin, J. E., J. C. Latourelle, M. F. Lew, C. Klein, O. Suchowersky, H. A. Shill, L. I. Golbe, M. H. Mark, J. H. Growdon, G. F. Wooten, B. A. Racette, J. S. Perlmutter, R. Watts, M. Guttman, K. B. Baker, S. Goldwurm, G. Pezzoli, C. Singer, M. H. Saint-Hilaire, A. E. Hendricks, S. Williamson, M. W. Nagle, J. B. Wilk, T. Massood, J. M. Laramie, A. L. Destefano, I. Litvan, G. Nicholson, A. Corbett, S. Isaacson, D. J. Burn, P. F. Chinnery, P. P. Pramstaller, S. Sherman, J. Al-Hinti, E. Drasby, M. Nance, A. T. Moller, K. Ostergaard, R. Roxburgh, B. Snow, J. T. Slevin, F. Cambi, J. F. Gusella, and R. H. Myers (2008). "Haplotypes and gene expression implicate the MAPT region for Parkinson disease: The GenePD Study". In: *Neurology* 71.1, pp. 28–34

Tong, Y., H. Yamaguchi, E. Giaime, S. Boyle, R. Kopan, R. J. Kelleher, and J. Shen (2010). "Loss of leucine-rich repeat kinase 2 causes impairment of protein degradation pathways, accumulation of alpha-synuclein, and apoptotic cell death in aged mice." In: *Proceedings of the National Academy of Sciences of the United States of America* 107.21, pp. 9879–9884

Tong, Y., E. Giaime, H. Yamaguchi, T. Ichimura, Y. Liu, H. Si, H. Cai, J. V. Bonventre, and J. Shen (2012). "Loss of leucine-rich repeat kinase 2 causes age-dependent bi-phasic alterations of the autophagy pathway". In: *Molecular Neurodegeneration* 7.1, p. 2

Trancikova, A., A. Mamais, P. J. Webber, K. Stafa, E. Tsika, L. Glauser, A. B. West, R. Bandopadhyay, and D. J. Moore (2012). "Phosphorylation of 4E-BP1 in the Mammalian Brain Is Not Altered by LRRK2 Expression or Pathogenic Mutations". In: *PLoS ONE* 7.10

Trinh, J. and M. J. Farrer (2013). "Advances in the genetics of Parkinson disease." In: *Nature reviews. Neurology* 9.8, pp. 445–54

Tsika, E. and D. J. Moore (2012). "Mechanisms of LRRK2-mediated neurodegeneration". In: *Current Neurology and Neuroscience Reports* 12.3, pp. 251–260

Tyynelä, J., I. Sohar, D. E. Sleat, R. M. Gin, R. J. Donnelly, M. Baumann, M. Haltia, and P. Lobel (2000). "A mutation in the ovine cathepsin D gene causes a congenital lysosomal storage disease with profound neurodegeneration." In: *The EMBO journal* 19.12, pp. 2786–92

Ujiie, S., T. Hatano, S.-I. Kubo, S. Imai, S. Sato, T. Uchihara, S. Yagishita, K. Hasegawa, H. Kowa, F. Sakai, and N. Hattori (2012). "LRRK2 I2020T

mutation is associated with tau pathology." In: *Parkinsonism & related disorders* 18.7, pp. 819–23

Valente, E. M., P. M. Abou-sleiman, V. Caputo, M. K. Muqit, K. Harvey, S. Gispert, Z. Ali, D. Del Turco, A. Bentivoglio, D. Healy, A. Albanese, R. Nussbaum, R. Gonza, T. Deller, S. Salvi, P. Cortelli, W. P. Gilks, D. S. Latchman, R. J. Harvey, B. Dallapiccola, G. Auburger, and N. W. Wood (2004). "Hereditary Early-Onset Parkinson ' s Disease Caused by Mutations in PINK1". In: *Science* 304.May, pp. 1158–1161. arXiv: `arXiv:1011.1669v3`

Van Den Eeden, S. K., C. M. Tanner, A. L. Bernstein, R. D. Fross, A. Leimpeter, D. A. Bloch, and L. M. Nelson (2003). "Incidence of Parkinson's disease: variation by age, gender, and race/ethnicity." In: *American journal of epidemiology* 157.11, pp. 1015–1022

Vanlandingham, P. A. and B. P. Ceresa (2009). "Rab7 regulates late endocytic trafficking downstream of multivesicular body biogenesis and cargo sequestration". In: *Journal of Biological Chemistry* 284.18, pp. 12110–12124

Varanese, S., Z. Birnbaum, R. Rossi, and A. Di Rocco (2011). "Treatment of advanced Parkinson's disease." In: *Parkinson's disease* 2010, p. 480260

Vilariño-Güell, C., C. Wider, O. A. Ross, J. C. Dachsel, J. Kachergus, S. J. Lincoln, A. I. Soto-Ortolaza, S. A. Cobb, G. J. Wilhoite, J. A. Bacon, B. Bahareh, H. L. Melrose, E. Hentati, A. Puschmann, D. M. Evans, E. Conibear, W. W. Wasserman, J. O. Aasly, P. R. Burkhard, R. Djaldetti, J. Ghika, F. Hentati, A. Krygowska-Wajs, T. Lynch, E. Melamed, A. Rajput, A. H. Rajput, A. Solida, R. M. Wu, R. J. Uitti, Z. K. Wszolek, F. Vingerhoets, and M. J. Farrer (2011). "VPS35 mutations in parkinson disease". In: *American Journal of Human Genetics* 89.1, pp. 162–167

Villarroel-Campos, D., L. Gastaldi, C. Conde, A. Caceres, and C. Gonzalez-Billault (2014). "Rab-mediated trafficking role in neurite formation". In: *Journal of Neurochemistry* 129.2, pp. 240–248

Visanji, N. P., P. L. Brooks, L.-N. Hazrati, and A. E. Lang (2013). "The prion hypothesis in Parkinson's disease: Braak to the future". In: *Acta Neuropathologica Communications* 1.1, p. 2

Vossel, K. A., K. Zhang, J. Brodbeck, A. C. Daub, P. Sharma, S. Finkbeiner, B. Cui, and L. Mucke (2010). "Tau reduction prevents Abeta-induced defects in axonal transport." In: *Science (New York, N.Y.)* 330.6001, p. 198

Wallings, R., C. Manzoni, and R. Bandopadhyay (2015). "Cellular processes associated with LRRK2 function and dysfunction". In: *FEBS Journal* 282.15, pp. 2806–26

Wang, X., M. H. Yan, H. Fujioka, J. Liu, A. L. Wilson-Delfosse, S. G. Chen, G. Perry, G. Casadesus, and X. Zhu (2012a). "LRRK2 regulates mitochondrial dynamics and function through direct interaction with DLP1". In: *Human Molecular Genetics* 21.9, pp. 1931–1944

Wang, X., T. G. Petrie, Y. Liu, J. Liu, H. Fujioka, and X. Zhu (2012b). "Parkinson's disease-associated DJ-1 mutations impair mitochondrial dynamics and cause mitochondrial dysfunction". In: *Journal of Neurochemistry* 121.5, pp. 830–839

Wang, X., T. Huang, G. Bu, and H. Xu (2014). "Dysregulation of protein trafficking in neurodegeneration". In: 9.1, pp. 1–9

Waschbüsch, D., H. Michels, S. Strassheim, E. Ossendorf, D. Kessler, C. J. Gloeckner, and A. Barnekow (2014). "LRRK2 transport is regulated by its novel interacting partner Rab32". In: *PLoS ONE* 9.10

Waterston, R. H. et al. (2002). "Initial sequencing and comparative analysis of the mouse genome". In: *Nature* 420.6915, pp. 520–562

Webb, J. L., B. Ravikumar, J. Atkins, J. N. Skepper, and D. C. Rubinsztein (2003). "Alpha-synuclein Is Degraded by Both Autophagy and the Proteasome". In: *Journal of Biological Chemistry* 278.27, pp. 25009–25013

West, A. B., D. J. Moore, S. Biskup, A. Bugayenko, W. W. Smith, C. A. Ross, V. L. Dawson, and T. M. Dawson (2005). "Parkinson's disease-associated mutations in leucine-rich repeat kinase 2 augment kinase activity." In: *Proceedings of the National Academy of Sciences of the United States of America* 102.46, pp. 16842–16847

West, A. B., R. M. Cowell, J. P. L. Daher, M. S. Moehle, K. M. Hinkle, H. L. Melrose, D. G. Standaert, and L. A. Volpicelli-Daley (2014). "Differential LRRK2 expression in the cortex, striatum, and substantia nigra in transgenic and nontransgenic rodents." In: *The Journal of comparative neurology* 522.11, pp. 2465–80

Wiese, S., K. A. Reidegeld, H. E. Meyer, and B. Warscheid (2007). "Protein labeling by iTRAQ: A new tool for quantitative mass spectrometry in proteome research". In: *Proteomics* 7, pp. 340–350

Winklhofer, K. F. and C. Haass (2010). "Mitochondrial dysfunction in Parkinson's disease". In: *Biochimica et Biophysica Acta (BBA) - Molecular Basis of Disease* 1802.1, pp. 29–44

Winner, B., H. L. Melrose, C. Zhao, K. M. Hinkle, M. Yue, C. Kent, and A. Braithwaite (2012). "Adult neurogenesis and neurite outgrowth are impaired in LRRK2 G2019S mice". In: *Neurobiology of disease* 41.3, pp. 706–716

Wittrup, A. and J. Lieberman (2015). "Knocking down disease: a progress report on siRNA therapeutics". In: *Nature Review Genetics* 16.9, pp. 543–552

Woodman, P. G. (2000). "Biogenesis of the sorting endosome: the role of Rab5." In: *Traffic* 1.9, pp. 695–701

Xie, R., S. Nguyen, W. L. McKeehan, and L. Liu (2010). "Acetylated microtubules are required for fusion of autophagosomes with lysosomes." In: *BMC cell biology* 11.1, p. 89

Xing, W., J. Liu, S. Cheng, P. Vogel, S. Mohan, and R. Brommage (2013). "Targeted disruption of leucine-rich repeat kinase 1 but not leucine-rich repeat kinase 2 in mice causes severe osteopetrosis." In: *Journal of bone and mineral research : the official journal of the American Society for Bone and Mineral Research* 28.9, pp. 1962–74

Yao, C., W. M. Johnson, Y. Gao, W. Wang, J. Zhang, M. Deak, D. R. Alessi, X. Zhu, J. J. Mieyal, H. Roder, A. L. Wilson-Delfosse, and S. G. Chen (2013).

"Kinase inhibitors arrest neurodegeneration in cell and C. elegans models of LRRK2 toxicity". In: *Human Molecular Genetics* 22.2, pp. 328–344

Yoshida, H., K. Okamoto, T. Iwamoto, E. Sakai, K. Kanaoka, J. Hu, M. Shibata, H. Hotokezaka, K. Nishishita, A. Mizuno, and Y. Kato (2006). "Pepstatin A, an Aspartic Proteinase Inhibitor, Suppresses RANKL-Induced Osteoclast Differentiation". In: *The Journal of Biochemistry* 139.3, p. 583

Young, P. R., C. Karanutilake, and A. P. Zygas (1991). "Binding of cathepsin D to the mannose receptor on rat peritoneal macrophages." In: *Biochimica et biophysica acta* 1095.1, pp. 1–4

Yue, M., K. M. Hinkle, P. Davies, E. Trushina, F. Fiesel, T. Christenson, A. Schroeder, L. Zhang, E. Bowles, B. Behrouz, S. J. Lincoln, J. E. Beevers, A. Milnerwood, A. Kurti, P. McLean, J. Fryer, W. Springer, D. W. Dickson, M. J. Farrer, and H. L. Melrose (2015). "Progressive dopaminergic alterations and mitochondrial abnormalities in LRRK2 G2019S knock in mice". In: *Neurobiology of Disease* 78, pp. 172–195

Zabetian, C. P., C. M. Hutter, S. A. Factor, J. G. Nutt, D. S. Higgins, A. Griffith, J. W. Roberts, B. C. Leis, D. M. Kay, D. Yearout, J. S. Montimurro, K. L. Edwards, A. Samii, and H. Payami (2007). "Association analysis of MAPT H1 haplotype and subhaplotypes in Parkinson's disease". In: *Annals of Neurology* 62.2, pp. 137–144

Zanetti, G., K. B. Pahuja, S. Studer, S. Shim, and R. Schekman (2012). "COPII and the regulation of protein sorting in mammals". In: *Nature Cell Biology* 14.1, pp. 20–28

Zhang, B., A. Maiti, S. Shively, F. Lakhani, G. McDonald-Jones, J. Bruce, E. B. Lee, S. X. Xie, S. Joyce, C. Li, P. M. Toleikis, V. M. Lee, and J. Q. Trojanowski (2005). "Microtubule-binding drugs offset tau sequestration by stabilizing microtubules and reversing fast axonal transport deficits in a tauopathy model." In: *Proceedings of the National Academy of Sciences of the United States of America* 102.1, pp. 227–231

Zhang, D., J. Lin, and J. Han (2010). "Receptor-interacting protein (RIP) kinase family." In: *Cellular & molecular immunology* 7.4, pp. 243–249

Zhang, Q., M. Tan, J. Yu, and L. Tan (2015). "The Role of Retromer in Alzheimer's Disease". In: *Molecular Neurobiology* 53, pp. 4201–4209

Zhou, J., M. Tawk, F. D. Tiziano, J. Veillet, M. Bayes, F. Nolent, V. Garcia, S. Servidei, E. Bertini, F. Castro-Giner, Y. Renda, S. Carpentier, N. Andrieu-Abadie, I. Gut, T. Levade, H. Topaloglu, and J. Melki (2012). "Spinal muscular atrophy associated with progressive myoclonic epilepsy is caused by mutations in ASAH1". In: *American Journal of Human Genetics* 91.1, pp. 5–14

Zhou, R. M., Y. X. Huang, X. L. Li, C. Chen, Q. Shi, G. R. Wang, C. Tian, Z. Y. Wang, Y. Y. Jing, C. Gao, and X. P. Dong (2010). "Molecular interaction of alpha-synuclein with tubulin influences on the polymerization of microtubule in vitro and structure of microtubule in cells". In: *Molecular Biology Reports* 37.7, pp. 3183–3192

Zimmerberg, J. and M. Kozlov (2006). "How proteins produce cellular membrane curvature." In: *Nature reviews. Molecular cell biology* 7.1, pp. 9–19

Zimprich, A., S. Biskup, P. Leitner, P. Lichtner, M. J. Farrer, S. J. Lincoln, J. Kachergus, M. Hulihan, R. J. Uitti, D. B. Calne, A. Stoessl, R. F. Pfeiffer, N. Patenge, I. C. Carbajal, P. Vieregge, F. Asmus, B. Müller-Myhsok, D. W. Dickson, T. Meitinger, T. M. Strom, Z. K. Wszolek, and T. Gasser (2004). "Mutations in LRRK2 cause autosomal-dominant parkinsonism with pleomorphic pathology". In: *Neuron* 44.4, pp. 601–607

Zimprich, A., A. Benet-Pagès, W. Struhal, E. Graf, S. H. Eck, M. N. Offman, D. Haubenberger, S. Spielberger, E. C. Schulte, P. Lichtner, S. C. Rossle, N. Klopp, E. Wolf, K. Seppi, W. Pirker, S. Presslauer, B. Mollenhauer, R. Katzenschlager, T. Foki, C. Hotzy, E. Reinthaler, A. Harutyunyan, R. Kralovics, A. Peters, F. Zimprich, T. Brücke, W. Poewe, E. Auff, C. Trenkwalder, B. Rost, G. Ransmayr, J. Winkelmann, T. Meitinger, and T. M. Strom (2011). "A mutation in VPS35, encoding a subunit of the retromer complex, causes late-onset parkinson disease". In: *American Journal of Human Genetics* 89.1, pp. 168–175